The Pennsylvania State University

The Graduate School

Eberly College of Science

INVESTIGATION OF LATE TRANSITION METAL BASED CATALYTIC SYSTEMS FOR POLYMERIZATION OF POLAR VINYL MONOMERS

A Thesis in

Chemistry

by

Myeongsoon Kang

Submitted in Partial Fulfillment
of the Requirements
for the Degree of

Doctor of Philosophy

August 2004

The thesis of Myeongsoon Kang was reviewed and approved* by the following:

Ayusman Sen
Professor of Chemistry
Thesis Advisor
Chair of Committee

Thomas E. Mallouk
DuPont Professor of Materials Chemistry

Alan J. Benesi
Director of the NMR Facility
Lecturer in Chemistry

Ralph H. Colby
Professor of
Materials Science and Engineering

Ayusman Sen
Professor of Chemistry
Head of the Department of Chemistry

*Signatures are on file in the Graduate School

ABSTRACT

Variable-temperature ^{1}H NMR studies of the reaction of cationic (α-diimine)Pd-alkyl complexes with alkenes are presented. The studies reveal that vinyl bromide coordinates to the Pd(II)-Me complex followed by migratory insertion and β-bromo elimination, to generate free propene. Propene further reacts to give β-agostic Pd(II)-*tert*-butyl species. From the reactions with vinyl bromide, stable chloro-bridged dicationic Pd complex was isolated and characterized. For a series of alkenes (CH_2=CHX), the rate for migratory insertion decreases as follows : X = CO_2Me > Br > H > Me.

Palladium(1,5-cyclooctadiene)(methyl)(chloride), is a catalyst for the living oligomerization of norbornene. The reaction is attenuated by additives in the following decreasing order, C=C > Cl^- > RC(=O)OR. The insertion of norbornene, *endo* and *exo*-5-ethylester-2-norbornene, and *endo*-5-methylacetate-2-norbornene into the palladium-methyl bond of Palladium(1,5-cyclooctadiene)(methyl)(chloride) was examined. Similar rates were found for all the norbornene derivatives, with the product in every case being derived from insertion through the *exo* face.

A series of neutral salicylaldiminato Pd(II) complexes, Pd(Me)(Ph-CH=N-R′)[3-^{t}Bu-2-(O)C_6H_3-CH=N-2,6-*di*-^{i}Pr-C_6H_3](R=CH3, n-Pr, tert-Bu, Ph, Benzyl) (**3a-3e**), and Pd(Me)[3-(CH=N-*t*-Bu)-Py][3-^{t}Bu-2-(O)C_6H_3-CH=N-2,6-*di*-^{i}Pr-C_6H_3] (**4**) have been synthesized and characterized. Their structure has been confirmed by an X-ray analysis of complexes **3a**, **3c-3e**, and **4**. Nuclear Magnetic Resonance (NMR) studies utilizing **3c**

indicate that the complex reacts with CO through a five-coordinate species. The neutral complexes **3a-3e** show moderate catalytic activity for the polymerization of methyl acrylate at ambient temperature. In the polymerization reaction, a radical mechanism rather than coordination insertion mechanism is invoked to be operative. The complexes **3a**, **3b**, **3d**, **3e** produced poly(norbornene) in low yield.

Neutral Pd(II) complexes, [3,5-di-^{t}Bu-2-(OH)C_6H_2N=CH-2-P$Ph_2C_6H_4$]PdMe_2 (**3**) and [3,5-di-^{t}Bu-2-(OH)C_6H_2CH=N-2-P$Ph_2C_6H_4$]PdMe_2 (**4**) have been synthesized and characterized. Their structures have been confirmed by an X-ray analysis of complexes **3** and **4**. In the solid state, the structure of the complex **3** significantly deviated from the idealized square planar geometry by virtue of the constraint caused by the large bond length difference between P(1)-C(14) and N(1)-C(8) (1.823(3) and 1.288(3), respectively in the [P,N] six-membered ring. Independently, the title compound did not show catalytic activity for the polymerization or oligomerization of an alkene without an assisting agent. In combination with $AlEt_3$, **3** and **4** have produced PMA, where **4** showed better activity. The complex **4** with $Al(C_6F_5)_3$ as a cocatalyst polymerized norbornene or *n*-butylnorbornene in excellent yield, but with $B(C_6F_5)_3$, it did not produce any polymeric product. Different reaction pathways between complexes **3** or **4** and $Al(C_6F_5)_3$ or $B(C_6F_5)_3$ have been proposed based on the results of the polymerization and the NMR experiments. Utilizing methylaluminoxane (MAO) as a co catalyst, **3** and **4** produced poly(norbornene) in good yield with no activity difference between **3** and **4**.

TABLE OF CONTENTS

LIST OF FIGURES viii

LIST OF TABLES x

ACKNOWLEDGEMENTS xii

Chapter 1 INTRODUCTION 1

References 3

Chapter 2 TRENDS IN ALKENE INSERTION IN LATE AND EARLY TRANSITION METAL COMPOUNDS: RELEVANCE TO TRANSITION METAL-CATALYZED POLYMERIZATION OF POLAR VINYL MONOMERS 4

2.1 Introduction 4
2.2 Results 5
2.2.1 Generation of Active Species 5
2.2.2 ^{1}H NMR Study of the Reaction of Cationic (α-diimine)Pd-methyl Complex with Vinyl bromide 7
2.2.3 Kinetics of the Reaction of Cationic (α-diimine)Pd-methyl Complex with Alkenes. 11
2.3 Discussion 13
2.3.1 Formation of Dimer and Deactivation Pathway. 13
2.3.2 Relative Insertion Rates of Alkenes. 13
2.4 Conclusions 15
2.5 Experimental Section 16
2.5.1 Low Temperature: methanol (with 0.03% concentrated HCl)[23] 17
2.5.2 High Temperature: ethylene glycol (neat)[24] 17
2.5.3 Interpretation of activation parameters 17
2.5.4 The Eyring Equation 18
2.5.5 Application of the Eyring Equation 18
2.6 References 19

Chapter 3 THE REACTION OF PALLADIUM(1,5-CYCLOOCTADIENE)-(ALKYL)(CHLORIDE) WITH NORBORNENE DERIVATIVES: RELEVANCE TO METAL-CATALYZED ADDITION POLYMERIZATION OF FUNCTIONALIZED NORBORNENE 22

3.1 Introduction 22
3.2 Results and Discussion 24
3.2.1 Reactions of Pd(1,5-cyclooctadiene)(CH_3)(Cl) with Norbornene Derivatives 24

3.2.2 Investigation of Reaction Mechanism 32
3.3 Conclusion 36
3.4 Experimental Section 37
3.4.1 Generation Considerations. 37
3.4.2 Synthesis of Complexes 38
3.4.3 General Procedure for NMR Experiments 41
3.4.4 General Procedures for Polymerization Reactions 41
3.5 References 42

Chapter 4 NEUTRAL PALLADIUM(II) COMPLEXES WITH N-O CHELATE: SYNTHESES, CHARACTERIZATION, AND THEIR REACTIVITIES 44

4.1 Introduction 44
4.2 Results and Discussion 45
4.2.1 Complex Synthesis 45
4.2.2 Mechanistic Studies of CO Insertion into Pd-Me Bond using Complex 3c 57
4.2.3 Polymerization of Polar or Nor-polar Vinyl Monomers 59
4.2.4 Reactivities of the complexes toward imine and CO 61
4.3 Conclusions 66
4.4 Experimental Section 67
4.4.1 Generation Considerations 67
4.4.2 Synthesis of Compounds 68
4.4.3 General Procedures for Polymerization Reactions 74
4.4.4 General Procedure for NMR Experiments 74
4.5 References 75

Chapter 5 NEUTRAL PALLADIUM(II) COMPLEXES WITH P-N-O CHELATE: SYNTHESES, CHARACTERIZATION, AND THEIR REACTIVITIES 78

5.1 Introduction 78
5.2 Results and Discussion 80
5.2.1 Ligand Synthesis 80
5.2.2 Complex Synthesis 81
5.2.3 Reactivity of the Complexes 86
5.3 Experimental Section 94
5.3.1 General Considerations 94
5.3.2 Synthesis of Compounds 96
5.3.3 General Procedures for Polymerization Reactions 98
5.4 References 99

Appendix A 103

Crystal structure information, compound 6 in Chapter 2 103

Appendix B Crystal structure information, compound 1a in Chapter 3 109

Appendix C Crystal structure information, compound 1b in Chapter 3 112

Appendix D Crystal structure information, compound 1c in Chapter 3 117

Appendix E Crystal structure information, compound 1d in Chapter 3 122

Appendix F Crystal structure information, compound 3a in Chapter 4..... 126

Appendix G Crystal structure information, compound 3c in Chapter 4 132

Appendix H Crystal structure information, compound 3d in Chapter 4..... 140

Appendix I Crystal structure information, compound 3e in Chapter 4..... 146

Appendix J Crystal structure information, compound 4 in Chapter 4 150

Appendix K Crystal structure information, compound 5 in Chapter 4..... 156

Appendix L Crystal structure information, compound 3 in Chapter 5 162

Appendix M Crystal structure information, compound 4 in Chapter 5 166

Appendix N Kinetic data sources for Table 2-1 and Figure 2-2..... 172

Appendix O Data sources for Figure 3-6 and 3-7..... 182

Appendix P Kinetic data sources for Table 4-7 185

LIST OF FIGURES

Figure 2-1: Generation of Active Species. Selected NMR spectra. 6

Figure 2-2: Selected variable temperature NMR spectra 8

Figure 2-3: ORTEP view of 6. Hydrogen atoms are not shown for clarity 10

Figure 2-4: Hammet plot for migratory insertion of alkenes into palladium(II)–methyl bond. 12

Figure 3-1: Modes of bonding for functionalized norbornene derivatives (X = coordinating functionality). 23

Figure 3-2: An ORTEP view of 1a, showing 50% probability thermal ellipsoids. Hydrogen atoms are omitted for clarity. 27

Figure 3-3: An ORTEP view of 1b, showing 50% probability thermal ellipsoids. Hydrogen atoms are omitted for clarity. 27

Figure 3-4: An ORTEP view of 1c, showing 50% probability thermal ellipsoids. Hydrogen atoms are omitted for clarity. 28

Figure 3-5: An ORTEP view of 1d, showing 50% probability thermal ellipsoids. Hydrogen atoms are omitted for clarity. 28

Figure 3-6: Molecular weight of norbornene oligomer *versus* time 32

– "Living" system 32

Figure 3-7: Plot of ln{[NB]/[NB]$_o$} versus time. Reaction conditions: 1 (3.7×10^{-5} mol), norbornenes (7.5×10^{-4} mol), CD_2Cl_2 (1 mL), 23°C. 33

Figure 4-1: ORTEP view of complex 3a. Hydrogen atoms are omitted for clarity. 49

Figure 4-2: ORTEP view of complex 3c. Hydrogen atoms are omitted for clarity. 49

Figure 4-3: ORTEP view of complex 3d. Hydrogen atoms are omitted for clarity. 50

Figure 4-4: ORTEP view of complex 3e. Hydrogen atoms are omitted for clarity. 50

Figure 4-5: ORTEP view of complex 4. Hydrogen atoms are omitted for clarity. 53

Figure 4-6: Selected VT ^{13}C NMR Spectra of the Reaction between 3e and Ph-CH=N-CH_2-Ph under ^{13}CO Atmosphere 62

Figure 4-7: ORTEP view of complex 5. Hydrogen atoms are omitted for clarity. 63

Figure 4-8: Selected proton coupled ^{13}C NMR spectrum 65

Figure 5-1: ORTEP view of complex 3. Hydrogen atoms are omitted for clarity. 83

Figure 5-2: ORTEP view of complex 4. Hydrogen atoms are omitted for clarity. 83

LIST OF TABLES

Table 2-1: Kinetic Data for Insertion of Alkenes into Pd(II)-Me bond[a] 11

Table 3-1: Selected Bond distances (Å) and Angles (°) for **1a** 29

Table 3-2: Selected Bond distances (Å) and Angles (°) for **1b** 29

Table 3-3: Selected Bond distances (Å) and Angles (°) for **1c** 30

Table 3-4: Selected Bond distances (Å) and Angles (°) for **1d** 30

Table 3-5: Crystallographic Data and data Collection Parameters for complexes **1a-d** 31

Table 3-6: Effect of Additives on the Polymerization of Norbornene using (1,5-COD)PdMeCl 35

Table 4-1: Selected Bond distances (Å) and Angles (°) for **3a** 51

Table 4-2: Selected Bond distances (Å) and Angles (°) for **3c** 51

Table 4-3: Selected Bond distances (Å) and Angles (°) for **3d** 52

Table 4-4: Selected Bond distances (Å) and Angles (°) for **3e** 52

Table 4-5: Selected Bond distances (Å) and Angles (°) for **4** 55

Table 4-6: Crystallographic Data and data Collection Parameters for complexes **3a-e** and **4** 56

Table 4-7: Kinetic Data for Insertion of CO into Pd(II)-Me Bond 58

Table 4-8: Polymerization of Vinyl Monomers using Complexes **3a-e**, and **4**[a] 59

Table 5-1: Selected Bond distances (Å) and Angles (°) for **3** 84

Table 5-2: Selected Bond distances (Å) and Angles (°) for **4** 84

Table 5-3: Crystallographic Data and data Collection Parameters for complexes **3a-e** and **4** 86

Table 5-4: Polymerization of vinyl monomers using complexes **3** and **4** with $AlEt_3$[a] 88

Table **5-4**: Polymerization of vinyl monomers using complexes **3** and **4** with $AlEt_3$[a] 89

Table **5-5**: Polymerization of vinyl monomers using complex **3** with FAL, $Al(C_6F_5)_3$, as a cocatalyst..... 91

Table **5-6**: Polymerization of vinyl monomers using 3 or 4 with MAO as a cocatalyst[a] 92

ACKNOWLEDGEMENTS

I have spent an exciting and enjoyable five years here at Penn State University, largely due to the amazing people that I have had the good fortune to associate with. The research described in this thesis is the culmination of years of hard work, and it would not have been possible without the help of a number of people. I want to take this opportunity to thank them for their help and support.

I am grateful to my advisor Dr. Ayusman Sen for his advice, encouragement, and support over five years. His enthusiasm for new ideas is infectious, and he has helped to broaden my interest in chemistry. I have enjoyed learning from him.

My committee members Dr. Thomas E. Mallouk, Dr. Alan J. Benesi, and Dr. Ralph H. Colby have helped me with their advice and suggestions, and I am especially grateful for that. Dr. Alan J. Benesi deserves a special thanks for his help and advice for my various NMR experiments. His help and advice in all experimental matters is indispensable. Besides being an excellent source of technical advice Dr. Benesi is a wonderful person, who is always ready to go out of his way to help people. Thanks Dr. Benesi.

A significant portion of my time was spent in Althouse Lab solving X-ray crystal structures of new compounds. Dr. Hemant Yennawar guided me very well to solve most of the structures with his great assistance. Thanks Hemant.

I was fortunate to have worked closely with former members in our group Dr. Jangsub Kim, Dr. Gregory S. Long, Dr. April Hennis, Dr. Sharon Elyashiv-Barad, Dr. Cecily Andes, Dr. Joseph E. Remias, Dr. Michelle Belz and Dr. Bin Gu. They patiently

showed me the ropes around the lab and have helped me to understand a great deal about the chemistry. Not only were they helpful in my experiments, they were also around to share my frustrations and excitements, provide support and encouragement. I was also lucky to have worked with current group members including new comers Dr. Minren Lin, Dr. Shengsheng Liu, Dr. Sachin Borkar, Jeffrey Funk, Walter Paxton, Varun Sambhy, Tim Kline, Megan Majcher, Shakuntala Sundararajan, Yiying Hong, Shikchya Tandukar, David Newsham, and Matthew R. Dirmyer. All of them were very helpful and inspiring. I wish them the very best in their endeavors.

Sungwoo, Minjoung, Soo-Young, Jae Hong, Youngkyu, Eunsun, Younhi, and Seung-Goo have been very good friends since they have been here. Talking to them has helped me through rough times. Thanks all of them for being great friends.

One person who cannot be thanked enough is Dr. Ik-Mo Lee at Inha University, Inchon, Korea. He was a tremendous influence on my life and encouraged me to decide to make chemistry my life's work by providing me a chance to come over here. Thanks Prof. Dr. Lee.

I specially thank my beautiful wife Jaehyun, my first son Eugene, and my soon-to-be-second-son Eubene for their love, patience, and unwavering support. They have transformed my life, and made it richer in countless ways.

I also want to take this opportunity to thank my parents, parents-in-law, sisters, sisters-in-law and brothers-in-law for their love and encouragement. This work would not have been possible without their support.

Most of my research was supported by a grant from the U.S. Department of Energy, Office of Basic Energy Sciences. I also thank NSF (CHE-0131112) for funding the X-ray diffractometer

Finally, I thank my Lord for being my guide and giving me strength for last five years' task. Thanks Lord. I go forth in Your strength alone. Please use me as You wish.

Myeongsoon Kang

Chapter 1

INTRODUCTION

International markets for plastics have greatly expanded. Within the $1,600 billion global chemicals industry, the largest segment, 40%, is the petrochemical industry. Within the petrochemical industry, commodity polymers account for 55 %, in terms of volume, of the consumption of basic petrochemicals. According to the industry estimates, global production and consumption of plastics is growing from 125,000 metric tons in 1997 to 210,000 metric tons by 2007, and 380,000 tons by 2020.[1] The overwhelming position of plastics in the petrochemical industry encourages researchers in this scientifically challenging field. High demand for the initiator which can control desired polymer properties underlines the importance of transition metal-catalyzed polymerization systems. The next four chapters are directed to the continued research field which involves developing new catalyst, understanding polymerization mechanisms and making materials with new or improved properties.

The consideration in chapter 2 is the mechanistic studies of the reaction between vinyl bromide and a palladium(II)-based cationic complex, which is relevant to transition metal-catalyzed polymerization of polar vinyl monomers. The Brookhart-type cationic Pd(II)-methyl species, $[(ArN=C(Me)C(Me)=NAr)Pd(Me)]^-$ has been employed for this study. In an attempt to gain mechanistic insights, the stepwise coordination and insertion of vinyl bromide were studied using variable temperature NMR spectroscopy. The active species generated in the presence of aluminum trichloride enabled us to investigate the

reaction of vinyl bromide with a late transition metal-based cationic complex, in which 1,2-alkene insertion followed by β-bromo elimination occurred. The results deduced from the migratory insertion of the polar and nonpolar vinyl monomers and the deactivation pathway observed here directed us to move to a neutral catalytic system for the polymerization of functionalized alkenes.

Chapter 3 describes the reaction of palladium (1,5-cyclooctadiene)(alkyl)-(chloride) with norbornene derivatives. Metal-catalyzed addition polymerization of functionalized alkenes is an area of great current interest in synthetic polymer chemistry because the addition of functionalities to a polymer which is otherwise non-polar can greatly enhance the range of attainable properties. However, a key problem in the development of metal-catalyzed routes to functionalized polyalkenes is the coordination of the functionality present both in the monomer and in the resulting polymer. From the point of view that Ziegler shows in his theoretical calculations,[2] the neutral complex is employed and investigated as a possible initiator for poly(norbornenes). All of the norbornene and norbornene derivatives with pendant *exo* and *endo* functionalities insert into the metal-alkyl bonds through the *exo* face with similar rates. Unlike cationic systems, no coordination of the ester group is observed. The implication of the work with respect to the metal-catalyzed polymerization of polar vinyl monomers is that the key to the efficient polymerization and copolymerization of functionalized norbornene derivatives lies in the use of less electrophilic, neutral metal species.

The syntheses of new neutral Pd(II)-based complexes and their applications have been addressed in chapters 4 and 5. A majority of the work done in those chapters is the syntheses of neutral complexes having [N-N], [N-O], and [P-N-O] chelate ligands and

characterizations of them with various spectroscopic methods including X-ray single-crystal structure analysis. In an attempt to test their possible applications for the polymerization and copolymerization of polar and non-polar monomers, their reactivities toward monomers, such as carbon monoxide, norbornene, and acrylates, have been studied. The main goal of the research in addition insertion polymerization utilizing transition metal-based is better control over the tacticity of the polymer and the possibility of copolymerizations with monomers otherwise inaccessible. Although extensive mechanistic studies need to be done to understand the mechanism involved in the polymerizations employing the new neutral complexes, the complexes have initiated polymerizations of vinyl monomers alone or with the assistance of an activator.

References

1. (a) http://www.americanplasticscouncil.org (b) http://www.bizsites.com
   (c) http://thakur.itgo.com/petro.htm
2. Michalak, A.; Ziegler, T. *Organometallics* **2001**, *20*, 1521-1532.

Chapter 2

TRENDS IN ALKENE INSERTION IN LATE AND EARLY TRANSITION METAL COMPOUNDS: RELEVANCE TO TRANSITION METAL-CATALYZED POLYMERIZATION OF POLAR VINYL MONOMERS

2.1 Introduction

Metal-catalyzed insertion copolymerization of polar vinyl monomers with nonpolar alkenes remains an area of great interest in synthetic polymer chemistry, because the addition of functionalities to a polymer which is otherwise non-polar can greatly enhance the range of attainable properties.[1] For vinyl monomers with pendant coordinating functionalities, such as acrylates, the principal problem has been catalyst poisoning through functional group coordination.[1-3] Interestingly, vinyl halides, which do not possess any strongly coordinating functionality, are also not polymerized by any known transition metal-catalyzed systems. Recently, Jordan[4] and Wolczanski[5] have reported the reaction of vinyl halides with *rac*-(EBI)ZrMe and $(t\text{-}Bu_3SiO)_3TaH_2$, respectively. It was demonstrated that, following 1,2-insertion of the alkene, β-halide elimination occurs to generate a metal-halide bond. Since the halophilicity of the transition metal ions tends to decrease on going from left to right in the periodic table, we undertook an examination of the reactivity of vinyl halides towards a late transition metal complex (palladium). Herein we report mechanistic investigations of the reactions of cationic (α-diimine)Pd-alkyl complexes with alkenes using variable-temperature ^1H NMR spectroscopy.[6]

2.2 Results

2.2.1 Generation of Active Species

The starting point of our investigation was the Brookhart-type cationic Pd(II)-methyl species, **2**, generated in our case by the addition of two equivalents of $AlCl_3$ to the corresponding neutral Pd(II)-methylchloride, **1**, (Schemes **2-1** and **2-2**). ^1H NMR studies revealed that the active species **2** forms through the intermediate **A** or **B** (Scheme 1).[7] The reaction of **1** and 1 *equiv*. of $AlCl_3$ resulted in the generation of **A**/**B** and trace amounts of **2** upon stirring for 2 h at room temperature. The addition of a second *equiv*. of $AlCl_3$ to the reaction mixture resulted in the formation of the active species **2** (Figure **2-1**). The ^1H NMR spectrum of **2** is similar to that of the Brookhart compound [(ArN=C(Me)C(Me)=NAr)Pd(Me)(NCMe)]BAr′F (Ar = 2,6-di-*i*-Pr-C_6H_3), implying similar structures for both. However, the Brookhart compound was unreactive towards vinyl bromide, presumambly because of the failure of the olefin to displace the coordinated MeCN. Reaction of **1** with $B(C_6F_5)_3$ or $NaB(3,5\text{-}(CF_3)_2\text{-}C_6H_3)_4$ generated similar species produced from the reaction of **1** with 1 *equiv*. of $AlCl_3$.

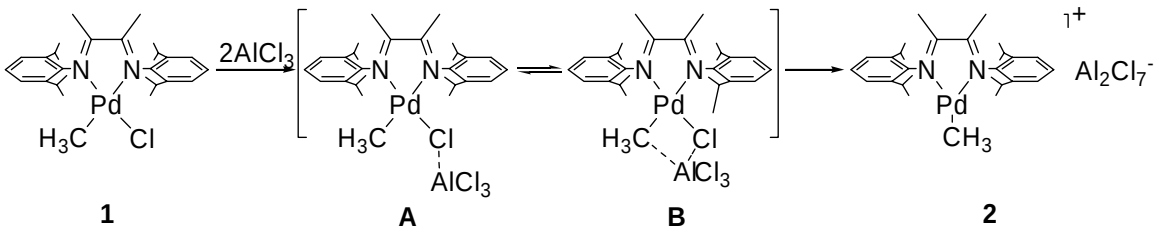

Scheme **2-1**

Figure 2-1

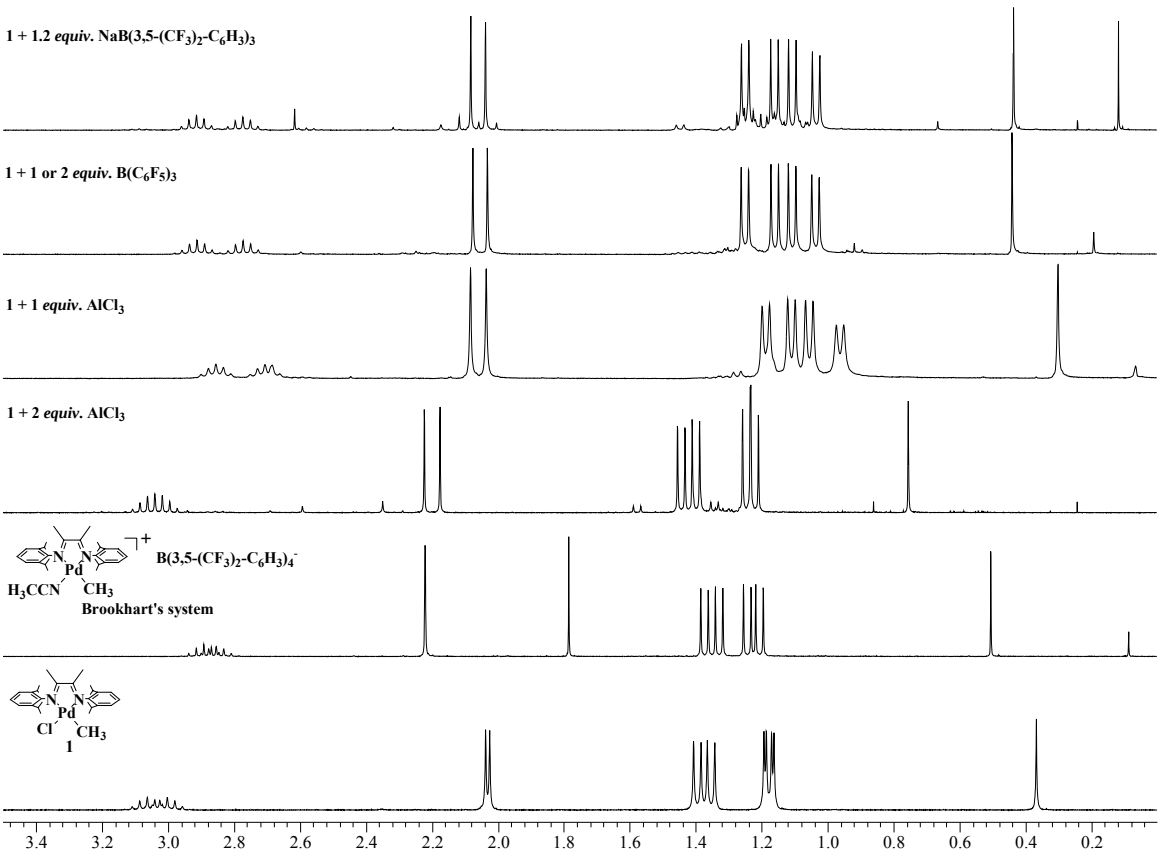

Figure **2-1**: Generation of Active Species. Selected NMR spectra.

2.2.2 ^{1}H NMR Study of the Reaction of Cationic (α-diimine)Pd-methyl Complex with Vinyl bromide

Several equivalents of vinyl bromide were added to a CD_2Cl_2 solution of **2** at -90°C and the reaction mixture was monitored by ^{1}H NMR spectroscopy as it was gradually warmed up (Figure **2-2** and Scheme **2-2**). The coordination of vinyl bromide to the metal center in **2** was observed even at -86°C, resulting in the formation of **3**. Warming the reaction mixture to -74°C resulted in the formation of the propene coordinated species, **4**, suggesting 1,2-alkene insertion followed by β-bromo elimination. Propene is gradually lost from **4** and is trapped by unreacted **2** to form **7**. Formation of complex **7** was confirmed by addition of free propene to the system, which caused the ratio of **7** to **4** to increase. The cationic Pd(II)-halide species arising from **4** by propene loss converts to the chloro-bridged dimer **6**. The structure of **6** as a dicationic complex with two aluminum tetrachloride counteranions was established by an X-ray crystal structure determination (Figure **2-3**).

Once formed, **7** undergoes 1,2-insertion of propene to form the known β-agostic Pd(II)-*tert*-butyl compound **8**[8]. The complexes **7** and **8** were also independently formed by the addition of propene to a CD_2Cl_2 solution of **2**. The initially formed **7** was found to convert to **8** when the solution was warmed to -36°C. At ambient temperature, the three methyl groups of the *tert*-butyl complex exchange rapidly on the NMR time scale and appear as a singlet at –0.28 ppm. Upon lowering the temperature to -86°C, a static ^{1}H NMR spectrum is observed and the agostic proton appears as a singlet at –8 ppm.

Figure **2-2**

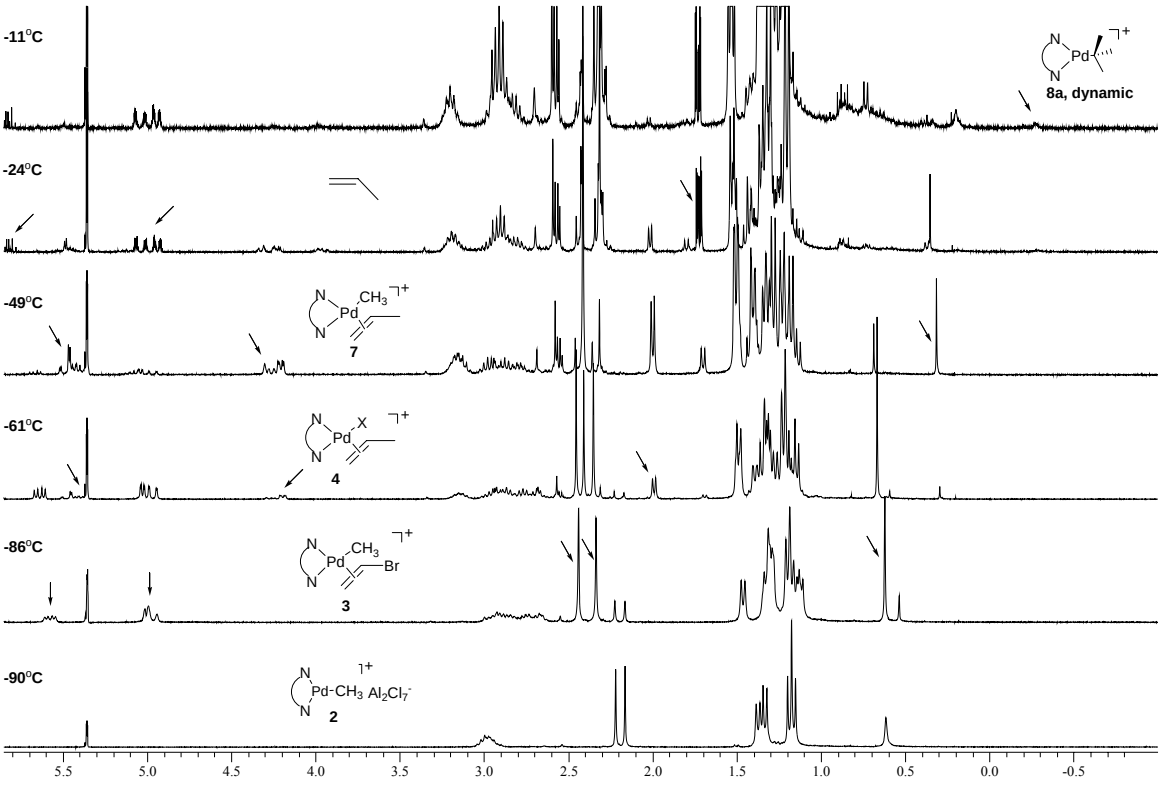

Figure **2-2**: Selected variable temperature NMR spectra

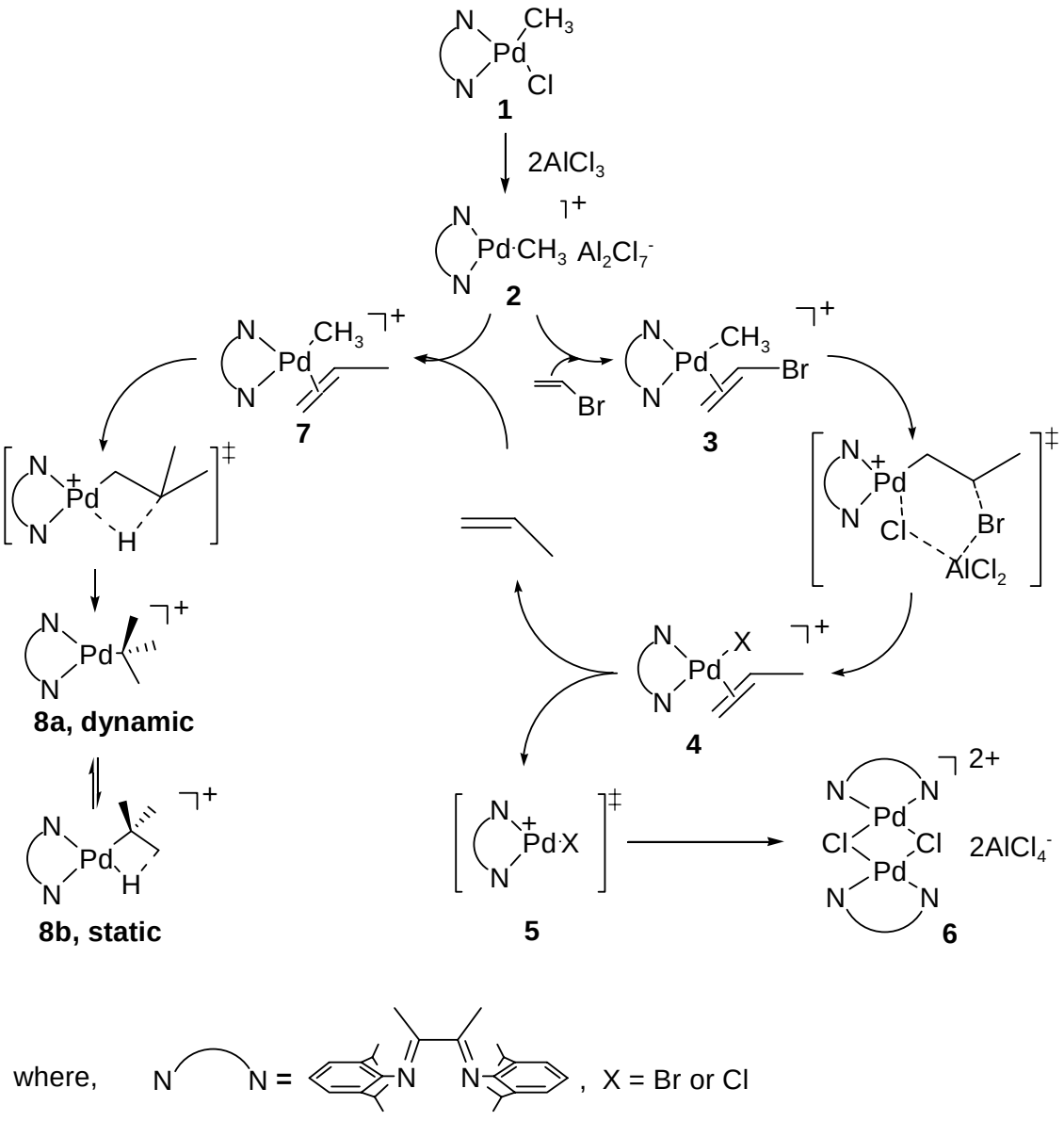

Scheme **2-2**. Proposed Reaction Pathway[6,7]

Figure 2-3

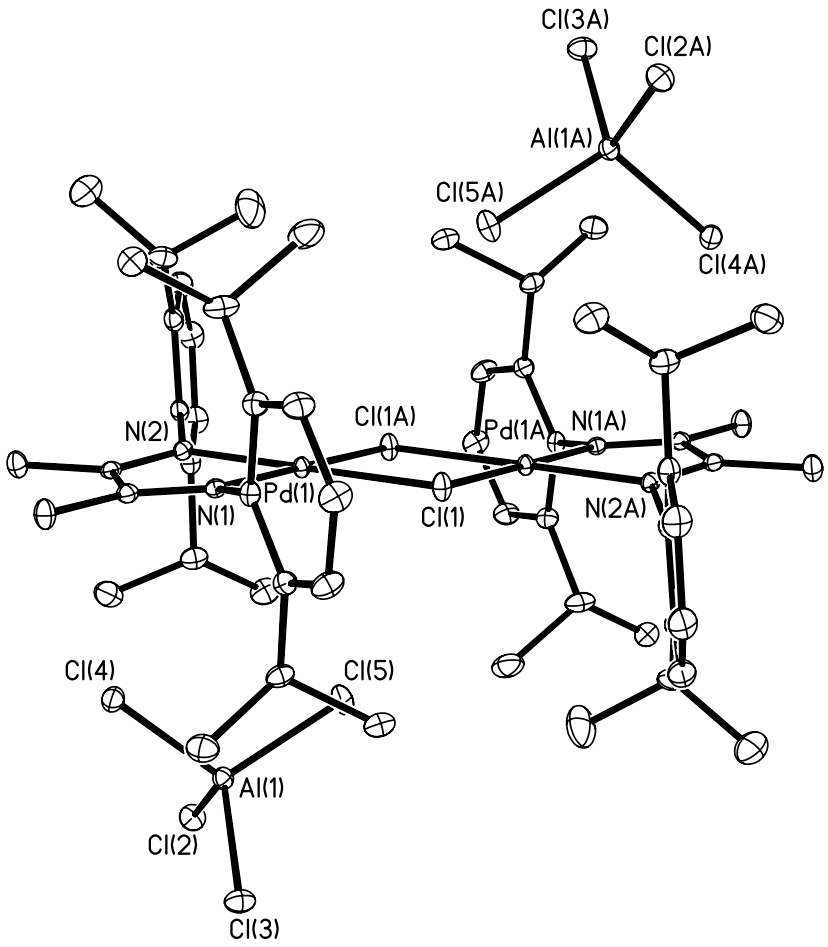

Figure 2-3: ORTEP view of 6. Hydrogen atoms are not shown for clarity

2.2.3 Kinetics of the Reaction of Cationic (α-diimine)Pd-methyl Complex with Alkenes.

The migratory insertion rates of bound vinyl bromide and propene in **3** and **7**, respectively, were directly measured by monitoring the disappearance of the corresponding Pd-CH_3 resonance. For propene our value was in close agreement with that reported by Brookhart.[10] For vinyl bromide, an Arrhenius plot was constructed from rate measurements done between -74 and -37°C. Our values together with those of Brookhart[9,10] are reported in Table **2-1**.

Table **2-1**

Table **2-1**: Kinetic Data for Insertion of Alkenes into Pd(II)-Me bond[a]

	k (x 10^3 s^{-1})	$\Delta H^{\ddagger}$ (kcal/mol)	$\Delta S^{\ddagger}$ (cal/K•mol)
Propene	0.54		
Ethene[10]	1.9	14.2 ± 0.1	-11.2 ± 0.8
Vinyl Bromide	22.0	11.9 ± 0.1	-16.8 ± 0.1
Methyl Acrylate[9]	55.0	12.1 ± 1.4	-14.1 ± 7.0

[a]Measured or extrapolated to 236.5K
** For kinetic data sources, see appendix N*

A Hammett plot[22] of the relative insertion rates of substituted alkenes versus σ_p[19] yielded a straight line with a *positive* ρ (+3.41) (Figure **2-4**). Of note is that the line encompasses values obtained by both Brookhart[9,10] and us.

Figure 2-4

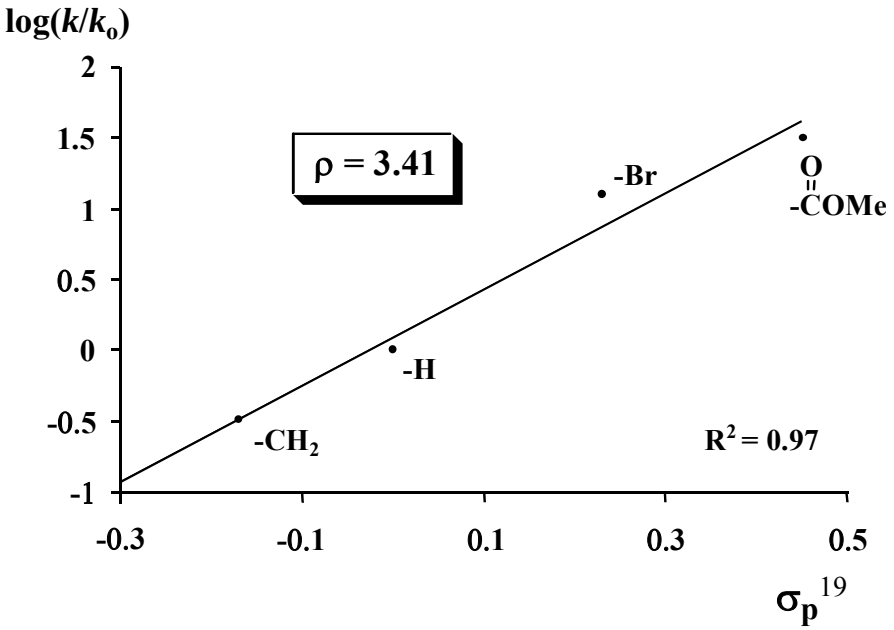

Figure 2-4: Hammet plot for migratory insertion of alkenes into palladium(II)-methyl bond.

2.3 Discussion

2.3.1 Formation of Dimer and Deactivation Pathway.

The identity of the halide ligand in **4** (Scheme **2-2**) has not been established but the formation of **6** opens up the possibility of an aluminum-assisted β-bromo abstraction pathway shown in Scheme **2-2**. The dimer formation is observed only when vinyl halides, such as vinyl bromide or vinylidene chloride, are utilized as monomers. Surprisingly, the β-bromopropyl-Pd(II) complex was not observed. It is likely that the β-bromoalkyl-metal intermediate rapidly reacts with excess aluminum chloride, followed by Cl/Br exchange, to form the dichloro-bridged palladium-diimine complex **6** which crystallizes out of solution due to its low solubility.

Prolonging the reaction time of **1** with 2 *equiv*. of $AlCl_3$ in CD_2Cl_2 also generates **6**, which implies another possible pathway for the formation of the dichloro-bridged dimer, **6**.

2.3.2 Relative Insertion Rates of Alkenes.

We have observed a linear *positive* Hammett correlation between the rate of insertion and the increasing electron-withdrawing effect of the substituent on the alkene. Theoretical calculations have also led to a lower insertion barrier for acrylates and vinyl halides compared to ethene.[11,12] This can be contrasted with a *negative* value of ρ obtained by Bercaw for alkene insertion in Cp^*_2NbH(alkene).[13] Additionally, The second-order rate constants obtained by Wolczanski for alkene insertion into Ta(V)-H

bond follow the trend H ≈ OR >> halide (F, Cl, Br).[5] The decrease in the rate of insertion with increasing electron withdrawing effect of the substituent on the alkene in the case of early transition metal compounds has been attributed to the development of positive charge on the carbon bearing the substituent either during alkene coordination or the subsequent insertion step.[5,13,14] In Wolczanski's case, it has not been possible to separate the effect of the substituent on binding versus insertion, and the trend for the actual insertion step remains an open question. We ascribe the increase in insertion rate for the palladium-methyl complex to a ground-state effect. An alkene with an electron-withdrawing substituent coordinates less strongly to the electrophilic metal (i.e. donation is more important than back-donation).[15] Thus, a weaker metal-alkene bond has to be broken for the insertion to proceed (i.e., the destabilization of the alkene complex leads to a lower insertion barrier).[15] Another surprising observation is that the observed correlation extends to propene. The slower insertion and polymerization rates of propene, when compared to ethene, are usually attributed to the steric bulk of the methyl group of the former.[10,16-18] Our results suggest that, at least for the late transition metal compounds, it is the donating ability of the methyl group, rather than its size, which results in a slower rate for propene insertion and, hence, polymerization. This argument applies even for the sterically encumbered Brookhart-type system. Likewise, for acrylates, the precoordination of the ester group appears to have little effect on its migratory insertion rate.

2.4 Conclusions

What is the implication of our work with respect to the metal-catalyzed polymerization of polar vinyl monomers? First, for the late transition metal compounds, the polar vinyl monomers can clearly outcompete ethene and simple 1-alkenes with respect to insertion. However, the ground-state destabilization of the alkene complex that favors the migratory insertion of the polar vinyl monomers is a two-edged sword because it biases the alkene coordination towards ethene and 1-alkenes. Indeed, we have observed the near quantitative displacement of vinyl bromide by propene to form **7** from **3**. Thus, the extent of incorporation of the polar vinyl monomer in the polymer will depend on the opposing trends in alkene coordination and migratory insertion. The above discussion does not take into account the problem of functional group coordination for acrylates or β-halide abstraction for vinyl halides. With respect to the latter, we are currently exploring approaches to suppress this "termination" step, e.g. decreasing the electrophilicity of the metal center.

2.5 Experimental Section

All work involving air and moisture sensitive compounds was carried out under an inert atmosphere of argon or nitrogen by using standard Schlenk or glove-box techniques. Variable-temperature ^{1}H NMR experiments were performed on a Brüker DPX 300 NMR spectrometer, using CD_2Cl_2 as solvent. Actual NMR probe temperatures were measured using anhydrous methanol (with 0.03% concentrated HCl) or ethylene glycol (neat) in a 5 mm NMR tube (see **2.5.1** and **2.5.2**).

All solvents were deoxygenated, dried via passage over a column of activated alumina, degassed by repeated freeze-pump-thaw cycles, and stored over 4 Å molecular sieves under nitrogen. The α-diimine ligand, 2,6-C_6H_4(*i*-Pr)$_2$-N=C(Me)-C(Me)=N-2,6-C_6H_4(*i*-Pr)$_2$, and complex, (2,6-C_6H_4(*i*-Pr)$_2$-N=C(Me)-C(Me)=N-2,6-C_6H_4(*i*-Pr)$_2$)Pd(Me)(Cl) were prepared as previously reported.[20,21] $AlCl_3$ (Strem) was stored in a nitrogen-filled drybox and used as received. Vinyl bromide (98%) was purchased from Aldrich and used without further purification.

Rates for migratory insertion of alkenes into the Pd(II)-Me bond were determined by adding 20 *equiv*. of alkenes to the pre-generated complex **2** solution in CD_2Cl_2 and monitoring the loss of the Pd(II)-Me resonance over time. The natural logarithm of the methyl integral was plotted versus time (first-order treatment) to obtain kinetic plots. Activation parameters ($\Delta G^{\ddagger}$, $\Delta H^{\ddagger}$,and $\Delta S^{\ddagger}$) were calculated from measured rate constants and temperatures using the Eyring equation.

2.5.1 Low Temperature: methanol (with 0.03% concentrated HCl)[23]

Temperature range: 175~330K (-100 to 55°C)

$T_{meas}[K]=403.0-29.46(\Delta\delta_M)-23.83(\Delta\delta_M)^2$

where $\Delta\delta_M$ is the chemical shift difference (in ppm) between the methyl and hydroxyl peaks.

2.5.2 High Temperature: ethylene glycol (neat)[24]

Temperature range: 310~440K (35 to 165°C)

$T_{meas}[K]=465.8-102.24(\Delta\delta_{EG})$

where $\Delta\delta_{EG}$ is the chemical shift difference (in ppm) between the methylene and hydroxyl peaks.

2.5.3 Interpretation of activation parameters

$\Delta G^{\ddagger}$, the Gibbs free energy of activation, determines at which rate a certain reaction will run at a given temperature

$\Delta H^{\ddagger}$ is a measure for the amount of binding energy that is lost in the transition state relative to the ground state (including solvent effects)

$\Delta S^{\ddagger}$ is a measure for the difference in (dis)order between the transition state and the ground state

2.5.4 The Eyring Equation

$k_{obs} = (\kappa T/h)\exp(-\Delta G^{\ddagger}/RT)$

$= (\kappa T/h)\exp(-\Delta H^{\ddagger}/RT)\exp(\Delta S^{\ddagger}/R)$

where, κ is the Boltzmann Constant, h is Planck's constant, T is the temperature in Kelvin, R is the universal gas constant, and $\Delta G^{\ddagger}$ is the free energy of activation.

$E_a = \Delta H^{\ddagger} + RT$

$\Delta G^{\ddagger} = \Delta H^{\ddagger} - T\Delta S^{\ddagger}$

2.5.5 Application of the Eyring Equation

After transforming the latter expression of the Eyring Equation,

$k_1/T = (\kappa/h)\exp(-\Delta H^{\ddagger}/RT)\exp(\Delta S^{\ddagger}/R)$

$\ln(k_{obs}/T) = -(\Delta H/R)(1/T)+(\Delta S/R)+\ln(\kappa/h)$

one can extract the values for $\Delta H^{\ddagger}$ and $\Delta S^{\ddagger}$ from kinetic data by plotting $\ln(k_{obs}/T)$ versus (1/T). Such a plot should provide a straight line of slope $-\Delta H/R$ and y-intercept $\Delta S/R+\ln(\kappa/h)$. It is necessary to extrapolate the data to 1/T = 0 to obtain the latter value.

2.6 References

1. Boffa, L. S.; Novak, B. M. *Chem. Rev*. **2000**, *100*, 1479-1493.
2. Brintzinger, H. H.; Fischer, D.; Mulhaupt, R.; Rieger, B.; Waymouth, R. M. *Angew. Chem. Int. Ed. Engl*. **1995**, *34*, 1143-1170.
3. Coates, G. W.; Waymouth, R. M. In *Comprehensive Organometallic Chemistry II*, Abel, E. W.; Stone, F. G. A.; Wilkinson, G., Eds.; Elsevier: New York, **1995**; Vol. 12, p. 1193.
4. Stockland, R. A. Jr.; Jordan, R. F. *J. Am. Chem. Soc*. **2000**, *122*, 6315-6316.
5. Strazisar, S. A.; Wolczanski, P. T. *J. Am. Chem. Soc*. **2001**, *123*, 4728-4740.
6. Kang, M.; Sen, A.; Zakharov, L.; Rheingold, A. L. *J. Am. Chem. Soc.,* **2002**, *124*, 12080-12081.
7. Selected ^{1}H NMR data (CD_2Cl_2, 300MHz, δ in ppm) (a) ^{1}H NMR of **A**/**B** (25˚C) 2.88 and 2.74 (septet, 2H each, Ar-C*H*MeMe′) 2.06 and 2.02 (s, 3H each, N=C(CH_3)-C(CH_3′)=N) 1.21, 1.13, 1.08, and 1.00 (d, 6H each, Ar-CHCH_3CH_3′) 0.39 (s, 3H, Pd-CH_3) (b) ^{1}H NMR of **2** (25˚C) 7.42~7.34 (m, 6H, Ar-*H*) 3.04 (septets, 4H, Ar-C*H*MeMe′) 2.22 and 2.17 (s, 3H each, N=C(CH_3)-C(CH_3′)=N) 0.76(s, 3H, Pd-CH_3) (c) ^{1}H NMR of **3** (-70˚C) 5.58 (m, 1H, coordinated CH_2=C*H*Br) 5.0 (m, 2H, coordinated CH_2=CHBr) 2.44 and 2.33 (s, 3H each, N=C(CH_3)-C(CH_3′)=N) 0.65 (s, 3H, Pd-CH_3) (d) ^{1}H NMR of **4** (-50˚C) 5.47 (m, 1H, coordinated CH_2=C*H*CH_3) 4.21 (m, 2H, coordinated CH_2=CHCH_3) 2.00 (m, coordinated CH_2=CHCH_3) (e) ^{1}H NMR of **7** (-40˚C) 4.31 (m, 2H, coordinated CH_2=CHCH_3) CH_2=C*H*CH_3 obscured CH_2=CHCH_3 obscured 0.32 (s, 3H, Pd-CH_3) (f) ^{1}H NMR of **8a**,dynamic (-20˚C) –

0.27 (br s, 9H, Pd(C(CH_3)$_3$), ^{1}H NMR of **8b**, static (-70˚C) 0.00 (br s, 6H, Pd(C(CH$_2$-μ-H)-(CH_3)$_2$)) –8.00 (br s, 1H, Pd(C(CH$_2$-*μ-H*)-(CH$_3$)$_2$)) (g) ^{1}H NMR of **6** (25˚C) 2.33 (s, 12H, N=C(CH_3)-C(CH_3')=N) 1.35 and 1.23 (d, 24H each, J = 6.59 and 6.86 Hz)

8. Shultz, L. H.; Tempel, D. J.; Brookhart, M. *J. Am. Chem. Soc*. **2001**, *123*, 11539-11555.
9. Mecking, S.; Johnson, L. K.; Wang, L.; Brookhart, M. *J. Am. Chem. Soc*. **1998**, *120*, 888-899.
10. Tempel, D. J.; Johnson, L. K.; Huff, R. L.; White, P. S.; Brookhart, M. *J. Am. Chem. Soc*. **2000**, *122*, 6686-6700.
11. Michalak, A.; Ziegler, T. *J. Am. Chem. Soc*. **2001**, *123*, 12266-12278.
12. Phillipp, D. M.; Muller, R. P.; Goddard, W. A.; Storer, J.; McAdon, M.; Mullins, M. *J. Am. Chem. Soc*. **2002**, *124*, 10198-10210.
13. Doherty, N. M.; Bercaw, J. E. *J. Am. Chem. Soc*. **1985**, *107*, 2670-2682.
14. Burger, B. J.; Santarsiero, B. D.; Trimmer, M. S.; Bercaw, J. E. *J. Am. Chem. Soc*. **1988**, *110*, 3134-3146.
15. von Schenck, H.; Strömberg, S.; Zetterberg, K.; Ludwig, M.; Åkermark, B.; Svensson, M *Organometallics*, **2001**, *20*, 2813-2819.
16. Michalak, A.; Ziegler, T. *Organometallics*, **1999**, *18*, 3998-4004.
17. Michalak, A.; Ziegler, T. *Organometallics*, **2000**, *19*, 1850-1858.
18. Michalak, A.; Ziegler, T. *Organometallics*, **2001**, *20*, 1521-1531.
19. Hansch, C.; Leo, A.; Taft, R. W. *Chem. Rev*. **1991**, *91*, 165-195.
20. Rülke, R. E.; Ernsting, J. M.; Spek, A. L.; Elsevier, C. J.; van Leeuwen, P. W. N. M.; Vrieze, K. *Inorg. Chem*. **1993**, *32*, 5769-5778

21. van Asselt, R.; Elsevier, C. J.; Smeets, W. J. J.; Spek, A. L.; Benedix, R. *Recl. Trav. Chim. Pays-Bas* **1994**, *113*, 88-98.

22. Carey, F. A.; Sundberg, R. J. In Advanced Organic Chemistry, Part A: Structure and Mechanisms, 3rd ed, Plenum press: New York and London, **1990**, p. 196-209.

23. Van Geet, A. L. *Anal. Chem.* **1970**, *42*, 679-680.

24. Kaplan, M. L.; Bovey, F. A.; Cheng, H. N. *Anal. Chem*. **1975**, *47*, 1703-1705

Chapter 3

THE REACTION OF PALLADIUM(1,5-CYCLOOCTADIENE)(ALKYL)(CHLORIDE) WITH NORBORNENE DERIVATIVES: RELEVANCE TO METAL-CATALYZED ADDITION POLYMERIZATION OF FUNCTIONALIZED NORBORNENE

3.1 Introduction

Metal-catalyzed addition polymerization of functionalized alkenes is an area of great current interest in synthetic polymer chemistry because the addition of functionalities to a polymer which is otherwise non-polar can greatly enhance the range of attainable properties.[1,2] One particular area of interest has been the addition polymerization of functionalized norbornene derivatives.[3,4] The resultant polymers exhibit superior etch resistance and thermal stability and are attractive candidates for deep UV photolithography.[5] A key problem in the development of metal-catalyzed routes to functionalized polyalkenes is the coordination of the functionality present both in the monomer and in the resulting polymer. Because they are synthesized by Diels-Alder reaction, functionalized norbornene derivatives sold commercially consist of *exo* and *endo* isomers with the latter predominating (approx. molar ratio: 1:3-1:4).[6] Earlier work in other labs,[7-10] as well as our own,[11,12] have shown that the *endo*-functionalized norbornenes are polymerized more slowly. The slow polymerization rate for commercial functionalized norbornene mixtures has previously been ascribed to the formation of a chelate by coordination of the functionality to the metal center and the C=C bond along the *endo* face (Figure **3-1**).[7-12] This has two detrimental effects on polymerization. First,

chelation strengthens metal-alkene interaction, thereby raising the barrier for the insertion step. Second, it forces insertion through the *endo* face, in sharp contrast to the known propensity for norbornene to insert into metal-carbon bonds through the less hindered *exo* face.[13-15] Indeed, we had earlier isolated and characterized a platinum complex formed by the insertion of *endo*-5-ethylester-2-norbornene into a Pt-H bond through the *endo* face.[12]

Figure **3-1**

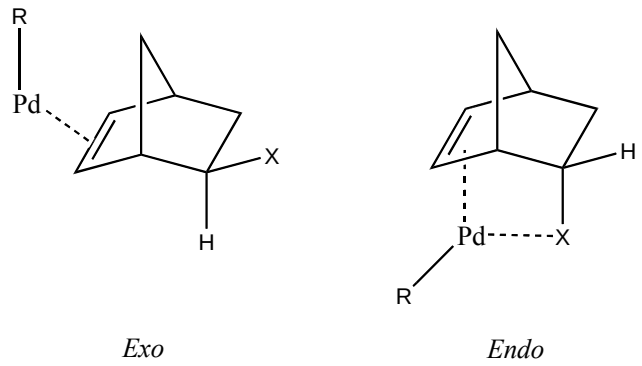

Figure **3-1**: Modes of bonding for functionalized norbornene derivatives (X = coordinating functionality).

The catalyst systems for which the relative *exo* versus *endo* reactivity have been reported are cationic. Theoretical calculations by Ziegler show that while the interaction of an oxygen functionality (e.g., ester group) with the metal center is weaker in neutral complexes when compared with the corresponding cationic species, the bonding of the vinyl functionality is not significantly affected because the weaker alkene to metal charge transfer in the neutral complex is compensated by stronger metal to alkene back-bonding.[16] We have conducted studies encompassing the insertion of norbornene

derivatives into palladium-carbon bonds in a neutral palladium compound, Pd(1,5-cyclooctadiene)(alkyl)(chloride). As described below, we have now succeeded in the first isolation of norbornene and functionalized-norbornene-inserted compounds, as well as the characterization using X-ray crystal structure analysis. The system showed "living"-type polymerization through coordination insertion mechanism.

3.2 Results and Discussion

3.2.1 Reactions of Pd(1,5-cyclooctadiene)(CH_3)(Cl) with Norbornene Derivatives

The result of the NMR scale reaction between (1,5-COD)Pd(CH_3)(Cl) (COD = 1,5-cyclooctadiene) and norbornene, indicating the formation of a norbornene-inserted complex and, consequently, norbornene oligomer, directed us to conduct isolation and characterization process of a desired norbornene-derivative-inserted complex. Four complexes, from norbornene, *endo*- and *exo*-5-ester norbornenes, and *endo*-5-methylacetate norbornene, have been synthesized under similar reaction conditions(Scheme **3-1**). All of the compounds have been isolated as a solid by triturating in diethyl ether or diethyl ether/pentane mixture at ambient temperature under the inert atmosphere or at -15^{o}C. For the compound **1a**, the apical protons of the norbornene moiety show resonances at 2.1 and 1.04 ppm with a geminal coupling constant of 9.8 Hz. A pair of doublet and multiplet at 1.83 and 1.76 ppm, respectively, are assigned to the two-carbon bridge protons, Pd-C*H*-C*H*-CH_3, of the norbornene framework. A coupling of 5.6 Hz was measured between the two protons. Since the vicinal coupling constant of 6 to

7 Hz is a typical value between the *endo* protons of the norbornene framework, *syn* addition across the *exo* face of the norbornene is deduced.

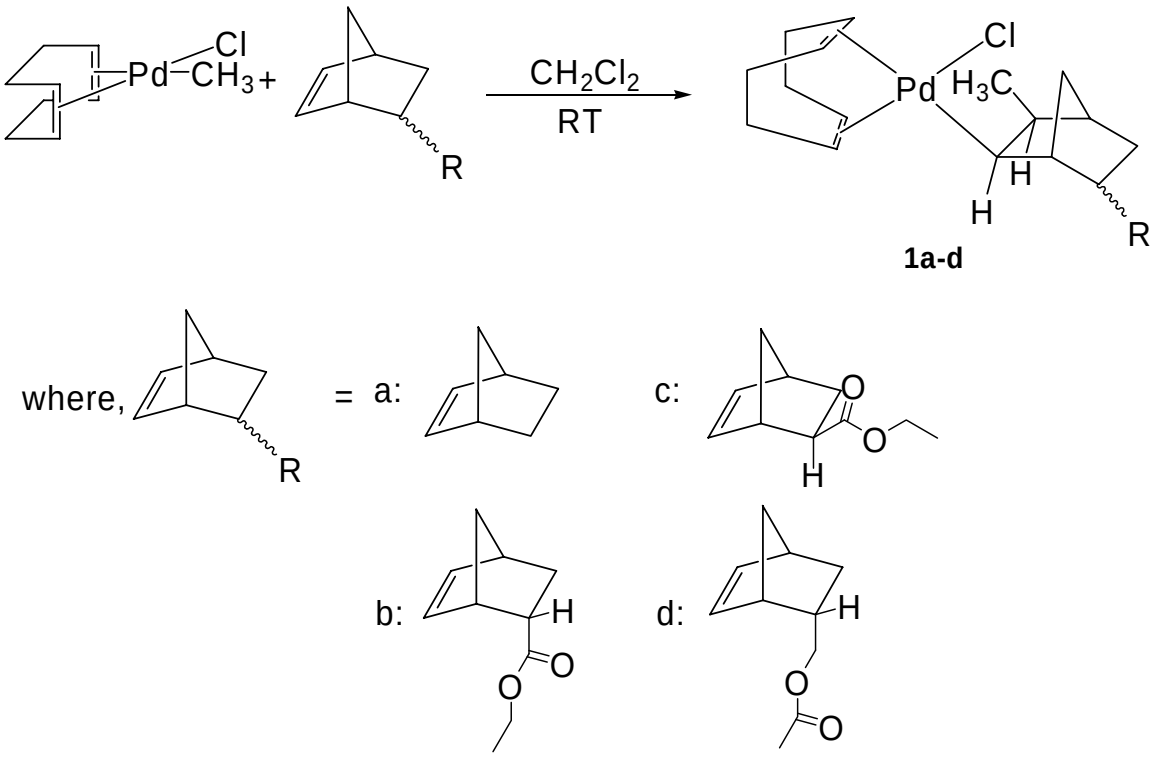

Scheme **3-1**

The products **1a-d** of the reaction of (1,5-COD)Pd(CH_3)(Cl) with norbornene (NB), *endo* and *exo*-5-ethylester-2-norbornene (EtEster-NB, NB-$COOCH_2CH_3$), and *endo*-5-methylacetate-2-norbornene (MeOAc-NB, NB-$CH_2OC(O)CH_3$) were isolated and their structures were determined by X-ray single-crystal structure analysis. X-ray quality crystals were prepared by slow diffusion of pentane into a concentrated solution of **1a, 1c** or **1d** in methylene chloride or by slow evaporation of solvent from a solution of **1b** in methylene chloride at ambient temperature. The ORTEP plots of **1a-d** are shown in

Figures **3-2**, **3-3**, **3-4**, and **3-5**. (For crystallographic data, see Table **3-5**). The selected bond lengths and angles for **1a-d** are given in Tables **3-1**, **3-2**, **3-3**, and **3-4**. In the solid state they adopt geometries best described as square planar about each palladium center having slight distortions from idealized geometry. In each case, the insertion of the monomer into the palladium-carbon bond had invariably occurred through the *exo* face with no evidence for interaction of the ester functionality with the metal (e.g., Figure **3-3**). In sharp contrast to the cationic systems, the coordination of alkene is favored over an ester functionality. Interestingly, in the crystals formed from the latter three monomers, the two possible regioisomers with the metal and the ester group in 1,3 and 1,4 relationships, were both present suggesting that the ester functionality exerted minimal steric and electronic effect in the insertion.

Figure 3-2

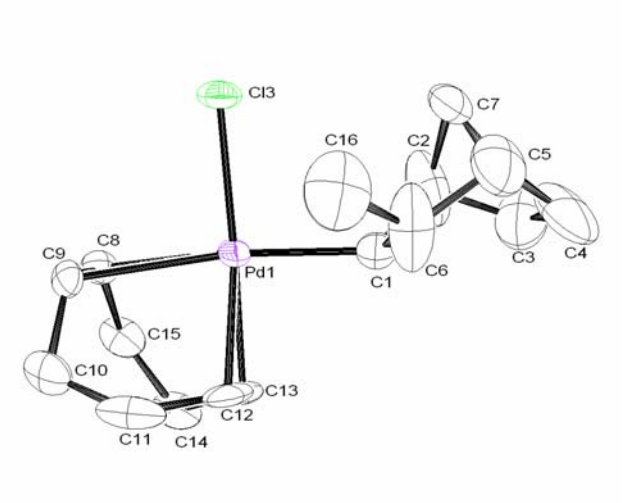

Figure 3-2: An ORTEP view of 1a, showing 50% probability thermal ellipsoids. Hydrogen atoms are omitted for clarity.

Figure 3-3

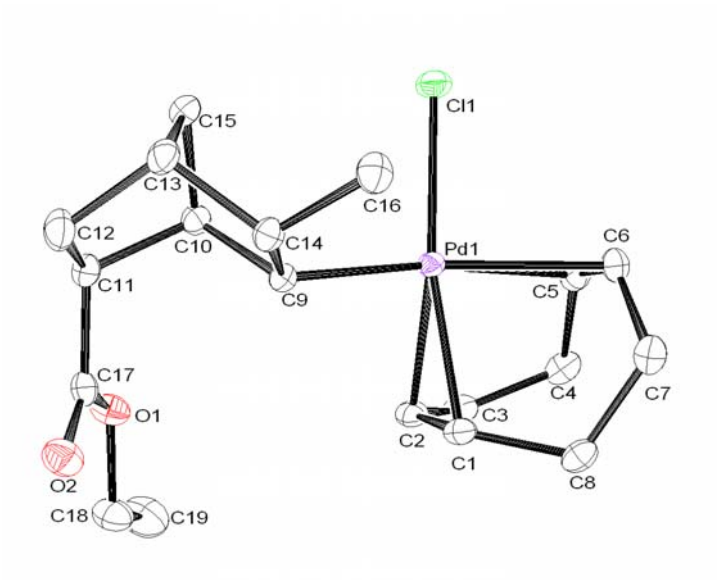

Figure 3-3: An ORTEP view of 1b, showing 50% probability thermal ellipsoids. Hydrogen atoms are omitted for clarity.

Figure 3-4

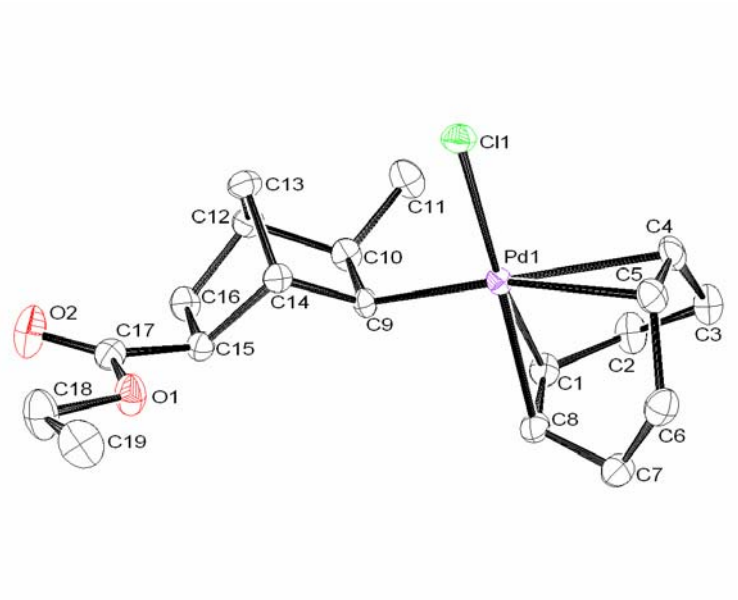

Figure 3-4: An ORTEP view of 1c, showing 50% probability thermal ellipsoids. Hydrogen atoms are omitted for clarity.

Figure 3-5

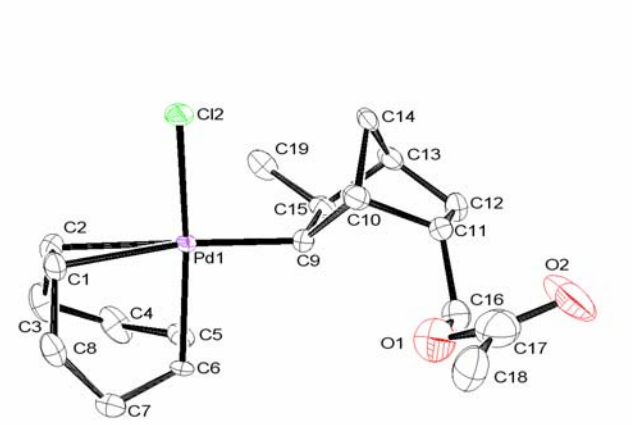

Figure 3-5: An ORTEP view of 1d, showing 50% probability thermal ellipsoids. Hydrogen atoms are omitted for clarity.

Table 3-1

Table 3-1: Selected Bond distances (Å) and Angles (°) for **1a**

Pd1-C1	2.074(10)	Pd1-C12	2.160(9)
Pd1-C13	2.188(7)	Pd1-Cl3	2.335(2)
Pd1-C8	2.364(8)	Pd1-C9	2.434(7)
C1-Pd1-C12	89.2(4)	Cl3-Pd1-C8	90.0(2)
C1-Pd1-C13	90.9(3)	C1-Pd1-C9	164.2(4)
C1-Pd1-Cl3	94.5(3)	C12-Pd1-C9	78.5(3)
C12-Pd1-Cl3	159.6(3)	C13-Pd1-C9	85.3(3)
C13-Pd1-Cl3	162.1(3)	Cl3-Pd1-C9	93.8(2)
C1-Pd1-C8	161.2(4)	C6-C1-Pd1	116.6(8)
C12-Pd1-C8	93.0(3)	C2-C1-Pd1	114.9(9)
C13-Pd1-C8	79.8(3)	C16-C6-C5	117.0(14)

Table 3-2

Table 3-2: Selected Bond distances (Å) and Angles (°) for **1b**

Pd1-C9	2.0717(19)	Pd1-C2	2.161(2)
Pd1-C1	2.184(2)	Pd1-Cl1	2.3486(7)
Pd1-C6	2.367(2)	Pd1-C5	2.442(2)
Cl1-Pd1-C6	89.02(5)	Cl1-Pd1-C5	88.90(5)
C1-Pd1-Cl1	168.74(6)	C2-Pd1-Cl1	150.43(6)
C9-Pd1-Cl1	98.05(6)	C14-C9-Pd1	115.90(12)
C9-Pd1-C5	167.03(8)	C9-Pd1-C6	157.28(8)
C16-C14-C9	116.75(16)	C16-C14-C13	113.28(17)
C9-Pd1-C1	89.17(8)	C9-Pd1-C2	89.69(8)
C17-C11-C10	114.06(16)	C17-C11-C12	113.80(18)

Table 3-3

Table 3-3: Selected Bond distances (Å) and Angles (°) for **1c**

Pd1-C9	2.064(2)	Pd1-C1	2.166(2)
Pd1-C8	2.187(3)	Pd1-Cl1	2.3426(7)
Pd1-C5	2.390(2)	Pd1-C4	2.436(2)
C9-Pd1-C1	87.34(9)	C9-Pd1-C8	90.36(10)
Cl1-Pd1-C4	94.81(7)	Cl1-Pd1-C5	89.75(7)
C1-Pd1-Cl1	162.53(7)	C8-Pd1-Cl1	159.78(7)
C9-Pd1-C4	162.20(9)	C9-Pd1-C5	162.30(9)
C9-Pd1-Cl1	94.67(7)	C10-C9-Pd1	115.67(15)
C11-C10-C9	116.6(2)	C11-C10-C12	111.8(2)
C17-C15-C16	114.7(2)	C17-C15-C14	112.3(2)

Table 3-4

Table 3-4: Selected Bond distances (Å) and Angles (°) for **1d**

Pd1-C9	2.078(6)	Pd1-Cl2	2.3403(17)
Pd1-C5	2.154(6)	Pd1-C1	2.391(7)
Pd1-C6	2.181(6)	Pd1-C2	2.406(7)
C9-Pd1-C5	88.7(3)	Cl2-Pd1-C1	88.87(18)
C9-Pd1-C6	92.9(3)	C9-Pd1-C2	160.7(3)
C9-Pd1-Cl2	94.58(19)	C5-Pd1-C2	78.8(3)
C5-Pd1-Cl2	161.7(2)	C6-Pd1-C2	86.0(3)
C6-Pd1-Cl2	159.9(2)	Cl2-Pd1-C2	92.95(19)
C9-Pd1-C1	165.0(3)	C10-C9-Pd1	117.5(5)
C5-Pd1-C1	92.5(3)	C15-C9-Pd1	113.8(4)
C6-Pd1-C1	79.4(3)	C19-C15-C13	113.0(6)

Table 3-5

Table 3-5: Crystallographic Data and data Collection Parameters for complexes **1a-d**

	1a	**1b**	**1c**	**1d**
formular	$C_{16}H_{25}ClPd$	$C_{38}H_{58}Cl_2O_4Pd_2$	$C_{19}H_{29}ClO_2Pd$	$C_{19}H_{29}ClO_2$ Pd
M_w	359.21	862.54	431.27	431.27
T(K)	95(2)	95(2)	96(2)	293(2)
λ(Å)	0.71073	0.71073	0.71073	0.71073
crystal structure	Monoclinic	triclinic	triclinic	Monoclinic
space group	*P*2(1)/*n*	*P*$\bar{1}$	*P*2(1)/*c*	*P*2(1)/*n*
a(Å)	10.899(5)	8.0473(17)	11.2420(18)	6.8659(17)
b(Å)	12.530(5)	10.216(2)	13.031(3)	23.248(6)
c(Å)	11.467(5)	12.347(3)	12.463(2)	11.502(3)
α(deg)	90°	105.751(3)	90	90
β(deg)	108.150(13)°	90.578(4)	92.048(4)	96.614(4)
γ(deg)	90	109.872(4)	90	90
V(Å^3)	1488.1(10)	912.9(3)	1825.5(5)	1823.7(8)
Z	4	2	4	4
F(000)	736	444	888	888
R(*F*)	0.0763	0.0250	0.0308	0.0685
$R_w(F)$	0.1818	0.0685	0.0765	0.1755
ρ_{calcd} (Mg/m^3)	1.603	1.569	1.569	1.571

3.2.2 Investigation of Reaction Mechanism

The neutral palladium(II) compound, Pd(1,5-cyclooctadiene)(methyl)(chloride)[17] was found to be effective for the oligomerization of norbornene. A linear increase in molecular weight was observed with time, with M_w reaching 1,600 (*versus* polystyrene standard) in approximately 60 min at ambient temperature (Figure **3-6**). The behavior suggests that the oligomerization is "living". The relatively slow reaction rate gave us the opportunity to examine the mechanism of norbornene insertion into the palladium-carbon bond in some detail.

Figure **3-6**

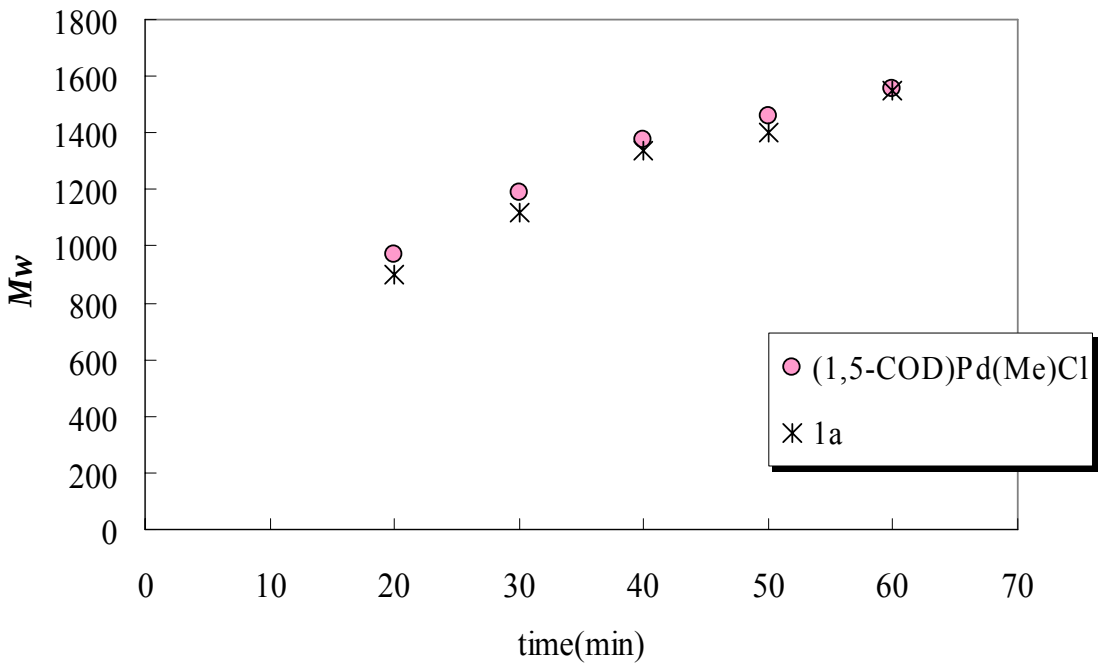

Figure **3-6**: Molecular weight of norbornene oligomer *versus* time – "Living" system

** For data sources, see Appendix O*

The oligomerization of norbornene by the insertion product **1a** derived from Pd(1,5-cyclooctadiene)(methyl)(chloride) and NB was also examined. A linear increase in molecular weight with a slope similar to that seen starting with Pd(1,5-cyclooctadiene)(methyl)(chloride) was observed (Figure **3-6**), strongly suggesting that the initial insertion product **1a** was an intermediate in norbornene oligomerization by Pd(1,5-cyclooctadiene)(methyl)(chloride).

Figure **3-7**

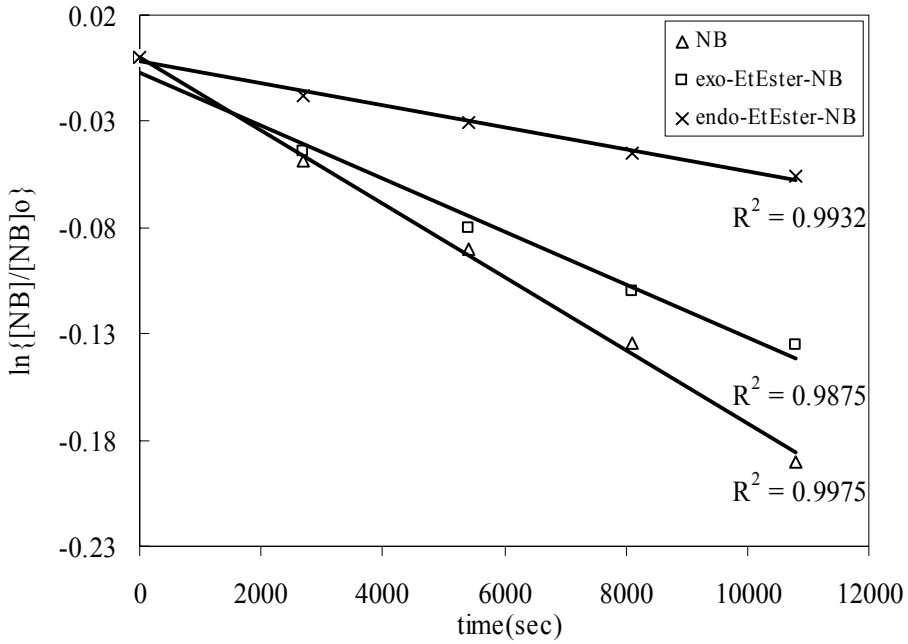

Figure **3-7**: Plot of $\ln\{[NB]/[NB]_o\}$ versus time. Reaction conditions: **1** (3.7×10^{-5} mol), norbornenes (7.5×10^{-4} mol), CD_2Cl_2 (1 mL), 23°C.

** For kinetic data sources, see Appendix O*

The kinetics of the reaction of Pd(1,5-cyclooctadiene)(methyl)(chloride) with NB, *exo*- and *endo*-EtEster-NB was investigated by ^{1}H NMR spectroscopy. In each case, the reaction was first-order in the monomer (Figure **3-7**) with rate constants of 2×10^{-5} s^{-1},

$1x10^{-5}$ s^{-1}, and $5x10^{-6}$ s^{-1}, respectively. This system is the first which exhibits similar insertion rates for norbornene and its *exo*- and *endo*-5-ester derivatives, thereby supporting Ziegler's calculations[16] and the notion that catalytic polymerization of functionalized monomers will be made more facile by moving from a cationic to a less electrophilic, neutral, metal center. The simplest mechanism that accounts for this observation involves alkene coordination to the fifth-coordination site of the metal, followed by insertion into the *cis* metal-carbon bond. The effect of potential coordinating moieties: C=C, chloride, and ester group, on the rate of norbornene polymerization (= rate of insertion) was probed by the addition of 1,5-cyclooctadiene, $NR_4^+Cl^-$, and ethyl acetate. As shown in Table **3-6**, the extent of inhibition clearly decreases in the order C=C > Cl- > RC(=O)OR with the ester group having minimal effect on the polymerization. This observation is in stark contrast to the cationic norbornene polymerization systems whose activities are sharply attenuated by the presence of a coordinating solvent such as ethyl acetate.[11,12] One interesting aspect of the above chemistry is that the insertion of a C=C bond of 1,5-cyclooctadiene is never observed. The reason for this is unclear although the norbornene C=C bond is expected to be more reactive due to greater ring strain.

Table 3-6

Table 3-6: Effect of Additives on the Polymerization of Norbornene using (1,5-COD)PdMeCl

(1,5-COD)PdMeCl ($x10^{-4}$ mol)	Additive (*equiv.*)	Norbornene (*equiv.*)	Yield[a] (%)
1.13	None	200	85
1.13	1,5-COD[b] (20)	200	n.r.
1.13	1,5-COD[b] (200)	200	n.r.
1.13	$(Butyl)_4NCl$ (20)	200	14
1.13	$MeCO_2Et$ (20)	200	67
1.13	$MeCO_2Et$ (200)	200	58

[a]Isolated solid polymer. Reaction conditions: 60°C, 2 h, PhCl (7 g). [b]1,5-cylclooctadiene

Taken together, the twin observations that (a) ethyl acetate does not inhibit norbornene polymerization and (b) norbornene derivatives with pendant *endo* ester functionalities insert into the metal-alkyl bond through the *exo* face with rates similar to that seen with norbornene, clearly demonstrate that there is no coordination of the ester group and suggests that the key to the efficient polymerization and copolymerization of functionalized norbornene derivatives lies in the use of less electrophilic, neutral metal species.

3.3 Conclusion

We have explored the reactivity of the complex, Pd(1,5-cyclooctadiene)(alkyl)(chloride), encompassing the insertion of norbornene and norbornene derivatives into palladium-carbon bonds in a neutral palladium compound. Norbornene and norbornene derivatives, such as *endo*- and *exo*-5-ester norbornenes, and *endo*-5-methylacetate norbornene, insert into metal-alkyl bond through the *exo* face. Insertion rate of the substituted norbornenes is similar to that seen with unsubstituted norbornene. Norbornene- and substituted-norbornene-inserted complexes are isolated and characterized using NMR spectroscopy as well as X-ray single-crystal structure analysis. Unlike cationic systems, no coordination of the ester group is observed. The plot of molecular weight of norbornene oligomer *versus* time indicates that the polymerization system is "living". The results that ethyl acetate does not inhibit norbornene polymerization and that there is no coordination of the ester group suggest that the use of less electrophilic, neutral metal species is the key to the efficient polymerization and copolymerization of functionalized norbornene derivatives.

3.4 Experimental Section

3.4.1 Generation Considerations.

All work involving air and moisture sensitive compounds was carried out under an inert atmosphere of argon or nitrogen by using standard Schlenk or glove-box techniques.

Nuclear magnetic resonance (NMR) spectra were recorded on a Bruker DRX 400 NMR spectrometer and DPX 300 NMR spectrometer. Variable-temperature ^{1}H NMR experiments were performed on a Bruker DPX 300 NMR spectrometer, using CD_2Cl_2, toluene-d_8, or chlorobenzene-d_5 as solvent. Actual NMR probe temperatures were measured using anhydrous methanol (with 0.03% concentrated HCl) or ethylene glycol (neat) in a 5 mm NMR tube (see **2.5.1** and **2.5.2**). NMR analyses of polymers were performed on a Brüker DPX 300 NMR spectrometer at ambient or elevated temperature, using $CDCl_3$ or chlorobenzene-d_5 as solvent unless otherwise noted.

Size exclusion chromatography data were obtained on a Shimadzu SEC System using a three-column bank (Styragel 7.8x300 mm columns, 100-5,000 D, 500-30,000 D, 2000-4,000,000 D), a Shimadzu RID-10A Differential Refractometer, and a Shimadzu LC-10AT pump/controller. Size exclusion chromatography was performed in chloroform at ambient temperature and calibrated to polystyrene standards.

Chlorobenzene and dichloromethane was obtained from Aldrich and dried over CaH_2 and freeze-thaw degassed three times prior to use. Norbornene was purchased from Acros Organics and used without further purification. Toluene, pentane, and diethyl ether were deoxygenated, dried via passage over a column of activated alumina, degassed by

repeated freeze-pump-thaw cycles, and stored over 4 Å molecular sieves under nitrogen. Palladium(1,5-cyclooctadiene)(methyl)(chloride), was prepared as previously reported[17]. *Endo*-Ethylester-norbornene, *exo*-ethylester-norbornene, and *endo*-methylacetate-norbornene were supplied by Jeffrey Funk.

3.4.2 Synthesis of Complexes

(1,5-COD)Pd(Cl)(2-Me-norbornanyl) (1a). To Pd(1,5-cyclooctadiene)(alkyl)(chloride) (100 mg, 0.38 mmol) in methylene dichloride (5 ml) was added norbornene (36 mg, 0.38 mmol) drop-wise at room temperature. The solution was stirred for 2 h at room temperature. After filtration to remove metallic palladium, removal of solvent in vacuo yielded an oily solid, which is triturated in ether. Upon filtering and washing with diethyl ether followed by pentane, the compound **1a** was obtained as an off-white solid. Recrystallization from methylene dichloride/pentane gave a clear crystalline solid which was suitable for X-ray crystal structure analysis. Yield 0.12 g, 89%. ^{1}H NMR(CD_2Cl_2): δ 5.83 (m, 2H, -C*H*=C*H*-), 5.01 (m, 2H, -C*H*´=C*H*´-), 2.85 (s, 1H, bridgeheat -C*H*), 2.73-2.38 (m, 8H, two =CH-CH_2-CH_2-CH=), 2.1 (br, 1H, *anti* apical -CH*H* and 1H, bridgehead -C*H*), 1.83 (d, 1H, Pd-C*H*-), 1.76 (m, 1H, CH_3-C*H*-), 1.51 (m, 1H, *exo*-CH*H*-), 1.46 (d, 3H, CH_3-), 1.29 (m, 1H, *exo*-CH*H*-), 1.04 (d, *syn* apical –C*H*H-), 1.13-0.99 (m, 2H, two *endo*-C*H*H-). ^{13}C NMR(CD_2Cl_2): 125.9 (=CH-*C*H_2-*C*H_2-CH=), 102.2 (=CH-*C*´H_2-*C*´H_2-CH=), 64.1 (bridge *C*H), 49.6 (CH_3-*C*H-), 45.7 (Pd-*C*H-), 44.9 (bridgehead *C*H), 35.6 (apical *C*H_2), 31.7 (*C*H_2), 31.6, 31.2 (-*C*H=*C*H-), 29.1 (*C*´H_2), 27.8, 27.5 (-*C*´H=*C*´H-) 22.2 (*C*H_3-)

(1,5-COD)Pd(Cl)(2-Me-*endo*-5-ethylester-norbornanyl) (1b). To Pd(1,5-cyclooctadiene)(alkyl)(chloride) (100 mg, 0.38 mmol) in methylene dichloride (5 ml) was added *endo*-5-ethylesternorbornene (63 mg, 0.38 mmol) drop-wise at room temperature. The solution was stirred for 2 h at room temperature. After filtration to remove metallic palladium, removal of solvent in vacuo yielded a yellow oil, which is solidified from ether/pentane mixture in freezer. Upon filtering and washing with pentane, the compound **1b** was obtained as an yellow solid. Recrystallization from methylene dichloride by slow evaporation gave a yellow crystalline solid which was suitable for X-ray crystal structure analysis. Yield 0.12 g, 74%. ^{1}H NMR(CD_2Cl_2): δ 5.87(m, 2H, -C*H*=C*H*-), 5.01 (m, 2H, -C*H*˝=C*H*´-), 4.12 (m, 2H, -O-CH_2-CH_3), 2.72-2.43 (m, 12H, two =CH-CH_2-CH_2-CH=, two bridgehead C*H*, and –C*H*-C(=O)O-), 1.86 (d, 1H, Pd-C*H*-), 1.75 (m, 1H, CH_3-C*H*-), 1.73 (m, 1H, *exo*-CH*H*-), 1.45 (m, 2H, two *endo*-C*H*H-), 1.44 (d, 3H, CH_3-), 1.31 (t, 3H, -O-CH_2-CH_3), 1.20 (m, 2H, *syn* and *anti* apical -C*H*H´- and -CH*H*´-). ^{13}C NMR(CD_2Cl_2): 125.8 (=CH-*C*H_2-*C*H_2-CH=), 60.4 (-O-*C*H_2-CH_3), 49.1 (CH_3-*C*H-), 47.4 (*C*H), 45.9 (Pd-*C*H-), 37.3 (apical *C*H_2), 32.0 (CH_2), 31.5, 31.4 (-*C*H=*C*H-), 27.8, 27.7 (-*C*´H=*C*´H-) 22.7 (*C*H_3-), 14.7 (-O-CH_2-*C*H_3).

(1,5-COD)Pd(Cl)(2-Me-*exo*-5-ethylester-norbornanyl) (1c). To Pd(1,5-cyclooctadiene)(alkyl)(chloride) (100 mg, 0.38 mmol) in methylene dichloride (5 ml) was added *exo*-5-ethylesternorbornene (63 mg, 0.38 mmol) drop-wise at room temperature. The solution was stirred for 2 h at room temperature. After filtration to remove metallic palladium, removal of solvent in vacuo yielded a yellow oil, which is triturated in ether. Upon filtering and washing with ether followed by pentane, the compound **1c** was

obtained as an off-white solid. Recrystallization from methylene dichloride/pentane gave a clear crystalline solid which was suitable for X-ray crystal structure analysis. Yield 0.14 g, 86%.

(1,5-COD)Pd(Cl)(2-Me-*endo*-5-methylacetate-norbornanyl) (1d). To Pd(1,5-cyclooctadiene)(alkyl)(chloride) (100 mg, 0.38 mmol) in methylene dichloride (5 ml) was added *endo*-5-methylacetatenorbornene (63 mg, 0.38 mmol) drop-wise at room temperature. The solution was stirred for 2 h at room temperature. After filtration to remove metallic palladium, removal of solvent in vacuo yielded a yellow oil, which is solidified from ether/pentane mixture in freezer. Upon filtering and washing with pentane, the compound **1d** was obtained as a yellow solid. Recrystallization from methylene dichloride/pentane gave a clear crystalline solid which was suitable for X-ray crystal structure analysis. Yield 0.13 g, 80%. ^{1}H NMR(CD_2Cl_2): δ 5.83(m, 2H, -C*H*=C*H*-), 5.08 (m, 2H, -C*H*´=C*H*´-), 3.96 (m, 2H, -O-CH_2-CH), 2.75-2.42 (m, 8H, two =CH-CH_2-CH_2-CH=), 2.18 (d, 1H, *anti* apical -C*H*H´-), 2.04 (s, 3H, CH_3-C(=O)-O-), 1.92 (d, 1H, Pd-C*H*-), 1.80 (m, 1H, CH_3-C*H*-), 1.61 (m, 1H, *exo*-CH*H*-), 1.46 (d, 3H, CH_3-), 1.18 (d, 2H, *syn* apical -CH*H*´-), 0.58 (m, 1H, *endo*-C*H*H-). ^{13}C NMR(CD_2Cl_2): 125.8 (=CH-*C*H_2-*C*H_2-CH=), 101.0 (=CH-*C*´H_2-*C*´H_2-CH=), 66.0 (-*C*H_2-O-C(=O)-CH_3), 50.0 (CH_3-*C*H-), 47.5 (*C*H), 45.8 (CH_3-*C*H-), 41.0 (Pd-*C*H-), 37.3 (apical *C*H_2), 33.1 (CH_2), 31.5, 31.3 (-*C*H=*C*H-), 27.8, 27.7 (-*C*´H=*C*´H-) 22.7 (*C*H_3-), 21.1 ((-CH_2-O-C(=O)-*C*H_3).

3.4.3 General Procedure for NMR Experiments

In a drybox under a nitrogen atmosphere, **1** (10 mg) was weighed into an NMR tube. CD_2Cl_2 (0.1 mL) was added to the NMR tube. The tube was then capped with a septum, removed from the drybox, and cooled to ca. -90^{o}C using liquid nitrogen/acetone slurry. 10 wt. % norbornene or functionalized norbornene in CD2Cl2 solution(1 mL) was then added to the NMR tube via a gas-tight syringe at that temperature, and the septum was wrapped with Parafilm. The tube was shaken very briefly, and transferred to the NMR probe. For conversion kinetics of norbornene derivatives, NMR spectra were acquired every 15 min at a desired temperature. TMS was employed as an external standard.

3.4.4 General Procedures for Polymerization Reactions

In a 100 mL Schlenk flask, 0.11 mmol of **1** was dissolved in 7 g of chlorobenzene. 22 mmol of norbornene or norbornene derivatives was introduced to the flask. The reaction mixture was stirred at a desired temperature. After the specified reaction time, the reaction was quenched with methanol. The precipitated polymer was filtered and washed with methanol. Volatiles were removed from the polymer in vacuo, and the polymer was dried under vacuum overnight.

To measure the molecular weight of poly(norbornene) versus time, 5 g of norbornene and 40 mL of chlorobenzene were used instead of the amounts listed above. 5 mL of reaction mixture was taken from the flask every 10 min, and quenched with methanol. Each sample was worked up as above.

3.5 References

1. Boffa, L. S.; Novak, B. M. *Chem. Rev*. **2000**, *100*, 1479-1493.
2. Gibson, V. C.; Spitzmesser, S. K. *Chem. Rev*. **2003**, *103*, 283-315.
3. Janiak, C.; Lassahn, P. G. *J. Mol. Catal. A. Chem*. **2001**, *166*, 193-209.
4. Janiak, C.; Lassahn, P. G. *Macromol. Rapid Commun*. **2001**, *22*, 479-492.
5. Reichmanis, E.; Nalamasu, O.; Houlihan, F. M. *Acc. Chem. Res*. **1999**, *32*, 659-667.
6. Martin, J. G.; Hill, R. K. *Chem. Rev*. **1961**, *61*, 537-562.
7. Mathew, J. P.; Reinmuth, A.; Risse, W.; Melia, J.; Swords, N. *Macromolecules* **1996**, *29*, 2755-2763.
8. Breunig, S.; Risse, W. *Makromol. Chem*. **1992**, *193*, 2915-2927.
9. Melia, J.; Connor, E.; Rush, S.; Breunig, S.; Mehler, C.; Risse, W. *Macrol. Symp*. **1995**, *89*, 433-442.
10. Heinz, B. S.; Alt, F. P.; Heitz, W. *Macromol. Rapid. Commun*. **1998**, *19*, 251-256.
11. Funk, J. K.; Andes, C. E.; Sen, A. *Organometallics* **2004**, *23*, 1680-1683.
12. Hennis, A. D.; Polley, J. D.; Long, G. S.; Sen, A.; Yandulov, D.; Lipian, J.; Benedikt, G. M.; Rhodes, L. F.; Huffman, J. *Organometallics* **2001**, *20*, 2802-2812.
13. Sen, A. *Acc. Chem. Res*. **1993**, *26*, 303-310.
14. Markies, B. A.; Kruis, D.; Rietveld, M. H. P.; Verkerk, K. A. N.; Boersma, J.; Kooijman, H.; Lakin, M. T.; Speck, A. L.; van Koten, G. *J. Am. Chem. Soc*. **1995**, *117*, 5263-5274.
15. Delis, J. G. P.; Aubel, P. B.; Vrieze, D.; van Leeuwen, P. W. N. M.; Veldman, N.; Spek, A. L. *Organometallics* **1997**, *16*, 4150-4160.

16. Michalak, A.; Ziegler, T. *Organometallics* **2001**, *20*, 1521-1532.

17. Rulke, R. E.; Ernsting, J. M.; Spek, A. L.; Elsevier, C. J.; van Leeuwen, P. W. N. M.; Vrieze, K. *Inorg. Chem*. **1993**, *32*, 5769-5778.

Chapter 4

NEUTRAL PALLADIUM(II) COMPLEXES WITH N-O CHELATE: SYNTHESES, CHARACTERIZATION, AND THEIR REACTIVITIES

4.1 Introduction

Since the revolution of metallocene-based catalysts for ethylene and α-olefin polymerization,[1,2] many efforts have been made to develop metallocene-[3] and non-metallocene-based[4-7] complexes for the successful homo- or co-polymerization of vinyl alkenes through a successive coordination insertion mechanism. Utilizing the late-transition-metal-based systems, the majority of the studies for the alkene polymerizations where an insertion mechanism is operative are the systems based on cationic palladium(II) complexes.[4] Although the sensitivity of metallocene-based catalysts to polar functionalities allowed the late-transition metal-based systems to attract considerable attention,[6,8] the electrophilicity of the cationic palladium compounds still limits their catalytic application to coordination polymerization of monomers having polar functionalities, such as acrylates.

In view of the limited compatibility of the cationic Ni and Pd complexes with a polar functional group of a monomer, considerable attention has been made in developing nickel-based neutral complexes for polymerization of polar- or non-polar vinyl monomers.[6,7] Recently, several neutral nickel catalysts based on [N,O] chelate ligands following SHOP-type catalysts,[9-13] where they have [P,O] chelate ligands, have been reported by the DuPont,[14] Grubbs,[15,16] Brookhart,[17,18,19] and other[20-22] groups. The most

important contribution of the results reported by them to the transition metal based polymerization research area is that they, especially the Grubbs group, showed the unprecedented functional group tolerance of the catalytic system by polymerizing alkenes having polar functionality or by carrying out polymerizations in the presence of polar impurities, which are poisons for cationic catalysts. Palladium-based neutral catalysts have also been reported by the Novak[23] and Sen.[24] Sen and Novak have homo- or co-polymerized methyl acrylate with or without 1-hexene. However, in both cases, a radical mechanism rather than a coordination insertion mechanism was suggested to be operative.

Synthesis of Pd(II)-based neutral complexes having [N,O] and [N,N] chelate ligands and their characterization using NMR spectroscopy as well as X-ray single-crystal analysis are reported in this chapter. The complexes showed reactivity toward carbon monoxide followed by an imine. They also produced norbornene oligomer and poly(methyl acrylate).

4.2 Results and Discussion

4.2.1 Complex Synthesis

A Salicylaldimine ligand was prepared by condensation of 3-*tert*-butyl-2-hydroxy-benzaldehyde with 2,6-*di*-isopropyl-aniline in the presence of formic acid as a catalyst (Scheme **4-1**).

In situ formation of the sodium salt from **1** upon deprotonation with sodium hydride at room temperature, followed by reaction with the palladium precursor,

cyclooctadienylpalladiummethylchloride, (COD)Pd(Me)Cl, [25] in toluene was not satisfactory in our case.[15] Only starting ligand was recovered without being deprotonated. However, upon attempted deprotonation of **1** with a slight excess of potassium hydride in THF, potassium salt **2** as the THF adduct with one *equiv*. of THF coordinated was successfully isolated as a yellow solid after triturating with pentane. The potassium salt **2** was relatively stable over the course of several months under nitrogen atmosphere.

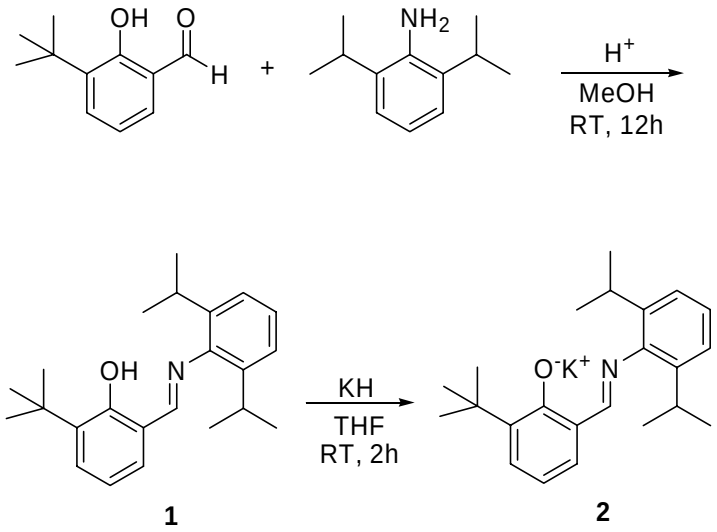

Scheme **4-1**. Preparation of Ligand

Neutral palladium complexes of **3a-3e** were first synthesized by combining the potassium salt **2** with (COD)PdMeCl in the presence of slight excess of an appropriate imine in toluene for *ca.* 12h. Potassium chloride was separated by filtration, and the product was isolated by triturating with ether, followed by washing with pentane.

Complexes **3a-3e** were obtained as yellow solid in yields of *ca*. 90% upon recrystallization from pentane or methylene chloride/pentane.

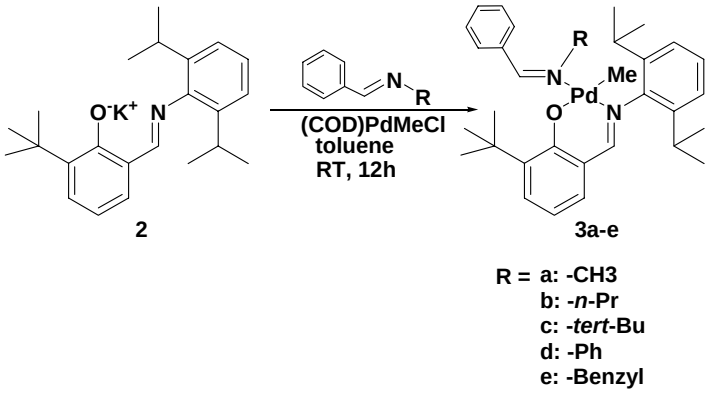

Scheme **4-2**. Preparation of the Complexes, **3a-e**

For all of complexes, coordination of an imine to the palladium center appears to affect rotation of the 2,6-*di*-isopropylphenyl group about the N-aryl bond, becoming slow on the NMR time scale and thus renders the individual methyl groups of an isopropyl unit inequivalent in the ^{1}H NMR spectrum. Four doublets, each of which integrates to three protons are observed. For complex **3e**, two doublets, each of which integrates to one proton, are observed at 5.61 and 5.10 ppm. As expected, two methylene protons on benzyl group (=N-CH_2-Ph) have different stereochemical environments, which resulted in two sets of doublets. The resonances attributed to the palladium-bound methyl groups are shown at -0.47 to -0.86ppm, with corresponding ^{13}C NMR resonances at -4.1 to -6.1 ppm.

The molecular structures of the complexes, **3a** and **3c-3e**, were determined by single-crystal X-ray structure analysis. X-ray quality crystals of the complexes were

obtained either by slow diffusion of pentane into a concentrated solution of **3e** in methylene chloride at room temperature or by cooling a concentrated solution of a complex in pentane down to room temperature(**3a** and **3d**) or to -25^{o}C(**3c**). The ORTEP plots of **3a** and **3c-3e** are shown in Figures **4-1**, **4-2**, **4-3**, and **4-4**. (For crystallographic data, see Table **4-6**). The selected bond lengths and angles for **3a** and **3c-3e** are given in Tables **4-1**, **4-2**, **4-3**, and **4-4**. In the solid state they adopt geometries best described as square planar about each palladium center having slight distortions from idealized geometry. An imine is coordinated through the nitrogen which is in the *trans* position to a nitrogen of a [N,O] chelate ring as a result of the sterics. The planes of C-N-C including palladium-bound nitrogen in imine ligands are roughly perpendicular to the square planes around each palladium. The *cis* N-Pd-O angles for the complexes **3a-e** exceed 90^{o}, due to the formation of six-membered [N,O] chelate rings. Conversely, the *cis* N-Pd-C, containing nitrogen of an imine and methyl group, angles are in the range of 85.7(3) to 89.28(9), which is smaller than 90^{o}.

Figure 4-1

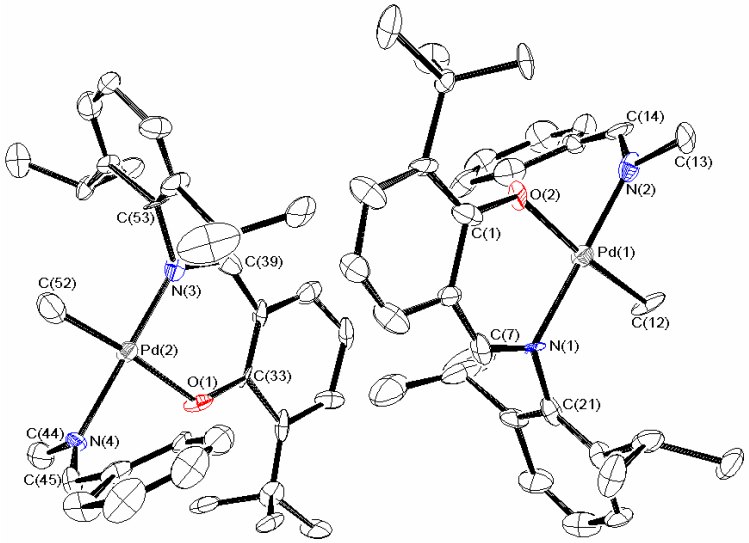

Figure 4-1: ORTEP view of complex 3a. Hydrogen atoms are omitted for clarity.

Figure 4-2

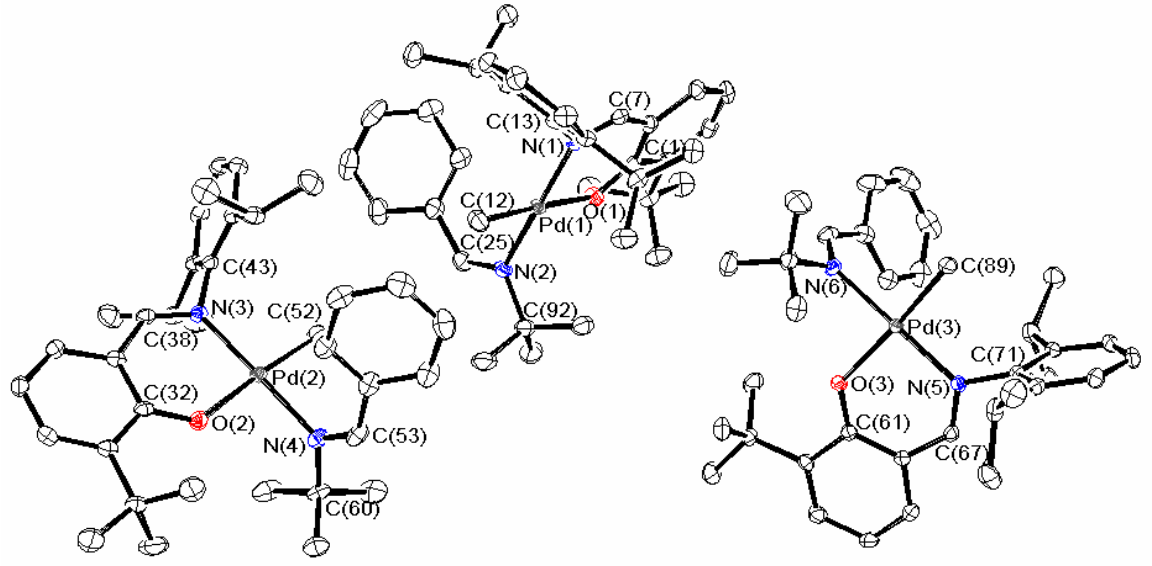

Figure 4-2: ORTEP view of complex 3c. Hydrogen atoms are omitted for clarity.

Figure 4-3

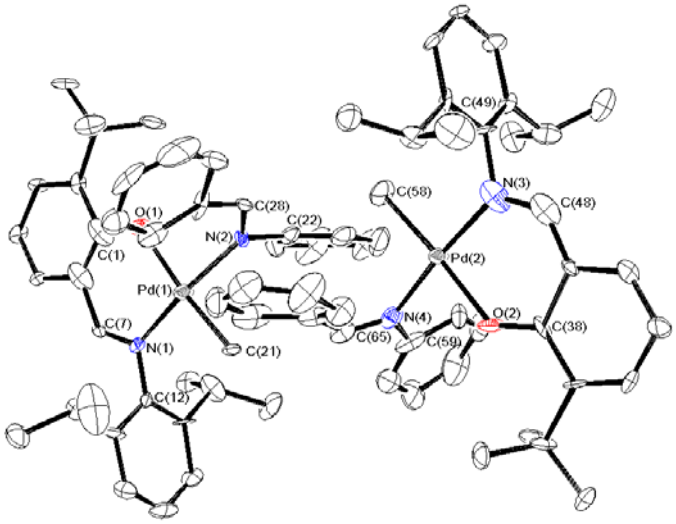

Figure 4-3: ORTEP view of complex 3d. Hydrogen atoms are omitted for clarity.

Figure 4-4

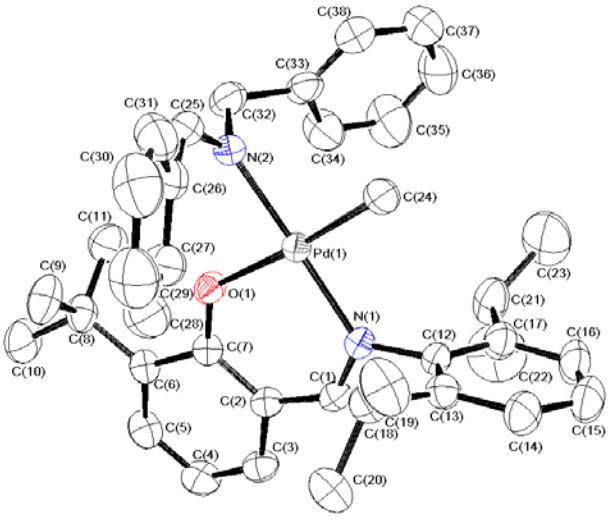

Figure 4-4: ORTEP view of complex 3e. Hydrogen atoms are omitted for clarity.

Table 4-1

Table 4-1: Selected Bond distances (Å) and Angles (°) for **3a**

Pd1-N2	1.989(10)	N1-C7	1.299(14)
Pd1-C12	2.035(10)	N1-C21	1.414(14)
Pd1-N1	2.038(9)	N2-C14	1.283(14)
Pd1-O2	2.051(7)	N2-C13	1.525(12)
O2-C1	1.275(13)		
N2-Pd1-C12	87.0(4)	C7-N1-C21	119.6(9)
N2-Pd1-N1	178.6(5)	C7-N1-Pd1	120.7(7)
C12-Pd1-N1	94.1(4)	C21-N1-Pd1	119.6(7)
N2-Pd1-O2	87.4(3)	C14-N2-C13	116.3(10)
C12-Pd1-O2	174.4(4)	C14-N2-Pd1	129.7(8)
N1-Pd1-O2	91.4(3)	C13-N2-Pd1	113.9(7)
C1-O2-Pd1	131.0(7)		

Table 4-2

Table 4-2: Selected Bond distances (Å) and Angles (°) for **3c**

Pd1-C12	2.026(3)	N2-C25	1.282(3)
Pd1-N1	2.0314(19)	N2-C92	1.517(3)
Pd1-N2	2.059(2)	N1-C7	1.294(3)
Pd1-O1	2.0990(16)	N1-C13	1.451(3)
O1-C1	1.285(3)		
C12-Pd1-N1	93.36(9)	C13-N1-Pd1	123.47(15)
C12-Pd1-N2	88.82(9)	C7-N1-C13	114.01(19)
N1-Pd1-N2	177.68(8)	C7-N1-Pd1	122.43(16)
C12-Pd1-O1	175.50(9)	C25-N2-C92	117.3(2)
N1-Pd1-O1	91.08(7)	C25-N2-Pd1	123.13(18)
N2-Pd1-O1	86.74(7)	C92-N2-Pd1	119.58(15)
C1-O1-Pd1	128.26(15)		

Table 4-3

Table 4-3: Selected Bond distances (Å) and Angles (°) for **3d**

Pd1-C21	2.009(9)	N1-C12	1.405(11)
Pd1-N1	2.024(8)	N1-C7	1.267(11)
Pd1-N2	2.048(4)	N2-C28	1.289(6)
Pd1-O1	2.105(6)	N2-C22	1.511(9)
O1-C1	1.275(11		
C21-Pd1-N1	94.7(3)	C7-N1-Pd1	122.4(6)
C21-Pd1-N2	85.7(3)	C12-N1-Pd1	119.0(6)
N1-Pd1-N2	165.9(2)	C28-N2-C22	114.4(5)
C21-Pd1-O1	173.3(3)	C28-N2-Pd1	128.7(4)
N1-Pd1-O1	91.9(3)	C22-N2-Pd1	116.9(4)
N2-Pd1-O1	87.7(2)	C7-N1-C12	118.3(7)
C1-O1-Pd1	124.4(5)		

Table 4-4

Table 4-4: Selected Bond distances (Å) and Angles (°) for **3e**

O1-C7	1.280(3)	N1-C1	1.296(3)
O1-Pd1	2.0880(16)	N1-C12	1.447(3)
Pd1-N1	2.0126(18)	N2-C25	1.280(3)
Pd1-C24	2.020(3)	N2-C32	1.468(3)
Pd1-N2	2.0386(19)		
C7-O1-Pd1	128.02(14)	C1-N1-C12	113.94(18)
N1-Pd1-C24	92.89(9)	C1-N1-Pd1	122.46(15)
N1-Pd1-N2	178.87(7)	C12-N1-Pd1	123.58(15)
C24-Pd1-N2	88.08(9)	C25-N2-C32	117.1(2)
N1-Pd1-O1	91.64(7)	C25-N2-Pd1	127.01(17)
C24-Pd1-O1	175.39(8)	C32-N2-Pd1	115.89(15)
N2-Pd1-O1	87.40(7)		

Complex **4** was prepared to compare the coordination ability of an imine to pyridine. The reaction of the potassium salt **2** with (COD)PdMeCl in the presence of *tert*-butyl-pyridin-2-ylmethylene-amine in toluene afforded the target compound **4** as a yellow solid in good yield after removing the solvent under *vacuo* following filtration.

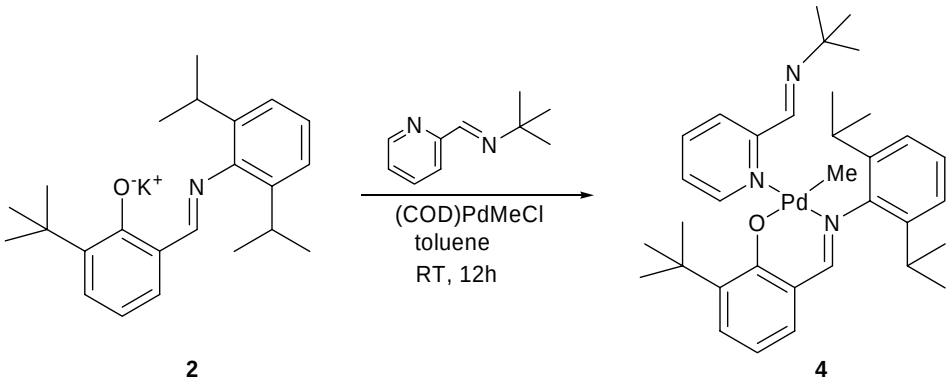

2 **4**

Scheme **4-3**. Preparation of the Complex **4**

Figure **4-5**

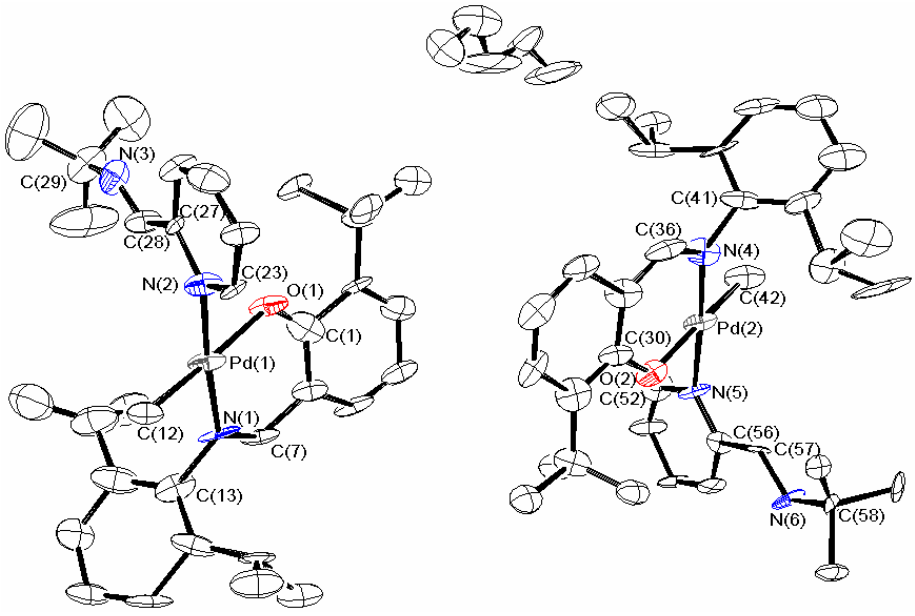

Figure **4-5**: ORTEP view of complex **4**. Hydrogen atoms are omitted for clarity.

The C*H* imine protons of the monodentate ligand and [N,O] chelate ring show resonances at 7.71 and 9.94 ppm, respectively. The palladium-bound methyl proton shows its resonance at -0.26 ppm. The molecular structure of complex **4** was confirmed by single crystal X-ray structure analysis. Cooling the concentrated compound **4** solution in pentane down to room temperature produced a yellow crystal which was suitable for the analysis. Figure **4-5** displays the ORTEP diagram of compound **4**. Selected bond distances and bond angles are collected in Table **4-5** (see Table **4-6** for crystallographic data). In the solid state it shows square planar coordination geometry about palladium, with bond angles slightly deviating from 90^{o} by virtue of the constraint arisen from the chelate ring. The imine is bound to palladium through the nitrogen of the pyridine ring, indicating that there is a steric reason for the coordination rather than an electronic reason. Nucleophilicity of pyridine is slightly smaller than that of an imine. However, steric forces have been proposed to control the ligand orientation as well as dictating the geometry of the imine ligand. The compound itself assigned the best place for each ligand to ease steric hindrance, in which an imine is positioned *trans* to the nitrogen of the [N,O] chelate rings, and the plane around the nitrogen in the imine is perpendicular to the square plane around palladium. With the same reason, the ligand is bound to the metal center through the nitrogen on pyridine rather than the nitrogen next to the *t*-butyl group.

Table 4-5

Table 4-5: Selected Bond distances (Å) and Angles (°) for **4**

Pd1-N2	2.023(10)	N1-C7	1.264(18)
Pd1-C12	2.029(17)	N1-C13	1.46(2)
Pd1-N1	2.039(11)	N2-C23	1.323(14)
Pd1-O1	2.069(12)	N2-C27	1.364(16)
O1-C1	1.23(2)	N3-C28	1.149(16)
		N3-C29	1.500(18)
N2-Pd1-C12	89.2(5)	C27-N2-Pd1	124.8(8)
N2-Pd1-N1	174.7(6)	C23-N2-C27	117.3(11)
C12-Pd1-N1	95.3(6)	C23-N2-Pd1	117.8(8)
N2-Pd1-O1	85.2(5)	C7-N1-C13	115.5(12)
C12-Pd1-O1	174.2(6)	C7-N1-Pd1	126.9(11)
N1-Pd1-O1	90.2(5)	C13-N1-Pd1	117.6(10)
C30-O2-Pd2	128.6(9)	C28-N3-C29	127.0(13)
C1-O1-Pd1	123.5(10)		

Table 4-6

Table 4-6: Crystallographic Data and data Collection Parameters for complexes **3a-e** and **4**

	3a	**3c**	**3d**	**3e**	**4**
Form.	$C_{32}H_{42}N_2OPd$	$C_{105}H_{144}N_6O_3Pd_3$	$C_{74}H_{88}N_4O_2Pd_2$	$C_{38}H_{46}N_2OPd$	$C_{34}H_{47}N_3OPd$
M_w	577.08	1857.46	1278.28	653.17	620.18
T(K)	98(2)	98(2)	98(2)	218(2)	98(2) K
λ(Å)	0.71073	0.71073	0.71073	0.71073	0.71073
c. s.	triclinic	monoclinic	triclinic	triclinic	triclinic
s. g.	*P*$\bar{1}$	*P*2(1)/*c*	*P*$\bar{1}$	*P*$\bar{1}$	*P*$\bar{1}$
a(Å)	11.1653(17)	11.4483(11)	11.9939(16)	9.6685(4)	10.895(2)
b(Å)	11.3688(17)	19.4368(19)	12.1298(16)	13.0421(6)	13.620(3)
c(Å)	13.611(2)	43.765(4)	13.9255(18)	14.8920(7)	13.959(3)
α(deg)	105.623(2)	90	82.955(2)	71.6700(10)	64.930(3)
β(deg)	99.448(2)	90	69.190(2)	81.2500(10)	71.179(3)
γ(deg)	113.062(2)	90	60.381(2)	71.0830(10)	73.707(3)
V(Å^3)	1458.3(4)	9738.5(17)	1642.8(4)	1683.65(13)	1750.8(6)
Z	2	4	2	2	2
F(000)	604	3912	668	684	694
R(*F*)	0.0380	0.0395	0.0447	0.0415	0.0604
R_w(*F*)	0.0905	0.0893	0.1051	0.0962	0.1637
ρ_{calcd} (Mg/m^3)	1.314	1.267	1.292	1.288	1.245

4.2.2 Mechanistic Studies of CO Insertion into Pd-Me Bond using Complex 3c

The reaction of the complexes **3a-3e** with CO was monitored by ^{1}H NMR spectroscopy. Treatment of neutral palladium complexes **3a-3e** with ^{13}CO in CD_2Cl_2 or chlorobenzene-d_5 at ambient temperature or 60^{o}C generates the corresponding palladium acyl species. The methyl group of the acyl appears as a doublet resonance at around 2.7 ppm (23^{o}C in CD_2Cl_2) in the ^{1}H NMR spectrum due to the labeled carbon in carbon monoxide. Disappearance of the Pd-methyl resonance and appearance of the acyl resonance indicates a clean insertion of carbon monoxide into Pd(II)-Me bond. The formation of acyl compounds was confirmed by the proton coupled ^{13}C NMR, in which the labeled acyl carbon appears as a quartet resonance at around 231 ppm (23^{o}C in CD_2Cl_2). The reaction of the complexes with CO was originally studied as a non-kinetic test for the formation an acyl compound. An intermediate has not been observed. However, in the course of an acyl compound formation, a system utilizing neutral Pd(II) compound may have two possible pathways for the formation of an acyl compound (Scheme **4-4**). The first possible pathway is through four-coordinated species – formation of a T-shaped three-coordinate species by releasing the coordinated imine, followed by the coordination of CO, migratory insertion, and the re-coordination of the imine. The other possible pathway is through a five-coordinated species – coordination of CO forming the pyramidal structure, followed by migratory insertion. To investigate the CO insertion pathway, the kinetics of initial carbon monoxide insertion into the palladium methyl bond were directly measured by monitoring the disappearance of the Pd-CH_3 resonance or the appearance of corresponding Pd-C(O)-Me resonance in the ^{1}H NMR

spectrum in CD_2Cl_2 over time. The first-order rate constants and corresponding enthalpy and entropy of activation for carbon monoxide insertion into the Pd(II)-Me bond for **3c** in the absence or presence of benzylidene-*tert*-butylamine are listed in Table **4-7**. The table shows that the system having an excess of the corresponding imine does not show any rate difference from the system having no imine at all. On the basis of results for the systems, we propose that carbon monoxide inserts into Pd(II)-Me bond in the neutral complexes **3a-e** through five-coordinate species (Route 2, Scheme **4-4**).

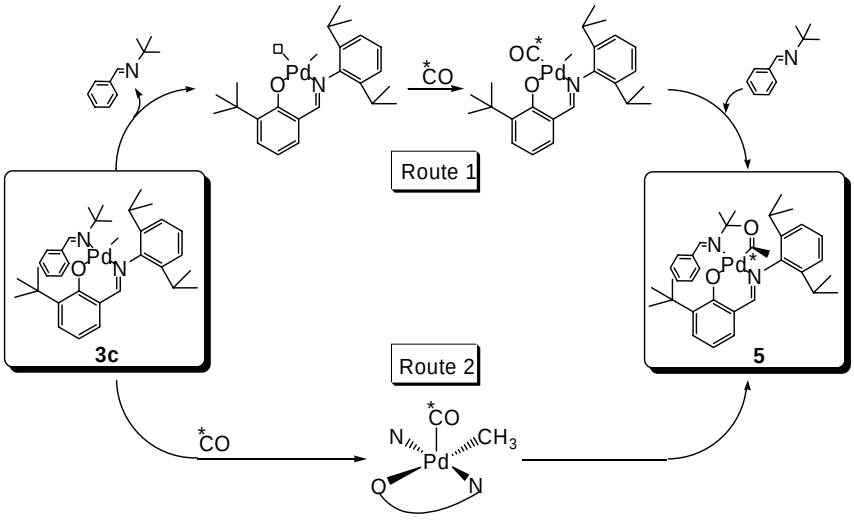

Scheme **4-4**. Proposed CO insertion Pathways

Table 4-7

Table **4-7**: Kinetic Data for Insertion of CO into Pd(II)-Me Bond

imine	T(K)	k(x10^4s^{-1})	$\Delta H^{\ddagger}$ (kcal/mol)	$\Delta S^{\ddagger}$ (cal/K•mol)
-	273.99	0.075	19.0	-12.5
	286.42	0.25		
50 *equiv*.	273.99	0.079	14.7	-28.1
	286.42	0.20		

* *For kinetic data sources, see Appendix P*

Table 4-8

Table 4-8: Polymerization of Vinyl Monomers using Complexes **3a-e**, and **4**[a]

entry	cat.	t(h)	monomer(g)		yield(g)	Mn(x10^{-3})[c]	Mw/Mn[c]
			MA	NB			
1	3a	3	8	-	1.1	211	1.78
2	3b	3	8	-	1.1	970	6.74
3	3c	3	8	-	1.1	1584	5.83
4	3d	3	8	-	1.7	1616	5.85
5[b]	3d	3	8	-	2.9	346	2.14
6	3e	3	8	-	2.0		
7	4	3	8	-	0.7	612	3.10
8	3a	18	-	1	0.05	-	-
9	3b	18	-	1	0.05	-	-
10	3d	18	-	1	0.05	-	-
11	3e	18	-	1	0.06	-	-

[a]Reaction conditions: complex (3.1x10^{-5} mol), chlorobenzene (6mL). [b]in chlorobenzene(30mL). [c]Molecular weight data were determined by GPC vs polystyrene standards.

4.2.3 Polymerization of Polar or Nor-polar Vinyl Monomers

Polymerization of non-polar vinyl monomers, such as ethene, propene, or 1-hexene, using the complexes **3a-e**, or **4** gave no polymeric product. It seems that the strongly coordinating donor ligands do not afford a vacant site for an incoming monomer. In this manner, the imine ligands provide inactivity to the title compounds. The reactivity

testing results of the complexes toward CO in this research also proved that the imine ligand is not dissociated during the reaction. NMR scale reactions of vinyl monomers with the complexes showed no reactions of either oligomerization or any other catalytic process occurred, except in the case of the system utilizing norbornene as a monomer. The ^{1}H NMR experiment using one of **3a-e** and 5 *equiv*. of norbornene showed resonances corresponding to oligomeric norbornene product at 23^{o}C. By adding *ca.*10 *equiv*. more of norbornene monomer to the system, we obtained increasing resonances in the ^{1}H NMR spectrum corresponding to norbornene oligomer or polymer at the same temperature. Upon having the evidence of the polynorbornene formation, we scaled-up the polymerization reaction of norbornene using catalyst **3a-e** in chlorobenzene at ambient temperature (entries 8-11, Table **4-8**). The yield of polynorbornene isolated as a solid after quenching with methanol did not reach the amount expected, as confirmed by NMR. Removing solvent under vacuum before quenching the reaction mixture with methanol left an oily product. The molecular weight of the oil was less than 500, which is the detection limit of the GPC. Although the exact molecular weight of the oily product could not be measured, the result revealed that most of the reaction product is oligomer, which is soluble in methanol.

Polymerization of methyl acrylate using catalysts **3a-e**, or **4** was carried out in chlorobenzene at ambient temperature (entries 1-7, Table **4-8**). Low to moderate yields of poly(methyl acrylate) were obtained at the conditions indicated. The polymers produced have high (Mn>211000) to ultrahigh (Mn> 1600000) molecular weight and showed wide polydispersity index. Formation of a sticky polymer started to prevent monomer diffusion to the active catalyst in 1 hr by blocking effective stirring, which seems to cause wide

polydispersity (entries 2-4). Decreasing the monomer concentration by increasing the amount of solvent from 6 mL to 30 mL gave a higher polymer yield with a narrower polydispersity index (entries 4, and 5). Our main interest in this study was the possible application of the palladium-based neutral complexes as a catalyst in the polymerization of polar or non-polar vinyl monomers. Recently, Sen[24] as well as Novak and co-workers[23] reported on the homopolymerization of methyl acrylate using neutral palladium compounds where a radical mechanism was invoked. Polyacrylates can be achieved through various routes including anionic, radical, or coordination insertion mechanism. We also tested the possible reaction mechanism by using two different monomers, methyl methacrylate and styrene, which are readily polymerized through a radical mechanism, or by using a radical inhibitor, galvinoxyl. Neither methyl methacrylate nor styrene was polymerized by any of the title complexes, **3a-e** or **4**. The polymerization of methyl acrylate was completely halted when galvinoxyl was utilized. Based on the results of the first experiments, we may rule out traditional free radical or metal based atom transfer radical polymerization mechanism. However, it seems to have a radical pathway for the polymerization of methyl acrylate, which agrees with the results reported by Novak and Sen, although there has been 'a warning on the use of radical traps as a test for radical mechanisms'.[26]

4.2.4 Reactivities of the complexes toward imine and CO

Reactions of the title complexes **3a-e** with an imine compound under ^{13}C labeled carbon monoxide atmosphere have been monitored using various NMR techniques.

Several equivalents of an imine were added to a chlorobenzene-d_5 solution of a title complex at ambient temperature and the reaction mixture was monitored by ^{1}H NMR, $^{13}C\{^{1}H\}$, or proton coupled ^{13}C NMR spectroscopy as it was gradually warmed up (Scheme **4-5**). The insertion of CO into Pd-Me bond was observed even at room temperature, resulting in the formation of acyl compound (compound **5**, Scheme **4-4** and resonance at 231.1 ppm in figure **4-6**).

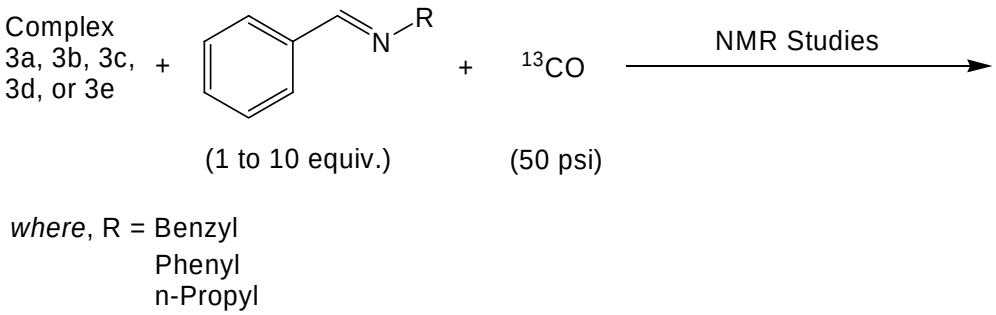

Scheme **4-5**. Reaction Scheme

Figure **4-6**

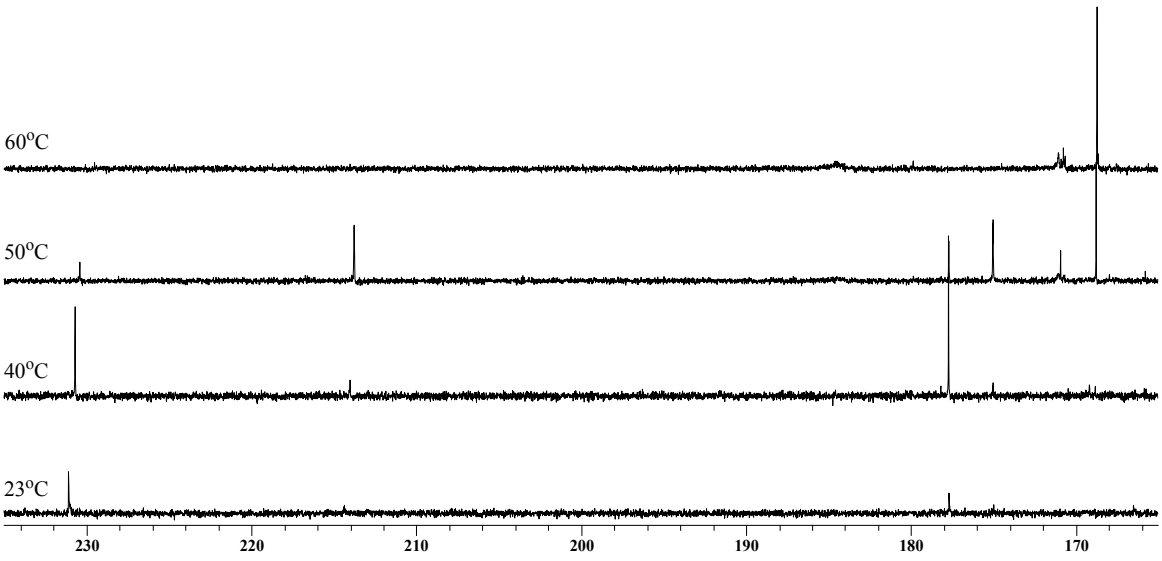

Figure **4-6**: Selected VT ^{13}C NMR Spectra of the Reaction between **3e** and Ph-CH=N-CH_2-Ph under ^{13}CO Atmosphere

Warming the reaction mixture to 40°C resulted in the formation of a new species which shows resonance at 213.8 ppm. The concentration of this species is gradually increased while an acyl compound slowly disappears as the system warms up to 50°C. All of these species disappears as the system temperature reachs at 60°C, leaving two resonances at 171.0ppm and 168.7ppm. From that point on, it seems no more reaction occurred.

Figure 4-7

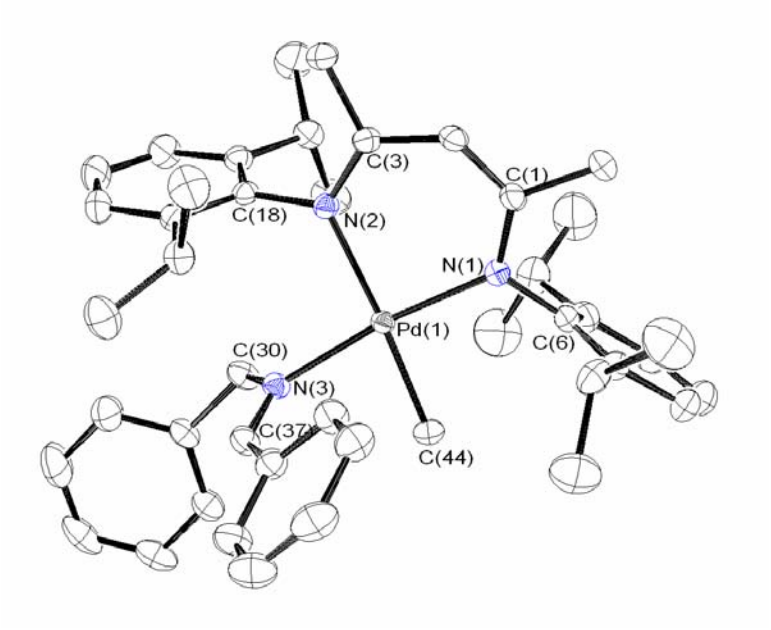

Figure 4-7: ORTEP view of complex 5. Hydrogen atoms are omitted for clarity.

To rule out the possibilities of the isomer formaton, proton coupled ^{13}C NMR experiment has been conducted. Since no desired data has been obtained, a new complex **5** having N-benzylbenzylideneimine, Ph-CH=N-CH_2-Ph, as a ligand has been prepared and utilized (Figure **4-7**). Fortunately, good spectroscopic data has been obtained from the reaction between the complex **5** and *N*-benzylbenzylideneimine under ^{13}C labeled

carbon monoxide atmosphere at 50^{o}C (Figure **4-8**). As already known, the peak at 231.1 ppm shows the resonance as a quartet indicating the presence of an acyl carbon formed by CO insertion into the Pd-Me bond. This compound undergoes an imine insertion into Pd-acyl bond in two possible pathways. It is generally known that an imine inserts into Pd-acyl bond via *path A* (Scheme 4-6). Although the insertion of an imine through carbon on carbon-nitrogen double bond has never been observed or proposed, the splitting pattern of the peak at 214.4 ppm, which is the resonance as a doublet of quartets suggests that a new insertion pathway of imine into Pd-acyl bond is possible. The acyl carbon on compound **6** formed through *path A* should show the resonance as a quartet instead of doublet of quartets. However, if the imine inserts into Pd-acyl bond via *path B*, the resulting compound **7** would show the resonance as a doublet of quartets for the acyl carbon. The resonance as a quartet at 168.7ppm is assigned as a carbonyl carbon right next to a methyl group, which is not chelated to palladium metal center through oxygen functionality. Based on the results above and the fact that the peaks at 176.8 and 175.0 ppm are the resonance as a singlet and a doublet, respectively, we propose two more possible structures, in which second insertion of carbon monoxide occurred (compound **8** and **9**, Scheme 4-6)). Because none of the intermediates and the final compound has been isolated and their structures have not been completely established yet, further research on this topic is in progress.

Figure **4-8**

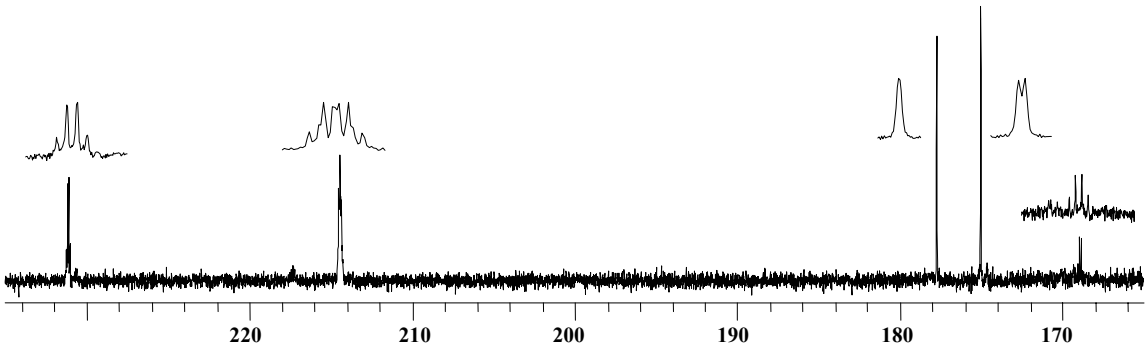

Figure **4-8**: Selected proton coupled ^{13}C NMR spectrum

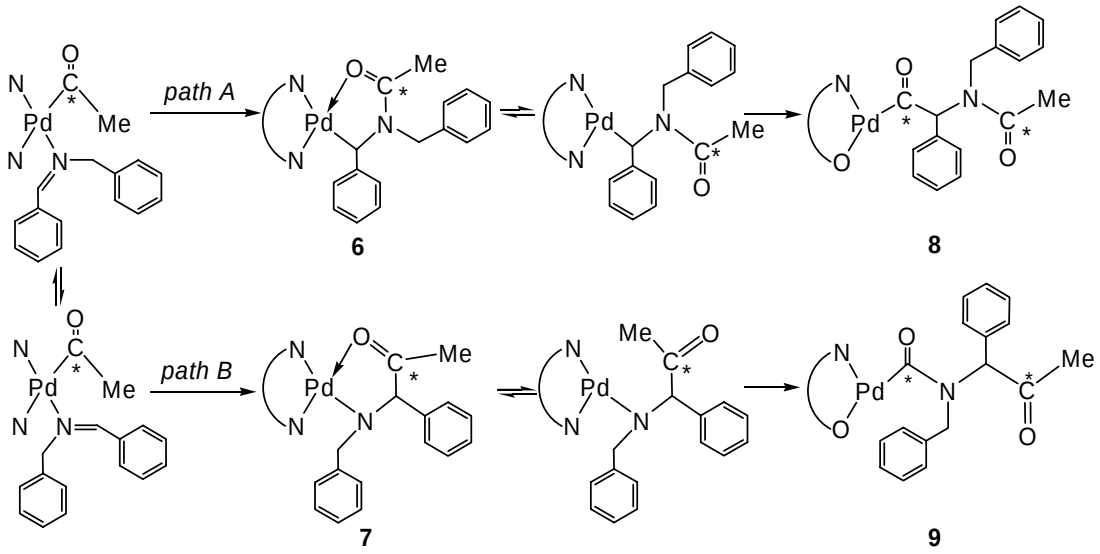

Scheme **4-6**. Proposed imine insertion pathways

4.3 Conclusions

We synthesized a serious of neutral salicylaldiminato Pd(II) complexes: Pd(Me)(Ph-CH=N-R´)[3-^{t}Bu-2-(O)C_6H_3-CH=N-2,6-*di*-^{i}Pr-C_6H_3](R=CH3, *n*-Pr, *tert*-Bu, Ph, Benzyl) (**3a-3e**), and Pd(Me)[3-(CH=N-*t*-Bu)-Py][3-^{t}Bu-2-(O)C_6H_3-CH=N-2,6-*di*-^{i}Pr-C_6H_3] (**4**). These complexes have been isolated and characterized spectroscopically, and the solid-state structures of the complexes have also been characterized by X-ray single-crystal structure analysis. According to the results of the NMR studies, the complexes reacted with carbon monoxide to form corresponding acyl complexes through five-coordinated intermediate. These acyl complexes undergo an imine insertion into Pd-acyl bond and two possible insertion pathways are proposed based on the results of NMR experiments. For the investigation of the imine insertion reaction, a neutral N-N chelated complex **5** has been prepared and its structure has been characterized by X-ray single-crystal structure analysis. The neutral complexes, **3a-e** and **4**, showed the reactivities toward norbornene with the main product of the reactions being norbornene oligomers. They also showed moderate catalytic activity for the polymerization of methyl acrylate at room temperature producing polymers with a high molecular weight but broad polydispersity index. The results of the preliminary polymerization reaction of methyl acrylate using complexes **3a-3e** suggest a radical mechanism rather than coordination insertion mechanism.

4.4 Experimental Section

4.4.1 Generation Considerations

All syntheses and manipulations of air- and moisture-sensitive compounds were carried out in flame dried Schlenk-type glassware on a dual-manifold Schlenk line, a high vacuum with argon line, or in a nitrogen-filled glovebox.

Nuclear magnetic resonance (NMR) spectra were recorded on a Bruker DRX 400 NMR spectrometer, DPX 300 NMR spectrometer, and CDPX 300 NMR spectrometer. Splitting patterns are designated as follows: s, singlet; bs, broad singlet; d, doublet; dd, doublet of doublets; t, triplet; td, triplet of doublets; sept, septet; m, multiplet. All ^{1}H NMR spectra are reported in δ units, parts per million (ppm) downfield from tetramethylsilane. All ^{13}C NMR spectra are reported in ppm relative to tetramethylsilane using CD_2Cl_2, toluene-d8, or chlorobenzene-d5 as an internal standard. Variable-temperature ^{1}H NMR experiments were performed on a Bruker DPX 300 NMR spectrometer, using CD_2Cl_2, toluene-d_8, or chlorobenzene-d_5 as solvent. Actual NMR probe temperatures were measured using anhydrous methanol (with 0.03% concentrated HCl) or ethylene glycol (neat) in a 5 mm NMR tube (see **2.5.1** and **2.5.2**). NMR analyses of polymers were performed on a Bruker DPX 300 NMR spectrometer at ambient or elevated temperature, using $CDCl_3$, chlorobenzene-d_5, dichlorobenzene-d_4, or tetrachloroethane-d_2 as solvents unless otherwise noted.

Size exclusion chromatography data were obtained on a Shimadzu SEC System using a three-column bank (Styragel 7.8x300 mm columns, 100-5,000 D, 500-30,000 D, 2000-4,000,000 D), a Shimadzu RID-10A Differential Refractometer, and a Shimadzu

LC-10AT pump/controller. Size exclusion chromatography was performed in chloroform at ambient temperature and calibrated to polystyrene standards.

Chlorobenzene and dichloromethane was obtained from Aldrich and dried via passage over a column of activated alumina (LaRoche A-2).[27] Toluene and diethyl ether were deoxygenated, dried via passage over a column of activated alumina (LaRoche A-2) and columns of Engelhard CU-0226S[27]. Pentane and tetrahydrofuran were distilled under nitrogen from sodium benzophenone ketyl. All solvents were degassed by repeated freeze-pump-thaw cycles, and stored over 4 Å molecular sieves under nitrogen. Norbornene was purchased from Acros Organics and used without further purification. Methyl acrylate and methyl methacrylate were purchased from Aldrich and used after repeated freeze-pump-thaw cycles prior to use. Cyclooctadienyl palladiummethylchloride[(COD)Pd(Me)(Cl) was prepared as previously reported. [25]

4.4.2 Synthesis of Compounds

3-^{t}Bu-2-(OH)C_6H_3-CH=N-2,6-*di*-^{i}Pr-C_6H_3 (1). To 3-tert-butyl-2-hydroxybenzaldehyde (1g, 5.6 mmol) in methanol(50 ml) was added 2,6-diisopropylaniline(1.5g, 8.4 mmol), followed catalytic amount of formic acid(2 drops), The solution was stirred at room temperature for 12h. Removal of solvent in Vacuo yielded a yellow oil, which is purified by vacuum distillation. ^{1}H NMR($CDCl_3$): δ 13.65 (br, 1H, -O*H*), 8.35 (s, 1H, -C*H*=N-), 7.49-6.91(m, 6H, Ar-*H*), 3.06 (sept, 2H, -C*H*(CH_3)$_2$), 1.52 (s, 9H, -C(C*H*$_3$)$_3$), 1.22 (d, 12H, -CH(C*H*$_3$)$_2$). ^{13}C NMR($CDCl_3$): δ

167.96 (-*C*H=N-), 160.99, 146.72, 139.31, 137.95, 131.08, 130.78, 125.70, 123.57, 118.96, 118.60 (Ar), 35.22 (-*C*Me$_3$), 29.51 (-C(*C*H$_3$)$_3$), 28.49 (-*C*H(CH$_3$)$_2$), 23.73 (-CH(*C*H$_3$)$_2$).

[3-^{t}Bu-2-(OK)C$_6$H$_3$-CH=N-2,6-*di*-^{i}Pr-C$_6$H$_3$]·THF (2). To a stirred suspension of KH (0.19g, 4.68mmol) in THF(30ml) was added ligand **1**(0.79g, 2.34mmol) in THF(20mL) at room temperature. The reaction mixture was stirred for 2h and filtered to remove excess KH. After removing solvent under vacuum, small amount of pentane was added to dissolve starting material. Upon filtering and washing with pentane, the potassium salt THF adduct was obtained as a yellow solid. Yield 0.97g, 92%.

Pd(Me)(Ph-CH=N-CH$_3$)[3-^{t}Bu-2-(O)C$_6$H$_3$-CH=N-2,6-*di*-^{i}Pr-C$_6$H$_3$] (3a) . To a mixture of [3-^{t}Bu-2-(OK)C$_6$H$_3$-CH=N-2,6-*di*-^{i}Pr-C$_6$H$_3$]·THF (0.42g, 0.94mmol) and Ph-CH=N-CH$_3$ (0.11g, 0.94mmol) in toluene (30mL) was added (COD)PdMeCl (0.25g, 0.94mmol) in toluene (10mL). The reaction mixture was stirred for 12 hours, which was filtered to remove a small quantity of dark insoluble material. The solvent was removed *in vacuo* to yield a yellow solid. Recrystallization from pentane gave a yellow crystalline solid which was suitable for X-ray crystal structure analysis. Yield 0.49g, 91%. ^{1}H NMR(CD$_2$Cl$_2$): δ 8.36 (s, 1H, Pd-O-Ar-C*H*=N-), 7.74 (s, 1H, Ph-C*H*=N-CH$_3$), 8.98(d), 7.58-7.49(m), 7.28(dd), 7.21-7.16(dd), 7.00(dd), 6.35(t) (11H, Ar-H), 3.99 (s, 3H, Ph-CH=N-C*H*$_3$) 3.55, 3.22 (hept each, 2H, Ar-C*H*(CH$_3$)$_2$), 1.29 (s, 9H, Ar-C(C*H*$_3$)$_3$), 1.38, 1.24, 1.18, 1.16 (d each, 12H, Ar-CH(C*H*$_3$)$_2$), -0.49 (s, 3H, Pd-C*H*$_3$). ^{13}C NMR(CD$_2$Cl$_2$): δ 167.7 (Pd-O-Ar-*C*H=N-), 166.1 (Ph-*C*H=N-CH$_3$), 141.6, 141.5, 134.9, 132.4, 131.3, 130.7, 129.1, 128.9, 128.6, 128.5, 126.4, 123.5, 119.9, 112.0 (Ar), 53.4 (Ph-CH=N-*C*H$_3$)

35.4 (Ar-*C*$(CH_3)_3$), 29.5 (Ar-C(*C*$H_3)_3$), 28.0 (Ar-*C*H$(CH_3)_2$), 25.2, 25.0, 23.0, 22.7 (Ar-CH(*C*$H_3)_2$), -5.6 (Pd-*C*H_3).

Pd(Me)(Ph-CH=N-CH_2-CH_2-CH_3)[3-^{t}Bu-2-(O)C_6H_3-CH=N-2,6-*di*-^{i}Pr-C_6H_3] (3b) . To a mixture of [3-^{t}Bu-2-(OK)C_6H_3-CH=N-2,6-*di*-^{i}Pr-C_6H_3]·THF (0.42g, 0.94mmol) and Ph-CH=N-CH_2-CH_2-CH_3 (0.14g, 0.94mmol) in toluene (30mL) was added (COD)PdMeCl (0.25g, 0.94mmol) in toluene (10mL). The reaction mixture was stirred for 12 hours, which was filtered to remove a small quantity of dark insoluble material. The solvent was removed *in vacuo* to yield a yellow solid. Recrystallization from pentane gave a yellow crystalline solid which was suitable for X-ray crystal structure analysis. Yield 0.51g, 89%. ^{1}H NMR(CD_2Cl_2): δ 8.38 (s, 1H, Pd-O-Ar-C*H*=N-), 7.70 (s, 1H, Ph-C*H*=N-CH_2-Ph), 8.93(d), 7.54-7.43(m), 7.24 (dd), 7.17-7.12(m), 6.96(dd), 6.31(t) (11H, Ar-*H*), 4.33, 3.68 (m each, 2H, Ph-CH=N-C*HH*'-CH_2-CH_3), 3.64, 3.39 (hept, 2H, Ar-C*H*$(CH_3)_2$), 2.31(sext, 2H, N-CH_2-CH_2-CH_3), 1.25 (s, 9H, Ar-C(C$H_3)_3$), 1.34, 1.21, 1.15, 1.12 (d each, 12H, Ar-CH(C$H_3)_2$), 1.02 (Ph-CH=N-CH_2-CH_2-CH_3), -0.62 (s, 3H, Pd-CH_3). ^{13}C NMR(CD_2Cl_2): δ 167.0 (Pd-O-Ar-*C*H=N-), 166.0 (Ph-*C*H=N-CH_2-CH_2-CH_3), 148.7, 141.5, 141.4, 135.0, 134.2, 132.3, 131.4, 130.7, 128.5, 126.3, 124.5, 123.5, 123.4, 120.0, 112.0 (Ar), 68.6 (Ph-CH=N-*C*H_2-CH_2-CH_3), 35.3 (Ar-*C*$(CH_3)_3$) 29.5 (Ar-C(*C*$H_3)_3$), 28.1, 28.0 (Ar-*C*H$(CH_3)_2$), 25.0 (Ph-CH=N-CH_2-*C*H_2-CH_3), 25.3, 25.1, 23.1, 22.6 (Ar-CH(*C*$H_3)_2$), 11.8 (Ph-CH=N-CH_2-CH_2-*C*H_3), -5.0 (Pd-*C*H_3).

Pd(Me)(Ph-CH=N-*t*-Bu)[3-^{t}Bu-2-(O)C_6H_3-CH=N-2,6-*di*-^{i}Pr-C_6H_3] (3c) . To a mixture of [3-^{t}Bu-2-(OK)C_6H_3-CH=N-2,6-*di*-^{i}Pr-C_6H_3]·THF (0.42g, 0.94mmol) and Ph-CH=N-t-Bu (0.15g, 0.94mmol) in toluene (30mL) was added (COD)PdMeCl (0.25g, 0.94mmol) in toluene (10mL). The reaction mixture was stirred for 12 hours, which was

filtered to remove a small quantity of dark insoluble material. The solvent was removed *in vacuo* to yield a yellow solid. Recrystallization from pentane at -25°C gave a yellow crystalline solid which was suitable for X-ray crystal structure analysis. Yield 0.52g, 90%. ^{1}H NMR(CD_2Cl_2): δ 8.51 (s, 1H, Pd-O-Ar-C*H*=N-), 7.69 (s, 1H, Ph-C*H*=N-*t*-Bu), 8.92(d), 7.52-7.43(m), 7.25(dd), 7.15-7.07(m), 6.95(dd), 6.31(t) (11H, Ar-*H*), 3.69, 3.21 (hept each, 2H, Ar-C*H*(CH_3)$_2$), 1.76 (s, 9H, -N-C(C*H*$_3$)$_3$), 1.29 (s, 9H, Ar-C(C*H*$_3$)$_3$), 1.24, 1.12, 1.10, 1.03 (d each, 12H, Ar-CH(C*H*$_3$)$_2$), -0.66(s, 3H, Pd-C*H*$_3$). ^{13}C NMR(CD_2Cl_2): δ 169.1 (Pd-O-Ar-*C*H=N-), 166.2 (Ph-*C*H=N-t-Bu), 148.8, 141.6, 141.5, 135.9, 135.1, 131.9, 131.4, 130.4, 128.3, 126.2, 123.5, 123.3, 120.0, 111.8(Ar), 64.7 (-N-*C*(CH_3)$_3$), 35.4(Ar-*C*(CH_3)$_3$), 32.1 (-N-C(*C*H$_3$)$_3$), 29.7 (Ar-C(*C*H$_3$)$_3$), 28.0 , 27.9 (Ar-*C*H(CH_3)$_2$), 25.3, 25.1, 23.0, 22.8 (Ar-CH(*C*H$_3$)$_2$), -6.01 (Pd-*C*H$_3$).

Pd(Me)(Ph-CH=N-Ph)[3-^{t}Bu-2-(O)C_6H_3-CH=N-2,6-*di*-^{i}Pr-C_6H_3] (3d) . To a mixture of [3-^{t}Bu-2-(OK)C_6H_3-CH=N-2,6-*di*-^{i}Pr-C_6H_3]·THF (0.42g, 0.94mmol) and Ph-CH=N-Ph (0.17g, 0.94mmol) in toluene (30mL) was added (COD)PdMeCl (0.25g, 0.94mmol) in toluene (10mL). The reaction mixture was stirred for 12 hours, which was filtered to remove a small quantity of dark insoluble material. The solvent was removed *in vacuo* to yield a yellow solid. Recrystallization from pentane gave a yellow crystalline solid which was suitable for X-ray crystal structure analysis. Yield 0.55g, 92%. ^{1}H NMR(CD_2Cl_2): δ 8.56 (s, 1H, Pd-O-Ar-C*H*=N-), 7.70 (s, 1H, Ph-C*H*=N-Ph), 9.17(d), 7.81(d), 7.61-7.15(m), 6.95(d), 6.30(t) (16H, Ar-*H*), 3.54, 3.47 (hept each, 2H, Ar-C*H*(CH_3)$_2$), 1.13 (s, 9H, Ar-C(C*H*$_3$)$_3$), 1.25, 1.24, 1.16, 1.10 (d each, 12H, Ar-CH(C*H*$_3$)$_2$), -0.47 (s, 3H, Pd-C*H*$_3$). ^{13}C NMR(CD_2Cl_2): δ 168.1 (Pd-O-Ar-*C*H=N-), 166.1 (Ph-*C*H=N-CH_2-Ph), 153.0, 148.7, 141.6, 141.4, 134.8, 133.3, 131.4, 131.3, 129.2, 128.7, 128.0,

126.4, 124.1, 123.6, 119.8, 112.0 (Ar), 35.3 (Ar-*C*$(CH_3)_3$) 29.4 (Ar-C(*C*$H_3)_3$), 28.0 (Ar-*C*H$(CH_3)_2$), 25.3, 25.0, 23.0, 22.6(Ar-CH(*C*$H_3)_2$), -4.1 (Pd-*C*H_3).

Pd(Me)(Ph-CH=N-CH_2-Ph)[3-^{t}Bu-2-(O)C_6H_3-CH=N-2,6-*di*-^{i}Pr-C_6H_3] (3e) . To a mixture of [3-^{t}Bu-2-(OK)C_6H_3-CH=N-2,6-*di*-^{i}Pr-C_6H_3]·THF (0.23g, 0.52mmol) and Ph-CH=N-CH_2-Ph (0.11g, 0.56mmol) in toluene (30mL) was added (COD)PdMeCl (0.15g, 0.57mmol) in toluene (10mL). The reaction mixture was stirred for 12 hours, which was filtered to remove a small quantity of dark insoluble material. The solvent was removed *in vacuo* to yield a yellow solid. Recrystallization from methylene dichloride and pentane gave a yellow crystalline solid which was suitable for X-ray crystal structure analysis. Yield 0.31g, 92%. ^{1}H NMR(CD_2Cl_2): δ 8.49 (s, 1H, Pd-O-Ar-C*H*=N-), 7.71 (s, 1H, Ph-C*H*=N-CH_2-Ph), 5.61 (d, 1H, Ph-CH=N-C*H*H′-Ph), 5.10 (d, 1H, Ph-CH=N-CH*H*′-Ph), 8.94(d), 7.65-6.98(m), 6.37(t) (16H, Ar-*H*), 3.42 (hept, 2H, Ar-C*H*$(CH_3)_2$), 1.38 (s, 9H, Ar-C(C$H_3)_3$), 1.22, 1.19, 1.16, 1.11 (d each, 12H, Ar-CH(C$H_3)_2$), -0.86 (s, 3H, Pd-CH_3). ^{13}C NMR(CD_2Cl_2): δ 166.9 (Pd-O-Ar-*C*H=N-), 166.3 (Ph-*C*H=N-CH_2-Ph), 148.6, 141.6, 136.4, 135.0, 132.5, 131.5, 130.7, 129.1, 129.0, 128.7, 128.5, 126.3, 123.4, 112.1 (Ar), 69.45 (=N-*C*H_2-Ph), 35.4 (Ar-*C*$(CH_3)_3$) 29.7 (Ar-C(*C*$H_3)_3$), 27.9 (Ar-*C*H$(CH_3)_2$), 25.2, 23.2 (Ar-CH(*C*$H_3)_2$), -4.4 (Pd-*C*H_3).

Pd(Me)[3-(CH=N-*t*-Bu)-Py][3-^{t}Bu-2-(O)C_6H_3-CH=N-2,6-*di*-^{i}Pr-C_6H_3] (4) . To a mixture of [3-^{t}Bu-2-(OK)C_6H_3-CH=N-2,6-*di*-^{i}Pr-C_6H_3]·THF (0.42g, 0.94mmol) and 3-(CH=N-*t*-Bu)-Py (0.15g, 0.94mmol) in toluene (30mL) was added (COD)PdMeCl (0.25g, 0.94mmol) in toluene (10mL). The reaction mixture was stirred for 12 hours, which was filtered to remove a small quantity of dark insoluble material. The solvent was removed *in vacuo* to yield a yellow solid. Recrystallization from pentane gave a yellow crystalline

solid which was suitable for X-ray crystal structure analysis. Yield 0.56g, 93%. ^{1}H NMR(CD_2Cl_2): δ 9.94 (s, 1H, Pd-O-Ar-C*H*=N-), 7.71 (s, 1H, Py-C*H*=N-*t*-Bu), 8.97(d), 8.24(s), 7.87(t), 7.36(dt), 7.26-7.14(m), 6.95(dd), 6.30(t) (10H, Ar-H), 3.69, 3.50 (hept each, 2H, Ar-C*H*(CH_3)$_2$), 1.33 (s, 9H, Ar-C(CH_3)$_3$), 1.02 (s, 9H, =N-C(CH_3)$_3$), 1.35, 1.16, 1.12 (d each, 12H, Ar-CH(CH_3)$_2$), -0.26 (s, 3H, Pd-CH_3). ^{13}C NMR(CD_2Cl_2): δ 166.4 (Ph-*C*H=N-t-Bu), 156.9 (Pd-O-Ar-*C*H=N-), 168.2, 155.9, 152.3, 141.5, 137.7, 134.7, 131.4, 129.4, 128.6, 126.5, 125.2, 123.7, 123.5, 123.1, 119.8, 112.1 (Ar), 58.7 (=N-*C*H(CH_3)$_2$), 35.1 (Ar-*C*H(CH_3)$_2$), 29.5 (Ar-C(*C*H_3)$_3$), 29.3 (=N-C(*C*H_3)$_3$), 28.3, 28.1 (Ar-*C*H(CH_3)$_2$), 25.0, 22.9 (Ar-CH(*C*H_3)$_2$), -4.0 (Pd-*C*H_3).

Pd(Me)(Ph-CH=N-CH2-Ph)[2,6-*di*-^{i}Pr-C_6H_3-N-C(Me)-CH-C(Me)-N-2,6-*di*-^{i}Pr-C_6H_3] (5) . To a mixture of [2,6-*di*-^{i}Pr-C_6H_3-N=C(Me)-CH=C(Me)-N(H)-2,6-*di*-^{i}Pr-C_6H_3]·Tl (0.50g, 0.8mmol) and Ph-CH=N-CH_2-Ph (0.15g, 0.8mmol) in toluene (30mL) was added (COD)PdMeCl (0.21g, 0.8mmol) in toluene (10mL). The reaction mixture was stirred for 12 hours, which was filtered to remove a small quantity of dark insoluble material. The solvent was removed *in vacuo* to yield a yellow solid. Recrystallization from methylene dichloride and pentane gave a yellow crystalline solid which was suitable for X-ray crystal structure analysis.Yield 0.57g, 97%. ^{1}H NMR(CD_2Cl_2): 7.30 (s, 1H, Ph-C*H*=N-), 9.05(d), 7.46-7.32(m), 7.22-6.86(m), 6.63(d) (16H, Ar-*H*), 4.68(s, N-C(CH_3)-C*H*-C(CH′$_3$)-N), 4.57, 3.29(d each, 2H, Ph-C*HH*′-N), 3.79, 3.66, 3.41, 2.86 (hept each, 4H, Ar-C*H*(CH_3)$_2$, Ar-C*H*′(CH_3)$_2$, Ar-C*H*″(CH_3)$_2$, Ar-C*H*‴(CH_3)$_2$), 1.56, 1.53 (s each, 6H, N-C(CH_3)-CH-C(C*H*′$_3$)-N), 1.50, 1.24, 1.20, 1.15, 1.06, 0.84, 1.82, 0.33 (d each, 24H, Ar-CH(CH_3)$_2$), -0.74(s, 3H, Pd-CH_3). ^{13}C DEPT135 NMR(CD_2Cl_2): δ 166.3 (-*C*H=N-), 132.4, 131.5, 129.2, 128.5, 125.0, 124.6, 124.2, 123.4, 123.2 (Ar), 94.5 (-C(CH_3)-*C*H-

C(CH′$_3$)-), 65.9 (Ph-*C*H$_2$-N), 28.4, 28.1, 27.7, 27.4 (Ar-*C*H(CH$_3$)$_2$), 26.2 ((-C(*C*H$_3$)-CH-C(*C*H′$_3$)-), 25.4, 25.1, 24.9, 24.8, 24.7, 24.2, 24.1, 23.8 (Ar-CH(*C*H$_3$)$_2$), 4.8 (Pd-*C*H$_3$).

4.4.3 General Procedures for Polymerization Reactions

In a drybox under a nitrogen atmosphere, a title complex ($3.1x10^{-5}$ mol) was dissolved in chlorobenzene(6 mL or 30 mL) in a 100 mL Schlenk flask. Then, a specified amount of methyl acrylate or norbornene was introduced to the flask. The reaction mixture was stirred at a desired temperature. After the specified reaction time, the reaction was quenched with methanol. The precipitated polymer was filtered and washed with methanol. Volatiles were removed from the polymer in *vacuo*, and the polymer was dried under vacuum overnight.

4.4.4 General Procedure for NMR Experiments

In a drybox under a nitrogen atmosphere, **3c** ($1.7x10^{-5}$ mol) with or without Ph-C=N-*n*-Pr($8.3x10^{-4}$ mol) was weighed into a High Pressure NMR tube. CD_2Cl_2 (1 mL) was added to the NMR tube. The tube was then capped, removed from the drybox, and cooled to *ca*. -90^{o}C. After applying vacuum briefly, the mixture was allowed to reach ambient temperature. The NMR tube was then charged with ^{13}C labeled carbon monoxide(50psi), and cooled again to *ca*. -90 °C using liquid nitrogen/acetone slurry. The tube was shaken very briefly, and transferred to the NMR probe which is at a preset temperature. NMR spectra were acquired every 10 min at a desired temperature.

4.5 References

1. Kaminsky, W.; Arndt, M. *Adv. Polym. Sci.* **1996**, *127*, 143-187.

2. Brintzinger, H. H.; Fischer, D.; Mulhaupt, R.; Rieger, B.; Waymouth, R. M. *Angew. Chem. Int. Ed. Engl.* **1995**, *34*, 1143-1170.

3. Alt, H.G.; Koeppl, A. *Chem. Rev.* **2000**, *100*, 1205-1221.

4. Ittel, S.D.; Johnson, L.K.; Brookhart, M. *Chem. Rev*. **2000**, *100*, 1169-1203.

5. Britovsek, G.J.P.; Gibson, V.C.; Wass, D.F. *Angew. Chem. Int. Ed. Engl.* **1999**, *38*, 428-447.

6. Mecking, S. *Angew. Chem. Int. Ed. Engl.* **2001**, *40*, 534-540.

7. Gibson, V.C.; Spitzmesser, S.K. *Chem. Rev.* **2003**, *103*, 283-315.

8. Boffa, L.S.; Novak, B.M. *Chem. Rev.* **2000**, *100*, 1479-1493.

9. Ostoja-Starzewski, K. A.; Witte, J. *Angew. Chem. Int. Ed. Engl.* **1985**, *24*, 599-601.

10. Ostoja-Starzewski, K. A.; Witte, J. *Angew. Chem. Int. Ed. Engl.* **1987**, *26*, 63-64.

11. Klabunde, U.; Ittel, S. D. *J. Mol. Catal.* **1987**, *41*, 123-134.

12. Klabunde, U.; Mülhaupt, R.; Herskovitz, T.; Janowicz, A. H.; Calabrese, J.; Ittel, S. D. *J. Polym. Sci., Part A: Polym. Chem.* **1987**, *25*, 1989-2003.

13. Kurtev, K.; Tomov, A. *J. Mol. Catal.* **1994**, *88*, 141-150.

14. Johnson, L. K.; Bennett, A. M. A.; Ittel, S. D.; Wang, L.; Parthasarathy, A.; Hauptman, E.; Simpson, R. D.; Feldman, J.; Coughlin, E. B. WO 98/30609, **1998**.

15. Wang, C.; Friedrich, S.; Younkin, T.R.; Li, R.T.; Grubbs, R.H.; Bansleben, D.A.; Day, M.W. *Organometallics* **1998**, *17*, 3149-3151.

16. Younkin, T.R.; Connor, E.F.; Henderson, J.I.; Friedrich, S.K.; Grubbs, R.H.; Bansleben, D.A. *Science* **2000**, *287*, 460-462.

17. Hicks, F.A.; Brookhart, M. *Organometallics* **2001**, *20*, 3217-3219.

18. Jenkins, J.C.; Brookhart, M. *Organometallics* **2003**, *22*, 250-256.

19. Hicks, F.A.; Jenkins, J.C.; Brookhart, M. *Organometallics* **2003**, *22*, 3533-3545.

20. Rachita, M. J.; Huff, R. L.; Bennett, J. L.; Brookhart, M. *J. Polym. Sci., Part A: Polym. Chem.* **2000**, *38*, 4627-4640.

21. Dohler, T.; Gorls, H.; Walther, D. *Chem. Commun*. **2000**, 945-946.

22. Walther, D.; Dohler, T.; Theyssen, N.; Gorls, H. *Eur. J. Inorg. Chem*. **2001**, 2049-2060.

23. Tian, G.; Boone, H.W.; Novak, B.M. *Macromolecules* **2001**, *34*, 7656-7663.

24. Elia, C.; Elyashiv-Barad, S.; Sen, A.; Lopez-Fernandez, R.; Albeniz, A.C.; Espinet, P. *Organometallics* **2002**, *21*, 4249-4256.

25. Rulke, R.E.; Ernsting, J.M.; Spek, A.L.; Elsevier, C.J.; van Leeuwen, Piet W. N. M.; Vrieze, K. *Inorg. Chem.* **1993**, *32*, 5769-5778.

26. Albeniz, A.C.; Espinet, P.; Lopez-Fernandez, R.; Sen, A. *J. Am. Chem. Soc.* **2002**, *124*, 11278-11279.

27. Pangborn, A.B.; Giardello, M.A.; Grubbs, R.H.; Rosen, R.K.; Timmers, F.J. *Organometallics* **1996**, *15*, 1518-1520.

Chapter 5

NEUTRAL PALLADIUM(II) COMPLEXES WITH P-N-O CHELATE: SYNTHESES, CHARACTERIZATION, AND THEIR REACTIVITIES

5.1 Introduction

Since the discovery of metallocene-based catalysts for ethene and α-olefin polymerization,[1,2] numerous efforts have been directed at the development of non-metallocene-based[3-6]complexes for the successful homo- or co-polymerization of polar- and nonpolar-alkenes through successive coordination insertion mechanism. The majority of the studies utilizing late transition metal complexes for the alkene polymerizations where an insertion mechanism is operative have been based on the cationic palladium(II) complexes.[3] Although there have been numerous achievements in the area of cationic palladium(II)-initiated addition polymerization, the electrophilicity of the cationic palladium compounds still limits their catalytic application to addition polymerization of monomers having polar functionalities, such as acrylates.

In light of the limited compatibility of the cationic Ni and Pd complexes with polar functional groups on a monomer, considerable attention has been made in developing nickel- or palladium-based neutral complexes for polymerization of polar- or non-polar vinyl monomers.[5,6] Recently, several neutral nickel catalysts based on [N,O] chelate ligands following SHOP(Shell Higher Olefin Process)-type catalysts[7-11] have been reported.[12-20] Furthermore, neutral palladium catalysts based on [N,N] chelate ligand[21] and non-chelate ligand[22] have been reported. On the other hand, there have been alternate

approaches developing overall-charge-neutral zwitterionic complexes based on nickel or palladium for the polymerization of alkenes.[23-28]

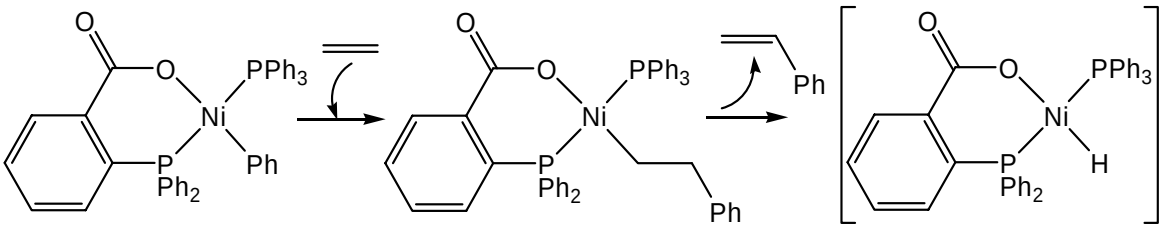

Generation of active SHOP catalyst

In most of the systems utilizing nickel-based neutral or zwitterionic complexes, non-polar alkenes have been tested for the polymerization. There has been only one case reported by Grubbs[14] where a neutral transition metal-based complex showed the unprecedented functional group tolerance of the catalytic system by polymerizing alkenes having polar functionality. A zwitterionic palladium complex showed copolymerization activity of carbon monoxide and ethene.[28] However, other palladium-based neutral systems produced poly(methyl acrylate) through a radical pathway.[21,22]

As a part of the aforementioned efforts, we decided to develop a serious of neutral palladium-based complexes to be utilized as catalysts with or without cocatalyst for the polymerization of polar- or non-polar alkenes. We report here the synthesis of neutral palladium complexes based on [P,N,O] chelate ligands, which can be converted to active species, such as a zwitterionic complex, by incorporating a Lewis acid. They are fully characterized in solution by spectroscopic methods and in solid-state by X-ray diffraction.

The complexes in combination with a different Lewis acid show characteristic reactivity toward polar- or non-polar alkenes

5.2 Results and Discussion

5.2.1 Ligand Synthesis

Hydroxyliminophosphine(P^N^O) ligands(**1** and **2**, Scheme **5-1**) were prepared by a condensation reaction between an aldehyde and an amine compound in the presence of formic acid as a catalyst. For ligand **1**, 2,4-di-*tert*-butylphenol was transformed by nitration[29] to 2-nitro-4,6-di-*tert*-butylphenol, which was converted to 2-amino-4,6-di-*tert*-butyl-phenol by hydrogenation over 10% Pd/C in ethanol at ambient temperature. The 2-amino-4,6-di-*tert*-butyl-phenol purified by recrystallization from methanol was then reacted with 2-(diphenylphosphino)benzaldehyde to afford ligand **1** as a yellow crystalline solid in good yield. The first step in the synthesis of ligand **2** was the preparation of (2-aminophenyl)diphenylphosphine,[30] which was condensed with 3,5-di-*tert*-butyl-2-hydroxybenzaldehyde giving the target compound **2**. The *CH* imine proton of these compounds shows resonances at 9.14 and 8.47 ppm, respectively, with the corresponding ^{13}C NMR resonances at 155.7 and 163.9 ppm, respectively. In the ^{1}H NMR spectrum of the ligand **1**, the imine proton (–N=C*H*) shows resonance as a doublet with a coupling constant $J_{P\text{-}H}$ = 4.333 Hz, indicating that there is a through-space coupling in which the imine proton is directed towards the lone pair electrons on the phosphorus atom.[31,32] In the case of complex **2**, there is no observed P-H coupling for the

corresponding imine proton. ^{31}P NMR spectra of **2** show resonances at -10.28 and -13.54 ppm, respectively.

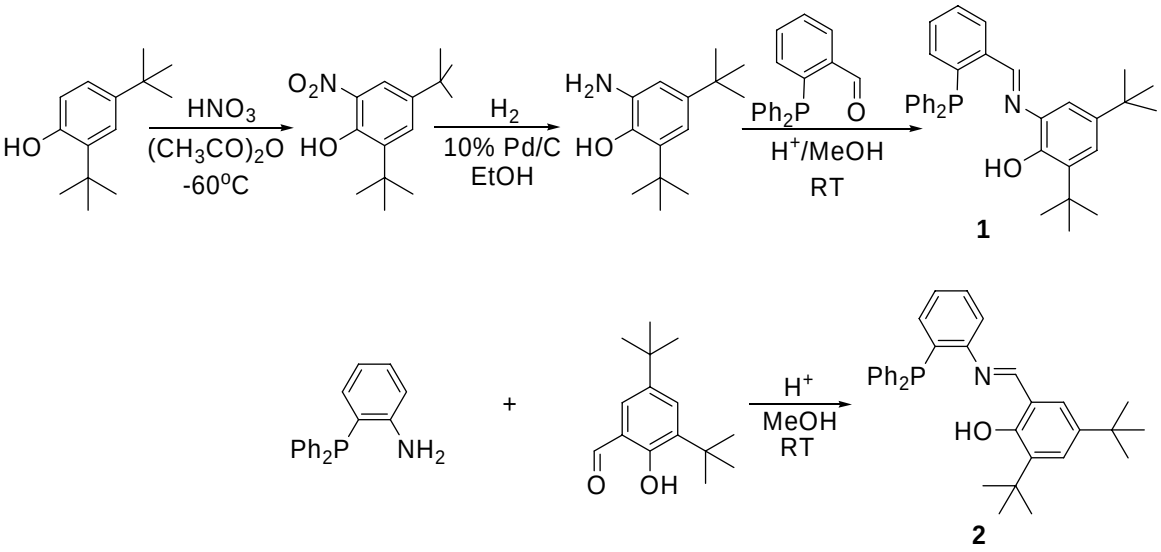

Scheme **5-1**

5.2.2 Complex Synthesis

Reaction of ligands **1** and **2** with (*N*,*N*,*N*',*N*'-tetramethylethylenediamine) dimethylpalladium(II) [(TMEDA)$PdMe_2$][33] in diethyl ether at ambient temperature caused the evolution of methane and generated the corresponding (P^N^O)PdMe complexes (Scheme **5-2**). Both compounds were obtained in almost quantitative yields as purple **3** or orange **4** solids. Recrystallization from methylene dichloride and pentane gave the analytically pure product. Spectroscopic analysis using 1D and 2D nuclear magnetic resonance (NMR) confirms the structure of the target complexes **3** and **4**.

As for the neutral complexes, palladium bound methyl groups in both cases show their ^{1}H NMR resonances at 0.60 and 0.72 ppm, with corresponding ^{13}C NMR resonances at -0.6 to -2.7 ppm, respectively, as a doublet with a coupling constant $^{3}J_{P\text{-}H}$ = 2.744 and 2.196 Hz, respectively. This is in the typical range for the methyl group *cis* to the phosphorus. ^{1}H NMR resonances for Ar-C*H*=N- are at 8.55 and 8.86 ppm with corresponding ^{13}C NMR resonances at 168.4 and 158.6 ppm, respectively. ^{31}P NMR spectra show resonances at 39.85 and 40.50 ppm, respectively. A downfield shift of *ca.* 50 ppm, in ^{31}P NMR, with respect to the free ligand reflects the coordination of the phosphine group to the palladium metal.

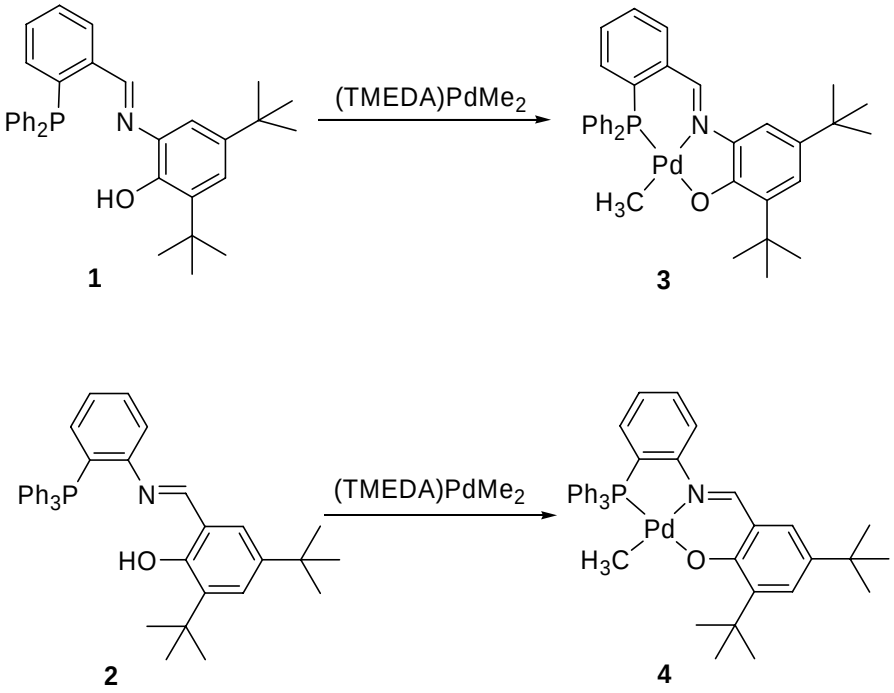

Scheme **5-2**

Figure 5-1

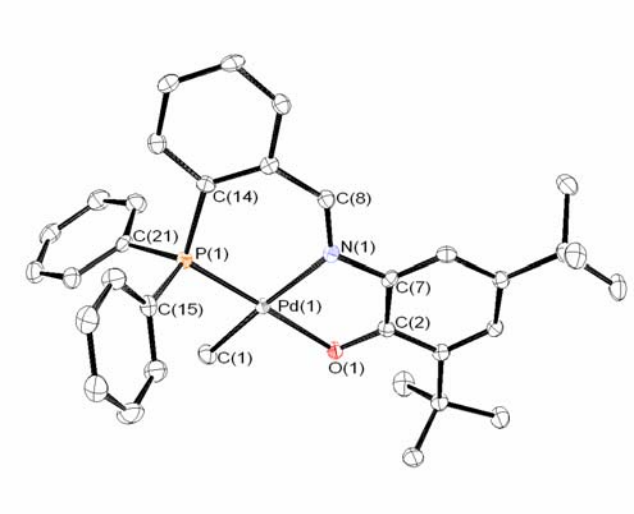

Figure 5-1: ORTEP view of complex 3. Hydrogen atoms are omitted for clarity.

Figure 5-2

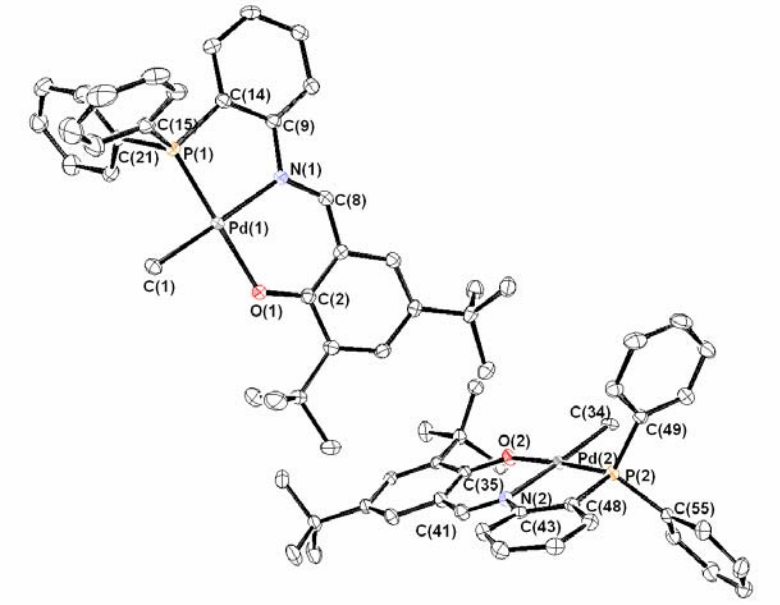

Figure 5-2: ORTEP view of complex 4. Hydrogen atoms are omitted for clarity.

Table 5-1

Table 5-1: Selected Bond distances (Å) and Angles (°) for **3**

C1-Pd1	2.033(2)	N1-C7	1.434(3)
Pd1-O1	2.0589(17)	N1-C8	1.288(3)
Pd1-N1	2.071(2)	P1-C14	1.823(3)
Pd1-P1	2.1809(7)	P1-C21	1.823(3)
O1-C2	1.314(3)	P1-C15	1.834(3)
C1-Pd1-O1	91.03(9)	C1-Pd1-N1	170.32(10)
O1-Pd1-N1	81.59(8)	C1-Pd1-P1	90.77(8)
O1-Pd1-P1	175.28(5)	N1-Pd1-P1	97.07(6)
C14-P1-C21	105.11(12)	C14-P1-C15	105.45(12)
C21-P1-C15	106.58(12)	C14-P1-Pd1	111.64(9)
C21-P1-Pd1	115.32(8)	C15-P1-Pd1	112.01(9)
C2-O1-Pd1	112.15(15)	C8-N1-C7	121.3(2)
C8-N1-Pd1	127.09(18)	C7-N1-Pd1	110.64(15)

Table 5-2

Table 5-2: Selected Bond distances (Å) and Angles (°) for **4**

Pd1-C1	2.0488(19)	Pd1-O1	2.0629(15)
Pd1-N1	2.0826(16)	Pd1-P1	2.1728(9)
P1-C14	1.8184(19)	P1-C15	1.815(2)
P1-C21	1.820(2)	O1-C2	1.300(2)
N1-C8	1.305(2)	N1-C9	1.440(2)
C1-Pd1-O1	90.34(7)	C1-Pd1-N1	176.20(7)
O1-Pd1-N1	91.80(6)	C1-Pd1-P1	91.27(6)
O1-Pd1-P1	176.36(4)	N1-Pd1-P1	86.78(5)
C15-P1-C14	106.91(9)	C15-P1-C21	103.51(9)
C14-P1-C21	105.46(9)	C15-P1-Pd1	119.80(7)
C14-P1-Pd1	101.39(6)	C21-P1-Pd1	118.44(7)
C8-N1-C9	120.32(16)	C2-O1-Pd1	127.18(12)
C8-N1-Pd1	122.41(13)	C9-N1-Pd1	117.27(12)

The molecular structures of complexes **3** and **4** were determined by single-crystal X-ray structure analysis. X-ray quality crystals were prepared by slow diffusion of pentane into a concentrated solution of **3** or **4** in methylene chloride at ambient temperature. The ORTEP plots of the complexes are shown in Figures **5-1** and **5-2**, respectively. The selected bond lengths and angles are given in Table **5-1** and **5-2**. The crystallographic data and the data collection parameters for complexes **3** and **4** are summarized in Table **5-3**. The ligand in complex **3** is isomeric with that in complex **4**, in that the relative positions of the five- and six-membered [P,N] and [N,O] chelate rings formed on complexation are reversed. As we expected, complex **3** has six-membered [P,N] and five-membered [N,O] chelate rings. Whereas, [P,N] and [N,O] chelate rings form five- and six-membered rings respectively in complex **4**.

In the solid state, the complexes adopt geometries about the palladium metal center best described as a distorted square planar arrangement due to the bulk of the phosphine group and the ring strain of the [P,N] chelate (complex **3**) or the [N,O] chelate (complex **4**) six-membered rings. For complex **3**, bond angles substantially deviated from idealized square planar geometry by virtue of the constraint. The bond angle of P(1)-Pd(1)-N(1) in complex **3** is 97.07(6)^{o}, which is similar to that of platinum-based analogue where Pt bound Cl instead of CH_3 and with no *t*-butyl groups on the aromatic ring.[34] It seems that the large bond length difference between P(1)-C(14) and N(1)-C(8) (1.823(3) and 1.288(3), respectively in the [P,N] six-membered ring in complex **3** caused severe distortion. The substantial decrease in the O(1)-Pd(1)-N(1) angle (81.59(8)^{o}) is observed due to the compensation by in large due to a concomitant increase in the P(1)-

Pd(1)-N(1) angle. On the other hand, in complex **4**, the [N,O] six-membered ring is quite symmetrical, thereby resulting in less ring strain than that of complex **3**.

Table 5-3

Table 5-3: Crystallographic Data and data Collection Parameters for complexes **3a-e** and **4**

	3	**4**
formula	$C_{34}H_{38}NOPPd$	$C_{34}H_{38}NOPPd$
mol wt	614.02	614.02
Temp.(K)	98(2)	98(2)
Wavelength(Å)	0.71073	0.71073
crystal system	monoclinic	triclinic
space group	P2(1)/c	$P\bar{1}$
a(Å)	11.8304(15)	12.620(6)
b(Å)	12.6496(16)	12.730(3)
c(Å)	20.121(3)	19.005(5)
α(deg)	90°	77.074(8)°
β(deg)	106.270(3)°	84.374(17)°
γ(deg)	90°	88.126(18)°
Volume($Å^3$)	2890.6(6)	2961.2(17)
Z	4	4
F(000)	1272	1272
R(*F*)	0.0373	0.0264
$R_w(F)$	0.0813	0.0668
$D_{calcd}(Mg/m^3)$	1.411	1.377

5.2.3 Reactivity of the Complexes

Catalytic activity of complexes **3** and **4** for polymerization of several vinyl monomers, such as ethene, methyl acrylate, and butylester norbornene, has been tested in dichloromethane at ambient temperature or chlorobenzene at 60°C. None of the tested reactions gave polymeric product. NMR scale experiments of vinyl monomers with one of the complexes showed no reactions of either oligomerization or any other catalytic

process occurred. Activation of the complexes by using a Lewis base, FAB, $B(C_6F_5)_3$, has been attempted. It was expected that FAB interacts with the complexes through oxygen of the aryloxy group to form a zwitterionic compound affording a vacant site for an incoming monomer. However, no polymeric product has been obtained from the reactions, except in the case of the reaction of methyl acrylate with complex **3**, in which a trace amount (*ca*. 7%) of product was produced. In the NMR scale experiment of the reaction between complex **3** or **4** with FAB in dichloromethane-d_2, we observed the abstraction of the palladium bound methyl group rather than the aryloxy group from **3** or **4** with FAB. Upon addition of the FAB to the purple solution of **3** in dichloromethane-d_2, the color of the solution changed to reddish brown in a few seconds, indicating a reaction occurred. ^{1}H NMR of the solution shows broad resonance as a singlet at 0.46 ppm, a typical resonance of the non-coordinating $MeB(C_6F_5)_3^-$. $^{11}B\{^1H\}$ NMR, one of the most notable spectroscopic evidences, shows sharp resonance at -15.29 ppm supporting the formation of the $[MeB(C_6F_5)_3]^-$ anion.[35] On the other hand, complex **4** also shows a similar reaction pattern with FAB, having 0.49 ppm in ^{1}H NMR and -15.29 ppm in $^{11}B\{^1H\}$ NMR.

Clear evidence that the complexes cannot be activated by FAB directed us to test several aluminum-based Lewis bases, such as aluminum trichloride, triethyl aluminum, $Al(C_6F_5)_3$ (FAL) or methyaluminoxane (MAO) for the polymerization of vinyl monomers. The system utilizing aluminum trichloride generated a small amount of polyethylene or no poly(methyl acrylate) in chlorobenzene at 60^{o}C. On the other hand, the polymerization reaction using triethyl aluminum as a cocatalyst showed interesting results (Table **5-4**).

Table 5-4

Table 5-4: Polymerization of vinyl monomers using complexes **3** and **4** with $AlEt_3$[a]

entry	Complex ($x10^{-5}$mol)	$AlEt_3$ ($x10^{-5}$mol)	ethene	Monomer MA(g)	MMA(g)	Yield(g)	M_n[b]	M_w/M_n[b]
1	**3**(3.3)	3.3	700psi	-	-	0.02		
2	**3**(3.3)	3.3	700psi	1	-	0.08		
3	**3**(3.3)	3.3	-	2	-	0.28		
4[c]	**3**(3.3)	3.3	-	2	-	0.35		
5[d]	**3**(3.3)	3.3	-	2	-	0.40		
6	**4**(3.3)	3.3	700psi	-	-	0.03		
7	**4**(3.3)	3.3	700psi	1	-	0.05		
8	**4**(3.3)	3.3	-	2	-	1.53		
9[c]	**4**(3.3)	3.3	-	2	-	1.65		
10[d]	**4**(3.3)	3.3	-	2	-	1.21		
11	-	3.3	-	2	-	0.61		
12[d]	-	3.3	-	2	-	0.40		

* table continued to next page

[a]Carried out in chlorobenzene (5g) at 60°C for 24h. [b]Number-average molecular weight (*M*n) and polydispersity index (PDI) determined by GPC relative to poly(styrene) standards. [c]Carried out in CH_2Cl_2 at ambient temperature. [d]Repeated reaction.

Table **5-4 continued**

Table **5-4**: Polymerization of vinyl monomers using complexes **3** and **4** with $AlEt_3$[a]

entry	Complex ($x10^{-5}$ mol)	$AlEt_3$ ($x10^{-5}$ mol)	Monomer ethene	MA(g)	MMA(g)	Yield(g)	M_n[b]	M_w/M_n[b]
13	**4**(0.8)	0.8	-	0.5	-	0.11	131k	1.4
14	**4**(0.8)	1.6	-	0.5	-	0.19	130k	1.2
15	**4**(0.8)	2.4	-	0.5	-	0.18	101k	1.2
16	**4**(0.8)	3.2	-	0.5	-	0.08		
17	**4**(0.8)	0.8	-	0.25	-	0.05	82k	1.2
18	**4**(0.8)	0.8	-	0.75	-	0.25	82k	1.5
19	**4**(0.8)	0.8	-	1.0	-	0.52	104k	1.3
20	**3**(3.3)	3.3	-	-	2	0.17	6674k	1.0
							126k	1.2
21	**4**(3.3)	3.3	-	-	2	1.01	4815k	1.1
							95k	1.2

[a]Carried out in chlorobenzene (5g) at 60°C for 24h. [b]Number-average molecular weight (*M*n) and polydispersity index (PDI) determined by GPC relative to poly(styrene) standards using chloroform as eluent.

As mentioned earlier, neutral complex **3** or **4** by itself is inactive for ethene, MA, or MMA polymerization. However, the polymerization by premixing the complex **3** or **4** with 1 *equiv*. of $AlEt_3$ in chlorobenzene followed by addition of MA or MMA is active, producing PMA or PMMA. The complex **3** mixture with $AlEt_3$ produced PMA or PMMA in relatively low yield (entries 3-5, 20, Table **5-4**). The complex **4** with $AlEt_3$ is more

active for the polymerization of MA or MMA (entries 8-10, 21, Table **5-4**) than the complex **3** with $AlEt_3$. Although overall running time was 24 hours, polymerization of MA using complex **4** with $AlEt_3$ seems to be almost finished in 2 hours, making the system hard to be stirred. Insolubility of the PMA produced from the reaction condition in chloroform or dichlorobenzene at ambient temperature or at high temperature (up to 150°C) did not allow us to analyze the polymer at all. The PMMA formed by complex **3** or **4** mixture has an extremely narrow polydispersity index of M_w/M_n=1.0 to 1.2 with bimodal characters. Polymerization of MA using $AlEt_3$ by itself was carried out (entries 11-12, Table **5-4**). It showed similar activity as the mixture of complex **3** and $AlEt_3$. In dilute solutions, polymerizations of MA using the complex **4** and $AlEt_3$ with different molar ratio of complex to $AlEt_3$ or with different molar ratio of complex mixture to monomer were also tested (entries 13-19, Table **5-4**). They did not show much difference in molecular weight or molecular weight distribution. Attempted homo- and co-polymerization of ethene with/without MA resulted in trace amount of polymeric product.

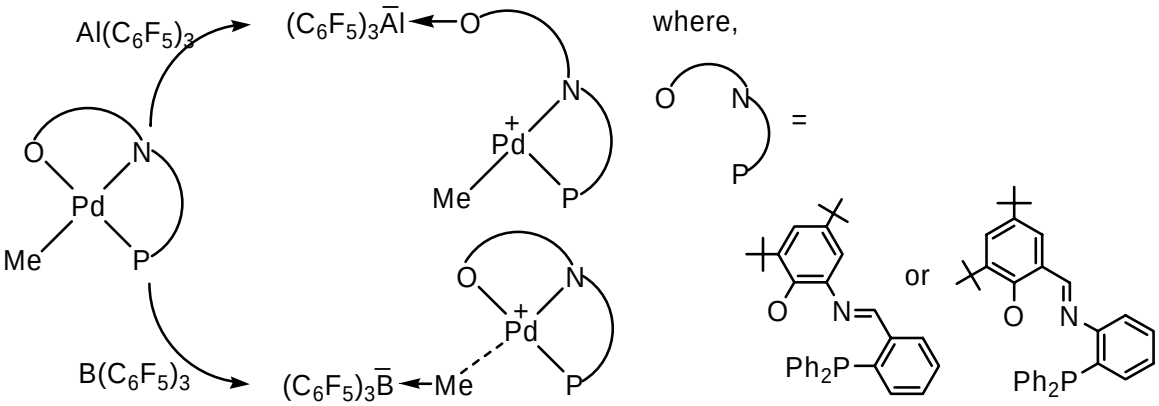

Scheme **5-3**

Table 5-5

Table 5-5: Polymerization of vinyl monomers using complex **3** with FAL, $Al(C_6F_5)_3$, as a cocatalyst

entry	**3**($x10^{-5}$ mol)	FAL ($x10^{-5}$ mol)	Monomers(g)	Yield(g)
1	0.8	0.8	NB(2)	trace
2[b]	0.8	2.4	NB (2)	~2
3	0.8	2.4	Bu-NB(1.5)	1.11
4	0.8	2.4	Etester-NB(2)	trace
5	0.8	2.4	MA(2)	trace
6	0.8	2.4	MMA(2)	trace

Polymerization of various vinyl monomers using premixed complex **3** and FAL, $Al(C_6F_5)_3$, was carred out in toluene at ambient temperature. Although the mixture did not show any activity for the polymerization of polar monomers (entries 4-6, Table **5-5**), poly(norbornene) or poly(*n*-butyl-nobornene) was produced in good to almost quantitative yield when 3 *equiv*. of FAL was pre-introduced (entires 1-3, Table **5-5**). Based on the results of the polymerizations using complex **3** or **4** with FAB or FAL and NMR experiments, two different reaction patterns of the Lewis acids, FAB and FAL, toward the title complexes are expected (Scheme **5-3**). As already mentioned above, FAB interacts with a palladium bound methyl group to give an ionic pair, in which there is a vacant site for an incoming monomer. However, the resultant compound cannot pursue the next insertion or a subsequent coordination reaction because there is no driving force for further reaction. On the other hand, FAL favors oxygen functionality to form a dative bond with it. In complex **3** or **4**, it looks to generate a zwitterionic

compound as shown in Scheme **5-3**, which can initiate the polymerization reaction of a non-polar vinyl monomer as a cationic complex.[36]

Table **5-6**

Table **5-6**: Polymerization of vinyl monomers using 3 or 4 with MAO as a cocatalyst[a]

entry	Complex	Monomers	Yield (g)
1	-	NB(2g)	n.r.
2	-	ethene (700psi)	Trace
3[b]	-	ethene (700psi)	Trace
4	**3**	NB(2g)	1.62
5	**4**	NB(2g)	1.58
6	**3**	ethene (700psi)	0.35
7[b]	**3**	ethene (700psi)	0.24
8	**3**	Bu-NB(2g)	0.38
9	**3**	Etester-NB(2g)	n.r.
10	**3**	MA(2g)	n.r.
11	**3**	MMA(2g)	n.r.

[a]Carried out in toluene (15mL) at ambient temperature for 3h, complex (3.13×10^{-5} mol), MAO (500mg). [b]60°C.

Polymerization activities of the complex **3** and **4** for vinyl monomers have been tested further with methylaluminoxane, MAO, as a cocatalyst. Both complexes have been activated by MAO, and polymerized non-polar vinyl monomers with no difference between complex **3** and **4** (entries 4 and 5, Table **5-6**). In the case of the norbornene

polymerization, the reactions have finished in a few minutes forming a lump of polymer, which blocks effective stirring.

In conclusion, we first synthesized two neutral Pd(II) complexes, [3,5-di-^{t}Bu-2-(OH)C_6H_2N=CH-2-P$Ph_2C_6H_4$]PdMe_2 (**3**) and [3,5-di-^{t}Bu-2-(OH)C_6H_2CH=N-2-P$Ph_2C_6H_4$]PdMe_2 (**4**) in almost quantitative yield from the ligands, 3,5-di-^{t}Bu-2-(OH)C_6H_2N=CH-2-P$Ph_2C_6H_4$ **(1)** and 3,5-di-^{t}Bu-2-(OH)C_6H_2CH=N-2-P$Ph_2C_6H_4$ **(2)**, respectively. The title complexes **3** and **4** have been characterized, and their structures have been confirmed by X-ray analysis. In the solid state, the complexes adopt geometries about the palladium metal center best described as a distorted square planar arrangement. The complex **3** showed much more deviation from the idealized square planar geometry by virtue of the constraint caused by the huge bond length difference between P(1)-C(14) and N(1)-C(8) (1.823(3) and 1.288(3), respectively in the [P,N] six-membered ring. Without the assistance of a cocatalyst, complexes **3** and **4** have not shown any catalytic activity for the polymerization or oligomerization of an alkene. In combination with $AlEt_3$, **3** and **4** produced PMA, where **4** was observed to have a higher activity than **3**. The complex **4** with $Al(C_6F_5)_3$ as a cocatalyst has polymerized norbornene or *n*-butylnorbornene in excellent yield, but with $B(C_6F_5)_3$, it has not produced any polymeric product. Different reaction pathways between complexes **3** or **4** and $Al(C_6F_5)_3$ or $B(C_6F_5)_3$ have been proposed based on the results of the polymerization and the NMR experiment. The title complexes have been expected to react with $Al(C_6F_5)_3$ affording a zwitterionic complex, which can initiate the polymerization of a non-polar alkene. The zwitterionic compounds produced have not polymerized polar alkenes due to their cationic character. Utilizing MAO as a co catalyst, **3** and **4** produced

poly(norbornene) in good yield with no activity difference between **3** and **4**. The combination has also not produced any polymer from monomers having polar functionality.

5.3 Experimental Section

5.3.1 General Considerations

All syntheses and manipulations of air- and moisture-sensitive compounds were carried out in flamed Schlenk-type glassware on a dual-manifold Schlenk line, a high vacuum with argon line, or in a nitrogen-filled glovebox.

Nuclear magnetic resonance (NMR) spectra were recorded on a Bruker DRX 400 NMR spectrometer, DPX 300 NMR spectrometer, and CDPX 300 NMR spectrometer. Splitting patterns are designated as follows: s, singlet; bs, broad singlet; d, doublet; dd, doublet of doublets; t, triplet; td, triplet of doublets; sept, septet; m, multiplet. All ^{1}H NMR spectra are reported in δ units, parts per million (ppm) downfield from tetramethylsilane. All ^{13}C NMR spectra are reported in ppm relative to tetramethylsilane using CD_2Cl_2, toluene-d8, or chlorobenzene-d5 as a secondary standard. Variable-temperature ^{1}H NMR experiments were performed on a Bruker DPX 300 NMR spectrometer, using CD_2Cl_2, toluene-d_8, or chlorobenzene-d_5 as solvent. Actual NMR probe temperatures were measured using anhydrous methanol (with 0.03% concentrated HCl) or ethylene glycol (neat) in a 5 mm NMR tube (see **2.5.1** and **2.5.2**). NMR analyses of polymers were performed on a Brüker DPX 300 NMR spectrometer at ambient or elevated temperature, using $CDCl_3$,

chlorobenzene-d_5, dichlorobenzene-d_4, or tetrachloroethane-d_2 as solvent unless otherwise noted.

Size exclusion chromatography data were obtained on a Shimadzu SEC System using a three-column bank (Styragel 7.8x300 mm columns, 100-5,000 D, 500-30,000 D, 2000-4,000,000 D), a Shimadzu RID-10A Differential Refractometer, and a Shimadzu LC-10AT pump/controller. Size exclusion chromatography was performed in chloroform at ambient temperature and calibrated to polystyrene standards.

Chlorobenzene and dichloromethane was obtained from Aldrich and dried via passage over a column of activated alumina (LaRoche A-2).[37] Toluene and diethyl ether were deoxygenated, dried via passage over a column of activated alumina (LaRoche A-2), and columns of Engelhard CU-0226S[37]. Pentane and tetrahydrofuran were distilled under nitrogen from sodium benzophenone ketyl. All solvents were degassed by repeated freeze-pump-thaw cycles, and stored over 4 Å molecular sieves under nitrogen. Norbornene was purchased from Acros Organics and used without further purification. Methyl acrylate and methyl methacrylate were purchased from Aldrich and used after repeated freeze-pump-thaw cycles prior to use. Aluminum trichloride and triethyl aluminium were purchased from Aldrich Chemical Co., and used without further purification. MAO, methylaluminoxane, purchased as 10 wt. % solution in toluene from Aldrich Chemical Co. was stored under nitrogen as a solid by removing solvent under vacuum, and prepared as a 20 wt.% solution in toluene before use. Tris(pentafluorophenyl)borane, $B(C_6F_5)_3$, was purchased from Strem and used without further purification. Tris(pentafluorophenyl)alane, $Al(C_6F_5)_3$, was prepared as a toluene adduct form of $Al(C_6F_5)_3 \cdot (toluene)_{1/2}$ according to a literature procedure.[38] *Extra caution*

should be taken for the handling this material because of its thermal and shock sensitivity.[39]

2-(diphenylphosphino)benzaldehyde, 3,5-di-*tert*-butyl-2-hydroxybenzaldehyde, and 2,4-di-*tert*-butylphenol were purchased from Aldrich and used without further purification. Palladiumdichloride(II) was purchased from Strem and used without further purification. 2-nitro-4,6-di-*tert*-butylphenol,[29] (N,N,N',N'-tetramethylethylenediamine)-dimethylpalladium(II) [(TMEDA)$PdMe_2$][33] and (2-aminophenyl)diphenylphosphine[30] were prepared as previously reported.

5.3.2 Synthesis of Compounds

2-Amino-4,6-di-*tert*-butyl-phenol. To 2-nitro-4,6-di-*tert*-butylphenol in ethanol was add 10% Pd/C. The flask was purged with hydrogen gas, and attached balloon inflated with hydrogen. The reaction mixture was stirred for 2 hours. After removing solvent, the white solid was recrystallized from methanol.

3,5-di-^{t}Bu-2-(OH)C_6H_2N=CH-2-$PPh_2C_6H_4$ (1). To 2-(diphenylphosphino)-benzaldehyde (1.13g, 3.9 mmol) in methanol(50 ml) was added 2-amino-4,6-di-*tert*-butyl-phenol (0.86g, 3.9 mmol), followed by catalytic amount of formic acid (2 drops). The solution was stirred at room temperature for 12h. The resulting yellow-colored precipitate was filtered off and was washed with methanol to provide **1** as a yellow crystalline solid. Yield 1.7g (86%). ^{1}H NMR($CDCl_3$): δ 9.14 (d, 1H, Ar-C*H*=N-), 8.10 (m, 1H), 7.48 (dt, 1H), 7.34 (br, 11H), 7.21 (d, 1H), 6.90 (m, 1H), 6.74 (d, 1H) (Ar*H*), 7.72

(s, 1H, *H*O-Ar), 1.45 (s, 9H), 1.30 (s, 9H) (-C(CH_3)$_3$. ^{13}C NMR($CDCl_3$): δ 155.7 (-*C*H=N-), 149.0, 141.5 139.4, 139.1, 137.0, 136.9, 135.5, 134.6, 134.5, 134.3, 131.0, 129.4, 129.2, 129.2, 129.1, 123.7, 110.8 (Ar), 35.3, 34.9 (-*C*Me$_3$), 32.0, 29.8 (-C(*C*H$_3$)$_3$). ^{31}P NMR ($CDCl_3$) -10.28 (Ph_2*P*-Ar)

3,5-di-^{t}Bu-2-(OH)C_6H_2CH=N-2-$PPh_2C_6H_4$ (2). To 3,5-di-*tert*-butyl-2-hydroxybenzaldehyde (1g, 4.3 mmol) in methanol(50 ml) was added (2-aminophenyl)diphenylphosphine (1.18g, 4.3 mmol), followed by catalytic amount of formic acid (2 drops). The solution was stirred at room temperature for 12h. Slow concentration of the resulting solution led to precipitation of the product. The yellow precipitate was filtered off and was washed with methanol to provide **1** as a yellow crystalline solid. The compound was recrystallized from methylene dichloride/methanol. Yield 1.6g (76%). ^{1}H NMR($CDCl_3$): δ 12.91 (s, 1H, *H*O-Ar) 8.47 (s, 1H, Ar-C*H*=N-), 7.44-6.94 (m, 16H, Ar*H*), 1.49 (s, 9H), 1.35 (s, 9H) (-C(CH_3)$_3$. ^{13}C NMR($CDCl_3$): δ 163.9 (-*C*H=N-), 158.6, 152.3, 140.6, 137.3, 136.7, 136.5, 134.9, 134.6, 133.7, 133.6, 133.4, 130.3, 129.1, 128.9, 128.8, 128.5, 127.3, 126.9, 118.6, 118.0 (Ar), 35.5, 34.6 (-*C*Me$_3$), 31.9, 29.8 (-C(*C*H$_3$)$_3$). ^{31}P NMR ($CDCl_3$) -13.54 (Ph_2*P*-Ar)

[3,5-di-^{t}Bu-2-(OH)C_6H_2N=CH-2-$PPh_2C_6H_4$]$PdMe_2$ (3) To (TMEDA)$PdMe_2$ (220mg, 0.87mmol) in diethyl ether (30mL) was added 3,5-di-^{t}Bu-2-(OH)C_6H_2N=CH-2-$PPh_2C_6H_4$ (**1**) (430mg, 0.0.87mmol) in diethyl ether (10mL). The reaction mixture was stirred for 12 hours, which was filtered to remove a small quantity of dark insoluble material. The solvent was removed *in vacuo* to yield a purple solid. Recrystallization from methylene/pentane gave a purple crystalline solid which was suitable for X-ray crystal structure analysis. Yield >99%. ^{1}H NMR($CDCl_3$): δ 8.55 (s, 1H, Ar-C*H*=N-), 7.58-

7.41(m, 14H), 7.20(m, 2H), (Ar-H), 1.51 (s, 9H, Ar-C(CH_3)$_3$), 1.32 (s, 9H, Ar-C(CH_3)$_3$), 0.60 (d, 3H, Pd-CH_3). ^{13}C NMR(CD_2Cl_2): δ 168.4 (Ar-*C*H=N-Ar), 149.0, 148.9, 140.7, 137.6, 137.5, 135.9, 135.2, 134.2, 134.1, 132.2, 132.1, 131.7, 131.6, 131.3, 131.2, 129.2, 129.1, 126.4, 124.1, 110.7 (Ar), 35.7, 34.5 (Ar-*C*(CH_3)$_3$), 31.8, 29.5 (Ar-C(*C*H_3)$_3$), -0.6 (Pd-*C*H_3). ^{31}P NMR ($CDCl_3$) 39.85 (Pd-*P*-Ar)

[3,5-di-^{t}Bu-2-(OH)C_6H_2CH=N-2-P$Ph_2C_6H_4$]$PdMe_2$ (4) To (TMEDA)$PdMe_2$ (240mg, 0.95mmol) in diethyl ether (30mL) was added 3,5-di-^{t}Bu-2-(OH)C_6H_2CH=N-2-P$Ph_2C_6H_4$ (**2**) (469mg, 0.95mmol) in diethyl ether (10mL). The reaction mixture was stirred for 12 hours, and then filtered to remove a small quantity of dark insoluble material. The solvent was removed *in vacuo* to yield an orange solid. Recrystallization from methylene/pentane gave an orange crystalline solid which was suitable for X-ray crystal structure analysis. Yield >99%. ^{1}H NMR(CD_2Cl_2): δ 8.86 (s, 1H, Ar-C*H*=N-), 7.79-7.64(m, 5H), 7.54-7.40 (m, 9H), 7.04 (t, 1H), 6.90 (d, 1H) (Ar-*H*), 1.52 (s, 9H, Ar-C(CH_3)$_3$), 1.33 (s, 9H, Ar-C(CH_3)$_3$), 0.72 (d, 3H, Pd-CH_3). ^{13}C NMR(CD_2Cl_2): δ 158.6 (-*C*H=N-), 155.9, 142.4, 135.5, 134.2, 134.0, 133.8, 132.9, 131.9, 131.5, 131.3, 131.3, 131.2, 130.7, 130.3, 129.2, 129.1, 119.8 (Ar), 36.2, 34.2 (-*C*Me_3), 31.7, 30.0 (-C(*C*H_3)$_3$). -2.7 (Pd-*C*H_3). ^{31}P NMR ($CDCl_3$) 43.50 (Pd-*P*-Ar)

5.3.3 General Procedures for Polymerization Reactions

In a drybox under a nitrogen atmosphere, a title complex was dissolved in chlorobenzene, dichloromethane, or toluene in a 100 mL Schlenk flask. To the complex solution was introduced a cocatalyst, and the mixture was allowed to generate active

species for 5 min. while stirring at ambient temperature. A desired monomer was introduced to the flask. The reaction mixture was stirred at a desired temperature. After the specified reaction time, the reaction was quenched with aqueous HCl solution (1 N), follow by methanol. The precipitated polymer was filtered and washed with methanol. Volatiles were removed from the polymer in *vacuo*, and the polymer was dried under vacuum overnight.

5.4 References

1. Kaminsky, W.; Arndt, M. *Adv. Polym. Sci.* **1996**, *127*, 143-187.

2. Brintzinger, H. H.; Fischer, D.; Mulhaupt, R.; Rieger, B.; Waymouth, R. M. *Angew. Chem. Int. Ed. Engl.* **1995**, *34*, 1143-1170.

3. Ittel, S.D.; Johnson, L.K.; Brookhart, M. *Chem. Rev*. **2000**, *100*, 1169-1203.

4. Britovsek, G.J.P.; Gibson, V.C.; Wass, D.F. *Angew. Chem. Int. Ed. Engl.* **1999**, *38*, 428-447.

5. Mecking, S. *Angew. Chem. Int. Ed. Engl.* **2001**, *40*, 534-540.

6. Gibson, V.C.; Spitzmesser, S.K. *Chem. Rev.* **2003**, *103*, 283-315.

7. Ostoja-Starzewski, K. A.; Witte, J. *Angew. Chem. Int. Ed. Engl.* **1985**, *24*, 599-601.

8. Ostoja-Starzewski, K. A.; Witte, J. *Angew. Chem. Int. Ed. Engl.* **1987**, *26*, 63-64.

9. Klabunde, U.; Ittel, S. D. *J. Mol. Catal.* **1987**, *41*, 123-134.

10. Klabunde, U.; Mülhaupt, R.; Herskovitz, T.; Janowicz, A. H.; Calabrese, J.; Ittel, S. D. *J. Polym. Sci., Part A: Polym. Chem.* **1987**, *25*, 1989-2003.

11. Kurtev, K.; Tomov, A. *J. Mol. Catal.* **1994**, *88*, 141-150.

12. Johnson, L. K.; Bennett, A. M. A.; Ittel, S. D.; Wang, L.; Parthasarathy, A.; Hauptman, E.; Simpson, R. D.; Feldman, J.; Coughlin, E. B. WO 98/30609, **1998**.

13. Wang, C.; Friedrich, S.; Younkin, T.R.; Li, R.T.; Grubbs, R.H.; Bansleben, D.A.; Day, M.W. *Organometallics* **1998**, *17*, 3149-3151.

14. Younkin, T.R.; Connor, E.F.; Henderson, J.I.; Friedrich, S.K.; Grubbs, R.H.; Bansleben, D.A. *Science* **2000**, *287*, 460-462.

15. Hicks, F.A.; Brookhart, M. *Organometallics* **2001**, *20*, 3217-3219.

16. Jenkins, J.C.; Brookhart, M. *Organometallics* **2003**, *22*, 250-256.

17. Hicks, F.A.; Jenkins, J.C.; Brookhart, M. *Organometallics* **2003**, *22*, 3533-3545.

18. Rachita, M. J.; Huff, R. L.; Bennett, J. L.; Brookhart, M. *J. Polym. Sci., Part A: Polym. Chem.* **2000**, *38*, 4627-4640.

19. Dohler, T.; Gorls, H.; Walther, D. *Chem. Commun*. **2000**, 945-946.

20. Walther, D.; Dohler, T.; Theyssen, N.; Gorls, H. *Eur. J. Inorg. Chem*. **2001**, 2049-2060.

21. Tian, G.; Boone, H.W.; Novak, B.M. *Macromolecules* **2001**, *34*, 7656-7663.

22. Elia, C.; Elyashiv-Barad, S.; Sen, A.; Lopez-Fernandez, R.; Albeniz, A.C.; Espinet, P. *Organometallics* **2002**, *21*, 4249-4256.

23. Lee, B.Y.; Bu, X.; Bazan, G.C. *Organometallics* **2001**, *20*, 5425-5431.

24. Lee, B.Y.; Bazan, G.C.; Vela, J.; Komon, Z.J.A.; Bu, X. *J. Am. Chem. Soc.* **2001**, *123*, 5352-5353.

25. Kim, Y.H.; Kim, T.H.; Lee, B.Y.; Woodmansee, D.; Bu, X.; Bazan, G.C. *Organometallics* **2002**, *21*, 3082-3084.

26. Lee, B.Y.; Kim, Y.H.; Shin, H.J.; Lee, C.H. *Organometallics* **2002**, *21*, 3481-3484.

27. Shim, C.B.; Kim, Y.H.; Lee, B.Y.; Shin, D.M.; Chung, Y.K. *J. Organomet. Chem.* **2003**, *675*, 72-76.

28. Lu, C.C.; Peters, J.C. *Journal of the American Chemical Society* **2002**, *124*, 5272-5273.

29. Cross, G. G.; Fischer, A.; Henderson, G. N. *Can. J. Chem*. **1984**, *62*, 2803-12.

30. Herd, O.; Hessler, A.; Hingst, M.; Tepper, M.; Stelzer, O. *J. Organomet. Chem.* **1996**, *522*, 69-76.

31. Jeffery, J. C.; Rauchfuss, T. B.; Tucker, P. A., *Inorg. Chem.* **1980**, *19*, 3306-3316.

32. Ankersmit, H. A.; Løken, B. H.; Kooijman, H.; Spek, A. L.; Vrieze, K.; van Koten, G. *Inorg. Chim. Acta* **1996**, *252*, 141-155.

33. De Graaf, W.; Boersma, J.; Smeets, W.J.J.; Spek, A.L.; Van Koten, G. *Organometallics* **1989**, *8*, 2907-2917.

34. Bhattacharyya, P.; Parr, J.; Slawin, A.M.Z. *J. Chem. Soc*., *Dalton Trans*., **1998**, 3609-3614.

35. Klosin, J.; Roof, G. R.; Chen, E. Y. X.; Abboud, K. A. *Organometallics* **2000**, *19*, 4684-4686.

36. Mecking, S.; Johnson, L.K.; Wang, L.; Brookhart, M. *J. Am. Chem. Soc.* **1998**, *120*, 888-899.

37. Pangborn, A.B.; Giardello, M.A.; Grubbs, R.H.; Rosen, R.K.; Timmers, F.J. *Organometallics* **1996**, *15*, 1518-1520.

38. Lee, C.H.; Lee, S.J.; Park, J.W.; Kim, K.H.; Lee, B.Y.; Oh, J.S. *J. Mol. Cat*., *A: Chem.* **1998**, *132*, 231-239.

39. K. Soga, M. Terano Eds. *Catalyst Design for Tailor-Made Polyolefins*; Elsevier: Amsterdam, 1994, pp. 405–410.

Appendix A

Crystal structure information, compound 6 in Chapter 2

Table 1. Crystal data and structure refinement for Complex **6**.

Empirical formula	C29 H42 Al Cl7 N2 Pd	
Formula weight	800.18	
Temperature	100(2) K	
Wavelength	0.71073 Å	
Crystal system	Triclinic	
Space group	P-1	
Unit cell dimensions	a = 12.9031(6) Å	α= 117.8510(10)°.
	b = 13.3823(7) Å	β= 117.3740(10)°.
	c = 13.8935(7) Å	γ = 91.0630(10)°.
Volume	1798.51(16) $Å^3$	
Z	2	
Density (calculated)	1.478 Mg/m^3	
Absorption coefficient	1.082 mm^{-1}	
F(000)	816	
Crystal size	0.30 x 0.10 x 0.05 mm^3	
Theta range for data collection	1.86 to 28.27°.	
Index ranges	-8<=h<=17, -17<=k<=17, -18<=l<=14	
Reflections collected	11565	
Independent reflections	8060 [R(int) = 0.0216]	
Completeness to theta = 28.27°	90.3 %	
Absorption correction	None	
Max. and min. transmission	0.9479 and 0.7372	
Refinement method	Full-matrix least-squares on F^2	
Data / restraints / parameters	8060 / 0 / 361	
Goodness-of-fit on F^2	1.034	
Final R indices [I>2sigma(I)]	R1 = 0.0338, wR2 = 0.0724	
R indices (all data)	R1 = 0.0447, wR2 = 0.0763	
Largest diff. peak and hole	0.680 and -0.649 $e.Å^{-3}$	

Table 2. Atomic coordinates (x 10^4) and equivalent isotropic displacement parameters ($Å^2$x 10^3)
for **6**. U(eq) is defined as one third of the trace of the orthogonalized U^{ij} tensor.

x	y	z	U(eq)

Pd(1)	5503(1)	5748(1)	6593(1)	13(1)
Al(1)	2820(1)	13265(1)	6704(1)	18(1)
Cl(1)	4100(1)	5766(1)	4800(1)	18(1)
Cl(2)	3126(1)	11753(1)	6828(1)	25(1)
Cl(3)	1006(1)	13262(1)	6281(1)	26(1)
Cl(4)	4096(1)	14843(1)	8505(1)	24(1)
Cl(5)	3047(1)	13163(1)	5244(1)	26(1)
Cl(6)	10326(1)	8962(1)	13593(1)	47(1)
Cl(7)	9219(1)	10168(1)	12262(1)	46(1)
N(1)	5190(2)	7014(2)	7839(2)	13(1)
N(2)	6706(2)	5815(2)	8190(2)	14(1)
C(1)	5591(2)	8014(2)	10033(2)	22(1)
C(2)	5734(2)	7162(2)	8966(2)	16(1)
C(3)	6619(2)	6476(2)	9170(2)	15(1)
C(4)	7398(2)	6641(2)	10452(2)	21(1)
C(5)	7677(2)	5272(2)	8256(2)	17(1)
C(6)	7473(2)	4074(2)	7863(2)	20(1)
C(7)	8401(2)	3583(2)	7823(3)	26(1)
C(8)	9471(2)	4229(3)	8141(3)	27(1)
C(9)	9655(3)	5411(3)	8535(3)	27(1)
C(10)	8771(2)	5958(2)	8605(2)	20(1)
C(11)	8999(2)	7261(2)	9014(3)	25(1)
C(12)	8922(4)	7386(3)	7959(3)	51(1)
C(13)	10221(3)	8046(3)	10269(3)	40(1)
C(14)	6308(2)	3341(2)	7526(3)	23(1)
C(15)	6553(3)	3211(3)	8644(3)	33(1)
C(16)	5795(3)	2116(2)	6290(3)	31(1)
C(17)	4449(2)	7737(2)	7504(2)	15(1)
C(18)	3181(2)	7337(2)	6880(2)	18(1)
C(19)	2515(2)	8025(2)	6502(3)	25(1)
C(20)	3077(2)	9054(2)	6715(3)	26(1)
C(21)	4339(2)	9425(2)	7326(3)	24(1)
C(22)	5059(2)	8780(2)	7733(2)	19(1)
C(23)	2515(2)	6205(2)	6615(2)	20(1)
C(24)	1502(2)	5397(2)	5197(3)	24(1)
C(25)	1993(3)	6501(2)	7481(3)	29(1)
C(26)	6440(2)	9202(2)	8369(3)	26(1)
C(27)	7006(3)	10390(3)	9651(3)	35(1)
C(28)	6760(3)	9298(3)	7475(3)	42(1)
C(29)	10449(3)	10296(3)	13641(3)	41(1)

Table 3. Bond lengths [Å] and angles [°] for **6**

Pd(1)-N(1)	1.990(2)	C(6)-C(14)	1.520(4)
Pd(1)-N(2)	1.9958(19)	C(7)-C(8)	1.375(4)
Pd(1)-Cl(1)	2.3230(6)	C(8)-C(9)	1.383(4)
Pd(1)-Cl(1)#1	2.3236(6)	C(9)-C(10)	1.384(4)
Al(1)-Cl(5)	2.1238(10)	C(10)-C(11)	1.533(4)
Al(1)-Cl(3)	2.1340(10)	C(11)-C(12)	1.510(4)
Al(1)-Cl(2)	2.1388(10)	C(11)-C(13)	1.526(4)
Al(1)-Cl(4)	2.1389(10)	C(14)-C(15)	1.531(4)
Cl(1)-Pd(1)#1	2.3236(6)	C(14)-C(16)	1.536(4)
Cl(6)-C(29)	1.757(3)	C(17)-C(18)	1.395(3)
Cl(7)-C(29)	1.762(3)	C(17)-C(22)	1.409(3)
N(1)-C(2)	1.295(3)	C(18)-C(19)	1.389(3)
N(1)-C(17)	1.453(3)	C(18)-C(23)	1.519(3)
N(2)-C(3)	1.292(3)	C(19)-C(20)	1.377(4)
N(2)-C(5)	1.448(3)	C(20)-C(21)	1.387(4)
C(1)-C(2)	1.486(3)	C(21)-C(22)	1.389(4)
C(2)-C(3)	1.488(3)	C(22)-C(26)	1.524(4)
C(3)-C(4)	1.486(3)	C(23)-C(24)	1.532(4)
C(5)-C(6)	1.405(3)	C(23)-C(25)	1.540(4)
C(5)-C(10)	1.406(3)	C(26)-C(28)	1.532(4)
C(6)-C(7)	1.387(4)	C(26)-C(27)	1.533(4)

N(1)-Pd(1)-N(2)	80.35(8)	C(8)-C(7)-C(6)	121.9(3)
N(1)-Pd(1)-Cl(1)	96.87(6)	C(7)-C(8)-C(9)	120.0(3)
N(2)-Pd(1)-Cl(1)	177.06(6)	C(8)-C(9)-C(10)	121.1(3)
N(1)-Pd(1)-Cl(1)#1	177.26(6)	C(9)-C(10)-C(5)	117.8(2)
N(2)-Pd(1)-Cl(1)#1	97.21(6)	C(9)-C(10)-C(11)	119.4(2)
Cl(1)-Pd(1)-Cl(1)#1	85.60(2)	C(5)-C(10)-C(11)	122.8(2)
Cl(5)-Al(1)-Cl(3)	111.29(4)	C(12)-C(11)-C(13)	110.7(3)
Cl(5)-Al(1)-Cl(2)	109.39(4)	C(12)-C(11)-C(10)	110.3(2)
Cl(3)-Al(1)-Cl(2)	107.42(4)	C(13)-C(11)-C(10)	112.2(2)
Cl(5)-Al(1)-Cl(4)	109.66(4)	C(6)-C(14)-C(15)	109.7(2)
Cl(3)-Al(1)-Cl(4)	109.45(4)	C(6)-C(14)-C(16)	112.0(2)
Cl(2)-Al(1)-Cl(4)	109.59(4)	C(15)-C(14)-C(16)	110.2(2)
Pd(1)-Cl(1)-Pd(1)#1	94.40(2)	C(18)-C(17)-C(22)	122.8(2)
C(2)-N(1)-C(17)	123.7(2)	C(18)-C(17)-N(1)	120.0(2)
C(2)-N(1)-Pd(1)	114.65(16)	C(22)-C(17)-N(1)	117.0(2)

C(17)-N(1)-Pd(1)	121.61(15)	C(19)-C(18)-C(17)	117.4(2)
C(3)-N(2)-C(5)	123.6(2)	C(19)-C(18)-C(23)	119.5(2)
C(3)-N(2)-Pd(1)	114.54(16)	C(17)-C(18)-C(23)	123.1(2)
C(5)-N(2)-Pd(1)	121.42(15)	C(20)-C(19)-C(18)	121.6(3)
N(1)-C(2)-C(3)	114.6(2)	C(19)-C(20)-C(21)	119.7(3)
N(1)-C(2)-C(1)	124.3(2)	C(20)-C(21)-C(22)	121.6(2)
C(3)-C(2)-C(1)	120.8(2)	C(21)-C(22)-C(17)	116.9(2)
N(2)-C(3)-C(4)	124.2(2)	C(21)-C(22)-C(26)	119.9(2)
N(2)-C(3)-C(2)	114.9(2)	C(17)-C(22)-C(26)	123.2(2)
C(4)-C(3)-C(2)	120.8(2)	C(18)-C(23)-C(24)	111.5(2)
C(6)-C(5)-C(10)	122.2(2)	C(18)-C(23)-C(25)	110.1(2)
C(6)-C(5)-N(2)	120.3(2)	C(24)-C(23)-C(25)	110.8(2)
C(10)-C(5)-N(2)	117.2(2)	C(22)-C(26)-C(28)	110.7(2)
C(7)-C(6)-C(5)	117.0(2)	C(22)-C(26)-C(27)	110.8(2)
C(7)-C(6)-C(14)	120.7(2)	C(28)-C(26)-C(27)	110.6(2)
C(5)-C(6)-C(14)	122.3(2)	Cl(6)-C(29)-Cl(7)	111.97(17)

Symmetry transformations used to generate equivalent atoms: #1 -x+1,-y+1,-z+1

Table 4. Anisotropic displacement parameters ($Å^2 x\ 10^3$) for **6**. The anisotropic displacement factor exponent takes the form: $-2\pi^2[\ h^2\ a^{*2}U^{11} + ... + 2\ h\ k\ a^*\ b^*\ U^{12}\ ]$

	U^{11}	U^{22}	U^{33}	U^{23}	U^{13}	U^{12}
Pd(1)	13(1)	16(1)	12(1)	8(1)	7(1)	7(1)
Al(1)	18(1)	19(1)	17(1)	11(1)	9(1)	6(1)
Cl(1)	21(1)	23(1)	14(1)	11(1)	10(1)	14(1)
Cl(2)	29(1)	22(1)	29(1)	18(1)	15(1)	10(1)
Cl(3)	20(1)	27(1)	34(1)	19(1)	14(1)	8(1)
Cl(4)	24(1)	23(1)	18(1)	11(1)	8(1)	2(1)
Cl(5)	35(1)	33(1)	24(1)	19(1)	20(1)	17(1)
Cl(6)	60(1)	29(1)	34(1)	15(1)	13(1)	6(1)
Cl(7)	46(1)	47(1)	46(1)	28(1)	21(1)	22(1)
N(1)	12(1)	13(1)	14(1)	7(1)	7(1)	4(1)
N(2)	13(1)	14(1)	14(1)	9(1)	6(1)	5(1)
C(1)	27(2)	23(1)	16(1)	9(1)	13(1)	11(1)
C(2)	15(1)	14(1)	16(1)	7(1)	8(1)	2(1)
C(3)	12(1)	16(1)	16(1)	10(1)	6(1)	1(1)
C(4)	22(1)	29(1)	17(1)	14(1)	11(1)	12(1)
C(5)	16(1)	23(1)	14(1)	11(1)	8(1)	8(1)
C(6)	21(1)	22(1)	18(1)	12(1)	11(1)	11(1)
C(7)	26(2)	27(1)	29(2)	17(1)	15(1)	16(1)
C(8)	21(1)	40(2)	30(2)	23(1)	16(1)	20(1)

C(9)	20(1)	38(2)	28(2)	19(1)	14(1)	12(1)
C(10)	18(1)	28(1)	16(1)	14(1)	9(1)	8(1)
C(11)	19(1)	28(1)	34(2)	19(1)	16(1)	9(1)
C(12)	76(3)	39(2)	37(2)	27(2)	23(2)	11(2)
C(13)	36(2)	34(2)	37(2)	15(2)	14(2)	4(2)
C(14)	18(1)	22(1)	31(2)	16(1)	12(1)	9(1)
C(15)	32(2)	38(2)	37(2)	23(2)	21(1)	11(1)
C(16)	30(2)	25(1)	36(2)	16(1)	15(1)	9(1)
C(17)	17(1)	16(1)	14(1)	8(1)	8(1)	8(1)
C(18)	18(1)	17(1)	18(1)	9(1)	10(1)	6(1)
C(19)	17(1)	22(1)	29(2)	14(1)	8(1)	7(1)
C(20)	25(2)	21(1)	32(2)	16(1)	13(1)	11(1)
C(21)	25(1)	17(1)	31(2)	15(1)	14(1)	7(1)
C(22)	20(1)	17(1)	21(1)	9(1)	12(1)	6(1)
C(23)	13(1)	20(1)	24(1)	13(1)	7(1)	6(1)
C(24)	18(1)	22(1)	30(2)	14(1)	11(1)	5(1)
C(25)	30(2)	24(1)	34(2)	16(1)	18(1)	6(1)
C(26)	18(1)	22(1)	39(2)	19(1)	13(1)	5(1)
C(27)	27(2)	44(2)	26(2)	17(1)	11(1)	0(1)
C(28)	28(2)	43(2)	35(2)	3(2)	20(2)	-2(1)
C(29)	40(2)	29(2)	36(2)	17(2)	10(2)	4(2)

Table 5. Hydrogen coordinates (x 10^4) and isotropic displacement parameters ($Å^2$x 10^3) for **6**

	x	y	z	U(eq)	
H(1A)	4975	8384	9724	33	
H(1B)	6374	8626	10737	33	
H(1C)	5331	7594	10340	33	
H(4A)	7920	6119	10406	32	
H(4B)	6878	6446	10715	32	
H(4C)	7911	7466	11080	32	
H(7A)	8293	2776	7570	31	
H(8A)	10084	3865	8090	33	
H(9A)	10401	5854	8761	32	
H(11A)		8337	7537	9153	29
H(12A)		8127	6887	7167	76
H(12B)		9575	7137	7817	76
H(12C)		9016	8214	8210	76
H(13A)		10328	8869	10497	61
H(13B)		10887	7784	10163	61
H(13C)		10235	7989	10952	61
H(14A)		5681	3771	7391	28

H(15A)	6873	3997	9425	49
H(15B)	7153	2775	8778	49
H(15C)	5789	2777	8444	49
H(16A)	5640	2211	5581	47
H(16B)	5030	1684	6087	47
H(16C)	6389	1672	6411	47
H(19A)	1650	7779	6085	30
H(20A)	2603	9509	6445	31
H(21A)	4720	10136	7471	28
H(23A)	3120	5771	6830	24
H(24A)	1854	5215	4664	36
H(24B)	888	5799	4971	36
H(24C)	1117	4661	5051	36
H(25A)	2655	7012	8383	43
H(25B)	1607	5768	7340	43
H(25C)	1383	6912	7273	43
H(26A)	6792	8603	8544	31
H(27A)	6796	10312	10212	53
H(27B)	6687	10994	9498	53
H(27C)	7897	10625	10064	53
H(28A)	6395	8531	6663	63
H(28B)	7650	9530	7883	63
H(28C)	6439	9895	7308	63
H(29A)	11225	10536	13713	49
H(29B)	10474	10924	14411	49

Appendix B

Crystal structure information, compound 1a in Chapter 3

Table 1. Sample and crystal data for Complex 1a

Empirical formula	C16 H25 Cl Pd	
Formula weight	359.21	
Temperature	95(2) K	
Wavelength	0.71073 Å	
Crystal size	0.33 x 0.33 x 0.18 mm	
Crystal habit	Clear cuboid	
Crystal system	Monoclinic	
Space group	P2(1)/n	
Unit cell dimensions	a = 10.899(5) Å	α= 90°
	b = 12.530(5) Å	β= 108.150(13)°
	c = 11.467(5) Å	γ = 90°
Volume	1488.1(10) $Å^3$	
Z	4	
Density (calculated)	1.603 g/cm^3	
Absorption coefficient	1.408 mm^{-1}	
F(000)	736	

Table 2. Data collection and structure refinement for Complex 1a

Diffractometer	CCD area detector
Radiation source	fine-focus sealed tube, MoK
Generator power	1600 watts (50 kV, 32mA)
Detector distance	5.8 cm
Data collection method	omega scans
Theta range for data collection	2.25 to 28.41°
Index ranges	$-14 \leq h \leq 10$, $-10 \leq k \leq 16$, $-12 \leq l \leq 15$

Table 3. Atomic coordinates and equivalent isotropic atomic displacement parameters (Å ^{2}) for **Complex 1a**

U(eq) is defined as one third of the trace of the orthogonalized U_{ij} tensor.

	x/a	y/b	z/c	U(eq)
Pd1	0.42167(6)	0.11703(5)	0.25430(5)	0.0283(2)
Cl3	0.4781(2)	0.23938(16)	0.41588(17)	0.0357(5)
C1	0.5487(11)	0.1788(9)	0.1695(9)	0.057(3)
C2	0.5441(14)	0.3003(12)	0.1542(13)	0.087(4)
C11	0.4063(10)	-0.1215(8)	0.2371(9)	0.053(3)
C10	0.3092(10)	-0.1090(7)	0.3038(9)	0.043(2)
C13	0.3147(9)	0.0332(8)	0.0860(7)	0.041(2)
C9	0.3073(7)	0.0002(6)	0.3549(7)	0.0280(17)
C8	0.2284(8)	0.0777(7)	0.2981(8)	0.0303(17)
C12	0.4159(9)	-0.0303(8)	0.1549(8)	0.045(2)
C14	0.1750(9)	0.0186(7)	0.0750(7)	0.042(2)
C15	0.1280(9)	0.0698(8)	0.1727(8)	0.042(2)
C7	0.6815(13)	0.3216(11)	0.2660(10)	0.074(4)
C5	0.7534(12)	0.2508(12)	0.2137(12)	0.072(4)
C3	0.5892(12)	0.3311(13)	0.0501(11)	0.076(4)
C6	0.6841(11)	0.1510(10)	0.2237(14)	0.074(4)
C4	0.7277(14)	0.2850(13)	0.0918(12)	0.097(6)
C16	0.7212(11)	0.0987(13)	0.3424(12)	0.082(4)

Table 4. Bond lengths (Å) for Complex 1a

Pd1-C1	2.074(10)	Pd1-C12	2.160(9)
Pd1-C13	2.188(7)	Pd1-Cl3	2.335(2)
Pd1-C8	2.364(8)	Pd1-C9	2.434(7)
C1-C6	1.454(16)	C1-C2	1.531(18)
C2-C3	1.477(17)	C2-C7	1.662(18)
C11-C10	1.495(14)	C11-C12	1.505(15)
C10-C9	1.491(12)	C13-C12	1.390(14)
C13-C14	1.500(13)	C9-C8	1.326(11)
C8-C15	1.515(11)	C14-C15	1.513(14)
C7-C5	1.434(19)	C5-C4	1.405(17)
C5-C6	1.483(17)	C3-C4	1.55(2)
C6-C16	1.450(17)		

Table 5. Bond angles (°) for Complex 1a

C1-Pd1-C12	89.2(4)	C1-Pd1-C13	90.9(3)
C12-Pd1-C13	37.3(4)	C1-Pd1-Cl3	94.5(3)
C12-Pd1-Cl3	159.6(3)	C13-Pd1-Cl3	162.1(3)
C1-Pd1-C8	161.2(4)	C12-Pd1-C8	93.0(3)
C13-Pd1-C8	79.8(3)	Cl3-Pd1-C8	90.0(2)
C1-Pd1-C9	164.2(4)	C12-Pd1-C9	78.5(3)
C13-Pd1-C9	85.3(3)	Cl3-Pd1-C9	93.8(2)
C8-Pd1-C9	32.0(3)	C6-C1-C2	106.2(10)
C6-C1-Pd1	116.6(8)	C2-C1-Pd1	114.9(9)
C3-C2-C1	110.1(13)	C3-C2-C7	97.7(10)
C1-C2-C7	94.7(10)	C10-C11-C12	116.0(8)
C9-C10-C11	113.4(8)	C12-C13-C14	125.7(8)
C12-C13-Pd1	70.3(4)	C14-C13-Pd1	112.4(6)
C8-C9-C10	124.5(7)	C8-C9-Pd1	71.1(5)
C10-C9-Pd1	107.1(6)	C9-C8-C15	125.7(8)
C9-C8-Pd1	76.9(5)	C15-C8-Pd1	103.9(6)
C13-C12-C11	126.4(9)	C13-C12-Pd1	72.4(5)
C11-C12-Pd1	108.4(6)	C13-C14-C15	117.1(7)
C14-C15-C8	114.8(7)	C5-C7-C2	93.2(9)
C4-C5-C7	105.2(13)	C4-C5-C6	112.7(11)
C7-C5-C6	97.6(10)	C2-C3-C4	101.1(11)
C16-C6-C1	117.3(10)	C16-C6-C5	117.0(14)
C1-C6-C5	103.8(9)	C5-C4-C3	107.1(13)

Appendix C

Crystal structure information, compound 1b in Chapter 3

Table 1. Sample and crystal data for complex 1b.

Empirical formula	C38 H58 Cl2 O4 Pd2	
Formula weight	862.54	
Temperature	95(2) K	
Wavelength	0.71073 Å	
Crystal size	0.26 x 0.24 x 0.12 mm	
Crystal habit	colourless cuboidal	
Crystal system	Triclinic	
Space group	P1	
Unit cell dimensions	a = 8.0473(17) Å	α= 105.751(3)°
	b = 10.216(2) Å	β= 90.578(4)°
	c = 12.347(3) Å	γ = 109.872(4)°
Volume	912.9(3) $Å^3$	
Z	1	
Density (calculated)	1.569 g/cm^3	
Absorption coefficient	1.170 mm^{-1}	
F(000)	444	

Table 2. Data collection and structure refinement for complex 1b.

Diffractometer	CCD area detector
Radiation source	fine-focus sealed tube, MoK
Generator power	1600 watts (50 kV, 32mA)
Detector distance	5.8 cm
Data collection method	omega scans
Theta range for data collection	1.72 to 28.32°
Index ranges	$-10 \leq h \leq 6$, $-10 \leq k \leq 13$, $-15 \leq l \leq 15$

Table 3. Atomic coordinates and equivalent isotropic atomic displacement parameters (Å ^{2}) for complex 1b.
U(eq) is defined as one third of the trace of the orthogonalized U_{ij} tensor.

	x/a	y/b	z/c	U(eq)
Pd1	0.40111(3)	0.75329(2)	0.449667(19)	0.01285(12)
C15	0.6582(12)	0.7849(10)	0.5305(8)	0.017(2)
C32	0.5864(13)	1.2441(10)	0.6559(9)	0.0221(19)
Cl2	0.1113(3)	0.6760(3)	0.3596(2)	0.0201(5)
C28	0.2849(13)	1.1599(10)	0.7258(9)	0.019(2)
C9	0.6812(12)	0.8582(12)	0.4554(9)	0.020(2)
C27	0.1591(10)	0.9971(8)	0.6759(8)	0.0163(17)
C26	0.2806(10)	0.8999(9)	0.6708(7)	0.0157(16)
C33	0.1342(11)	0.9863(8)	0.5532(8)	0.0211(19)
C29	0.4021(12)	1.1875(10)	0.6251(7)	0.0191(17)
C24	0.1623(12)	0.7419(10)	0.6577(8)	0.0197(18)
C14	0.6870(11)	0.6397(9)	0.5186(7)	0.0169(16)
C12	0.4656(10)	0.5826(10)	0.2946(7)	0.0182(18)
C30	0.3193(11)	1.0357(8)	0.5293(8)	0.0176(17)
C25	0.3887(9)	0.9315(9)	0.5702(7)	0.0142(16)
C13	0.5153(11)	0.5006(9)	0.4650(7)	0.0192(16)
C11	0.6617(9)	0.6507(10)	0.2746(7)	0.0179(17)
C10	0.7337(11)	0.8131(10)	0.3326(6)	0.0183(18)
Pd2	0.50100(3)	1.00970(2)	0.081257(19)	0.01312(12)
Cl1	0.7915(3)	1.0879(3)	0.1701(2)	0.0202(5)
O1	0.2314(9)	0.4885(7)	-0.2215(6)	0.0241(14)
C1	0.2143(12)	0.9043(10)	0.0783(9)	0.0135(19)
C8	0.2469(11)	0.9855(10)	-0.0041(7)	0.0136(19)
C21	0.6205(15)	0.6101(11)	-0.1920(8)	0.024(2)
C23	0.7755(10)	0.7753(9)	-0.0181(6)	0.0172(17)
C17	0.6284(10)	0.8622(8)	-0.1408(6)	0.0156(16)
C20	0.5102(10)	0.5738(8)	-0.0984(7)	0.0158(16)
C22	0.7319(11)	0.7672(10)	-0.1452(7)	0.0216(19)
C5	0.4980(8)	1.2469(9)	0.1581(7)	0.0187(17)
C19	0.5678(10)	0.7246(9)	-0.0058(7)	0.0125(16)
C3	0.2492(13)	1.1168(10)	0.2557(7)	0.0241(19)
C16	0.7324(12)	1.0240(10)	-0.1253(8)	0.0200(18)
C4	0.4367(13)	1.1815(9)	0.2436(7)	0.0201(18)
C7	0.2251(11)	1.1318(10)	0.0172(7)	0.0181(16)
C2	0.1644(11)	0.9479(9)	0.1900(8)	0.0232(19)
C18	0.5008(11)	0.8285(8)	-0.0479(7)	0.0128(15)
O3	0.2144(8)	0.4988(7)	-0.0413(6)	0.0238(15)
O4	0.6824(8)	1.2646(7)	0.5715(5)	0.0219(14)

C34	0.8724(12)	1.3178(10)	0.5955(7)	0.0227(19)
C36	0.0187(11)	0.4459(12)	-0.0649(10)	0.034(2)
O2	0.6608(9)	1.2701(7)	0.7563(6)	0.0232(15)
C35	0.9548(12)	1.3199(11)	0.4857(7)	0.0284(19)
C31	0.3017(10)	0.5157(9)	-0.1355(8)	0.0116(16)
C38	0.4001(12)	0.5141(8)	0.3687(7)	0.0226(19)
C6	0.3972(11)	1.2578(8)	0.0647(8)	0.0217(18)
C37	-0.0518(14)	0.4343(12)	0.0448(9)	0.050(3)

Table 4. Bond lengths (Å) for complex 1b.

Pd1-C25	2.048(8)	Pd1-C9	2.133(9)
Pd1-C15	2.170(10)	Pd1-Cl2	2.349(3)
Pd1-C38	2.373(8)	Pd1-C12	2.408(8)
C15-C9	1.319(14)	C15-C14	1.546(13)
C32-O2	1.289(11)	C32-O4	1.324(12)
C32-C29	1.402(13)	C28-C27	1.568(11)
C28-C29	1.597(13)	C9-C10	1.567(13)
C27-C33	1.495(12)	C27-C26	1.605(11)
C26-C24	1.533(12)	C26-C25	1.565(11)
C33-C30	1.463(12)	C29-C30	1.592(12)
C14-C13	1.582(11)	C12-C38	1.308(12)
C12-C11	1.546(10)	C30-C25	1.546(12)
C13-C38	1.564(11)	C11-C10	1.514(12)
Pd2-C18	2.089(7)	Pd2-C1	2.184(9)
Pd2-C8	2.196(9)	Pd2-Cl1	2.347(3)
Pd2-C5	2.359(8)	Pd2-C4	2.469(8)
O1-C31	1.116(11)	C1-C2	1.435(14)
C1-C8	1.452(12)	C8-C7	1.517(13)
C21-C22	1.490(13)	C21-C20	1.513(13)
C23-C22	1.579(11)	C23-C19	1.595(10)
C17-C22	1.469(12)	C17-C16	1.535(11)
C17-C18	1.576(11)	C20-C19	1.563(10)
C20-C31	1.593(11)	C5-C4	1.404(11)
C5-C6	1.454(12)	C19-C18	1.540(12)
C3-C4	1.455(12)	C3-C2	1.591(12)
C7-C6	1.510(11)	O3-C31	1.386(11)
O3-C36	1.478(11)	O4-C34	1.435(11)
C34-C35	1.517(11)	C36-C37	1.492(15)

Table 5. Bond angles (°) for complex 1b.

C25-Pd1-C9	90.4(4)	C25-Pd1-C15	90.7(3)
C9-Pd1-C15	35.7(4)	C25-Pd1-Cl2	96.5(2)
C9-Pd1-Cl2	150.5(3)	C15-Pd1-Cl2	170.0(3)
C25-Pd1-C38	158.9(3)	C9-Pd1-C38	95.3(4)
C15-Pd1-C38	82.3(3)	Cl2-Pd1-C38	88.5(2)
C25-Pd1-C12	167.5(3)	C9-Pd1-C12	79.4(4)
C15-Pd1-C12	85.1(3)	Cl2-Pd1-C12	89.22(19)
C38-Pd1-C12	31.7(3)	C9-C15-C14	127.3(9)
C9-C15-Pd1	70.6(6)	C14-C15-Pd1	112.5(5)
O2-C32-O4	121.2(9)	O2-C32-C29	124.3(9)
O4-C32-C29	114.4(9)	C27-C28-C29	102.6(7)
C15-C9-C10	127.6(10)	C15-C9-Pd1	73.7(6)
C10-C9-Pd1	108.0(6)	C33-C27-C28	101.1(7)
C33-C27-C26	100.0(6)	C28-C27-C26	106.7(7)
C24-C26-C25	117.5(7)	C24-C26-C27	109.6(7)
C25-C26-C27	101.0(6)	C30-C33-C27	100.7(7)
C32-C29-C30	118.3(7)	C32-C29-C28	114.8(8)
C30-C29-C28	102.2(7)	C15-C14-C13	113.5(7)
C38-C12-C11	129.3(8)	C38-C12-Pd1	72.6(5)
C11-C12-Pd1	108.3(5)	C33-C30-C25	100.9(7)
C33-C30-C29	101.7(6)	C25-C30-C29	104.5(7)
C30-C25-C26	105.2(6)	C30-C25-Pd1	117.2(6)
C26-C25-Pd1	116.0(6)	C38-C13-C14	114.6(7)
C10-C11-C12	110.8(6)	C11-C10-C9	114.2(7)
C18-Pd2-C1	89.0(3)	C18-Pd2-C8	87.7(3)
C1-Pd2-C8	38.7(3)	C18-Pd2-Cl1	99.7(2)
C1-Pd2-Cl1	150.4(3)	C8-Pd2-Cl1	167.4(2)
C18-Pd2-C5	155.6(3)	C1-Pd2-C5	94.2(3)
C8-Pd2-C5	79.9(3)	Cl1-Pd2-C5	89.46(18)
C18-Pd2-C4	166.3(3)	C1-Pd2-C4	78.6(3)
C8-Pd2-C4	86.2(3)	Cl1-Pd2-C4	88.6(2)
C5-Pd2-C4	33.7(3)	C2-C1-C8	127.3(8)
C2-C1-Pd2	109.3(6)	C8-C1-Pd2	71.1(5)
C1-C8-C7	122.8(8)	C1-C8-Pd2	70.2(5)
C7-C8-Pd2	110.9(6)	C22-C21-C20	104.8(7)
C22-C23-C19	89.1(6)	C22-C17-C16	117.4(7)
C22-C17-C18	103.5(6)	C16-C17-C18	115.4(7)
C21-C20-C19	102.2(7)	C21-C20-C31	113.1(8)
C19-C20-C31	109.9(6)	C17-C22-C21	112.3(8)
C17-C22-C23	105.5(6)	C21-C22-C23	100.4(7)
C4-C5-C6	129.4(7)	C4-C5-Pd2	77.4(5)
C6-C5-Pd2	100.1(5)	C18-C19-C20	109.5(6)
C18-C19-C23	105.5(6)	C20-C19-C23	97.5(6)

C4-C3-C2	113.5(7)	C5-C4-C3	123.4(8)
C5-C4-Pd2	68.9(5)	C3-C4-Pd2	106.6(5)
C6-C7-C8	112.5(7)	C1-C2-C3	115.8(7)
C19-C18-C17	101.3(6)	C19-C18-Pd2	113.5(5)
C17-C18-Pd2	115.7(5)	C31-O3-C36	113.3(7)
C32-O4-C34	117.8(7)	O4-C34-C35	109.0(7)
O3-C36-C37	105.9(8)	O1-C31-O3	123.4(8)
O1-C31-C20	128.3(8)	O3-C31-C20	108.2(7)
C12-C38-C13	124.2(8)	C12-C38-Pd1	75.6(5)
C13-C38-Pd1	100.4(5)	C5-C6-C7	115.6(7)

Appendix D

Crystal structure information, compound 1c in Chapter 3

Table 1. Sample and crystal data for complex 1c.

Empirical formula	C38 H58 Cl2 O4 Pd2	
Formula weight	862.54	
Temperature	96(2) K	
Wavelength	0.71073 Å	
Crystal size	0.29 x 0.17 x 0.07 mm	
Crystal habit	light plate	
Crystal system	Triclinic	
Space group	P-1	
Unit cell dimensions	a = 11.2420(18) Å	α= 89.876(3)°
	b = 12.466(2) Å	β= 89.940(3)°
	c = 13.034(2) Å	γ = 87.950(3)°
Volume	1825.5(5) $Å^3$	
Z	2	
Density (calculated)	1.569 g/cm^3	
Absorption coefficient	1.170 mm^{-1}	
F(000)	888	

Table 2. Data collection and structure refinement for complex 1c.

Diffractometer	CCD area detector
Radiation source	fine-focus sealed tube, MoK
Generator power	1600 watts (50 kV, 32mA)
Detector distance	5.8 cm
Data collection method	omega scans
Theta range for data collection	1.56 to 28.30°
Index ranges	$-9 \leq h \leq 14$, $-13 \leq k \leq 16$, $-17 \leq l \leq 15$

Table 3. Atomic coordinates and equivalent isotropic atomic displacement parameters (Å ^{2}) for complex 1c.
U(eq) is defined as one third of the trace of the orthogonalized U_{ij} tensor.

	x/a	y/b	z/c	U(eq)	
Pd1	0.474673(19)		0.922949(17)	0.210048(15)	0.01421(7)
Pd2	0.474717(19)		0.422957(17)	0.289941(15)	0.01418(7)
Cl1	0.36614(7)	0.78299(6)	0.14145(6)	0.02081(16)	
Cl2	0.36605(7)	0.28285(6)	0.35854(6)	0.02057(16)	
C27	0.3314(2)	0.4930(2)	0.2132(2)	0.0158(6)	
C17	0.3317(3)	0.9932(2)	0.2868(2)	0.0154(6)	
O4	0.05690(19)	0.64037(19)	0.37991(16)	0.0242(5)	
O2	0.05649(19)	1.14044(19)	0.12038(16)	0.0238(5)	
C24	0.0283(3)	1.1177(3)	0.2183(2)	0.0198(6)	
C34	0.0281(3)	0.6174(3)	0.2817(2)	0.0207(6)	
C21	0.1393(3)	1.0907(2)	0.2788(2)	0.0179(6)	
C22	0.2078(3)	0.9884(2)	0.2365(2)	0.0149(6)	
C31	0.1392(3)	0.5909(2)	0.2212(2)	0.0180(6)	
C33	0.1465(3)	0.4003(3)	0.2041(2)	0.0219(6)	
C18	0.3113(3)	0.9522(3)	0.3989(2)	0.0211(6)	
O1	-0.0724(2)	1.1213(2)	0.24945(18)	0.0340(6)	
C1	0.5881(3)	1.0154(3)	0.3081(2)	0.0215(7)	
C32	0.2083(3)	0.4884(2)	0.2636(2)	0.0166(6)	
C10	0.5691(3)	0.5733(3)	0.2818(2)	0.0212(6)	
C11	0.5882(3)	0.5154(3)	0.1920(2)	0.0216(7)	
C14	0.6686(3)	0.3381(3)	0.3270(2)	0.0210(6)	
C29	0.1739(3)	0.4468(3)	0.0987(2)	0.0212(6)	
C16	0.6613(3)	0.4966(3)	0.4496(2)	0.0224(7)	
O3	-0.0724(2)	0.6208(2)	0.25024(18)	0.0341(6)	
C2	0.5685(3)	1.0733(3)	0.2186(2)	0.0211(6)	
C23	0.1464(3)	0.8998(3)	0.2960(2)	0.0208(6)	
C3	0.6580(3)	1.0852(3)	0.1327(2)	0.0244(7)	
C4	0.6611(3)	0.9969(3)	0.0499(2)	0.0242(7)	
C13	0.7569(3)	0.3858(3)	0.2548(2)	0.0251(7)	
C28	0.3115(3)	0.4518(3)	0.1015(2)	0.0214(6)	
C7	0.7571(3)	0.8851(3)	0.2448(2)	0.0260(7)	
C6	0.6684(3)	0.8385(3)	0.1731(2)	0.0217(7)	
C15	0.6280(3)	0.3874(3)	0.4135(2)	0.0214(6)	
C19	0.1738(3)	0.9468(3)	0.4014(2)	0.0213(7)	
C9	0.6578(3)	0.5849(3)	0.3678(2)	0.0238(7)	
C35	-0.0405(3)	0.6729(3)	0.4475(2)	0.0301(8)	
C12	0.6980(3)	0.4468(3)	0.1648(2)	0.0263(7)	
C20	0.1174(3)	1.0603(3)	0.3922(2)	0.0220(7)	

C30	0.1175(3)	0.5599(3)	0.1076(2)	0.0221(7)
C5	0.6279(3)	0.8875(3)	0.0865(2)	0.0196(6)
C25	-0.0403(3)	1.1732(3)	0.0526(2)	0.0302(8)
C36	0.0058(3)	0.6720(3)	0.5547(2)	0.0292(8)
C8	0.6980(3)	0.9474(3)	0.3351(2)	0.0269(7)
C26	0.0053(3)	1.1722(3)	-0.0545(2)	0.0305(8)
C37	0.3717(3)	0.3447(3)	0.0729(3)	0.0302(8)
C38	0.3714(3)	0.8449(3)	0.4270(2)	0.0296(8)

Table 4. Bond lengths (Å) for complex 1c.

Pd1-C17	2.062(3)	Pd1-C1	2.168(3)
Pd1-C2	2.186(3)	Pd1-Cl1	2.3438(8)
Pd1-C5	2.388(3)	Pd1-C6	2.433(3)
Pd2-C27	2.063(3)	Pd2-C11	2.163(3)
Pd2-C10	2.189(3)	Pd2-Cl2	2.3422(8)
Pd2-C15	2.389(3)	Pd2-C14	2.437(3)
C27-C32	1.534(4)	C27-C28	1.563(4)
C17-C22	1.543(4)	C17-C18	1.566(4)
O4-C34	1.354(4)	O4-C35	1.451(4)
O2-C24	1.347(4)	O2-C25	1.449(4)
C24-O1	1.201(4)	C24-C21	1.505(4)
C34-O3	1.202(4)	C34-C31	1.503(4)
C21-C20	1.546(4)	C21-C22	1.567(4)
C22-C23	1.533(4)	C31-C30	1.553(4)
C31-C32	1.571(4)	C33-C29	1.525(4)
C33-C32	1.533(4)	C18-C38	1.520(4)
C18-C19	1.550(4)	C1-C2	1.383(4)
C1-C8	1.514(4)	C10-C11	1.389(4)
C10-C9	1.512(4)	C11-C12	1.518(4)
C14-C15	1.356(4)	C14-C13	1.504(5)
C29-C30	1.530(4)	C29-C28	1.551(4)
C16-C15	1.502(5)	C16-C9	1.530(4)
C2-C3	1.516(4)	C23-C19	1.530(4)
C3-C4	1.542(5)	C4-C5	1.504(4)
C13-C12	1.535(4)	C28-C37	1.522(4)
C7-C6	1.500(5)	C7-C8	1.548(4)
C6-C5	1.355(4)	C19-C20	1.534(4)
C35-C36	1.491(4)	C25-C26	1.486(4)

Table 5. Bond angles (°) for kms22t.

C17-Pd1-C1	87.26(11)	C17-Pd1-C2	90.15(12)
C1-Pd1-C2	37.05(12)	C17-Pd1-Cl1	94.79(9)
C1-Pd1-Cl1	162.56(9)	C2-Pd1-Cl1	159.82(9)
C17-Pd1-C5	162.23(11)	C1-Pd1-C5	93.60(11)
C2-Pd1-C5	80.10(11)	Cl1-Pd1-C5	89.70(8)
C17-Pd1-C6	162.18(11)	C1-Pd1-C6	79.18(11)
C2-Pd1-C6	85.97(12)	Cl1-Pd1-C6	94.81(8)
C5-Pd1-C6	32.62(10)	C27-Pd2-C11	87.48(11)
C27-Pd2-C10	90.60(12)	C11-Pd2-C10	37.21(12)
C27-Pd2-Cl2	94.54(9)	C11-Pd2-Cl2	162.51(9)
C10-Pd2-Cl2	159.68(9)	C27-Pd2-C15	162.30(11)
C11-Pd2-C15	93.46(11)	C10-Pd2-C15	79.73(11)
Cl2-Pd2-C15	89.86(8)	C27-Pd2-C14	162.26(11)
C11-Pd2-C14	79.19(11)	C10-Pd2-C14	85.86(11)
Cl2-Pd2-C14	94.78(8)	C15-Pd2-C14	32.62(10)
C32-C27-C28	104.3(2)	C32-C27-Pd2	117.97(19)
C28-C27-Pd2	115.58(19)	C22-C17-C18	104.0(2)
C22-C17-Pd1	117.92(19)	C18-C17-Pd1	115.76(19)
C34-O4-C35	116.7(2)	C24-O2-C25	117.2(2)
O1-C24-O2	122.7(3)	O1-C24-C21	127.2(3)
O2-C24-C21	110.1(2)	O3-C34-O4	123.2(3)
O3-C34-C31	126.9(3)	O4-C34-C31	109.8(3)
C24-C21-C20	114.7(2)	C24-C21-C22	112.1(2)
C20-C21-C22	102.5(2)	C23-C22-C17	104.1(2)
C23-C22-C21	100.8(2)	C17-C22-C21	103.7(2)
C34-C31-C30	114.7(3)	C34-C31-C32	112.2(2)
C30-C31-C32	102.1(2)	C29-C33-C32	94.7(2)
C38-C18-C19	111.7(3)	C38-C18-C17	116.4(3)
C19-C18-C17	101.0(2)	C2-C1-C8	126.8(3)
C2-C1-Pd1	72.19(18)	C8-C1-Pd1	108.9(2)
C33-C32-C27	104.0(2)	C33-C32-C31	100.5(2)
C27-C32-C31	103.9(2)	C11-C10-C9	125.8(3)
C11-C10-Pd2	70.41(19)	C9-C10-Pd2	112.9(2)
C10-C11-C12	126.7(3)	C10-C11-Pd2	72.38(18)
C12-C11-Pd2	108.7(2)	C15-C14-C13	123.8(3)
C15-C14-Pd2	71.74(17)	C13-C14-Pd2	107.30(19)
C33-C29-C30	101.4(2)	C33-C29-C28	102.0(2)
C30-C29-C28	110.0(3)	C15-C16-C9	115.6(3)
C1-C2-C3	125.3(3)	C1-C2-Pd1	70.76(18)
C3-C2-Pd1	112.7(2)	C19-C23-C22	94.3(2)
C2-C3-C4	116.5(3)	C5-C4-C3	115.3(3)
C14-C13-C12	113.2(3)	C37-C28-C29	111.8(3)
C37-C28-C27	117.0(3)	C29-C28-C27	101.0(2)

C6-C7-C8	112.9(3)	C5-C6-C7	124.3(3)
C5-C6-Pd1	71.85(17)	C7-C6-Pd1	107.82(19)
C14-C15-C16	125.7(3)	C14-C15-Pd2	75.64(18)
C16-C15-Pd2	104.22(19)	C23-C19-C20	101.7(2)
C23-C19-C18	102.3(2)	C20-C19-C18	109.8(3)
C10-C9-C16	116.6(3)	O4-C35-C36	107.9(3)
C11-C12-C13	115.3(2)	C19-C20-C21	103.6(2)
C29-C30-C31	103.8(2)	C6-C5-C4	125.5(3)
C6-C5-Pd1	75.53(17)	C4-C5-Pd1	104.15(19)
O2-C25-C26	108.4(3)	C1-C8-C7	115.5(3)

Appendix E

Crystal structure information, compound 1d in Chapter 3

Table 1. Sample and crystal data for complex 1d.

Empirical formula	C19 H29 Cl O2 Pd	
Formula weight	431.27	
Temperature	293(2) K	
Wavelength	0.71073 Å	
Crystal size	0.41 x 0.21 x 0.1 mm	
Crystal habit	colourless needle	
Crystal system	Monoclinic	
Space group	P2(1)/n	
Unit cell dimensions	a = 6.8659(17) Å	α= 90°
	b = 23.248(6) Å	β= 96.614(4)°
	c = 11.502(3) Å	γ = 90°
Volume	1823.7(8) $Å^3$	
Z	4	
Density (calculated)	1.571 g/cm^3	
Absorption coefficient	1.171 mm^{-1}	
F(000)	888	

Table 2. Data collection and structure refinement for complex 1d.

Diffractometer	CCD area detector
Radiation source	fine-focus sealed tube, MoK
Generator power	1600 watts (50 kV, 32mA)
Detector distance	5.8 cm
Data collection method	omega scans
Theta range for data collection	1.75 to 28.40°
Index ranges	$-9 \leq h \leq 8$, $-30 \leq k \leq 21$, $-15 \leq l \leq 15$

Table 3. Atomic coordinates and equivalent isotropic atomic displacement parameters (Å ^{2}) for complex 1d.

U(eq) is defined as one third of the trace of the orthogonalized U_{ij} tensor.

	x/a	y/b	z/c	U(eq)
Pd1	0.91482(6)	0.87777(2)	0.51353(4)	0.01383(16)
Cl2	1.2314(2)	0.85452(9)	0.59819(16)	0.0319(4)
C2	1.0074(11)	0.8757(3)	0.3181(6)	0.0276(15)
C9	0.7814(9)	0.8557(3)	0.6605(5)	0.0183(13)
C5	0.6323(9)	0.8725(3)	0.4110(6)	0.0245(15)
C10	0.8924(10)	0.8695(3)	0.7806(6)	0.0223(14)
C11	0.7431(12)	0.8731(4)	0.8720(6)	0.0314(17)
C1	1.0561(10)	0.9280(3)	0.3624(6)	0.0249(15)
C14	0.9874(9)	0.8118(3)	0.8199(6)	0.0184(13)
C13	0.7928(10)	0.7780(3)	0.7993(6)	0.0241(15)
C6	0.6650(10)	0.9293(3)	0.4401(6)	0.0218(14)
C8	0.9388(11)	0.9817(3)	0.3404(6)	0.0261(15)
C3	0.8286(13)	0.8640(4)	0.2347(7)	0.0354(19)
C15	0.7298(9)	0.7901(3)	0.6674(6)	0.0207(14)
C7	0.7193(11)	0.9754(3)	0.3551(7)	0.0268(15)
C4	0.6552(13)	0.8438(4)	0.2955(6)	0.0355(19)
C12	0.6605(12)	0.8108(4)	0.8730(7)	0.0321(18)
O1	0.6745(11)	0.9779(3)	0.8471(6)	0.0550(18)
O2	0.7165(10)	0.9860(4)	1.0523(7)	0.082(3)
C16	0.5808(13)	0.9176(4)	0.8535(7)	0.0368(19)
C17	0.7309(15)	1.0053(5)	0.9531(9)	0.052(3)
C18	0.7894(14)	1.0637(4)	0.9298(8)	0.040(2)
C19	0.8275(12)	0.7501(3)	0.5869(6)	0.0279(16)

Table 4. Bond lengths (Å) for complex 1d.

Pd1-C9	2.078(6)	Pd1-C5	2.154(6)
Pd1-C6	2.181(6)	Pd1-Cl2	2.3403(17)
Pd1-C1	2.391(7)	Pd1-C2	2.406(7)
C2-C1	1.347(11)	C2-C3	1.493(11)
C9-C10	1.532(9)	C9-C15	1.571(9)
C5-C6	1.373(10)	C5-C4	1.510(11)
C10-C14	1.536(9)	C10-C11	1.553(10)
C11-C16	1.518(11)	C11-C12	1.556(12)
C1-C8	1.491(10)	C14-C13	1.545(9)
C13-C12	1.517(10)	C13-C15	1.555(9)
C6-C7	1.525(10)	C8-C7	1.543(10)
C3-C4	1.523(12)	C15-C19	1.521(10)
O1-C17	1.391(12)	O1-C16	1.548(12)
O2-C17	1.240(12)	C17-C18	1.449(14)

Table 5. Bond angles (°) for complex 1d.

C9-Pd1-C5	88.7(3)	C9-Pd1-C6	92.9(3)
C5-Pd1-C6	36.9(3)	C9-Pd1-Cl2	94.58(19)
C5-Pd1-Cl2	161.7(2)	C6-Pd1-Cl2	159.9(2)
C9-Pd1-C1	165.0(3)	C5-Pd1-C1	92.5(3)
C6-Pd1-C1	79.4(3)	Cl2-Pd1-C1	88.87(18)
C9-Pd1-C2	160.7(3)	C5-Pd1-C2	78.8(3)
C6-Pd1-C2	86.0(3)	Cl2-Pd1-C2	92.95(19)
C1-Pd1-C2	32.6(3)	C1-C2-C3	123.8(7)
C1-C2-Pd1	73.1(4)	C3-C2-Pd1	108.5(5)
C10-C9-C15	104.4(5)	C10-C9-Pd1	117.5(5)
C15-C9-Pd1	113.8(4)	C6-C5-C4	127.4(7)
C6-C5-Pd1	72.6(4)	C4-C5-Pd1	109.1(5)
C9-C10-C14	103.5(5)	C9-C10-C11	108.8(6)
C14-C10-C11	98.0(5)	C16-C11-C10	118.3(6)
C16-C11-C12	112.0(7)	C10-C11-C12	103.0(6)
C2-C1-C8	125.9(7)	C2-C1-Pd1	74.3(4)
C8-C1-Pd1	106.0(4)	C10-C14-C13	93.9(5)
C12-C13-C14	102.8(6)	C12-C13-C15	109.7(6)
C14-C13-C15	101.3(5)	C5-C6-C7	124.3(6)
C5-C6-Pd1	70.5(4)	C7-C6-Pd1	113.3(4)
C1-C8-C7	114.6(6)	C2-C3-C4	112.9(6)
C19-C15-C13	113.0(6)	C19-C15-C9	116.5(6)
C13-C15-C9	100.7(5)	C6-C7-C8	116.9(6)
C5-C4-C3	115.7(6)	C13-C12-C11	102.8(6)
C17-O1-C16	116.6(8)	C11-C16-O1	108.8(7)

O2-C17-O1	126.7(11)	O2-C17-C18	124.2(10)
O1-C17-C18	108.7(9)		

Appendix F

Crystal structure information, compound 3a in Chapter 4

Table 1. Sample and crystal data for complex 3a.

Empirical formula	C32 H42 N2 O Pd	
Formula weight	577.08	
Temperature	98(2) K	
Wavelength	0.71073 Å	
Crystal size	0.20 x 0.19 x 0.09 mm	
Crystal habit	Yellow-clear Brick	
Crystal system	Triclinic	
Space group	P1	
Unit cell dimensions	a = 11.1653(17) Å	α= 105.623(2)°
	b = 11.3688(17) Å	β= 99.448(2)°
	c = 13.611(2) Å	γ = 113.062(2)°
Volume	1458.3(4) $Å^3$	
Z	2	
Density (calculated)	1.314 g/cm^3	
Absorption coefficient	0.662 mm^{-1}	
F(000)	604	

Table 2. Data collection and structure refinement for complex 3a.

Diffractometer	CCD area detector
Radiation source	fine-focus sealed tube, MoK
Generator power	1600 watts (50 kV, 32mA)
Detector distance	5.8 cm
Data collection method	omega scans
Theta range for data collection	1.63 to 28.04°
Index ranges	$-14 \leq h \leq 14$, $-14 \leq k \leq 14$, $-17 \leq l \leq 17$

Table 3. Atomic coordinates and equivalent isotropic atomic displacement parameters (Å ^{2}) for complex 3a.

U(eq) is defined as one third of the trace of the orthogonalized U_{ij} tensor.

	x/a	y/b	z/c	U(eq)
Pd1	0.86458(3)	0.79906(3)	0.87833(2)	0.01813(17)
Pd2	0.35917(2)	0.75628(3)	0.23499(2)	0.01837(17)
O2	0.7092(7)	0.8461(8)	0.9011(6)	0.0254(19)
N4	0.2312(9)	0.5785(9)	0.1047(8)	0.021(2)
N1	0.7321(10)	0.6213(9)	0.7531(8)	0.022(2)
N2	0.9903(10)	0.9720(10)	1.0022(8)	0.023(2)
O1	0.5201(8)	0.7120(7)	0.2135(6)	0.0218(19)
N3	0.4849(10)	0.9289(10)	0.3575(7)	0.021(2)
C12	1.0309(11)	0.7687(10)	0.8687(10)	0.028(3)
C52	0.1934(13)	0.7826(13)	0.2461(10)	0.043(3)
C6	0.5199(11)	0.6368(10)	0.7676(7)	0.021(2)
C38	0.6983(10)	0.9149(11)	0.3461(9)	0.022(2)
C33	0.6497(8)	0.7932(9)	0.2649(8)	0.0134(17)
C36	0.9319(12)	0.9487(13)	0.3676(10)	0.032(3)
C43	0.7996(12)	0.5583(12)	0.1246(9)	0.033(3)
C8	0.5447(10)	0.9620(11)	0.9727(8)	0.0180(19)
C14	1.0697(11)	1.0905(9)	1.0036(9)	0.030(3)
C4	0.2934(12)	0.6082(13)	0.7527(9)	0.026(3)
C42	0.6175(11)	0.5984(10)	0.0358(8)	0.033(3)
C7	0.6018(9)	0.5838(9)	0.7259(8)	0.026(2)
C39	0.6178(11)	0.9792(10)	0.3894(8)	0.020(2)
C40	0.6938(11)	0.5980(12)	0.1411(10)	0.025(2)
C1	0.5805(11)	0.7784(10)	0.8552(8)	0.026(2)
C53	0.4338(10)	1.0106(9)	0.4277(8)	0.024(2)
C5	0.3741(9)	0.5603(10)	0.7196(8)	0.020(2)
C2	0.4780(11)	0.8150(9)	0.8797(8)	0.021(2)
C21	0.7829(10)	0.5397(11)	0.6935(8)	0.023(2)
C10	0.6088(10)	0.9585(11)	1.0802(7)	0.026(3)
C9	0.4235(12)	0.9992(13)	0.9919(10)	0.040(3)
C45	0.1483(10)	0.4629(11)	0.1055(8)	0.021(2)
C35	0.8762(11)	0.8154(10)	0.2782(8)	0.028(2)
C27	0.7653(11)	0.4091(11)	0.8124(10)	0.029(2)
C34	0.7350(10)	0.7298(11)	0.2274(8)	0.024(2)
C37	0.8364(11)	0.9936(11)	0.3949(9)	0.029(2)
C25	0.8494(11)	0.3576(11)	0.6543(8)	0.024(2)
C60	0.4637(11)	1.1458(12)	0.2961(9)	0.022(2)
C3	0.3441(9)	0.7345(11)	0.8263(8)	0.025(2)
C55	0.3710(12)	1.1884(12)	0.4560(10)	0.039(3)

C41	0.5825(12)	0.4852(11)	0.1673(9)	0.027(2)
C15	1.0881(10)	1.1284(11)	0.9175(8)	0.021(2)
C13	0.9857(11)	0.9609(11)	1.1108(8)	0.025(2)
C54	0.4215(11)	1.1191(9)	0.3931(9)	0.028(3)
C20	0.9788(13)	1.0747(12)	0.8226(10)	0.032(3)
C51	0.2515(11)	0.4882(10)	0.2969(9)	0.023(2)
C44	0.2375(11)	0.5981(12)	0.0083(9)	0.032(3)
C11	0.6394(12)	1.0798(11)	0.9454(10)	0.031(3)
C46	0.1420(12)	0.4307(11)	0.2091(9)	0.026(2)
C26	0.7959(10)	0.4379(10)	0.7158(7)	0.022(2)
C24	0.8905(13)	0.3942(13)	0.5706(10)	0.041(3)
C47	0.0091(10)	0.3233(11)	0.1954(10)	0.033(3)
C56	0.3307(13)	1.1616(13)	0.5395(9)	0.033(3)
C23	0.8828(14)	0.4966(14)	0.5477(10)	0.040(3)
C22	0.8253(13)	0.5829(12)	0.6082(9)	0.029(2)
C16	1.2061(12)	1.2213(13)	0.9138(10)	0.042(3)
C50	0.2290(15)	0.4423(13)	0.3797(9)	0.039(3)
C19	0.9886(13)	1.1101(11)	0.7331(11)	0.033(3)
C57	0.3405(14)	1.0491(12)	0.5631(9)	0.030(3)
C58	0.3895(13)	0.9819(11)	0.5074(9)	0.029(2)
C48	0.0001(14)	0.2894(14)	0.2884(12)	0.047(3)
C18	1.1201(15)	1.2163(14)	0.7372(12)	0.040(3)
C49	0.1092(16)	0.3507(16)	0.3721(12)	0.043(3)
C17	1.2282(14)	1.2697(14)	0.8347(12)	0.047(3)
C63	0.8571(11)	0.3649(12)	0.8740(10)	0.037(3)
C68	0.3771(10)	1.2042(12)	0.2476(9)	0.032(2)
C64	0.6151(12)	0.3045(13)	0.7823(11)	0.043(3)
C72	0.935(2)	0.7769(17)	0.5511(15)	0.097(6)
C71	0.672(2)	0.6457(18)	0.4991(12)	0.077(5)
C70	0.8143(18)	0.6959(15)	0.5775(12)	0.043(3)
C69	0.6150(11)	1.2448(10)	0.3223(10)	0.032(2)
C74	0.4007(19)	0.8579(16)	0.5275(12)	0.043(4)
C76	0.2756(19)	0.7703(15)	0.5573(14)	0.071(5)
C75	0.5246(17)	0.9072(13)	0.6231(10)	0.059(3)

Table 4. Bond lengths (Å) for complex 3a.

Pd1-N2	1.989(10)	Pd1-C12	2.035(10)
Pd1-N1	2.038(9)	Pd1-O2	2.051(7)
Pd2-N3	1.978(10)	Pd2-C52	2.010(12)
Pd2-N4	2.060(9)	Pd2-O1	2.090(7)
O2-C1	1.275(13)	N4-C45	1.281(13)
N4-C44	1.397(14)	N1-C7	1.299(14)
N1-C21	1.414(14)	N2-C14	1.283(14)

N2-C13	1.525(12)	O1-C33	1.308(11)
N3-C39	1.307(14)	N3-C53	1.489(12)
C6-C7	1.392(14)	C6-C5	1.439(13)
C6-C1	1.524(13)	C38-C33	1.350(14)
C38-C37	1.372(14)	C38-C39	1.465(13)
C33-C34	1.479(13)	C36-C37	1.410(16)
C36-C35	1.479(16)	C43-C40	1.449(15)
C8-C11	1.528(15)	C8-C10	1.538(12)
C8-C2	1.589(13)	C8-C9	1.607(15)
C14-C15	1.373(15)	C4-C5	1.303(15)
C4-C3	1.336(16)	C42-C40	1.544(15)
C40-C34	1.473(16)	C40-C41	1.567(15)
C1-C2	1.420(15)	C53-C58	1.329(15)
C53-C54	1.478(13)	C2-C3	1.347(14)
C21-C26	1.327(13)	C21-C22	1.456(15)
C45-C46	1.556(14)	C35-C34	1.410(15)
C27-C26	1.497(15)	C27-C63	1.535(15)
C27-C64	1.532(16)	C25-C24	1.400(16)
C25-C26	1.439(12)	C60-C69	1.531(15)
C60-C54	1.539(16)	C60-C68	1.529(14)
C55-C56	1.354(17)	C55-C54	1.346(15)
C15-C16	1.346(16)	C15-C20	1.415(16)
C20-C19	1.390(16)	C51-C46	1.351(16)
C51-C50	1.383(15)	C46-C47	1.447(15)
C24-C23	1.312(18)	C47-C48	1.427(17)
C56-C57	1.439(16)	C23-C22	1.511(15)
C22-C70	1.495(18)	C16-C17	1.350(18)
C50-C49	1.300(19)	C19-C18	1.472(18)
C57-C58	1.268(15)	C58-C74	1.554(18)
C48-C49	1.31(2)	C18-C17	1.43(2)
C72-C70	1.47(2)	C71-C70	1.54(2)
C74-C75	1.53(2)	C74-C76	1.56(2)

Table 5. Bond angles (°) for complex 3a.

N2-Pd1-C12	87.0(4)	N2-Pd1-N1	178.6(5)
C12-Pd1-N1	94.1(4)	N2-Pd1-O2	87.4(3)
C12-Pd1-O2	174.4(4)	N1-Pd1-O2	91.4(3)
N3-Pd2-C52	93.5(4)	N3-Pd2-N4	178.4(5)
C52-Pd2-N4	87.3(4)	N3-Pd2-O1	91.4(3)
C52-Pd2-O1	175.0(4)	N4-Pd2-O1	87.8(3)
C1-O2-Pd1	131.0(7)	C45-N4-C44	120.9(10)
C45-N4-Pd2	127.4(8)	C44-N4-Pd2	111.7(7)
C7-N1-C21	119.6(9)	C7-N1-Pd1	120.7(7)
C21-N1-Pd1	119.6(7)	C14-N2-C13	116.3(10)
C14-N2-Pd1	129.7(8)	C13-N2-Pd1	113.9(7)
C33-O1-Pd2	125.8(6)	C39-N3-C53	113.0(9)
C39-N3-Pd2	125.0(7)	C53-N3-Pd2	121.9(7)
C7-C6-C5	118.6(9)	C7-C6-C1	122.0(9)
C5-C6-C1	119.2(9)	C33-C38-C37	120.1(10)
C33-C38-C39	126.7(8)	C37-C38-C39	113.1(10)
O1-C33-C38	124.3(8)	O1-C33-C34	111.1(8)
C38-C33-C34	124.5(8)	C37-C36-C35	116.4(10)
C11-C8-C10	113.6(9)	C11-C8-C2	114.5(8)
C10-C8-C2	111.3(8)	C11-C8-C9	104.3(9)
C10-C8-C9	104.3(8)	C2-C8-C9	107.8(8)
N2-C14-C15	127.6(10)	C5-C4-C3	120.9(10)
N1-C7-C6	134.1(9)	N3-C39-C38	126.5(9)
C43-C40-C34	117.5(10)	C43-C40-C42	110.0(9)
C34-C40-C42	108.5(9)	C43-C40-C41	109.1(9)
C34-C40-C41	106.1(9)	C42-C40-C41	104.9(9)
O2-C1-C2	127.6(9)	O2-C1-C6	120.2(9)
C2-C1-C6	112.1(9)	C58-C53-C54	121.9(9)
C58-C53-N3	124.3(9)	C54-C53-N3	113.5(9)
C4-C5-C6	121.0(10)	C3-C2-C1	122.6(9)
C3-C2-C8	126.7(9)	C1-C2-C8	110.7(9)
C26-C21-N1	123.5(9)	C26-C21-C22	123.4(10)
N1-C21-C22	113.1(9)	N4-C45-C46	123.7(10)
C34-C35-C36	123.1(10)	C26-C27-C63	117.4(10)
C26-C27-C64	109.7(9)	C63-C27-C64	110.0(10)
C35-C34-C40	117.3(9)	C35-C34-C33	113.2(9)
C40-C34-C33	129.3(9)	C38-C37-C36	122.3(10)
C24-C25-C26	116.7(10)	C69-C60-C54	114.2(9)
C69-C60-C68	108.9(9)	C54-C60-C68	108.4(9)
C4-C3-C2	123.9(9)	C56-C55-C54	125.4(11)
C16-C15-C14	125.4(10)	C16-C15-C20	112.9(11)
C14-C15-C20	121.7(10)	C55-C54-C53	112.2(10)
C55-C54-C60	125.8(9)	C53-C54-C60	122.0(9)

C19-C20-C15	125.1(11)	C46-C51-C50	115.5(11)
C51-C46-C47	124.9(11)	C51-C46-C45	123.3(10)
C47-C46-C45	111.6(10)	C21-C26-C25	122.1(9)
C21-C26-C27	120.7(9)	C25-C26-C27	117.0(9)
C23-C24-C25	123.1(12)	C46-C47-C48	113.2(10)
C55-C56-C57	118.0(11)	C24-C23-C22	122.6(12)
C21-C22-C70	127.0(10)	C21-C22-C23	112.0(10)
C70-C22-C23	121.0(11)	C17-C16-C15	128.1(12)
C49-C50-C51	121.2(13)	C20-C19-C18	118.6(12)
C58-C57-C56	119.2(11)	C57-C58-C53	123.3(10)
C57-C58-C74	121.7(11)	C53-C58-C74	115.0(10)
C49-C48-C47	119.0(11)	C17-C18-C19	114.9(12)
C50-C49-C48	126.0(13)	C16-C17-C18	120.3(12)
C72-C70-C22	112.7(13)	C72-C70-C71	117.7(15)
C22-C70-C71	111.6(13)	C75-C74-C76	105.2(13)
C75-C74-C58	110.7(13)	C76-C74-C58	111.8(13)

Appendix G

Crystal structure information, compound 3c in Chapter 4

Table 1. Sample and crystal data for complex 3c.

Empirical formula	C105 H144 N6 O3 Pd3	
Formula weight	1857.46	
Temperature	98(2) K	
Wavelength	0.71073 Å	
Crystal size	0.45 x 0.15 x 0.15 mm	
Crystal habit	yellow Brick	
Crystal system	Monoclinic	
Space group	P2(1)/c	
Unit cell dimensions	a = 11.4483(11) Å	α= 90°
	b = 19.4368(19) Å	β= 90°
	c = 43.765(4) Å	γ = 90°
Volume	9738.5(17) $Å^3$	
Z	4	
Density (calculated)	1.267 g/cm^3	
Absorption coefficient	0.599 mm^{-1}	
F(000)	3912	

Table 2. Data collection and structure refinement for complex 3c.

Diffractometer	CCD area detector
Radiation source	fine-focus sealed tube, MoK
Generator power	1600 watts (50 kV, 32mA)
Detector distance	5.8 cm
Data collection method	omega scans
Theta range for data collection	0.93 to 28.03°
Index ranges	$-15 \leq h \leq 15$, $-24 \leq k \leq 25$, $-57 \leq l \leq 57$

Table 3. Atomic coordinates and equivalent isotropic

atomic displacement parameters (Å ^{2}) for **complex 3c**.
U(eq) is defined as one third of the trace of the orthogonalized U_{ij} tensor.

	x/a	y/b	z/c	U(eq)	
Pd1	0.319165(15)		0.481161(9)	0.902213(4)	0.01518(4)
Pd2	0.342551(15)		0.740692(9)	0.766371(4)	0.01543(4)
Pd3	-0.025818(14)		0.066242(9)	0.912278(4)	0.01425(4)
N1	0.23332(16)	0.49114(10)	0.94259(4)	0.0156(4)	
O1	0.39995(14)	0.39041(8)	0.91735(4)	0.0197(3)	
N5	-0.11592(16)	-0.01487(10)	0.89541(4)	0.0158(4)	
N6	0.07631(17)	0.14494(10)	0.92938(4)	0.0181(4)	
O3	0.06252(14)	0.07908(8)	0.87074(4)	0.0183(3)	
N2	0.41095(17)	0.46845(11)	0.86215(4)	0.0198(4)	
O2	0.26153(14)	0.80991(8)	0.73644(4)	0.0212(4)	
C89	-0.1081(2)	0.06047(14)	0.95324(5)	0.0247(5)	
N4	0.23813(17)	0.66485(10)	0.74746(5)	0.0199(4)	
N3	0.44093(16)	0.81728(10)	0.78444(4)	0.0163(4)	
C12	0.2497(2)	0.56857(13)	0.88473(6)	0.0261(5)	
C44	0.6398(2)	0.80030(12)	0.80424(5)	0.0184(5)	
C33	0.2172(2)	0.91351(12)	0.71037(5)	0.0179(5)	
C38	0.43573(19)	0.88018(12)	0.77452(5)	0.0166(5)	
C7	0.23914(19)	0.44515(12)	0.96390(5)	0.0162(4)	
C2	0.4545(2)	0.29840(12)	0.94975(6)	0.0184(5)	
C6	0.30584(19)	0.38305(12)	0.96590(5)	0.0166(5)	
C80	-0.3620(2)	0.02136(13)	0.89214(6)	0.0247(5)	
C67	-0.09609(19)	-0.03987(12)	0.86831(5)	0.0167(5)	
C37	0.36825(19)	0.91036(12)	0.75037(5)	0.0161(4)	
C62	-0.0173(2)	-0.01780(12)	0.84473(5)	0.0170(5)	
C18	0.0346(2)	0.53737(12)	0.94737(5)	0.0181(5)	
C60	0.2761(2)	0.62871(13)	0.71843(6)	0.0226(5)	
C34	0.2434(2)	0.98215(13)	0.70634(5)	0.0208(5)	
C61	0.05939(19)	0.04026(12)	0.84701(5)	0.0151(4)	
C66	0.13515(19)	0.05468(12)	0.82134(5)	0.0161(4)	
C52	0.4149(2)	0.66919(13)	0.79413(6)	0.0272(6)	
C54	0.0893(2)	0.66806(13)	0.78802(6)	0.0233(5)	
C73	-0.3971(2)	-0.08130(13)	0.92667(6)	0.0208(5)	
C53	0.1418(2)	0.64442(13)	0.75917(6)	0.0245(5)	
C43	0.5202(2)	0.80904(12)	0.81008(5)	0.0174(5)	
C13	0.1554(2)	0.54789(12)	0.94950(5)	0.0168(5)	
C35	0.3308(2)	1.01620(13)	0.72299(6)	0.0216(5)	
C1	0.38708(19)	0.35946(12)	0.94308(5)	0.0166(5)	
C5	0.2889(2)	0.34426(13)	0.99283(6)	0.0203(5)	
C83	0.2233(2)	0.06781(14)	0.95198(6)	0.0240(5)	
C46	0.6734(2)	0.80792(12)	0.85884(6)	0.0228(5)	

C88	0.2199(2)	0.01068(14)	0.93282(6)	0.0244(5)
C71	-0.1994(2)	-0.05477(12)	0.91290(5)	0.0160(4)
C68	0.2179(2)	0.11668(12)	0.82269(5)	0.0183(5)
C3	0.4328(2)	0.26354(13)	0.97655(6)	0.0228(5)
C32	0.28226(19)	0.87439(12)	0.73283(5)	0.0167(5)
C76	-0.1583(2)	-0.10845(12)	0.93108(5)	0.0171(5)
C70	0.1459(2)	0.18331(13)	0.82388(6)	0.0258(5)
C19	-0.0201(2)	0.46980(13)	0.93754(6)	0.0225(5)
C47	0.5545(2)	0.81188(13)	0.86399(6)	0.0231(5)
C26	0.5735(2)	0.54210(14)	0.87821(6)	0.0243(5)
C15	0.1275(2)	0.66450(13)	0.96575(6)	0.0235(5)
C25	0.5101(2)	0.49695(14)	0.85711(6)	0.0250(5)
C75	-0.2400(2)	-0.15021(13)	0.94578(5)	0.0212(5)
C63	-0.0187(2)	-0.05813(13)	0.81786(6)	0.0228(5)
C36	0.3912(2)	0.98045(12)	0.74465(5)	0.0189(5)
C17	-0.0376(2)	0.59325(13)	0.95449(6)	0.0229(5)
C64	0.0537(2)	-0.04399(14)	0.79387(6)	0.0265(6)
C48	0.4749(2)	0.81298(12)	0.83971(5)	0.0188(5)
C9	0.4844(2)	0.24810(14)	0.89758(6)	0.0310(6)
C16	0.0079(2)	0.65564(13)	0.96368(6)	0.0249(5)
C8	0.5464(2)	0.27294(13)	0.92688(6)	0.0240(5)
C59	0.0985(2)	0.73485(14)	0.79917(6)	0.0246(5)
C87	0.2707(2)	-0.05039(15)	0.94191(7)	0.0311(6)
C45	0.7154(2)	0.80091(12)	0.82939(6)	0.0211(5)
C14	0.2039(2)	0.61099(12)	0.95857(5)	0.0182(5)
C77	-0.0283(2)	-0.12269(13)	0.93478(6)	0.0227(5)
C74	-0.3587(2)	-0.13706(13)	0.94338(6)	0.0229(5)
C72	-0.3186(2)	-0.03919(12)	0.91084(5)	0.0177(5)
C41	0.1854(3)	0.82469(16)	0.66997(7)	0.0379(7)
C23	0.3792(2)	0.59576(15)	0.99257(6)	0.0296(6)
C22	0.3355(2)	0.61953(13)	0.96119(6)	0.0210(5)
C24	0.3762(2)	0.69343(14)	0.95489(7)	0.0310(6)
C27	0.5714(2)	0.53446(14)	0.90996(6)	0.0263(6)
C50	0.3075(2)	0.89339(15)	0.85036(7)	0.0336(6)
C69	0.2990(2)	0.11185(14)	0.85075(6)	0.0270(6)
C78	0.0099(3)	-0.18153(16)	0.91402(7)	0.0365(7)
C10	0.6172(2)	0.21267(15)	0.93976(7)	0.0341(6)
C82	0.1704(2)	0.13476(14)	0.94441(6)	0.0227(5)
C81	-0.4753(2)	0.05176(14)	0.90507(7)	0.0338(6)
C58	0.0503(2)	0.75129(15)	0.82727(7)	0.0292(6)
C39	0.1242(2)	0.87738(13)	0.69087(6)	0.0231(5)
C28	0.6292(2)	0.58132(15)	0.92836(7)	0.0324(6)
C65	0.1299(2)	0.01247(13)	0.79598(6)	0.0222(5)
C4	0.3496(2)	0.28524(13)	0.99815(6)	0.0236(5)
C84	0.2820(2)	0.06313(18)	0.97983(6)	0.0356(7)

C30	0.6961(3)	0.64192(15)	0.88375(8)	0.0405(8)
C79	0.0053(2)	-0.13730(14)	0.96792(6)	0.0275(6)
C21	-0.1070(2)	0.44354(14)	0.96147(6)	0.0299(6)
C29	0.6897(2)	0.63602(15)	0.91527(8)	0.0389(7)
C42	0.0601(3)	0.92788(15)	0.66997(7)	0.0363(7)
C49	0.3446(2)	0.81861(14)	0.84583(6)	0.0234(5)
C40	0.0319(2)	0.84171(16)	0.71094(7)	0.0355(7)
C20	-0.0793(3)	0.47702(17)	0.90657(7)	0.0412(8)
C51	0.3072(3)	0.77490(16)	0.87297(7)	0.0342(7)
C56	-0.0202(3)	0.63607(16)	0.83282(7)	0.0374(7)
C85	0.3311(3)	0.00168(19)	0.98915(7)	0.0427(8)
C31	0.6388(2)	0.59503(15)	0.86531(7)	0.0337(6)
C11	0.6338(2)	0.33024(16)	0.91854(7)	0.0332(6)
C57	-0.0069(2)	0.70151(16)	0.84436(7)	0.0349(7)
C55	0.0262(2)	0.61942(15)	0.80471(7)	0.0321(6)
C86	0.3251(2)	-0.05492(18)	0.97037(7)	0.0397(8)
C102	0.0395(2)	0.21941(13)	0.92484(6)	0.0232(5)
C99	0.6866(2)	0.79116(14)	0.77192(6)	0.0233(5)
C92	0.3590(2)	0.42546(13)	0.83660(6)	0.0236(5)
C98	0.1796(2)	0.63176(15)	0.69419(6)	0.0286(6)
C91	-0.3819(2)	0.00145(15)	0.85855(6)	0.0300(6)
C93	0.2608(2)	0.38228(14)	0.84999(6)	0.0272(6)
C103	0.1402(3)	0.26118(15)	0.91096(7)	0.0339(6)
C94	0.4511(3)	0.37781(15)	0.82249(7)	0.0331(6)
C90	0.2969(2)	0.12077(15)	0.79451(6)	0.0288(6)
C104	-0.0635(2)	0.22051(14)	0.90302(7)	0.0285(6)
C105	0.0048(3)	0.24875(15)	0.95599(7)	0.0392(7)
C101	0.7335(3)	0.85871(16)	0.75895(7)	0.0348(7)
C95	0.3103(3)	0.47541(15)	0.81279(6)	0.0377(7)
C96	0.3038(3)	0.55387(15)	0.72646(7)	0.0370(7)
C100	0.7822(3)	0.73624(17)	0.77054(7)	0.0382(7)
C97	0.3851(2)	0.66474(16)	0.70633(7)	0.0343(7)

Table 4. Bond lengths (Å) for complex 3c.

Pd1-C12	2.026(3)	Pd1-N1	2.0314(19)
Pd1-N2	2.059(2)	Pd1-O1	2.0990(16)
Pd2-N3	2.0272(19)	Pd2-C52	2.023(2)
Pd2-N4	2.071(2)	Pd2-O2	2.0944(16)
Pd3-N5	2.0234(19)	Pd3-C89	2.028(2)
Pd3-N6	2.066(2)	Pd3-O3	2.0950(16)
N1-C7	1.294(3)	N1-C13	1.451(3)
O1-C1	1.285(3)	N5-C67	1.302(3)
N5-C71	1.449(3)	N6-C82	1.277(3)
N6-C102	1.521(3)	O3-C61	1.284(3)

N2-C25	1.282(3)	N2-C92	1.517(3)
O2-C32	1.285(3)	N4-C53	1.280(3)
N4-C60	1.515(3)	N3-C38	1.299(3)
N3-C43	1.453(3)	C44-C45	1.400(3)
C44-C43	1.403(3)	C44-C99	1.523(3)
C33-C34	1.379(3)	C33-C32	1.449(3)
C33-C39	1.535(3)	C38-C37	1.435(3)
C7-C6	1.431(3)	C2-C3	1.377(4)
C2-C1	1.446(3)	C2-C8	1.534(3)
C6-C5	1.412(3)	C6-C1	1.440(3)
C80-C72	1.517(3)	C80-C81	1.533(4)
C80-C91	1.537(4)	C67-C62	1.437(3)
C37-C36	1.410(3)	C37-C32	1.431(3)
C62-C63	1.413(3)	C62-C61	1.433(3)
C18-C17	1.400(3)	C18-C13	1.401(3)
C18-C19	1.517(3)	C60-C97	1.526(4)
C60-C96	1.530(4)	C60-C98	1.532(3)
C34-C35	1.403(3)	C61-C66	1.447(3)
C66-C65	1.381(3)	C66-C68	1.534(3)
C54-C59	1.391(4)	C54-C55	1.396(4)
C54-C53	1.471(4)	C73-C74	1.380(3)
C73-C72	1.399(3)	C43-C48	1.399(3)
C13-C14	1.404(3)	C35-C36	1.364(3)
C5-C4	1.361(3)	C83-C88	1.392(4)
C83-C84	1.395(4)	C83-C82	1.473(4)
C46-C47	1.382(4)	C46-C45	1.382(3)
C88-C87	1.380(4)	C71-C76	1.393(3)
C71-C72	1.402(3)	C68-C90	1.531(3)
C68-C70	1.536(3)	C68-C69	1.542(3)
C3-C4	1.406(4)	C76-C75	1.395(3)
C76-C77	1.523(3)	C19-C20	1.522(4)
C19-C21	1.532(4)	C47-C48	1.400(3)
C26-C31	1.392(4)	C26-C27	1.398(4)
C26-C25	1.466(4)	C15-C16	1.382(4)
C15-C14	1.395(3)	C75-C74	1.386(3)
C63-C64	1.366(3)	C17-C16	1.380(4)
C64-C65	1.405(3)	C48-C49	1.519(3)
C9-C8	1.543(4)	C8-C10	1.532(4)
C8-C11	1.541(4)	C59-C58	1.385(4)
C87-C86	1.395(4)	C14-C22	1.520(3)
C77-C78	1.525(4)	C77-C79	1.527(3)
C41-C39	1.542(4)	C23-C22	1.533(3)
C22-C24	1.535(3)	C27-C28	1.384(4)
C50-C49	1.527(4)	C58-C57	1.387(4)
C39-C42	1.529(4)	C39-C40	1.539(4)

C28-C29	1.393(4)	C84-C85	1.382(4)
C30-C31	1.383(4)	C30-C29	1.386(5)
C49-C51	1.522(4)	C56-C57	1.377(4)
C56-C55	1.379(4)	C85-C86	1.375(5)
C102-C104	1.517(4)	C102-C105	1.530(4)
C102-C103	1.535(4)	C99-C101	1.528(4)
C99-C100	1.530(4)	C92-C93	1.520(4)
C92-C95	1.529(4)	C92-C94	1.533(4)

Table 5. Bond angles (°) for complex 3c.

C12-Pd1-N1	93.36(9)	C12-Pd1-N2	88.82(9)
N1-Pd1-N2	177.68(8)	C12-Pd1-O1	175.50(9)
N1-Pd1-O1	91.08(7)	N2-Pd1-O1	86.74(7)
N3-Pd2-C52	92.45(9)	N3-Pd2-N4	178.13(8)
C52-Pd2-N4	89.28(9)	N3-Pd2-O2	91.05(7)
C52-Pd2-O2	176.50(9)	N4-Pd2-O2	87.22(7)
N5-Pd3-C89	92.45(9)	N5-Pd3-N6	176.09(8)
C89-Pd3-N6	89.05(9)	N5-Pd3-O3	91.28(7)
C89-Pd3-O3	176.08(9)	N6-Pd3-O3	87.31(7)
C7-N1-C13	114.01(19)	C7-N1-Pd1	122.43(16)
C13-N1-Pd1	123.47(15)	C1-O1-Pd1	128.26(15)
C67-N5-C71	113.35(19)	C67-N5-Pd3	122.30(16)
C71-N5-Pd3	124.08(14)	C82-N6-C102	116.6(2)
C82-N6-Pd3	123.31(18)	C102-N6-Pd3	120.04(15)
C61-O3-Pd3	128.19(14)	C25-N2-C92	117.3(2)
C25-N2-Pd1	123.13(18)	C92-N2-Pd1	119.58(15)
C32-O2-Pd2	128.42(15)	C53-N4-C60	116.1(2)
C53-N4-Pd2	123.94(18)	C60-N4-Pd2	119.98(15)
C38-N3-C43	113.00(19)	C38-N3-Pd2	122.37(16)
C43-N3-Pd2	124.59(15)	C45-C44-C43	117.3(2)
C45-C44-C99	120.9(2)	C43-C44-C99	121.8(2)
C34-C33-C32	118.8(2)	C34-C33-C39	121.5(2)
C32-C33-C39	119.6(2)	N3-C38-C37	131.0(2)
N1-C7-C6	130.9(2)	C3-C2-C1	118.6(2)
C3-C2-C8	121.4(2)	C1-C2-C8	120.0(2)
C5-C6-C7	115.3(2)	C5-C6-C1	119.8(2)
C7-C6-C1	124.8(2)	C72-C80-C81	112.1(2)
C72-C80-C91	111.7(2)	C81-C80-C91	108.9(2)
N5-C67-C62	130.7(2)	C36-C37-C32	120.4(2)
C36-C37-C38	115.2(2)	C32-C37-C38	124.5(2)
C63-C62-C61	120.1(2)	C63-C62-C67	115.1(2)
C61-C62-C67	124.7(2)	C17-C18-C13	117.0(2)
C17-C18-C19	119.4(2)	C13-C18-C19	123.5(2)
N4-C60-C97	108.2(2)	N4-C60-C96	107.9(2)

C97-C60-C96	110.3(2)	N4-C60-C98	110.9(2)
C97-C60-C98	109.4(2)	C96-C60-C98	110.2(2)
C33-C34-C35	123.0(2)	O3-C61-C62	122.4(2)
O3-C61-C66	119.8(2)	C62-C61-C66	117.7(2)
C65-C66-C61	118.9(2)	C65-C66-C68	121.6(2)
C61-C66-C68	119.5(2)	C59-C54-C55	119.2(2)
C59-C54-C53	124.2(2)	C55-C54-C53	116.7(2)
C74-C73-C72	121.1(2)	N4-C53-C54	126.8(2)
C48-C43-C44	122.5(2)	C48-C43-N3	118.6(2)
C44-C43-N3	118.8(2)	C18-C13-C14	122.5(2)
C18-C13-N1	118.9(2)	C14-C13-N1	118.7(2)
C36-C35-C34	118.8(2)	O1-C1-C6	122.2(2)
O1-C1-C2	120.0(2)	C6-C1-C2	117.8(2)
C4-C5-C6	121.5(2)	C88-C83-C84	119.2(3)
C88-C83-C82	123.9(2)	C84-C83-C82	116.9(3)
C47-C46-C45	120.0(2)	C87-C88-C83	120.1(3)
C76-C71-C72	121.8(2)	C76-C71-N5	118.7(2)
C72-C71-N5	119.5(2)	C90-C68-C66	112.0(2)
C90-C68-C70	107.5(2)	C66-C68-C70	109.40(19)
C90-C68-C69	106.8(2)	C66-C68-C69	110.8(2)
C70-C68-C69	110.3(2)	C2-C3-C4	123.2(2)
O2-C32-C37	122.5(2)	O2-C32-C33	120.0(2)
C37-C32-C33	117.5(2)	C71-C76-C75	118.2(2)
C71-C76-C77	121.7(2)	C75-C76-C77	120.0(2)
C18-C19-C20	110.9(2)	C18-C19-C21	111.2(2)
C20-C19-C21	110.5(2)	C46-C47-C48	121.2(2)
C31-C26-C27	119.4(3)	C31-C26-C25	116.9(2)
C27-C26-C25	123.7(2)	C16-C15-C14	120.9(2)
N2-C25-C26	126.0(2)	C74-C75-C76	121.0(2)
C64-C63-C62	121.4(2)	C35-C36-C37	121.4(2)
C16-C17-C18	121.6(2)	C63-C64-C65	118.9(2)
C43-C48-C47	117.5(2)	C43-C48-C49	122.1(2)
C47-C48-C49	120.4(2)	C17-C16-C15	120.2(2)
C10-C8-C2	111.7(2)	C10-C8-C11	107.2(2)
C2-C8-C11	111.5(2)	C10-C8-C9	108.0(2)
C2-C8-C9	109.2(2)	C11-C8-C9	109.1(2)
C58-C59-C54	119.8(3)	C88-C87-C86	120.0(3)
C46-C45-C44	121.3(2)	C15-C14-C13	117.8(2)
C15-C14-C22	121.5(2)	C13-C14-C22	120.6(2)
C76-C77-C78	110.7(2)	C76-C77-C79	112.4(2)
C78-C77-C79	110.7(2)	C73-C74-C75	119.9(2)
C73-C72-C71	117.9(2)	C73-C72-C80	120.7(2)
C71-C72-C80	121.4(2)	C14-C22-C23	111.0(2)
C14-C22-C24	112.9(2)	C23-C22-C24	110.1(2)
C28-C27-C26	120.0(3)	N6-C82-C83	126.8(2)

C59-C58-C57	120.4(3)	C42-C39-C33	111.8(2)
C42-C39-C40	107.6(2)	C33-C39-C40	111.4(2)
C42-C39-C41	106.8(2)	C33-C39-C41	108.6(2)
C40-C39-C41	110.6(2)	C27-C28-C29	120.1(3)
C66-C65-C64	122.9(2)	C5-C4-C3	118.9(2)
C85-C84-C83	120.7(3)	C31-C30-C29	120.1(3)
C30-C29-C28	119.9(3)	C48-C49-C51	111.9(2)
C48-C49-C50	111.4(2)	C51-C49-C50	110.6(2)
C57-C56-C55	120.1(3)	C86-C85-C84	119.6(3)
C30-C31-C26	120.4(3)	C56-C57-C58	119.9(3)
C56-C55-C54	120.5(3)	C85-C86-C87	120.4(3)
C104-C102-N6	108.1(2)	C104-C102-C105	110.7(2)
N6-C102-C105	108.1(2)	C104-C102-C103	109.1(2)
N6-C102-C103	110.3(2)	C105-C102-C103	110.5(2)
C44-C99-C101	111.6(2)	C44-C99-C100	111.7(2)
C101-C99-C100	109.5(2)	N2-C92-C93	108.0(2)
N2-C92-C95	107.2(2)	C93-C92-C95	110.1(2)
N2-C92-C94	111.1(2)	C93-C92-C94	109.3(2)
C95-C92-C94	111.1(2)		

Appendix H

Crystal structure information, compound 3d in Chapter 4

Table 1. Sample and crystal data for complex 3d.

Empirical formula	C74 H88 N4 O2 Pd2	
Formula weight	1278.28	
Temperature	98(2) K	
Wavelength	0.71073 Å	
Crystal size	0.12 x 0.11 x 0.10 mm	
Crystal habit	yellow-clear brick	
Crystal system	Triclinic	
Space group	P1	
Unit cell dimensions	a = 11.9939(16) Å	α= 82.955(2)°
	b = 12.1298(16) Å	β= 69.190(2)°
	c = 13.9255(18) Å	γ = 60.381(2)°
Volume	1642.8(4) $Å^3$	
Z	1	
Density (calculated)	1.292 g/cm^3	
Absorption coefficient	0.595 mm^{-1}	
F(000)	668	

Table 2. Data collection and structure refinement for complex 3d.

Diffractometer	CCD area detector
Radiation source	fine-focus sealed tube, MoK
Generator power	1600 watts (50 kV, 32mA)
Detector distance	5.8 cm
Data collection method	omega scans
Theta range for data collection	1.94 to 28.05°
Index ranges	$-15 \leq h \leq 15$, $-15 \leq k \leq 15$, $-18 \leq l \leq 17$

Table 3. Atomic coordinates and equivalent isotropic atomic displacement parameters (Å ^{2}) for complex 3d.
U(eq) is defined as one third of the trace of the orthogonalized U_{ij} tensor.

	x/a	y/b	z/c	U(eq)
Pd1	0.38267(3)	0.71631(3)	0.23606(2)	0.02613(15)
Pd2	0.06482(3)	0.38239(3)	0.64543(2)	0.02503(14)
N1	0.3781(8)	0.8071(7)	0.1044(6)	0.0269(18)
N3	0.0738(6)	0.2896(6)	0.7732(5)	0.0122(13)
O2	-0.0846(7)	0.3480(7)	0.6419(5)	0.0328(17)
O1	0.5379(7)	0.7470(7)	0.2426(5)	0.0299(16)
C21	0.2371(9)	0.6748(9)	0.2440(7)	0.025(2)
C58	0.2151(11)	0.4243(11)	0.6396(8)	0.039(3)
C6	0.5587(7)	0.8596(8)	0.0936(6)	0.0182(16)
C43	-0.1093(8)	0.2393(7)	0.7976(6)	0.0171(16)
C41	-0.2841(9)	0.1710(9)	0.8459(8)	0.032(2)
C49	0.1643(8)	0.2772(9)	0.8300(6)	0.0220(18)
C12	0.2810(8)	0.8238(7)	0.0619(6)	0.0142(15)
C8	0.7306(9)	0.7707(7)	0.2945(7)	0.0227(18)
C2	0.6916(8)	0.8188(8)	0.1999(6)	0.0200(17)
C48	-0.0093(6)	0.2428(7)	0.8236(6)	0.0165(16)
C4	0.7201(8)	0.9341(8)	0.0418(6)	0.0230(18)
C53	0.2164(9)	0.3673(8)	0.9374(7)	0.028(2)
C14	0.2226(9)	0.7409(9)	-0.0523(6)	0.0263(19)
C7	0.4516(9)	0.8591(7)	0.0633(6)	0.0206(18)
C39	-0.2562(7)	0.2796(7)	0.6895(6)	0.0188(17)
C50	0.2865(9)	0.1710(7)	0.8056(6)	0.0192(17)
C44	-0.2929(9)	0.3388(9)	0.5905(6)	0.0256(19)
C38	-0.1497(8)	0.2930(7)	0.7041(5)	0.0213(18)
C3	0.7616(7)	0.8777(7)	0.1275(6)	0.0176(16)
C51	0.3764(9)	0.1623(9)	0.8525(7)	0.0264(19)
C16	0.0632(10)	0.9495(9)	0.0333(7)	0.027(2)
C1	0.5890(7)	0.8078(7)	0.1778(6)	0.0197(17)
C40	-0.3091(10)	0.2174(8)	0.7547(8)	0.034(2)
C13	0.3174(7)	0.7243(8)	-0.0049(6)	0.0243(18)
C17	0.1510(8)	0.9412(8)	0.0833(6)	0.0241(18)
C42	-0.1850(9)	0.1822(8)	0.8636(6)	0.0221(18)
C52	0.3405(9)	0.2587(8)	0.9188(6)	0.0249(18)
C54	0.1260(9)	0.3796(7)	0.8927(6)	0.0230(19)
C15	0.0977(9)	0.8528(9)	-0.0310(7)	0.035(2)
C5	0.6197(8)	0.9276(8)	0.0243(7)	0.0214(17)
C10	0.7908(10)	0.6249(9)	0.2903(8)	0.039(2)
C11	0.8453(11)	0.7931(10)	0.3001(9)	0.045(3)

C55	-0.0131(8)	0.5051(8)	0.9123(7)	0.031(2)
C46	-0.3463(10)	0.4816(7)	0.5892(7)	0.029(2)
C35	0.4502(9)	0.6068(7)	-0.0245(6)	0.0264(19)
C72	0.3343(10)	0.0577(9)	0.7297(8)	0.039(2)
C73	0.4508(11)	0.0525(9)	0.6335(7)	0.041(2)
C18	0.1124(9)	1.0380(7)	0.1562(6)	0.0251(19)
C47	-0.1644(11)	0.2732(10)	0.4911(7)	0.038(2)
C9	0.6072(11)	0.8326(11)	0.3902(7)	0.041(3)
C74	0.3781(12)	-0.0679(10)	0.7765(9)	0.049(3)
C20	0.0712(11)	1.1698(9)	0.1086(7)	0.037(2)
C56	-0.1149(10)	0.4910(11)	1.0055(8)	0.055(3)
C36	0.5713(9)	0.6068(8)	-0.1193(7)	0.033(2)
C37	0.4339(11)	0.4858(9)	-0.0300(10)	0.053(3)
C57	-0.0121(10)	0.6239(8)	0.9252(8)	0.039(2)
C19	-0.0006(16)	1.0489(12)	0.2578(9)	0.086(5)
C67	-0.1528(11)	0.6691(10)	0.6686(7)	0.038(2)
C71	-0.0450(13)	0.7766(14)	0.5444(9)	0.064(4)
C70	-0.1237(10)	0.8822(8)	0.6214(7)	0.043(2)
C66	-0.0513(9)	0.6619(10)	0.5709(7)	0.034(2)
C45	-0.3969(10)	0.3079(9)	0.5806(7)	0.033(2)
C68	-0.2087(10)	0.7629(11)	0.7358(8)	0.056(3)
C69	-0.1970(8)	0.8674(8)	0.7170(6)	0.048(2)
C65	0.0276(5)	0.5646(6)	0.4871(5)	0.0312(11)
N2	0.4234(4)	0.5865(4)	0.3448(3)	0.0183(8)
C25	0.6470(8)	0.2108(8)	0.2131(8)	0.055(2)
C26	0.5399(9)	0.2417(8)	0.3035(8)	0.052(3)
C22	0.5056(8)	0.4478(8)	0.3075(7)	0.0249(18)
C24	0.6794(11)	0.3071(12)	0.1647(9)	0.074(4)
C27	0.4758(11)	0.3522(11)	0.3487(9)	0.041(2)
C23	0.5960(11)	0.4328(9)	0.2149(8)	0.041(3)
C29	0.2990(7)	0.7331(7)	0.4906(8)	0.035(3)
C30	0.2296(11)	0.8537(10)	0.4625(7)	0.040(2)
C31	0.1606(11)	0.9565(11)	0.5278(9)	0.043(2)
C32	0.1373(11)	0.9455(11)	0.6327(8)	0.051(3)
C34	0.2755(14)	0.7233(12)	0.5991(11)	0.063(3)
C33	0.1852(15)	0.8334(14)	0.6675(9)	0.077(4)
C28	0.3850(5)	0.6064(5)	0.4430(4)	0.0213(9)
C59	0.1501(10)	0.3624(10)	0.3955(8)	0.044(3)
N4	0.0758(4)	0.4484(4)	0.4978(4)	0.0257(9)
C64	0.1562(17)	0.3913(12)	0.3002(12)	0.074(4)
C62	0.3004(13)	0.1768(13)	0.2450(9)	0.066(4)
C63	0.2213(15)	0.3012(11)	0.2264(8)	0.068(4)
C60	0.2079(9)	0.2413(7)	0.4240(7)	0.029(2)
C61	0.2958(10)	0.1435(8)	0.3415(9)	0.039(3)

Table 4. Bond lengths (Å) for complex 3d.

Pd1-C21	2.009(9)	Pd1-N1	2.024(8)
Pd1-N2	2.048(4)	Pd1-O1	2.105(6)
Pd2-N3	1.992(6)	Pd2-O2	2.048(7)
Pd2-C58	2.075(10)	Pd2-N4	2.096(5)
N1-C7	1.267(11)	N1-C12	1.405(11)
N3-C48	1.332(9)	N3-C49	1.499(10)
O2-C38	1.303(10)	O1-C1	1.275(11)
C6-C1	1.341(11)	C6-C5	1.431(11)
C6-C7	1.490(11)	C43-C48	1.391(11)
C43-C42	1.421(12)	C43-C38	1.511(10)
C41-C42	1.367(13)	C41-C40	1.395(13)
C49-C50	1.345(12)	C49-C54	1.391(11)
C12-C13	1.406(11)	C12-C17	1.458(11)
C8-C9	1.509(13)	C8-C2	1.508(12)
C8-C10	1.544(13)	C8-C11	1.557(13)
C2-C3	1.430(10)	C2-C1	1.437(11)
C4-C5	1.351(11)	C4-C3	1.423(12)
C53-C54	1.371(12)	C53-C52	1.374(13)
C14-C15	1.395(13)	C14-C13	1.430(11)
C39-C40	1.301(12)	C39-C38	1.448(11)
C39-C44	1.576(11)	C50-C51	1.403(12)
C50-C72	1.575(12)	C44-C45	1.520(12)
C44-C46	1.522(12)	C44-C47	1.571(13)
C51-C52	1.375(12)	C16-C15	1.365(13)
C16-C17	1.417(12)	C13-C35	1.478(11)
C17-C18	1.429(11)	C54-C55	1.563(11)
C55-C57	1.480(13)	C55-C56	1.494(14)
C35-C36	1.578(13)	C35-C37	1.587(12)
C72-C74	1.494(15)	C72-C73	1.534(14)
C18-C19	1.536(14)	C18-C20	1.560(12)
C67-C68	1.297(14)	C67-C66	1.445(13)
C71-C66	1.428(16)	C71-C70	1.451(15)
C70-C69	1.357(12)	C66-C65	1.449(10)
C68-C69	1.328(14)	C65-N4	1.245(7)
N2-C28	1.289(6)	N2-C22	1.511(9)
C25-C26	1.366(13)	C25-C24	1.428(16)
C26-C27	1.276(14)	C22-C23	1.319(13)
C22-C27	1.378(14)	C24-C23	1.439(15)
C29-C30	1.369(14)	C29-C28	1.437(9)
C29-C34	1.436(16)	C30-C31	1.338(14)
C31-C32	1.389(16)	C32-C33	1.295(18)
C34-C33	1.419(18)	C59-C64	1.316(17)
C59-C60	1.357(14)	C59-N4	1.567(10)

C64-C63	1.312(18)	C62-C61	1.345(17)
C62-C63	1.381(19)	C60-C61	1.440(12)

Table 5. Bond angles (°) for complex 3d.

C21-Pd1-N1	94.7(3)	C21-Pd1-N2	85.7(3)
N1-Pd1-N2	165.9(2)	C21-Pd1-O1	173.3(3)
N1-Pd1-O1	91.9(3)	N2-Pd1-O1	87.7(2)
N3-Pd2-O2	90.8(3)	N3-Pd2-C58	93.3(4)
O2-Pd2-C58	175.9(4)	N3-Pd2-N4	170.0(2)
O2-Pd2-N4	87.3(2)	C58-Pd2-N4	88.7(3)
C7-N1-C12	118.3(7)	C7-N1-Pd1	122.4(6)
C12-N1-Pd1	119.0(6)	C48-N3-C49	112.0(6)
C48-N3-Pd2	124.0(5)	C49-N3-Pd2	123.7(5)
C38-O2-Pd2	132.7(5)	C1-O1-Pd1	124.4(5)
C1-C6-C5	124.6(7)	C1-C6-C7	124.0(7)
C5-C6-C7	111.3(7)	C48-C43-C42	119.2(7)
C48-C43-C38	126.3(7)	C42-C43-C38	114.4(7)
C42-C41-C40	116.4(9)	C50-C49-C54	124.3(8)
C50-C49-N3	115.9(7)	C54-C49-N3	119.3(7)
C13-C12-N1	116.8(7)	C13-C12-C17	122.0(7)
N1-C12-C17	121.2(7)	C9-C8-C2	110.1(7)
C9-C8-C10	111.0(8)	C2-C8-C10	108.1(6)
C9-C8-C11	108.7(7)	C2-C8-C11	113.9(7)
C10-C8-C11	105.0(7)	C3-C2-C1	118.1(8)
C3-C2-C8	118.1(7)	C1-C2-C8	123.8(7)
N3-C48-C43	129.3(8)	C5-C4-C3	121.1(8)
C54-C53-C52	120.9(7)	C15-C14-C13	120.0(7)
N1-C7-C6	129.6(8)	C40-C39-C38	118.8(7)
C40-C39-C44	125.8(8)	C38-C39-C44	115.3(7)
C49-C50-C51	116.6(7)	C49-C50-C72	124.9(8)
C51-C50-C72	118.5(8)	C45-C44-C46	109.9(7)
C45-C44-C47	104.9(7)	C46-C44-C47	108.4(8)
C45-C44-C39	109.4(7)	C46-C44-C39	113.8(7)
C47-C44-C39	110.2(7)	O2-C38-C39	124.8(7)
O2-C38-C43	116.8(7)	C39-C38-C43	118.4(7)
C4-C3-C2	119.9(7)	C52-C51-C50	121.1(8)
C15-C16-C17	122.0(8)	O1-C1-C6	127.6(7)
O1-C1-C2	114.1(7)	C6-C1-C2	118.3(7)
C39-C40-C41	126.7(8)	C12-C13-C14	118.0(7)
C12-C13-C35	120.3(6)	C14-C13-C35	121.7(7)
C16-C17-C18	122.5(7)	C16-C17-C12	116.3(7)
C18-C17-C12	121.1(7)	C41-C42-C43	124.9(8)
C53-C52-C51	119.7(8)	C53-C54-C49	117.3(8)

C53-C54-C55	120.2(7)	C49-C54-C55	122.5(8)
C16-C15-C14	121.8(8)	C4-C5-C6	117.6(8)
C57-C55-C56	109.8(8)	C57-C55-C54	116.2(7)
C56-C55-C54	107.5(7)	C13-C35-C36	115.2(7)
C13-C35-C37	110.6(7)	C36-C35-C37	112.2(7)
C74-C72-C73	110.2(8)	C74-C72-C50	113.6(8)
C73-C72-C50	108.7(8)	C17-C18-C19	114.2(9)
C17-C18-C20	111.4(7)	C19-C18-C20	110.1(8)
C68-C67-C66	120.3(10)	C66-C71-C70	118.6(9)
C69-C70-C71	119.2(8)	C71-C66-C67	115.3(9)
C71-C66-C65	113.7(8)	C67-C66-C65	129.8(9)
C67-C68-C69	124.7(9)	C68-C69-C70	120.0(8)
N4-C65-C66	124.8(7)	C28-N2-C22	114.4(5)
C28-N2-Pd1	128.7(4)	C22-N2-Pd1	116.9(4)
C26-C25-C24	119.1(8)	C27-C26-C25	120.8(10)
C23-C22-C27	121.5(9)	C23-C22-N2	110.0(8)
C27-C22-N2	127.1(8)	C25-C24-C23	117.4(9)
C26-C27-C22	122.6(10)	C22-C23-C24	117.8(9)
C30-C29-C28	138.0(9)	C30-C29-C34	114.6(8)
C28-C29-C34	107.2(8)	C31-C30-C29	122.9(9)
C30-C31-C32	121.3(11)	C33-C32-C31	119.2(9)
C33-C34-C29	120.1(10)	C32-C33-C34	120.8(11)
N2-C28-C29	120.8(6)	C64-C59-C60	123.4(10)
C64-C59-N4	131.2(10)	C60-C59-N4	105.3(8)
C65-N4-C59	115.4(6)	C65-N4-Pd2	119.1(5)
C59-N4-Pd2	125.4(5)	C63-C64-C59	120.4(11)
C61-C62-C63	120.5(10)	C64-C63-C62	120.1(11)
C59-C60-C61	116.2(9)	C62-C61-C60	118.1(9)

Appendix I

Crystal structure information, compound 3e in Chapter 4

Table 1. Sample and crystal data for complex 3e

Empirical formula	C38 H46 N2 O Pd	
Formula weight	653.17	
Temperature	218(2) K	
Wavelength	0.71073 Å	
Crystal system	Triclinic	
Space group	P-1	
Unit cell dimensions	a = 9.6685(4) Å	= 71.6700(10)°.
	b = 13.0421(6) Å	= 81.2500(10)°.
	c = 14.8920(7) Å	= 71.0830(10)°.
Volume	1683.65(13) $Å^3$	
Z	2	
Density (calculated)	1.288 Mg/m^3	
Absorption coefficient	0.582 mm^{-1}	
F(000)	684	
Crystal size	0.30 x 0.28 x 0.10 mm^3	
Theta range for data collection	1.44 to 28.28°.	
Index ranges	-12<=h<=12, -17<=k<=17, -18<=l<=19	
Reflections collected	12607	
Independent reflections	7806 [R(int) = 0.0210]	
Completeness to theta = 28.28°	93.6 %	
Absorption correction	None	
Max. and min. transmission	0.9441 and 0.8448	
Refinement method	Full-matrix least-squares on F^2	
Data / restraints / parameters	7806 / 0 / 379	
Goodness-of-fit on F^2	1.056	
Final R indices [I>2sigma(I)]	R1 = 0.0364, wR2 = 0.0937	
R indices (all data)	R1 = 0.0415, wR2 = 0.0962	
Largest diff. peak and hole	1.078 and -0.878 $e.Å^{-3}$	

Table 2. Atomic coordinates (x 10^4) and equivalent isotropic displacement parameters ($Å^2$x 10^3)
for complex 3e.

U(eq) is defined as one third of the trace of the orthogonalized U^{ij} tensor.

	x	y	z	U(eq)
O(1)	-1839(2)	3153(1)	2655(1)	37(1)
Pd(1)	-1545(1)	1973(1)	1913(1)	29(1)
N(1)	567(2)	1269(2)	2238(1)	30(1)
N(2)	-3681(2)	2717(2)	1584(1)	35(1)
C(1)	1174(2)	1629(2)	2747(2)	32(1)
C(2)	590(2)	2541(2)	3165(2)	32(1)
C(3)	1591(3)	2716(2)	3660(2)	39(1)
C(4)	1190(3)	3577(2)	4064(2)	46(1)
C(5)	-236(3)	4302(2)	3987(2)	43(1)
C(6)	-1282(3)	4192(2)	3517(2)	34(1)
C(7)	-886(2)	3279(2)	3089(1)	30(1)
C(8)	-2830(3)	5003(2)	3442(2)	43(1)
C(9)	-3171(4)	5590(3)	2398(2)	60(1)
C(10)	-3050(4)	5934(3)	3917(3)	67(1)
C(11)	-3946(3)	4371(3)	3930(2)	57(1)
C(12)	1553(2)	342(2)	1907(2)	33(1)
C(13)	2206(2)	587(2)	993(2)	37(1)
C(14)	3230(3)	-305(2)	719(2)	49(1)
C(15)	3570(3)	-1379(2)	1316(2)	58(1)
C(16)	2841(3)	-1611(2)	2194(2)	54(1)
C(17)	1801(3)	-758(2)	2505(2)	43(1)
C(18)	1796(3)	1768(2)	319(2)	39(1)
C(19)	1760(4)	1772(3)	-706(2)	62(1)
C(20)	2796(3)	2433(2)	377(2)	53(1)
C(21)	961(3)	-1031(2)	3453(2)	57(1)
C(22)	1864(5)	-1234(4)	4270(2)	99(2)
C(23)	401(5)	-2034(3)	3585(3)	93(1)
C(24)	-1437(3)	873(2)	1188(2)	45(1)
C(25)	-4164(3)	3389(2)	789(2)	42(1)
C(26)	-3260(3)	3837(2)	-28(2)	43(1)
C(27)	-2030(3)	4107(2)	60(2)	48(1)
C(28)	-1239(3)	4547(3)	-737(2)	58(1)
C(29)	-1680(4)	4733(3)	-1621(2)	66(1)
C(30)	-2928(5)	4501(3)	-1717(2)	69(1)
C(31)	-3731(4)	4063(2)	-921(2)	57(1)
C(32)	-4772(3)	2468(2)	2355(2)	45(1)
C(33)	-4396(3)	1234(2)	2897(2)	43(1)
C(34)	-3723(4)	864(3)	3740(2)	61(1)

C(35)	-3357(5)	-256(3)	4244(2)	79(1)
C(36)	-3693(4)	-1022(3)	3926(3)	71(1)
C(37)	-4347(3)	-672(3)	3090(3)	64(1)
C(38)	-4700(3)	463(3)	2579(2)	53(1)

Table 3. Bond lengths [Å] and angles [°] for complex 3e.

O(1)-C(7)	1.280(3)	C(13)-C(18)	1.514(3)
O(1)-Pd(1)	2.0880(16)	C(14)-C(15)	1.367(4)
Pd(1)-N(1)	2.0126(18)	C(15)-C(16)	1.381(4)
Pd(1)-C(24)	2.020(3)	C(16)-C(17)	1.386(4)
Pd(1)-N(2)	2.0386(19)	C(17)-C(21)	1.517(3)
N(1)-C(1)	1.296(3)	C(18)-C(20)	1.520(4)
N(1)-C(12)	1.447(3)	C(18)-C(19)	1.531(4)
N(2)-C(25)	1.280(3)	C(21)-C(22)	1.511(5)
N(2)-C(32)	1.468(3)	C(21)-C(23)	1.519(5)
C(1)-C(2)	1.429(3)	C(25)-C(26)	1.465(3)
C(2)-C(3)	1.413(3)	C(26)-C(27)	1.380(4)
C(2)-C(7)	1.438(3)	C(26)-C(31)	1.383(4)
C(3)-C(4)	1.358(4)	C(27)-C(28)	1.380(4)
C(4)-C(5)	1.393(4)	C(28)-C(29)	1.371(5)
C(5)-C(6)	1.381(3)	C(29)-C(30)	1.372(5)
C(6)-C(7)	1.441(3)	C(30)-C(31)	1.384(5)
C(6)-C(8)	1.524(3)	C(32)-C(33)	1.505(4)
C(8)-C(11)	1.527(4)	C(33)-C(38)	1.363(4)
C(8)-C(10)	1.532(4)	C(33)-C(34)	1.377(4)
C(8)-C(9)	1.535(4)	C(34)-C(35)	1.371(5)
C(12)-C(17)	1.395(3)	C(35)-C(36)	1.371(5)
C(12)-C(13)	1.396(3)	C(36)-C(37)	1.362(5)
C(13)-C(14)	1.389(3)	C(37)-C(38)	1.389(4)

Table 5. Bond angles (°) for Complex 3e

C(7)-O(1)-Pd(1)	128.02(14)	C(13)-C(12)-N(1)	118.4(2)
N(1)-Pd(1)-C(24)	92.89(9)	C(14)-C(13)-C(12)	117.3(2)
N(1)-Pd(1)-N(2)	178.87(7)	C(14)-C(13)-C(18)	121.1(2)
C(24)-Pd(1)-N(2)	88.08(9)	C(12)-C(13)-C(18)	121.6(2)
N(1)-Pd(1)-O(1)	91.64(7)	C(15)-C(14)-C(13)	121.2(2)
C(24)-Pd(1)-O(1)	175.39(8)	C(14)-C(15)-C(16)	120.4(2)
N(2)-Pd(1)-O(1)	87.40(7)	C(15)-C(16)-C(17)	120.9(3)
C(1)-N(1)-C(12)	113.94(18)	C(16)-C(17)-C(12)	117.4(2)
C(1)-N(1)-Pd(1)	122.46(15)	C(16)-C(17)-C(21)	120.4(2)
C(12)-N(1)-Pd(1)	123.58(15)	C(12)-C(17)-C(21)	122.2(2)
C(25)-N(2)-C(32)	117.1(2)	C(13)-C(18)-C(20)	111.7(2)
C(25)-N(2)-Pd(1)	127.01(17)	C(13)-C(18)-C(19)	112.7(2)
C(32)-N(2)-Pd(1)	115.89(15)	C(20)-C(18)-C(19)	110.4(2)
N(1)-C(1)-C(2)	130.6(2)	C(22)-C(21)-C(17)	111.9(3)
C(3)-C(2)-C(1)	115.3(2)	C(22)-C(21)-C(23)	110.4(3)
C(3)-C(2)-C(7)	119.8(2)	C(17)-C(21)-C(23)	111.6(3)
C(1)-C(2)-C(7)	124.8(2)	N(2)-C(25)-C(26)	125.2(2)
C(4)-C(3)-C(2)	121.3(2)	C(27)-C(26)-C(31)	119.4(3)
C(3)-C(4)-C(5)	119.3(2)	C(27)-C(26)-C(25)	122.8(2)
C(6)-C(5)-C(4)	123.2(2)	C(31)-C(26)-C(25)	117.7(2)
C(5)-C(6)-C(7)	118.5(2)	C(26)-C(27)-C(28)	120.2(3)
C(5)-C(6)-C(8)	121.9(2)	C(29)-C(28)-C(27)	120.2(3)
C(7)-C(6)-C(8)	119.6(2)	C(28)-C(29)-C(30)	120.1(3)
O(1)-C(7)-C(2)	122.3(2)	C(29)-C(30)-C(31)	120.1(3)
O(1)-C(7)-C(6)	119.78(19)	C(26)-C(31)-C(30)	120.0(3)
C(2)-C(7)-C(6)	117.9(2)	N(2)-C(32)-C(33)	112.6(2)
C(6)-C(8)-C(11)	110.5(2)	C(38)-C(33)-C(34)	118.4(3)
C(6)-C(8)-C(10)	112.6(2)	C(38)-C(33)-C(32)	122.0(3)
C(11)-C(8)-C(10)	106.7(2)	C(34)-C(33)-C(32)	119.6(3)
C(6)-C(8)-C(9)	110.2(2)	C(35)-C(34)-C(33)	120.8(3)
C(11)-C(8)-C(9)	109.6(2)	C(34)-C(35)-C(36)	120.2(3)
C(10)-C(8)-C(9)	107.1(2)	C(37)-C(36)-C(35)	119.8(3)
C(17)-C(12)-C(13)	122.5(2)	C(36)-C(37)-C(38)	119.5(3)
C(17)-C(12)-N(1)	119.1(2)	C(33)-C(38)-C(37)	121.2(3)

Appendix J

Crystal structure information, compound 4 in Chapter 4

Table 1. Sample and crystal data for complex 4.

Empirical formula	C34H47 N3 O Pd	
Formula weight	620.18	
Temperature	98(2) K	
Wavelength	0.71073 Å	
Crystal size	0.20 x 0.07 x 0.05 mm	
Crystal habit	Yellow-clear Needle	
Crystal system	Triclinic	
Space group	P1	
Unit cell dimensions	a = 10.895(2) Å	α= 64.930(3)°
	b = 13.620(3) Å	β= 71.179(3)°
	c = 13.959(3) Å	γ = 73.707(3)°
Volume	1750.8(6) $Å^3$	
Z	2	
Density (calculated)	1.245 g/cm^3	
Absorption coefficient	0.560 mm^{-1}	
F(000)	694	

Table 2. Data collection and structure refinement for complex 4.

Diffractometer	CCD area detector
Radiation source	fine-focus sealed tube, MoK
Generator power	1600 watts (50 kV, 32mA)
Detector distance	5.8 cm
Data collection method	omega scans
Theta range for data collection	1.67 to 28.05°
Index ranges	$-14 \leq h \leq 14$, $-17 \leq k \leq 17$, $-17 \leq l \leq 17$

Table 3. Atomic coordinates and equivalent isotropic atomic displacement parameters (Å ^{2}) for complex 4.

U(eq) is defined as one third of the trace of the orthogonalized U_{ij} tensor.

	x/a	y/b	z/c	U(eq)
Pd1	-0.06814(5)	0.30085(4)	0.61823(4)	0.0344(3)
Pd2	0.65544(4)	0.56202(4)	0.92882(4)	0.0349(3)
N2	-0.2066(11)	0.4373(9)	0.5857(8)	0.025(3)
N5	0.7993(12)	0.4234(9)	0.9606(9)	0.032(3)
N4	0.5180(12)	0.6937(9)	0.8925(9)	0.039(3)
N1	0.0797(12)	0.1708(9)	0.6550(9)	0.044(4)
O2	0.5240(10)	0.4566(8)	0.9718(8)	0.037(3)
O1	0.0586(11)	0.4086(9)	0.5756(9)	0.043(3)
N3	-0.1076(13)	0.5520(11)	0.3026(10)	0.041(3)
C42	0.7915(18)	0.6564(15)	0.8873(16)	0.053(5)
C12	-0.2075(16)	0.2080(12)	0.6609(13)	0.038(4)
N6	0.6892(12)	0.2994(10)	1.2512(9)	0.033(3)
C28	-0.1036(11)	0.4954(10)	0.3906(9)	0.024(3)
C23	-0.2984(12)	0.4545(10)	0.6688(9)	0.021(3)
C30	0.4144(9)	0.4777(9)	0.9408(9)	0.027(3)
C52	0.8916(14)	0.4009(13)	0.8758(12)	0.043(4)
C56	0.7927(11)	0.3478(10)	1.0614(10)	0.022(3)
C57	0.6924(13)	0.3680(9)	1.1515(10)	0.029(3)
C35	0.3526(15)	0.3952(14)	0.9547(12)	0.048(4)
C36	0.4109(17)	0.6827(13)	0.8797(12)	0.051(5)
C55	0.8858(13)	0.2553(10)	1.0768(10)	0.033(3)
C26	-0.2993(12)	0.6147(11)	0.4657(12)	0.037(4)
C7	0.1898(13)	0.1728(11)	0.6658(11)	0.033(3)
C1	0.1620(17)	0.3814(13)	0.6050(11)	0.056(5)
C27	-0.2094(14)	0.5155(11)	0.4847(10)	0.024(3)
C32	0.2440(16)	0.6192(14)	0.8528(12)	0.046(4)
C2	0.2307(13)	0.4714(11)	0.5921(9)	0.027(3)
C31	0.3593(12)	0.5909(12)	0.8956(11)	0.038(4)
C6	0.2358(15)	0.2703(12)	0.6559(9)	0.044(4)
C53	0.9818(13)	0.3129(10)	0.8859(11)	0.041(4)
C8	0.1761(14)	0.5920(12)	0.5351(8)	0.035(4)
C37	0.4112(14)	0.2745(12)	1.0150(13)	0.044(4)
C38	0.4143(16)	0.2571(11)	1.1257(12)	0.042(4)
C5	0.3502(13)	0.2542(12)	0.6868(11)	0.038(4)
C58	0.5871(12)	0.3259(10)	1.3413(8)	0.026(3)
C29	-0.0051(15)	0.5493(14)	0.2012(13)	0.050(4)
C33	0.1864(14)	0.5283(15)	0.8700(12)	0.046(5)
C4	0.4023(17)	0.3299(13)	0.6853(12)	0.047(4)

C9	0.1765(17)	0.6079(13)	0.4153(10)	0.043(4)
C10	0.0337(16)	0.6194(13)	0.5960(10)	0.046(4)
C40	0.5530(12)	0.2401(12)	0.9523(12)	0.040(4)
C24	-0.3920(14)	0.5522(12)	0.6571(10)	0.037(4)
C13	0.0584(13)	0.0635(13)	0.6713(13)	0.042(4)
C18	0.0775(18)	0.0394(14)	0.5780(17)	0.060(6)
C41	0.5257(16)	0.8032(11)	0.8761(14)	0.048(5)
C47	0.5095(16)	0.8318(13)	0.9647(11)	0.044(4)
C25	-0.3925(15)	0.6205(13)	0.5586(15)	0.051(4)
C20	-0.0037(18)	0.0078(11)	0.8792(11)	0.047(4)
C54	0.9800(13)	0.2291(10)	0.9922(8)	0.034(3)
C34	0.2442(13)	0.4269(14)	0.9118(11)	0.041(4)
C3	0.3422(16)	0.4455(13)	0.6279(12)	0.045(4)
C49	0.5872(16)	0.8423(12)	0.6756(15)	0.062(5)
C15	0.0004(18)	-0.1212(12)	0.7943(15)	0.055(5)
C43	0.5659(15)	0.8792(12)	0.7704(10)	0.048(5)
C11	0.2517(16)	0.6763(13)	0.5294(13)	0.047(4)
C44	0.5792(19)	0.9734(14)	0.7634(16)	0.064(6)
C14	0.0212(15)	-0.0107(11)	0.7770(14)	0.054(5)
C39	0.3230(15)	0.1986(13)	1.0287(13)	0.042(4)
C16	0.018(2)	-0.1476(14)	0.7030(17)	0.057(5)
C45	0.5589(18)	1.0024(15)	0.8504(17)	0.058(5)
C17	0.0568(18)	-0.0686(14)	0.6007(14)	0.052(5)
C61	0.6447(8)	0.3867(7)	1.3878(5)	0.0329(18)
C21	-0.1421(17)	-0.0061(15)	0.9601(15)	0.064(5)
C46	0.5249(16)	0.9307(14)	0.9552(17)	0.063(5)
C51	0.7116(18)	0.8830(13)	0.5942(13)	0.065(5)
C19	0.1201(18)	0.1164(16)	0.4621(16)	0.070(6)
C48	0.476(2)	0.7375(15)	1.0827(12)	0.068(6)
C59	0.4599(7)	0.3964(6)	1.3136(5)	0.0295(15)
C50	0.479(2)	0.9013(15)	0.6130(15)	0.072(6)
C22	0.1126(18)	-0.0494(13)	0.9319(16)	0.059(5)
C60	0.5722(9)	0.2138(6)	1.4249(6)	0.037(2)
C62	0.562(3)	0.7247(17)	1.1517(17)	0.145(10)
C65	0.047(3)	0.1237(16)	0.3905(18)	0.097(7)
C63	0.3377(11)	0.8113(10)	1.1420(10)	0.083(4)
C64	0.2601(10)	0.1325(10)	0.4295(7)	0.066(3)
C82	0.8474(17)	0.9603(18)	0.2537(14)	0.082(5)
C83	0.736(2)	0.9050(17)	0.277(2)	0.172(17)
C81	0.984(2)	0.9191(15)	0.2783(19)	0.147(11)
C84	0.6106(16)	0.9771(12)	0.2611(16)	0.091(6)
C85	0.5029(17)	0.9132(12)	0.2992(14)	0.103(5)
C67	-0.0793(15)	0.5780(13)	0.1213(12)	0.107(4)
C68	0.0835(15)	0.6403(13)	0.1535(13)	0.091(5)
C69	0.0853(19)	0.4466(16)	0.2218(16)	0.128(7)

Table 4. Bond lengths (Å) for complex 4.

Pd1-N2	2.023(10)	Pd1-C12	2.029(17)
Pd1-N1	2.039(11)	Pd1-O1	2.069(12)
Pd2-N4	1.981(11)	Pd2-C42	2.017(19)
Pd2-N5	2.073(11)	Pd2-O2	2.084(12)
N2-C23	1.323(14)	N2-C27	1.364(16)
N5-C56	1.339(16)	N5-C52	1.368(18)
N4-C36	1.29(2)	N4-C41	1.433(19)
N1-C7 1.264(18)	N1-C13	1.46(2)	O2-C30
1.316(14)	O1-C1	1.23(2)	N3-C28
1.149(16)	N3-C29	1.500(18)	N6-C57
1.303(15)	N6-C58	1.485(15)	C28-C27
1.510(16)	C23-C24	1.414(17)	C30-C35
1.38(2)	C30-C31	1.427(16)	C52-C53
1.31(2)	C56-C55	1.363(17)	C56-C57
1.445(17)	C35-C34	1.38(2)	C35-C37
1.55(2)	C36-C31	1.42(2)	C55-C54
1.394(16)	C26-C25	1.38(2)	C26-C27
1.405(17)	C7-C6	1.48(2)	C1-C6
1.49(2)	C1-C2	1.53(2)	C32-C33
1.44(2)	C32-C31	1.45(2)	C2-C3
1.36(2)	C2-C8	1.528(17)	C6-C5
1.38(2)	C53-C54	1.436(15)	C8-C10
1.537(19)	C8-C11	1.55(2)	C8-C9
1.591(17)	C37-C38	1.47(2)	C37-C39
1.52(2)	C37-C40	1.563(18)	C5-C4
1.30(2)	C58-C59	1.509(15)	C58-C60
1.493(12)	C58-C61	1.584(13)	C29-C67
1.44(2)	C29-C69	1.44(2)	C29-C68
1.57(2)	C33-C34	1.31(2)	C4-C3
1.50(2)	C24-C25	1.29(2)	C13-C14
1.39(2)	C13-C18	1.41(3)	C18-C17
1.43(2)	C18-C19	1.51(2)	C41-C43
1.408(18)	C41-C47	1.39(2)	C47-C46
1.35(2)	C47-C48	1.61(2)	C20-C14
1.48(2)	C20-C22	1.52(2)	C20-C21
1.57(2)	C49-C43	1.54(3)	C49-C51
1.53(2)	C49-C50	1.53(2)	C15-C16
1.41(3)	C15-C14	1.49(2)	C43-C44
1.29(3)	C44-C45	1.37(3)	C16-C17
1.39(2)	C45-C46	1.37(2)	C19-C65
1.42(3)	C19-C64	1.50(2)	C48-C62
1.48(3)	C48-C63	1.74(2)	C82-C83
1.479(15)	C82-C81	1.529(15)	C83-C84

1.465(16)	C84-C85	1.481(15)	

Table 5. Bond angles (°) for complex 4.

N2-Pd1-C12	89.2(5)	N2-Pd1-N1	174.7(6)
C12-Pd1-N1	95.3(6)	N2-Pd1-O1	85.2(5)
C12-Pd1-O1	174.2(6)	N1-Pd1-O1	90.2(5)
N4-Pd2-C42	91.3(6)	N4-Pd2-N5	177.5(5)
C42-Pd2-N5	89.4(6)	N4-Pd2-O2	92.0(5)
C42-Pd2-O2	176.6(6)	N5-Pd2-O2	87.2(4)
C23-N2-C27	117.3(11)	C23-N2-Pd1	117.8(8)
C27-N2-Pd1	124.8(8)	C56-N5-C52	119.0(12)
C56-N5-Pd2	120.8(9)	C52-N5-Pd2	119.5(9)
C36-N4-C41	115.2(13)	C36-N4-Pd2	118.4(10)
C41-N4-Pd2	126.4(12)	C7-N1-C13	115.5(12)
C7-N1-Pd1	126.9(11)	C13-N1-Pd1	117.6(10)
C30-O2-Pd2	128.6(9)	C1-O1-Pd1	123.5(10)
C28-N3-C29	127.0(13)	C57-N6-C58	119.1(12)
N3-C28-C27	120.5(12)	N2-C23-C24	122.7(10)
O2-C30-C35	122.2(11)	O2-C30-C31	116.4(12)
C35-C30-C31	121.4(11)	C53-C52-N5	124.8(14)
N5-C56-C55	118.5(10)	N5-C56-C57	119.9(10)
C55-C56-C57	121.5(11)	N6-C57-C56	121.2(12)
C34-C35-C30	116.9(14)	C34-C35-C37	124.8(16)
C30-C35-C37	118.2(14)	N4-C36-C31	133.7(14)
C56-C55-C54	123.7(12)	C25-C26-C27	113.1(13)
N1-C7-C6	126.7(13)	O1-C1-C6	130.4(16)
O1-C1-C2	118.6(14)	C6-C1-C2	111.0(15)
N2-C27-C26	123.5(12)	N2-C27-C28	116.9(11)
C26-C27-C28	119.5(11)	C33-C32-C31	116.0(14)
C3-C2-C1	120.9(13)	C3-C2-C8	119.4(13)
C1-C2-C8	119.7(12)	C36-C31-C30	126.8(13)
C36-C31-C32	114.2(14)	C30-C31-C32	118.8(14)
C5-C6-C7	118.6(13)	C5-C6-C1	122.9(16)
C7-C6-C1	118.4(14)	C52-C53-C54	118.5(12)
C2-C8-C10	109.5(11)	C2-C8-C11	115.2(12)
C10-C8-C11	106.2(12)	C2-C8-C9	107.5(11)
C10-C8-C9	108.8(12)	C11-C8-C9	109.6(11)
C38-C37-C39	105.9(12)	C38-C37-C35	111.1(12)
C39-C37-C35	109.4(13)	C38-C37-C40	109.1(13)
C39-C37-C40	109.1(12)	C35-C37-C40	111.9(12)
C4-C5-C6	126.3(14)	N6-C58-C59	116.3(9)
N6-C58-C60	101.4(9)	C59-C58-C60	114.1(9)
N6-C58-C61	109.5(9)	C59-C58-C61	107.5(8)

C60-C58-C61	107.8(8)	C67-C29-C69	117.4(16)
C67-C29-N3	104.5(12)	C69-C29-N3	111.3(15)
C67-C29-C68	105.2(13)	C69-C29-C68	105.0(14)
N3-C29-C68	113.5(13)	C34-C33-C32	120.8(15)
C5-C4-C3	115.1(15)	C25-C24-C23	116.4(11)
C14-C13-C18	123.0(17)	C14-C13-N1	119.1(15)
C18-C13-N1	117.9(14)	C13-C18-C17	114.5(16)
C13-C18-C19	124.8(18)	C17-C18-C19	120.7(19)
C43-C41-C47	118.8(15)	C43-C41-N4	120.5(16)
C47-C41-N4	120.3(14)	C46-C47-C41	123.6(14)
C46-C47-C48	120.2(16)	C41-C47-C48	116.1(15)
C24-C25-C26	126.1(14)	C14-C20-C22	110.4(14)
C14-C20-C21	118.1(16)	C22-C20-C21	114.7(13)
C55-C54-C53	115.0(11)	C33-C34-C35	125.4(17)
C2-C3-C4	123.2(15)	C43-C49-C51	106.2(16)
C43-C49-C50	111.8(13)	C51-C49-C50	104.3(14)
C16-C15-C14	118.9(16)	C44-C43-C41	116.5(16)
C44-C43-C49	126.7(14)	C41-C43-C49	116.8(15)
C43-C44-C45	124.5(18)	C13-C14-C15	119.5(17)
C13-C14-C20	126.9(14)	C15-C14-C20	113.6(14)
C15-C16-C17	117.4(17)	C46-C45-C44	121.9(19)
C16-C17-C18	126.6(18)	C45-C46-C47	114.7(19)
C65-C19-C64	125.2(18)	C65-C19-C18	114.3(18)
C64-C19-C18	114.4(16)	C62-C48-C47	111.8(17)
C62-C48-C63	97.2(15)	C47-C48-C63	98.6(12)
C83-C82-C81	133.3(16)	C84-C83-C82	116.0(13)
C83-C84-C85	111.6(16)		

Appendix K

Crystal structure information, compound 5 in Chapter 4

Table 1. Crystal data and structure refinement for complex 5.

Empirical formula	C44 H57 N3 Pd	
Formula weight	734.33	
Temperature	150(2) K	
Wavelength	0.71073 Å	
Crystal system	Monoclinic	
Space group	P2(1)/c	
Unit cell dimensions	a = 8.8271(4) Å	= 90°.
	b = 19.8265(10) Å	= 94.9130(10)°.
	c = 22.4034(11) Å	= 90°.
Volume	3906.4(3) $Å^3$	
Z	4	
Density (calculated)	1.249 Mg/m^3	
Absorption coefficient	0.508 mm^{-1}	
F(000)	1552	
Crystal size	0.35 x 0.25 x 0.20 mm^3	
Theta range for data collection	1.82 to 28.27°.	
Index ranges	-11<=h<=9, -26<=k<=21, -27<=l<=28	
Reflections collected	23985	
Independent reflections	8937 [R(int) = 0.0153]	
Completeness to theta = 28.27°	92.4 %	
Absorption correction	SADABS	
Max. and min. transmission	1.00 and 0.92	
Refinement method	Full-matrix least-squares on F^2	
Data / restraints / parameters	8937 / 0 / 445	
Goodness-of-fit on F^2	1.056	
Final R indices [I>2sigma(I)]	R1 = 0.0256, wR2 = 0.0677	
R indices (all data)	R1 = 0.0282, wR2 = 0.0693	
Largest diff. peak and hole	0.483 and -0.405 $e.Å^{-3}$	

Table 2. Atomic coordinates (x 10^4) and equivalent isotropic displacement parameters ($Å^2$x 10^3)
for complex 5. U(eq) is defined as one third of the trace of the orthogonalized U^{ij} tensor.

	x	y	z	U(eq)
Pd(1)	3469(1)	1040(1)	1990(1)	16(1)
N(1)	3006(1)	1264(1)	1102(1)	20(1)
N(2)	2320(1)	93(1)	1886(1)	18(1)
N(3)	3971(2)	953(1)	2899(1)	20(1)
C(1)	2005(2)	920(1)	740(1)	23(1)
C(2)	1214(2)	346(1)	892(1)	24(1)
C(3)	1431(2)	-65(1)	1403(1)	20(1)
C(4)	1707(3)	1136(1)	90(1)	37(1)
C(5)	623(2)	-740(1)	1353(1)	28(1)
C(6)	3716(2)	1831(1)	837(1)	23(1)
C(7)	2971(2)	2459(1)	797(1)	26(1)
C(8)	3654(2)	2988(1)	508(1)	34(1)
C(9)	5039(2)	2904(1)	274(1)	39(1)
C(10)	5788(2)	2294(1)	338(1)	37(1)
C(11)	5158(2)	1748(1)	624(1)	29(1)
C(12)	1469(2)	2585(1)	1066(1)	31(1)
C(13)	200(3)	2796(1)	595(1)	57(1)
C(14)	1632(3)	3124(1)	1554(1)	49(1)
C(15)	6037(2)	1091(1)	712(1)	37(1)
C(16)	6434(4)	779(2)	125(1)	73(1)
C(17)	7470(3)	1189(2)	1136(1)	67(1)
C(18)	2701(2)	-438(1)	2310(1)	19(1)
C(19)	2019(2)	-460(1)	2856(1)	22(1)
C(20)	2467(2)	-968(1)	3266(1)	30(1)
C(21)	3557(2)	-1437(1)	3145(1)	36(1)
C(22)	4207(2)	-1412(1)	2606(1)	33(1)
C(23)	3795(2)	-922(1)	2176(1)	23(1)
C(24)	4556(2)	-914(1)	1591(1)	26(1)
C(25)	6075(2)	-548(1)	1670(1)	47(1)
C(26)	4766(3)	-1624(1)	1338(1)	48(1)
C(27)	819(2)	50(1)	2993(1)	26(1)
C(28)	-754(2)	-127(1)	2694(1)	38(1)
C(29)	715(2)	165(1)	3664(1)	38(1)
C(30)	5359(2)	536(1)	3050(1)	26(1)
C(31)	6132(2)	597(1)	3675(1)	25(1)
C(32)	6027(2)	82(1)	4088(1)	38(1)
C(33)	6822(3)	129(1)	4653(1)	51(1)
C(34)	7712(2)	684(1)	4802(1)	46(1)

C(35)	7811(2)	1197(1)	4397(1)	40(1)
C(36)	7024(2)	1153(1)	3834(1)	31(1)
C(37)	3385(2)	1282(1)	3314(1)	24(1)
C(38)	2035(2)	1722(1)	3250(1)	24(1)
C(39)	1035(2)	1775(1)	2733(1)	28(1)
C(40)	-240(2)	2184(1)	2723(1)	32(1)
C(41)	-524(2)	2553(1)	3226(1)	37(1)
C(42)	461(2)	2513(1)	3739(1)	41(1)
C(43)	1730(2)	2098(1)	3754(1)	33(1)
C(44)	4683(2)	1910(1)	2137(1)	31(1)

Table 3. Bond lengths [Å] and angles [°] for complex 5.

Pd(1)-C(44)	2.0423(17)	C(18)-C(19)	1.409(2)
Pd(1)-N(1)	2.0432(12)	C(18)-C(23)	1.411(2)
Pd(1)-N(3)	2.0550(13)	C(19)-C(20)	1.397(2)
Pd(1)-N(2)	2.1380(12)	C(19)-C(27)	1.516(2)
N(1)-C(1)	1.335(2)	C(20)-C(21)	1.382(3)
N(1)-C(6)	1.4398(19)	C(21)-C(22)	1.382(3)
N(2)-C(3)	1.3192(19)	C(22)-C(23)	1.394(2)
N(2)-C(18)	1.4368(18)	C(23)-C(24)	1.524(2)
N(3)-C(37)	1.281(2)	C(24)-C(25)	1.522(3)
N(3)-C(30)	1.4925(19)	C(24)-C(26)	1.534(2)
C(1)-C(2)	1.393(2)	C(27)-C(28)	1.530(2)
C(1)-C(4)	1.518(2)	C(27)-C(29)	1.531(2)
C(2)-C(3)	1.404(2)	C(30)-C(31)	1.509(2)
C(3)-C(5)	1.516(2)	C(31)-C(36)	1.384(2)
C(6)-C(11)	1.407(2)	C(31)-C(32)	1.386(2)
C(6)-C(7)	1.407(2)	C(32)-C(33)	1.397(3)
C(7)-C(8)	1.398(2)	C(33)-C(34)	1.377(3)
C(7)-C(12)	1.523(2)	C(34)-C(35)	1.370(3)
C(8)-C(9)	1.382(3)	C(35)-C(36)	1.388(2)
C(9)-C(10)	1.379(3)	C(37)-C(38)	1.474(2)
C(10)-C(11)	1.397(2)	C(38)-C(43)	1.398(2)
C(11)-C(15)	1.520(2)	C(38)-C(39)	1.398(2)
C(12)-C(14)	1.527(3)	C(39)-C(40)	1.386(2)
C(12)-C(13)	1.531(3)	C(40)-C(41)	1.383(3)
C(15)-C(16)	1.520(3)	C(41)-C(42)	1.383(3)
C(15)-C(17)	1.528(3)	C(42)-C(43)	1.388(3)

C(44)-Pd(1)-N(1)	91.87(6)	C(16)-C(15)-C(17)	110.5(2)
C(44)-Pd(1)-N(3)	81.11(6)	C(11)-C(15)-C(17)	111.03(18)
N(1)-Pd(1)-N(3)	172.29(5)	C(19)-C(18)-C(23)	120.88(14)
C(44)-Pd(1)-N(2)	175.53(6)	C(19)-C(18)-N(2)	120.18(13)
N(1)-Pd(1)-N(2)	91.83(5)	C(23)-C(18)-N(2)	118.92(13)
N(3)-Pd(1)-N(2)	95.33(5)	C(20)-C(19)-C(18)	118.42(15)
C(1)-N(1)-C(6)	115.87(12)	C(20)-C(19)-C(27)	120.71(15)
C(1)-N(1)-Pd(1)	123.22(10)	C(18)-C(19)-C(27)	120.87(13)
C(6)-N(1)-Pd(1)	120.86(9)	C(21)-C(20)-C(19)	121.22(16)
C(3)-N(2)-C(18)	117.28(12)	C(20)-C(21)-C(22)	119.74(16)
C(3)-N(2)-Pd(1)	122.67(10)	C(21)-C(22)-C(23)	121.64(16)
C(18)-N(2)-Pd(1)	119.31(9)	C(22)-C(23)-C(18)	118.09(15)
C(37)-N(3)-C(30)	119.46(13)	C(22)-C(23)-C(24)	119.54(14)
C(37)-N(3)-Pd(1)	127.61(11)	C(18)-C(23)-C(24)	122.36(14)
C(30)-N(3)-Pd(1)	112.04(9)	C(25)-C(24)-C(23)	110.70(14)
N(1)-C(1)-C(2)	126.01(14)	C(25)-C(24)-C(26)	110.30(16)
N(1)-C(1)-C(4)	119.40(14)	C(23)-C(24)-C(26)	112.64(15)
C(2)-C(1)-C(4)	114.54(14)	C(19)-C(27)-C(28)	112.40(14)
C(1)-C(2)-C(3)	129.57(14)	C(19)-C(27)-C(29)	113.56(14)
N(2)-C(3)-C(2)	124.20(13)	C(28)-C(27)-C(29)	109.65(14)
N(2)-C(3)-C(5)	120.77(13)	N(3)-C(30)-C(31)	117.63(13)
C(2)-C(3)-C(5)	114.95(13)	C(36)-C(31)-C(32)	118.97(16)
C(11)-C(6)-C(7)	120.86(14)	C(36)-C(31)-C(30)	120.29(15)
C(11)-C(6)-N(1)	119.16(14)	C(32)-C(31)-C(30)	120.65(16)
C(7)-C(6)-N(1)	119.97(14)	C(31)-C(32)-C(33)	119.92(19)
C(8)-C(7)-C(6)	118.45(16)	C(34)-C(33)-C(32)	120.3(2)
C(8)-C(7)-C(12)	118.99(15)	C(35)-C(34)-C(33)	120.06(17)
C(6)-C(7)-C(12)	122.55(14)	C(34)-C(35)-C(36)	119.96(19)
C(9)-C(8)-C(7)	121.04(17)	C(31)-C(36)-C(35)	120.84(18)
C(10)-C(9)-C(8)	119.90(16)	N(3)-C(37)-C(38)	127.23(14)
C(9)-C(10)-C(11)	121.42(17)	C(43)-C(38)-C(39)	118.50(15)
C(10)-C(11)-C(6)	118.18(16)	C(43)-C(38)-C(37)	116.58(15)
C(10)-C(11)-C(15)	120.30(16)	C(39)-C(38)-C(37)	124.90(14)
C(6)-C(11)-C(15)	121.50(15)	C(40)-C(39)-C(38)	120.75(16)
C(7)-C(12)-C(14)	111.48(15)	C(41)-C(40)-C(39)	120.00(17)
C(7)-C(12)-C(13)	112.49(16)	C(40)-C(41)-C(42)	120.09(16)
C(14)-C(12)-C(13)	108.67(17)	C(41)-C(42)-C(43)	120.15(17)
C(16)-C(15)-C(11)	112.92(18)	C(42)-C(43)-C(38)	120.50(17)

Table 4. Anisotropic displacement parameters ($Å^2 x\ 10^3$) for complex 5. The anisotropic displacement factor exponent takes the form: $-2\ ^2[\ h^2\ a^{*2} U^{11} + ... + 2\ h\ k\ a^*\ b^*\ U^{12}\ ]$

	U^{11}	U^{22}	U^{33}	U^{23}	U^{13}	U^{12}
Pd(1)	17(1)	16(1)	16(1)	-1(1)	-1(1)	0(1)
N(1)	23(1)	19(1)	18(1)	1(1)	0(1)	-1(1)
N(2)	19(1)	16(1)	19(1)	0(1)	0(1)	1(1)
N(3)	19(1)	21(1)	20(1)	-1(1)	-3(1)	0(1)
C(1)	29(1)	20(1)	19(1)	0(1)	-3(1)	3(1)
C(2)	27(1)	22(1)	21(1)	-2(1)	-8(1)	-2(1)
C(3)	19(1)	18(1)	23(1)	-1(1)	0(1)	0(1)
C(4)	56(1)	32(1)	21(1)	4(1)	-12(1)	-10(1)
C(5)	31(1)	23(1)	28(1)	0(1)	-5(1)	-7(1)
C(6)	27(1)	23(1)	17(1)	1(1)	-1(1)	-4(1)
C(7)	30(1)	23(1)	24(1)	2(1)	-2(1)	-4(1)
C(8)	45(1)	24(1)	32(1)	6(1)	-1(1)	-6(1)
C(9)	49(1)	36(1)	33(1)	7(1)	6(1)	-17(1)
C(10)	36(1)	44(1)	32(1)	1(1)	9(1)	-11(1)
C(11)	30(1)	33(1)	23(1)	0(1)	4(1)	-3(1)
C(12)	32(1)	22(1)	39(1)	4(1)	2(1)	2(1)
C(13)	37(1)	72(2)	58(1)	-2(1)	-9(1)	9(1)
C(14)	44(1)	50(1)	54(1)	-15(1)	7(1)	6(1)
C(15)	32(1)	41(1)	40(1)	4(1)	12(1)	7(1)
C(16)	103(2)	60(2)	57(2)	-6(1)	23(2)	28(2)
C(17)	45(1)	74(2)	81(2)	1(2)	-9(1)	17(1)
C(18)	19(1)	16(1)	21(1)	1(1)	-3(1)	-2(1)
C(19)	22(1)	22(1)	23(1)	1(1)	0(1)	-1(1)
C(20)	38(1)	29(1)	23(1)	6(1)	2(1)	0(1)
C(21)	49(1)	27(1)	31(1)	10(1)	-3(1)	9(1)
C(22)	39(1)	24(1)	34(1)	1(1)	-2(1)	12(1)
C(23)	26(1)	20(1)	24(1)	-1(1)	-1(1)	2(1)
C(24)	26(1)	25(1)	27(1)	-3(1)	3(1)	6(1)
C(25)	37(1)	65(1)	42(1)	-8(1)	8(1)	-12(1)
C(26)	68(1)	33(1)	47(1)	-10(1)	21(1)	8(1)
C(27)	24(1)	29(1)	26(1)	2(1)	5(1)	3(1)
C(28)	24(1)	51(1)	40(1)	2(1)	3(1)	1(1)
C(29)	39(1)	48(1)	30(1)	0(1)	9(1)	7(1)
C(30)	23(1)	31(1)	24(1)	-5(1)	-4(1)	7(1)
C(31)	21(1)	32(1)	21(1)	-3(1)	-2(1)	6(1)
C(32)	42(1)	38(1)	34(1)	5(1)	-2(1)	1(1)
C(33)	62(1)	59(1)	30(1)	14(1)	-3(1)	12(1)
C(34)	42(1)	70(2)	23(1)	-9(1)	-10(1)	17(1)

C(35)	29(1)	55(1)	34(1)	-18(1)	-5(1)	1(1)
C(36)	28(1)	38(1)	27(1)	-3(1)	0(1)	2(1)
C(37)	25(1)	27(1)	20(1)	-1(1)	-2(1)	1(1)
C(38)	24(1)	22(1)	27(1)	-1(1)	4(1)	2(1)
C(39)	29(1)	28(1)	28(1)	-1(1)	3(1)	6(1)
C(40)	29(1)	28(1)	40(1)	2(1)	1(1)	5(1)
C(41)	33(1)	26(1)	54(1)	-5(1)	8(1)	9(1)
C(42)	45(1)	33(1)	45(1)	-14(1)	10(1)	8(1)
C(43)	37(1)	31(1)	30(1)	-7(1)	2(1)	2(1)
C(44)	39(1)	25(1)	28(1)	-1(1)	-4(1)	-12(1)

Appendix L

Crystal structure information, compound 3 in Chapter 5

Table 1. Sample and crystal data for complex 3.

Empirical formula	C34 H38 N O P Pd	
Formula weight	614.02	
Temperature	98(2) K	
Wavelength	0.71073 Å	
Crystal size	0.21 x 0.15 x 0.10 mm	
Crystal habit	Purple Prism	
Crystal system	Monoclinic	
Space group	P2(1)/c	
Unit cell dimensions	a = 11.8304(15) Å	α= 90°
	b = 12.6496(16) Å	β= 106.270(3)°
	c = 20.121(3) Å	γ = 90°
Volume	2890.6(6) $Å^3$	
Z	4	
Density (calculated)	1.411 g/cm^3	
Absorption coefficient	0.725 mm^{-1}	
F(000)	1272	

Table 2. Data collection and structure refinement for complex 3.

Diffractometer	CCD area detector
Radiation source	fine-focus sealed tube, MoK
Generator power	1600 watts (50 kV, 32mA)
Detector distance	5.8 cm
Data collection method	omega scans
Theta range for data collection	1.79 to 28.03°
Index ranges	$-15 \leq h \leq 15$, $-16 \leq k \leq 16$, $-26 \leq l \leq 26$

Table 3. Atomic coordinates and equivalent isotropic atomic displacement parameters (Å ^{2}) for complex 3.

U(eq) is defined as one third of the trace of the orthogonalized U_{ij} tensor.

	x/a	y/b	z/c	U(eq)	
C1	0.0185(2)	0.6440(2)	0.07066(13)	0.0189(6)	
Pd1	0.109043(16)		0.608864(15)	0.169860(9)	0.01192(6)
P1	-0.00344(6)	0.71434(5)	0.20895(3)	0.01279(13)	
O1	0.20917(15)	0.49909(14)	0.13621(9)	0.0150(4)	
N1	0.22599(18)	0.57206(17)	0.26465(11)	0.0136(4)	
C8	0.2425(2)	0.6236(2)	0.32177(13)	0.0150(5)	
C14	0.0673(2)	0.7554(2)	0.29770(13)	0.0144(5)	
C3	0.3733(2)	0.3814(2)	0.17581(13)	0.0141(5)	
C9	0.1710(2)	0.7077(2)	0.33969(13)	0.0142(5)	
C21	-0.0447(2)	0.8370(2)	0.16065(13)	0.0150(5)	
C2	0.2925(2)	0.4588(2)	0.18753(13)	0.0139(5)	
C20	-0.1835(3)	0.5697(2)	0.16450(15)	0.0237(6)	
C4	0.4568(2)	0.3406(2)	0.23270(13)	0.0139(5)	
C6	0.3906(2)	0.4460(2)	0.31215(13)	0.0158(5)	
C17	-0.3039(2)	0.6185(2)	0.25902(15)	0.0238(6)	
C12	0.0559(2)	0.8656(2)	0.39457(14)	0.0183(5)	
C5	0.4679(2)	0.36966(19)	0.30166(13)	0.0146(5)	
C10	0.2150(2)	0.7438(2)	0.40804(13)	0.0169(5)	
C7	0.3058(2)	0.4906(2)	0.25699(13)	0.0140(5)	
C13	0.0135(2)	0.8349(2)	0.32589(13)	0.0175(5)	
C18	-0.3441(3)	0.5382(2)	0.21294(16)	0.0250(6)	
C11	0.1588(2)	0.8204(2)	0.43571(13)	0.0187(6)	
C23	-0.1781(3)	0.9347(2)	0.06922(15)	0.0241(6)	
C22	-0.1561(2)	0.8502(2)	0.11532(14)	0.0197(6)	
C26	0.0433(3)	0.9108(2)	0.16133(15)	0.0220(6)	
C16	-0.2036(2)	0.6746(2)	0.25894(15)	0.0222(6)	
C24	-0.0897(3)	1.0055(2)	0.06837(14)	0.0239(6)	
C19	-0.2845(3)	0.5143(2)	0.16416(17)	0.0289(7)	
C15	-0.1411(2)	0.6500(2)	0.21152(13)	0.0159(5)	
C25	0.0202(3)	0.9945(2)	0.11517(15)	0.0251(6)	
C31	0.5600(2)	0.3211(2)	0.36328(13)	0.0165(5)	
C27	0.3659(2)	0.3453(2)	0.10192(13)	0.0173(5)	
C30	0.4641(3)	0.2666(2)	0.10023(14)	0.0232(6)	
C28	0.3776(3)	0.4407(2)	0.05664(14)	0.0269(6)	
C29	0.2475(3)	0.2896(2)	0.07051(14)	0.0246(6)	
C32	0.4983(3)	0.2685(2)	0.41236(14)	0.0228(6)	
C34	0.6347(3)	0.2374(2)	0.34091(15)	0.0271(7)	
C33	0.6428(3)	0.4089(2)	0.40254(15)	0.0266(7)	

Table 4. Bond lengths (Å) for complex 3.

C1-Pd1	2.033(2)	Pd1-O1	2.0589(17)
Pd1-N1	2.071(2)	Pd1-P1	2.1809(7)
P1-C14	1.823(3)	P1-C21	1.823(3)
P1-C15	1.834(3)	O1-C2	1.314(3)
N1-C8	1.288(3)	N1-C7	1.434(3)
C8-C9	1.466(3)	C14-C13	1.392(4)
C14-C9	1.415(3)	C3-C4	1.386(3)
C3-C2	1.433(3)	C3-C27	1.535(3)
C9-C10	1.403(3)	C21-C22	1.386(4)
C21-C26	1.396(4)	C2-C7	1.420(3)
C20-C15	1.383(4)	C20-C19	1.383(4)
C4-C5	1.406(3)	C6-C5	1.386(4)
C6-C7	1.391(4)	C17-C18	1.368(4)
C17-C16	1.384(4)	C12-C13	1.387(4)
C12-C11	1.389(4)	C5-C31	1.531(3)
C10-C11	1.379(4)	C18-C19	1.393(4)
C23-C24	1.381(4)	C23-C22	1.391(4)
C26-C25	1.385(4)	C16-C15	1.396(4)
C24-C25	1.383(4)	C31-C34	1.526(4)
C31-C32	1.534(4)	C31-C33	1.544(4)
C27-C30	1.537(4)	C27-C29	1.537(4)
C27-C28	1.542(4)		

Table 5. Bond angles (°) for complex 3.

C1-Pd1-O1	91.03(9)	C1-Pd1-N1	170.32(10)
O1-Pd1-N1	81.59(8)	C1-Pd1-P1	90.77(8)
O1-Pd1-P1	175.28(5)	N1-Pd1-P1	97.07(6)
C14-P1-C21	105.11(12)	C14-P1-C15	105.45(12)
C21-P1-C15	106.58(12)	C14-P1-Pd1	111.64(9)
C21-P1-Pd1	115.32(8)	C15-P1-Pd1	112.01(9)
C2-O1-Pd1	112.15(15)	C8-N1-C7	121.3(2)
C8-N1-Pd1	127.09(18)	C7-N1-Pd1	110.64(15)
N1-C8-C9	129.3(2)	C13-C14-C9	118.9(2)
C13-C14-P1	117.92(19)	C9-C14-P1	123.14(19)
C4-C3-C2	118.2(2)	C4-C3-C27	121.5(2)
C2-C3-C27	120.2(2)	C10-C9-C14	117.9(2)
C10-C9-C8	113.3(2)	C14-C9-C8	128.8(2)
C22-C21-C26	119.7(2)	C22-C21-P1	121.1(2)
C26-C21-P1	118.4(2)	O1-C2-C7	121.0(2)

O1-C2-C3	121.6(2)	C7-C2-C3	117.4(2)
C15-C20-C19	121.5(3)	C3-C4-C5	124.4(2)
C5-C6-C7	121.4(2)	C18-C17-C16	121.0(3)
C13-C12-C11	119.4(2)	C6-C5-C4	116.7(2)
C6-C5-C31	120.4(2)	C4-C5-C31	122.8(2)
C11-C10-C9	122.4(2)	C6-C7-C2	121.8(2)
C6-C7-N1	123.7(2)	C2-C7-N1	114.5(2)
C12-C13-C14	122.0(2)	C17-C18-C19	119.4(3)
C10-C11-C12	119.4(2)	C24-C23-C22	120.4(3)
C21-C22-C23	119.8(3)	C25-C26-C21	119.9(3)
C17-C16-C15	120.3(3)	C23-C24-C25	119.8(3)
C20-C19-C18	119.6(3)	C20-C15-C16	118.2(2)
C20-C15-P1	117.5(2)	C16-C15-P1	124.3(2)
C26-C25-C24	120.3(3)	C34-C31-C5	112.3(2)
C34-C31-C32	108.0(2)	C5-C31-C32	109.6(2)
C34-C31-C33	108.2(2)	C5-C31-C33	109.3(2)
C32-C31-C33	109.3(2)	C3-C27-C30	112.1(2)
C3-C27-C29	109.4(2)	C30-C27-C29	107.6(2)
C3-C27-C28	110.4(2)	C30-C27-C28	107.5(2)
C29-C27-C28	109.7(2)		

Appendix M

Crystal structure information, compound 4 in Chapter 5

Table 1. Sample and crystal data for complex 4.

Empirical formula	C34 H38 N O P Pd	
Formula weight	614.02	
Temperature	98(2) K	
Wavelength	0.71073 Å	
Crystal size	0.31 x 0.28 x 0.11 mm	
Crystal habit	Yellow Square	
Crystal system	Triclinic	
Space group	P-1	
Unit cell dimensions	a = 12.620(6) Å	α= 77.074(8)°
	b = 12.730(3) Å	β= 84.374(17)°
	c = 19.005(5) Å	γ = 88.126(18)°
Volume	2961.2(17) $Å^3$	
Z	4	
Density (calculated)	1.377 g/cm^3	
Absorption coefficient	0.707 mm^{-1}	
F(000)	1272	

Table 2. Data collection and structure refinement for complex 4.

Diffractometer	CCD area detector
Radiation source	fine-focus sealed tube, MoK
Generator power	1600 watts (50 kV, 32mA)
Detector distance	5.8 cm
Data collection method	omega scans
Theta range for data collection	1.10 to 28.01°
Index ranges	$-16 \leq h \leq 16$, $-16 \leq k \leq 16$, $-25 \leq l \leq 25$

Table 3. Atomic coordinates and equivalent isotropic atomic displacement parameters (Å ^{2}) for complex 4.
U(eq) is defined as one third of the trace of the orthogonalized U_{ij} tensor.

	x/a	y/b	z/c	U(eq)	
Pd2	0.701389(10)		0.777768(10)	0.332405(7)	0.01212(4)
Pd1	0.021974(10)		0.318050(11)	0.176913(7)	0.01296(4)
P2	0.83928(4)	0.67238(4)	0.32011(2)	0.01306(9)	
P1	-0.10903(4)	0.20524(4)	0.19888(3)	0.01556(9)	
O2	0.57392(10)	0.88261(11)	0.33775(7)	0.0168(3)	
O1	0.14084(10)	0.43084(11)	0.16011(7)	0.0179(3)	
N2	0.68436(12)	0.78191(12)	0.22450(8)	0.0142(3)	
N1	0.04566(12)	0.26814(12)	0.28635(8)	0.0150(3)	
C34	0.71530(15)	0.76414(14)	0.44331(9)	0.0141(3)	
C1	0.00029(15)	0.35675(15)	0.06867(10)	0.0176(4)	
C55	0.97114(14)	0.72106(15)	0.32773(10)	0.0153(3)	
C64	0.31065(16)	1.08639(16)	0.11673(10)	0.0196(4)	
C7	0.19868(15)	0.38720(15)	0.28092(10)	0.0163(3)	
C37	0.36265(14)	1.03821(14)	0.24681(10)	0.0151(3)	
C41	0.61728(15)	0.84632(15)	0.18752(10)	0.0176(4)	
C43	0.75373(14)	0.71510(14)	0.18860(10)	0.0146(3)	
C5	0.35465(15)	0.47928(15)	0.30521(10)	0.0169(4)	
C48	0.83714(15)	0.66080(14)	0.22624(10)	0.0147(3)	
C26	-0.26128(16)	0.36894(16)	0.17895(11)	0.0198(4)	
C49	0.83792(14)	0.53528(15)	0.37408(10)	0.0159(3)	
C57	1.07963(18)	0.86517(17)	0.34429(12)	0.0258(4)	
C4	0.36030(15)	0.53548(15)	0.23199(10)	0.0178(4)	
C38	0.38317(15)	1.02846(15)	0.17379(10)	0.0162(3)	
C10	-0.02030(15)	0.14651(15)	0.40460(10)	0.0190(4)	
C6	0.27317(15)	0.40694(15)	0.32793(10)	0.0177(4)	
C35	0.51524(14)	0.92542(14)	0.28634(10)	0.0144(3)	
C45	0.81724(16)	0.64194(15)	0.08493(10)	0.0193(4)	
C3	0.29075(15)	0.52219(15)	0.18293(10)	0.0172(4)	
C60	0.40027(15)	1.01276(15)	0.37870(10)	0.0164(4)	
C14	-0.10403(15)	0.14867(15)	0.29525(10)	0.0160(3)	
C44	0.74191(15)	0.70036(15)	0.11897(10)	0.0181(4)	
C54	0.87771(16)	0.51527(17)	0.44184(11)	0.0223(4)	
C39	0.46947(15)	0.96622(15)	0.15882(10)	0.0184(4)	
C47	0.91199(15)	0.60140(15)	0.19130(10)	0.0171(4)	
C8	0.12058(15)	0.30747(15)	0.31526(10)	0.0164(3)	
C36	0.42438(14)	0.99210(14)	0.30203(10)	0.0142(3)	
C27	0.30144(17)	0.59055(17)	0.10464(11)	0.0251(4)	
C46	0.90424(15)	0.59460(15)	0.12018(10)	0.0182(4)	

C21	-0.24369(15)0.25860(16)	0.18944(10)	0.0187(4)
C50	0.78958(16)0.45224(15)	0.35214(11)	0.0200(4)
C40	0.53530(15)0.91275(15)	0.21314(10)	0.0162(3)
C65	0.19658(17)1.0444(2)	0.13777(12)	0.0282(5)
C61	0.37805(16)0.90607(17)	0.43463(10)	0.0215(4)
C12	-0.17439(15)0.03610(15)	0.40917(10)	0.0189(4)
C11	-0.09509(15)0.07261(15)	0.44333(11)	0.0196(4)
C53	0.86905(17)0.41322(18)	0.48729(11)	0.0267(4)
C13	-0.17801(15)0.07326(15)	0.33524(11)	0.0187(4)
C15	-0.10440(16)0.09268(15)	0.15448(11)	0.0200(4)
C63	0.30204(17)1.08694(18)	0.38372(11)	0.0251(4)
C56	0.97981(16)0.82074(15)	0.34542(11)	0.0196(4)
C62	0.49527(16)1.07054(16)	0.39811(11)	0.0216(4)
C16	-0.05925(16)-0.00606(16)	0.18438(11)	0.0220(4)
C33	0.49253(16)0.38818(17)	0.38540(12)	0.0240(4)
C52	0.82073(17)0.33143(17)	0.46539(12)	0.0267(5)
C31	0.43482(15)0.49559(16)	0.35771(11)	0.0195(4)
C59	1.06439(16)0.66419(16)	0.31185(11)	0.0208(4)
C58	1.17114(17)0.81144(18)	0.32455(11)	0.0262(4)
C51	0.78156(17)0.34997(16)	0.39839(12)	0.0254(4)
C66	0.34804(18)1.0676(2)	0.04130(11)	0.0290(5)
C2	0.20589(14)0.44452(14)	0.20622(10)	0.0154(3)
C32	0.37534(17)0.53331(18)	0.42249(11)	0.0253(4)
C25	-0.36403(17)0.41186(18)	0.17363(12)	0.0257(4)
C17	-0.04982(19)-0.08822(17)	0.14638(13)	0.0292(5)
C9	-0.02481(14)0.18740(14)	0.33015(10)	0.0147(3)
C30	0.3976(2) 0.6666(2)	0.09022(13)	0.0381(6)
C23	-0.43274(18)0.2339(2)	0.18927(14)	0.0351(5)
C67	0.30970(19)1.20868(18)	0.11229(13)	0.0306(5)
C20	-0.1397(2) 0.10886(19)	0.08545(13)	0.0337(5)
C19	-0.1299(2) 0.0265(2)	0.04781(14)	0.0419(6)
C22	-0.33031(18)0.19066(18)	0.19412(13)	0.0309(5)
C24	-0.44964(17)0.34388(19)	0.17920(12)	0.0280(5)
C28	0.3174(2) 0.5180(2)	0.04931(12)	0.0357(5)
C29	0.2009(2) 0.66153(19)	0.09187(14)	0.0356(5)
C18	-0.0854(2) -0.0716(2)	0.07836(14)	0.0383(6)
C69	0.51852(17)0.58055(18)	0.32185(12)	0.0268(4)
C68	1.16317(16)0.71007(18)	0.30934(11)	0.0248(4)

Table 4. Bond lengths (Å) for complex 4.

Pd2-O2	2.0658(15)	Pd2-N2	2.0717(16)
Pd2-C34	2.1002(18)	Pd2-P2	2.1887(9)
Pd1-C1	2.0488(19)	Pd1-O1	2.0629(15)

Pd1-N1	2.0826(16)	Pd1-P1	2.1728(9)
P2-C49	1.8155(19)	P2-C55	1.824(2)
P2-C48	1.8256(19)	P1-C15	1.815(2)
P1-C14	1.8184(19)	P1-C21	1.820(2)
O2-C35	1.295(2)	O1-C2	1.300(2)
N2-C41	1.302(2)	N2-C43	1.431(2)
N1-C8	1.305(2)	N1-C9	1.440(2)
C55-C56	1.394(3)	C55-C59	1.404(3)
C64-C38	1.533(3)	C64-C67	1.540(3)
C64-C65	1.536(3)	C64-C66	1.532(3)
C7-C6	1.423(3)	C7-C8	1.439(3)
C7-C2	1.439(3)	C37-C36	1.381(3)
C37-C38	1.419(3)	C41-C40	1.432(3)
C43-C44	1.400(3)	C43-C48	1.406(3)
C5-C6	1.374(3)	C5-C4	1.411(3)
C5-C31	1.538(3)	C48-C47	1.400(3)
C26-C21	1.387(3)	C26-C25	1.395(3)
C49-C54	1.395(3)	C49-C50	1.397(3)
C57-C58	1.386(3)	C57-C56	1.394(3)
C4-C3	1.382(3)	C38-C39	1.371(3)
C10-C11	1.389(3)	C10-C9	1.400(3)
C35-C40	1.433(2)	C35-C36	1.452(3)
C45-C44	1.387(3)	C45-C46	1.392(3)
C3-C2	1.449(3)	C3-C27	1.542(3)
C60-C62	1.543(3)	C60-C36	1.538(2)
C60-C63	1.542(3)	C60-C61	1.541(3)
C14-C13	1.401(3)	C14-C9	1.411(3)
C54-C53	1.391(3)	C39-C40	1.427(3)
C47-C46	1.387(3)	C27-C30	1.542(3)
C27-C28	1.542(3)	C27-C29	1.541(3)
C21-C22	1.400(3)	C50-C51	1.399(3)
C12-C13	1.383(3)	C12-C11	1.390(3)
C53-C52	1.384(3)	C15-C16	1.387(3)
C15-C20	1.396(3)	C16-C17	1.394(3)
C33-C31	1.538(3)	C52-C51	1.379(3)
C31-C69	1.534(3)	C31-C32	1.539(3)
C59-C68	1.386(3)	C58-C68	1.393(3)
C25-C24	1.387(3)	C17-C18	1.379(4)
C23-C24	1.382(3)	C23-C22	1.392(3)
C20-C19	1.391(3)	C19-C18	1.380(4)

Table 5. Bond angles (°) for complex 4.

O2-Pd2-N2	91.26(6)	O2-Pd2-C34	89.85(6)
N2-Pd2-C34	176.60(6)	O2-Pd2-P2	176.52(4)
N2-Pd2-P2	86.02(5)	C34-Pd2-P2	92.99(5)
C1-Pd1-O1	90.34(7)	C1-Pd1-N1	176.20(7)
O1-Pd1-N1	91.80(6)	C1-Pd1-P1	91.27(6)
O1-Pd1-P1	176.36(4)	N1-Pd1-P1	86.78(5)
C49-P2-C55	104.05(9)	C49-P2-C48	105.89(8)
C55-P2-C48	106.51(8)	C49-P2-Pd2	119.09(6)
C55-P2-Pd2	118.47(7)	C48-P2-Pd2	101.54(6)
C15-P1-C14	106.91(9)	C15-P1-C21	103.51(9)
C14-P1-C21	105.46(9)	C15-P1-Pd1	119.80(7)
C14-P1-Pd1	101.39(6)	C21-P1-Pd1	118.44(7)
C35-O2-Pd2	127.42(12)	C2-O1-Pd1	127.18(12)
C41-N2-C43	119.12(16)	C41-N2-Pd2	122.75(12)
C43-N2-Pd2	118.04(12)	C8-N1-C9	120.32(16)
C8-N1-Pd1	122.41(13)	C9-N1-Pd1	117.27(12)
C56-C55-C59	119.02(18)	C56-C55-P2	118.99(14)
C59-C55-P2	121.87(15)	C38-C64-C67	110.35(16)
C38-C64-C65	109.45(16)	C67-C64-C65	108.74(18)
C38-C64-C66	111.61(16)	C67-C64-C66	108.01(17)
C65-C64-C66	108.61(17)	C6-C7-C8	113.91(17)
C6-C7-C2	120.29(17)	C8-C7-C2	125.80(17)
C36-C37-C38	124.73(17)	N2-C41-C40	128.58(17)
C44-C43-C48	118.84(16)	C44-C43-N2	123.54(17)
C48-C43-N2	117.62(16)	C6-C5-C4	116.32(17)
C6-C5-C31	120.76(17)	C4-C5-C31	122.91(17)
C47-C48-C43	119.66(17)	C47-C48-P2	123.94(14)
C43-C48-P2	116.39(13)	C21-C26-C25	120.55(19)
C54-C49-C50	119.65(18)	C54-C49-P2	118.67(15)
C50-C49-P2	121.43(14)	C58-C57-C56	120.35(19)
C3-C4-C5	124.68(17)	C39-C38-C37	116.34(17)
C39-C38-C64	123.75(17)	C37-C38-C64	119.91(16)
C11-C10-C9	120.30(18)	C5-C6-C7	122.78(17)
O2-C35-C40	123.88(16)	O2-C35-C36	119.25(16)
C40-C35-C36	116.86(16)	C44-C45-C46	120.57(18)
C4-C3-C2	119.24(17)	C4-C3-C27	120.65(17)
C2-C3-C27	120.10(16)	C62-C60-C36	109.48(15)
C62-C60-C63	106.84(16)	C36-C60-C63	111.73(15)
C62-C60-C61	110.33(16)	C36-C60-C61	110.67(15)
C63-C60-C61	107.72(16)	C13-C14-C9	120.16(17)
C13-C14-P1	122.41(15)	C9-C14-P1	117.36(14)
C45-C44-C43	120.48(17)	C49-C54-C53	120.1(2)
C38-C39-C40	122.54(17)	C46-C47-C48	120.77(17)

N1-C8-C7	128.67(17)	C37-C36-C35	118.94(16)
C37-C36-C60	121.22(16)	C35-C36-C60	119.81(16)
C30-C27-C28	106.92(19)	C30-C27-C29	107.31(19)
C28-C27-C29	110.37(19)	C30-C27-C3	112.14(17)
C28-C27-C3	110.91(18)	C29-C27-C3	109.11(18)
C47-C46-C45	119.29(17)	C26-C21-C22	119.21(19)
C26-C21-P1	119.27(14)	C22-C21-P1	121.50(16)
C51-C50-C49	119.62(19)	C39-C40-C35	120.54(17)
C39-C40-C41	113.97(16)	C35-C40-C41	125.47(17)
C13-C12-C11	119.31(17)	C10-C11-C12	121.09(18)
C52-C53-C54	120.0(2)	C12-C13-C14	120.54(18)
C16-C15-C20	118.99(19)	C16-C15-P1	122.08(15)
C20-C15-P1	118.73(16)	C57-C56-C55	120.31(19)
C15-C16-C17	120.6(2)	C53-C52-C51	120.50(19)
C69-C31-C33	108.48(17)	C69-C31-C32	107.76(17)
C33-C31-C32	109.27(17)	C69-C31-C5	112.45(16)
C33-C31-C5	109.26(16)	C32-C31-C5	109.56(16)
C68-C59-C55	120.14(19)	C57-C58-C68	119.55(19)
C50-C51-C52	120.1(2)	O1-C2-C7	123.79(17)
O1-C2-C3	119.53(16)	C7-C2-C3	116.68(16)
C26-C25-C24	119.9(2)	C16-C17-C18	119.9(2)
C10-C9-C14	118.54(17)	C10-C9-N1	124.25(17)
C14-C9-N1	117.20(16)	C24-C23-C22	120.5(2)
C15-C20-C19	120.1(2)	C18-C19-C20	120.3(2)
C21-C22-C23	120.0(2)	C23-C24-C25	119.9(2)
C19-C18-C17	120.1(2)	C59-C68-C58	120.46(19)

Appendix N

Kinetic data sources for Table 2-1 and Figure 2-2

199.01 K

t (/s)	[A]	ln([A]t/[A]0)		
0	15388.3	0		
1200	13627.1	-0.121547023		
2400	13030.7	-0.166299369		
3600	11890.6	-0.257859308		
T (K)	R(J/K.mol)	kB (J/K)	h (J.s)	k
199.01	8.314	1.38E-23	6.63E-34	6.82E-05

Gibbs Activation Energy

63943.577

63.944 kJ/mol

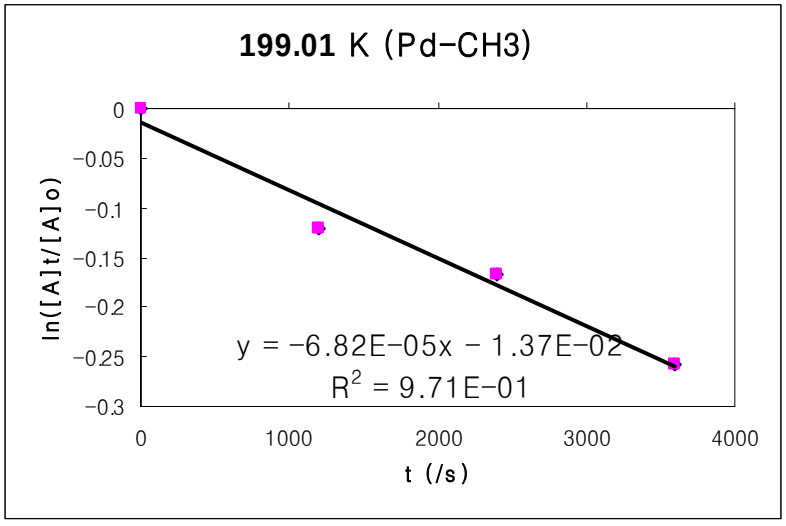

205.85 K

t (/s)	[A]	ln([A]t/[A]0)
0	15277.9	0
300	13968.8	-0.089581069
600	13503.8	-0.123436212
900	13156.8	-0.149468605
1200	12326.7	-0.214639698

T (K)	R(J/K.mol)	kB (J/K)	h (J.s)	k
205.85	8.314	1.38E-23	6.63E-34	1.63E-04

Gibbs Activation Energy

64707.976

64.708 kJ/mol

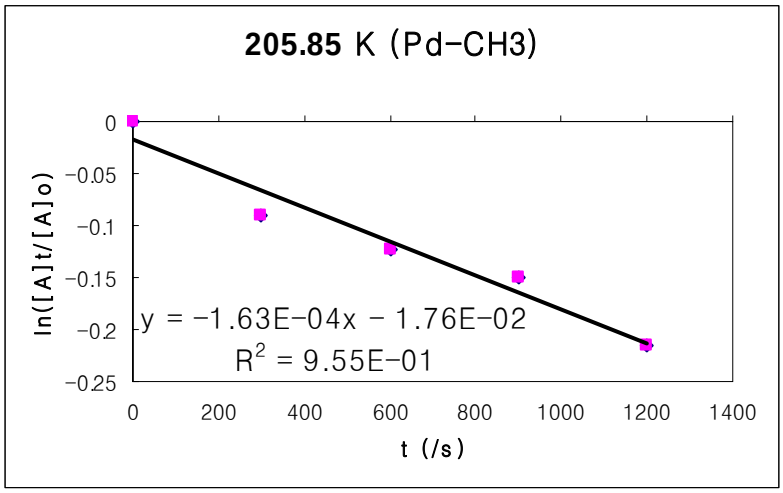

211.96 K 1st

t (/s)	[A]	ln([A]t/[A]0)		
0	14744.4	0		
600	10714.7	-0.319246719		
1200	7245.8	-0.710441359		
1800	3912.3	-1.326737913		
2400	2180.5	-1.911309141		
3000	1333.3	-2.403206278		
3600	938.1	-2.754762076		
4200	439	-3.514119216		
T (K)	R(J/K.mol)	kB (J/K)	h (J.s)	k
211.96	8.314	1.38E-23	6.63E-34	8.42E-04

Gibbs Activation Energy

63786.527

63.787 kJ/mol

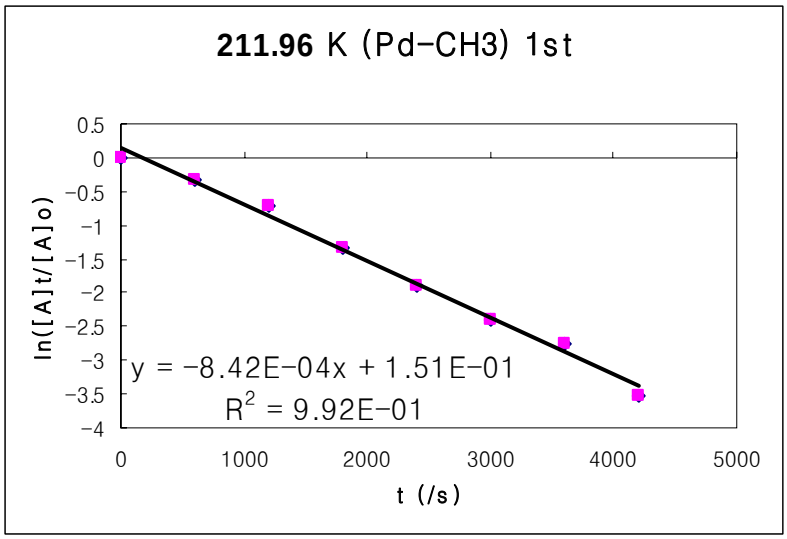

211.96 K 2nd

t (/s)	[A]	ln([A]t/[A]0)
0	15632.1	0
600	10345	-0.412823181
1200	5892.3	-0.975680079
1800	3985.4	-1.366688809
2400	2679.1	-1.763845575
3000	1632.5	-2.25921391
3600	961.9	-2.788171276
4200	725.3	-3.070496409

T (K)	R(J/K.mol)	kB (J/K)	h (J.s)	k
211.96	8.314	1.38E-23	6.63E-34	7.46E-04

Gibbs Activation Energy

63999.854

64.000 kJ/mol

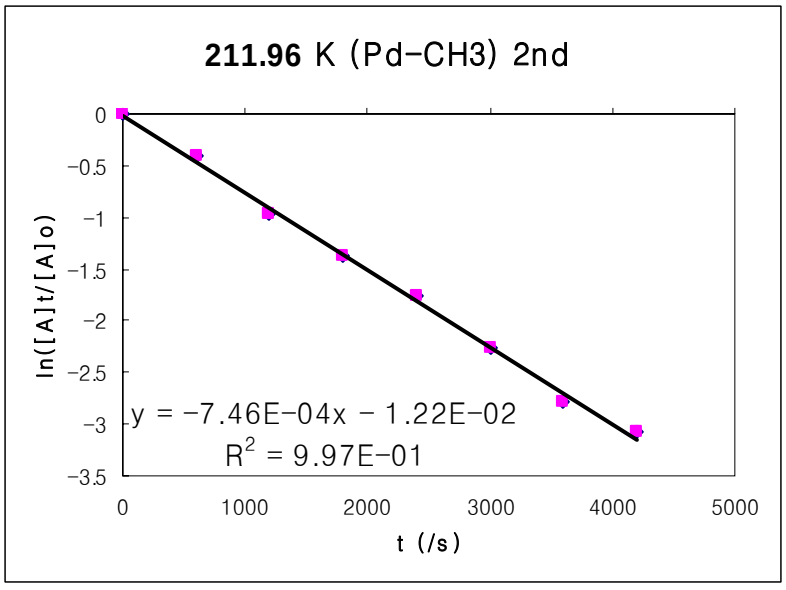

218.28 K

t (/s)	[A]	ln([A]t/[A]0)		
0	9699.2	0		
300	6163.4	-0.453414835		
600	4214.3	-0.833559904		
900	3078.3	-1.147665911		
1200	2326.1	-1.427850362		
T (K)	R(J/K.mol)	kB (J/K)	h (J.s)	k
218.28	8.314	1.38E-23	6.63E-34	1.18E-03

Gibbs Activation Energy

65129.297

65.129 kJ/mol

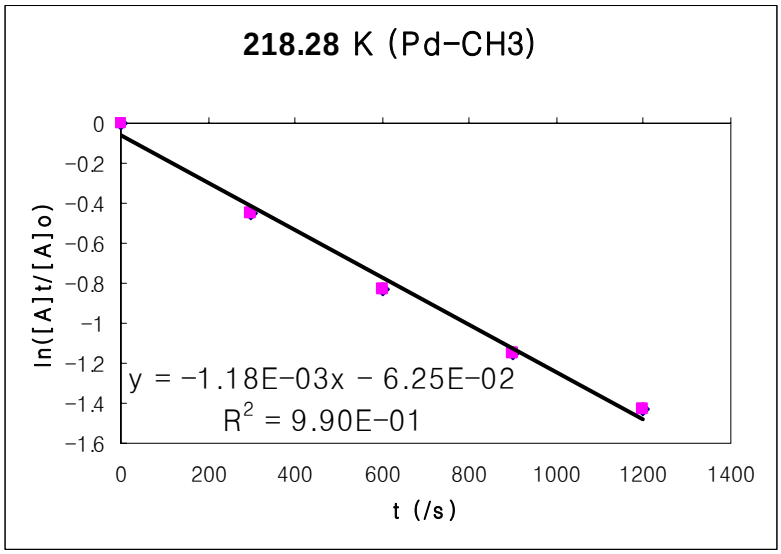

224.25 K

t (/s)	[A]	ln([A]t/[A]0)
0	5135.9	0
300	2472.4	-0.731065757
600	1410.6	-1.29223995
900	881.5	-1.762385373

T (K)	R(J/K.mol)	kB (J/K)	h (J.s)	k
224.25	8.314	1.38E-23	6.63E-34	1.95E-03

Gibbs Activation Energy

66024.38

66.024 kJ/mol

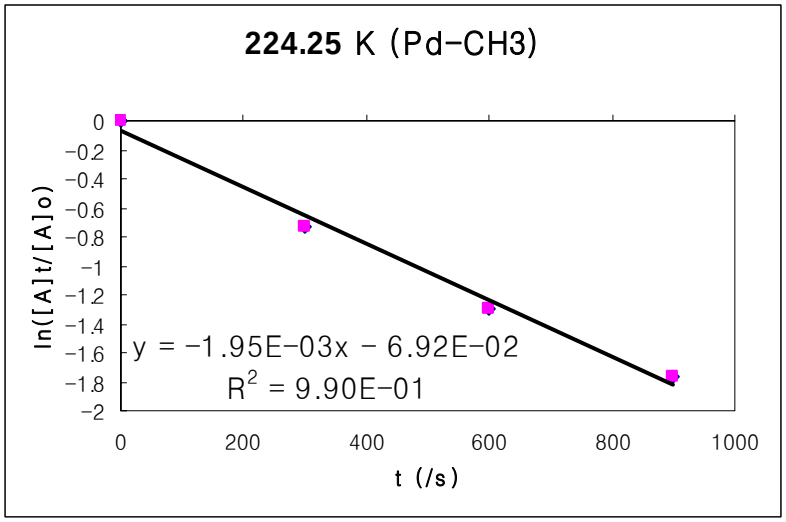

T	k	1/RT	lnk
199.01	6.82E-05	5.024873	-9.59307
205.85	1.63E-04	4.857906	-8.72176
211.96	7.46E-04	4.717871	-7.20078
218.28	1.18E-03	4.581272	-6.74224
224.25	1.95E-03	4.459309	-6.23993

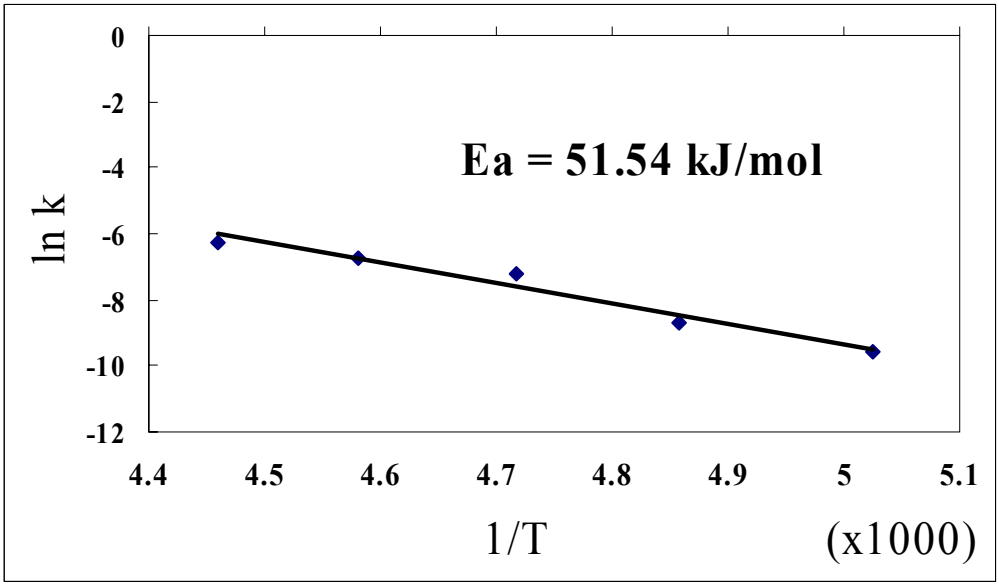

T	k(-CH3)	1/T	ln(k/T)	
199.01	6.82E-05	0.005025	-14.8864	
205.85	0.000163	0.004858	-14.0489	
211.96	0.000842	0.004718	-12.4361	
218.28	0.00118	0.004581	-12.128	
224.25	0.00195	0.004459	-11.6527	
R(J/K.mol)	kB (J/K)	h (J.s)	slope	y-intercept
8.314	1.38E-23	6.63E-34	5994.5	15.313

Activation enthalpy (J/mol)	**Activation Entropy (J/K.mol)**
721.01275	-70.2304
0.721 kJ/mol	-16.7851
172.322047	**-70.230 J/K.mol**
0.172 kcal/mol	**-16.785 cal/K.mol**

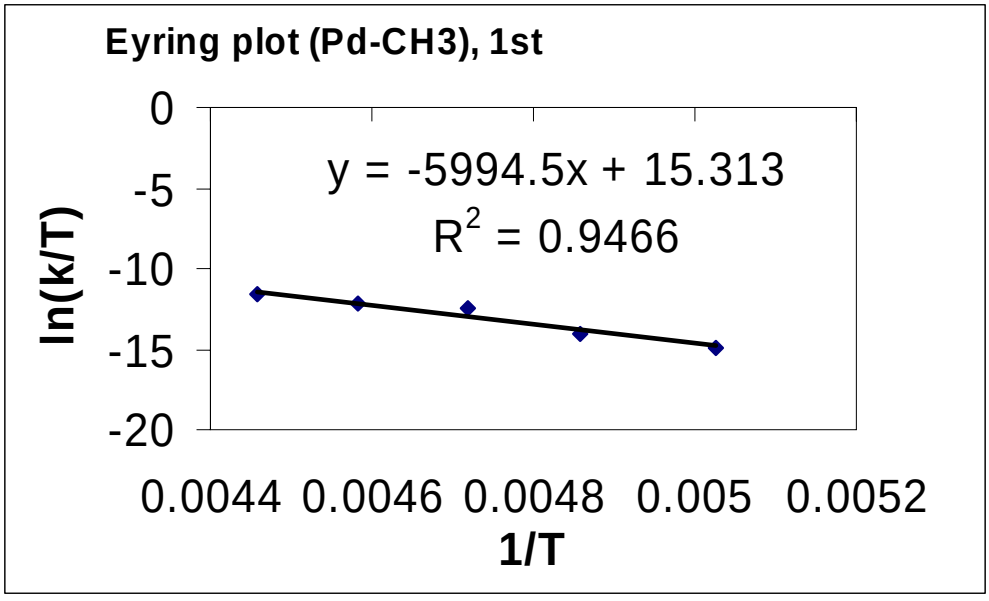

T	k(-CH3)	1/T	ln(k/T)	
199.01	6.82E-05	0.005025	-14.8864	
205.85	0.000163	0.004858	-14.0489	
211.96	0.000746	0.004718	-12.5572	
218.28	0.00118	0.004581	-12.128	
224.25	0.00195	0.004459	-11.6527	
R(J/K.mol)	kB (J/K)	h (J.s)	slope	y-intercept
8.314	1.38E-23	6.63E-34	5988.2	15.259

Activation enthalpy (J/mol)	**Activation Entropy (J/K.mol)**
720.254992	-70.6793
0.720 kJ/mol	**-70.679 J/K.mol**
172.140943	-16.8924
0.172 kcal/mol	**-16.892 cal/K.mol**

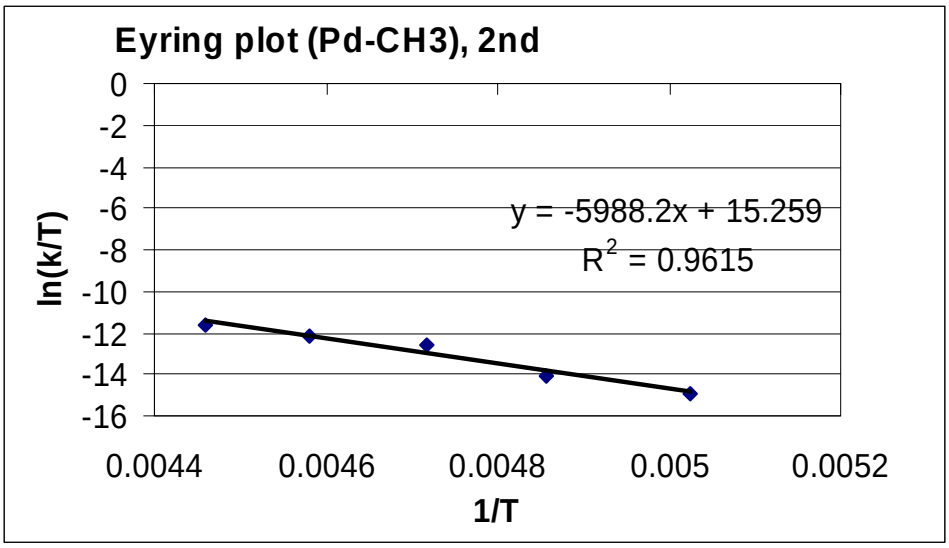

	k	sigma m	p	(+)	sigma p	log(k/ko)	
C(O)OMe	5.49E-02	0.35	0.44		0.45	1.509123	
F					0.06		0.774584
Br	2.15E-02	0.37	0.26	0.15	0.23	1.10199	0
Cl					0.23		-0.49065
H	1.70E-03	0	0	0	0	0	
CH3	5.40E-04	-0.06	-0.14	-0.31	-0.17	-0.49806	
OiPr	600		-0.12	2.088842	-0.45		2.088842
F	29.1		0.15	0.774584			
Br	4.89		0.26	0			
Cl	1.58		0.24	-0.49065			

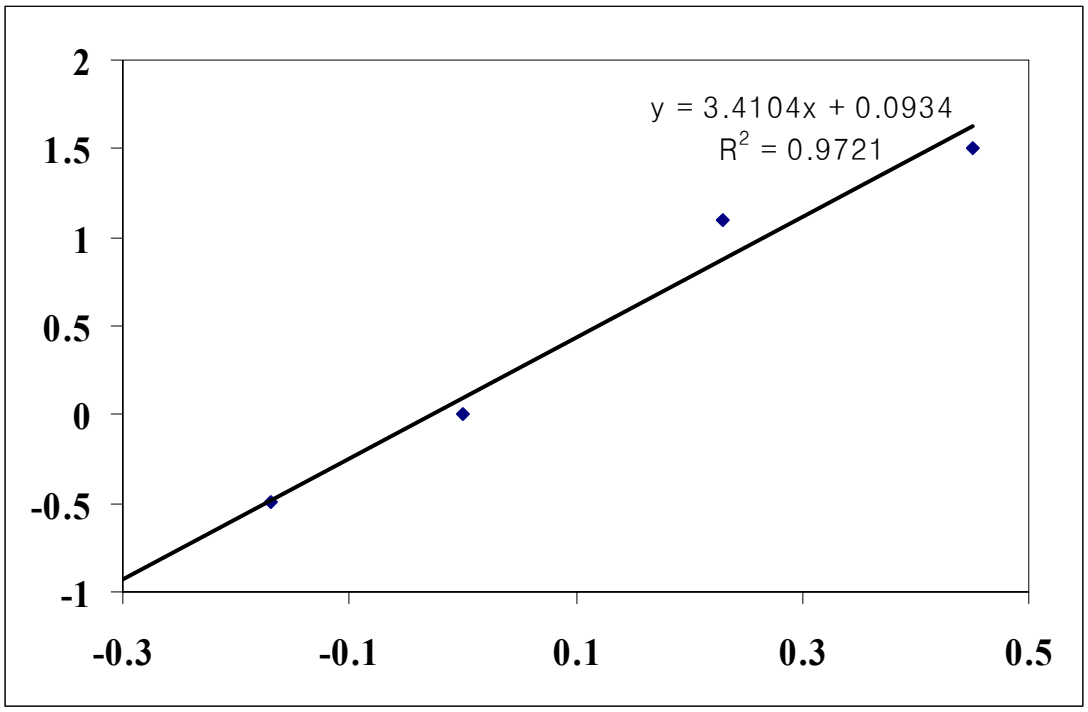

Appendix O

Data sources for Figure 3-6 and 3-7

1. Scaled-up Reaction : Molecular *vs* time [using (COD)PdMeCl)]

time(min)	20	30	40	50	60
Mw	973	1192	1376	1459	1558
Mn	628	749	793	789	879

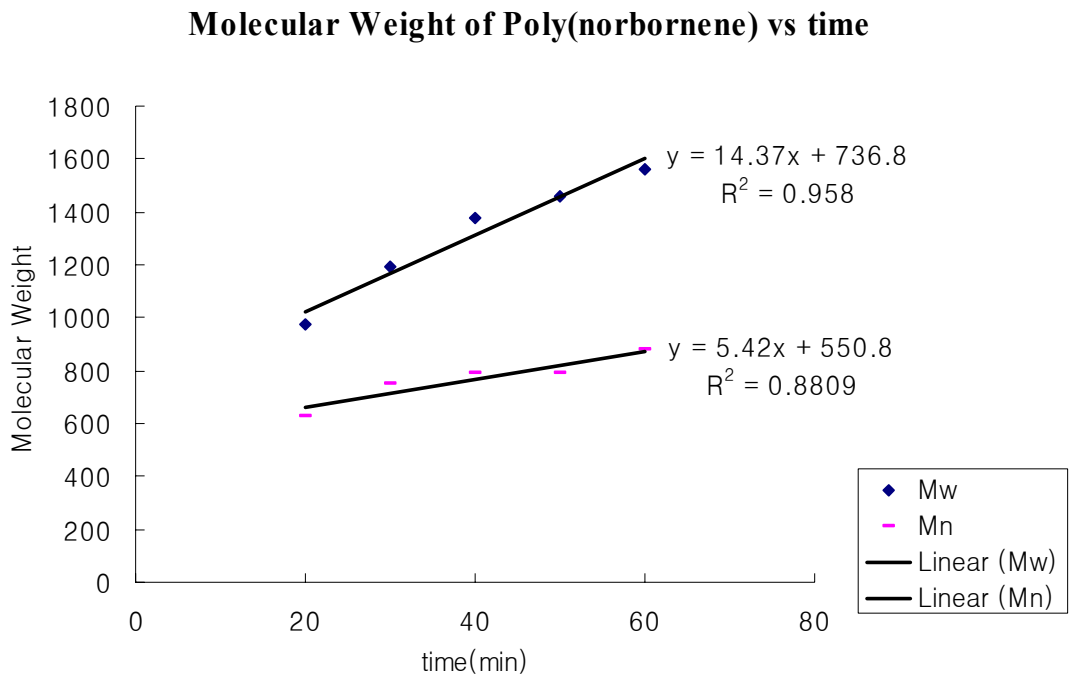

2. Scaled-up Reaction : Molecular *vs* time [using **1a**]

time(min)	20	30	40	50	60
Mw	901	1119	1338	1399	1550
Mn	552	655	723	733	922

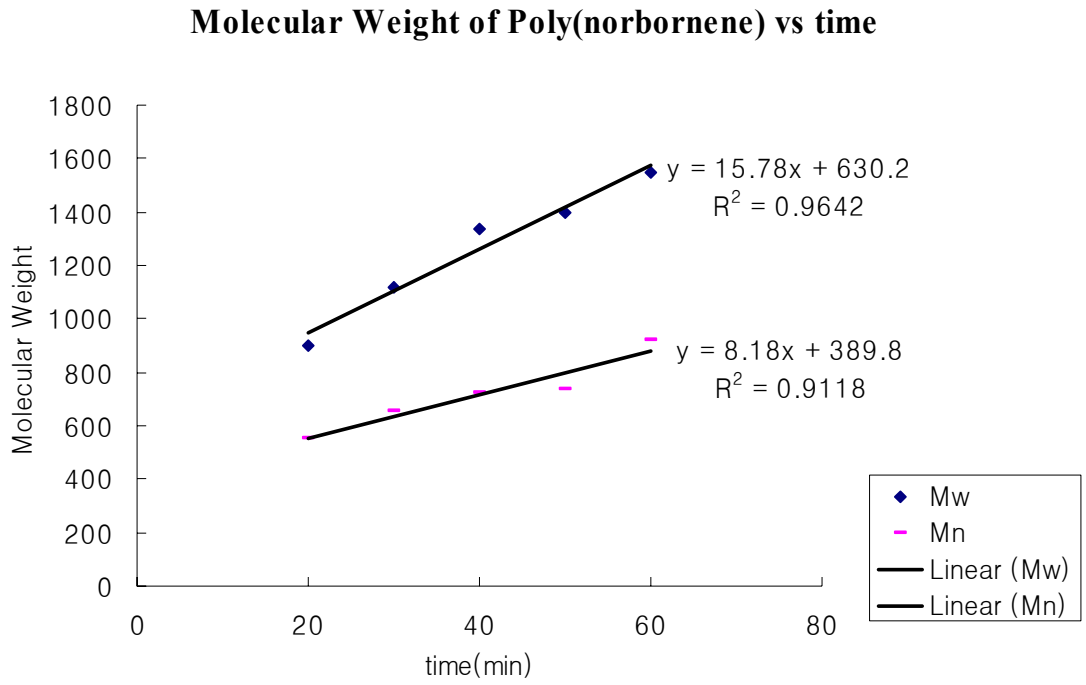

0	2700	5400	8100	10800
Conversion of Norbornene vs time				
0.94726	0.90217	0.86584	0.82789	0.78334
Conversion of Exo-Ethylesternorbornene vs time				
0.94726	0.93497	0.92535	0.91752	0.9113
Conversion of Endo-Ethylesternorbornene vs time				
0.94726	0.93824	0.93208	0.92501	0.91974

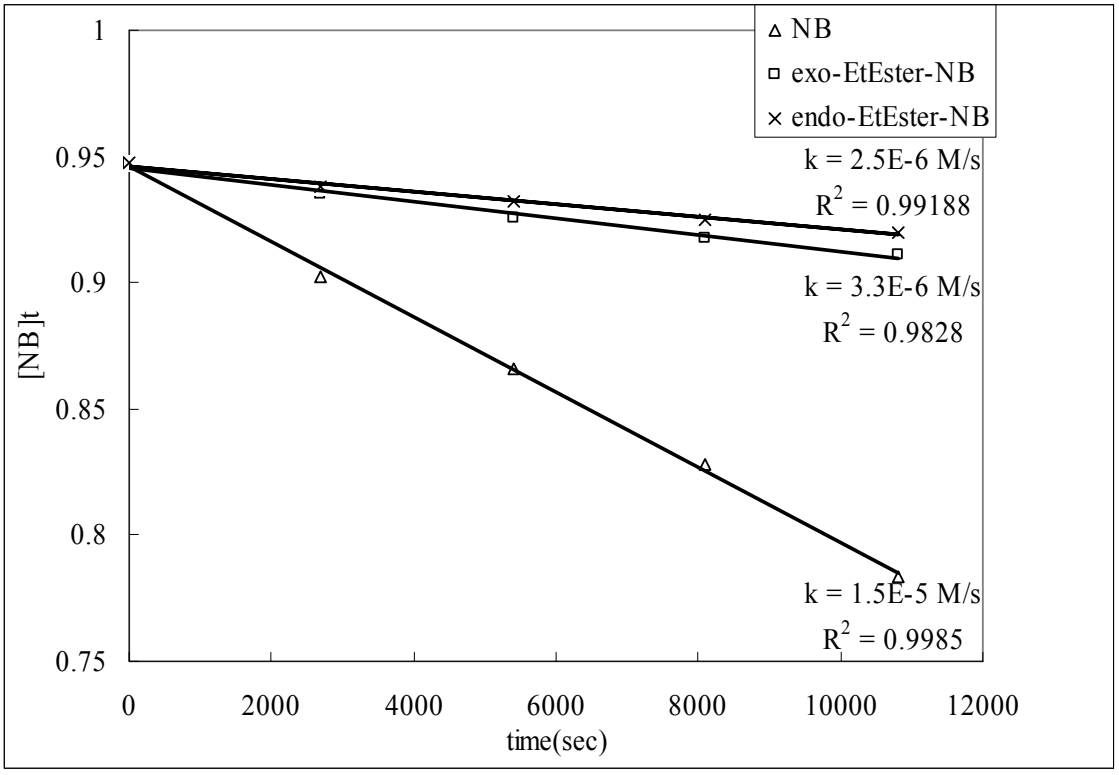

Appendix P

Kinetic data sources for Table 4-7

	0oC	3c + *CO		
time	0	900	1800	2700
ln([A]t/[A]0)	0	-0.024456068	-0.030814613	-0.04053898
time	3600	4500	5400	6300
ln([A]t/[A]0)	-0.0455890	-0.05178	-0.06125921	-0.06348
time	7200	8100	9000	9900
ln([A]t/[A]0)	-0.07526761	-0.07981	-0.08852	-0.09603
time	10800	11700	12600	13500
ln([A]t/[A]0)	-0.10032	-0.10785	-0.11382	-0.11905
time	14400	15300		
ln([A]t/[A]0)	-0.127	-0.13006		

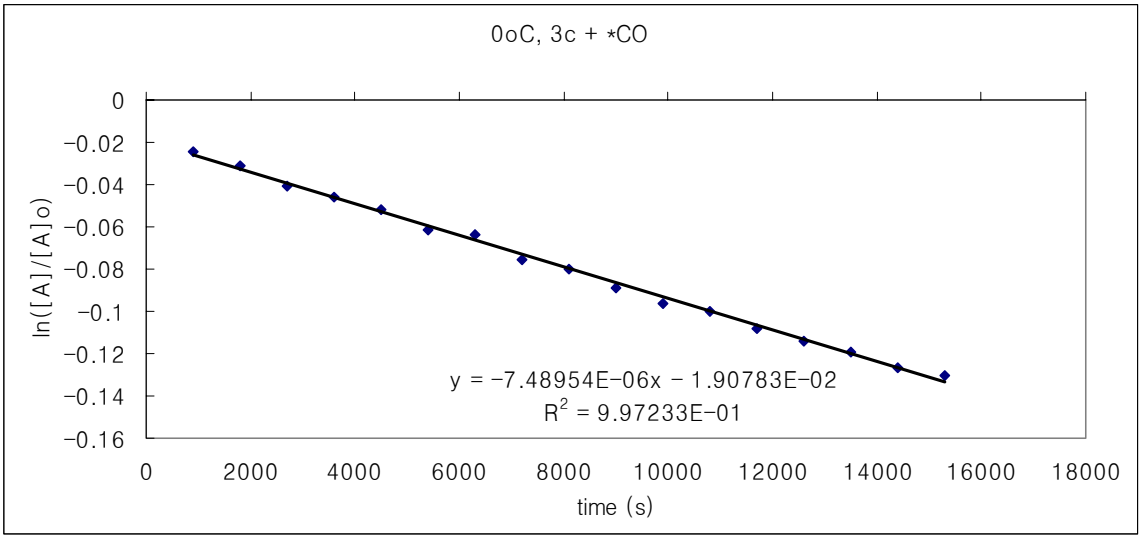

	10oC	3c + *CO		
time	0	600	1200	1800
ln([A]t/[A]0)	0	-0.012758866	-0.03045737	-0.04629046
time	2400	3000	3600	4200
ln([A]t/[A]0)	-0.06165	-0.07753855	-0.08785	-0.1064788
time	4800	5400	6000	
ln([A]t/[A]0)	-0.1179	-0.13748	-0.14677	

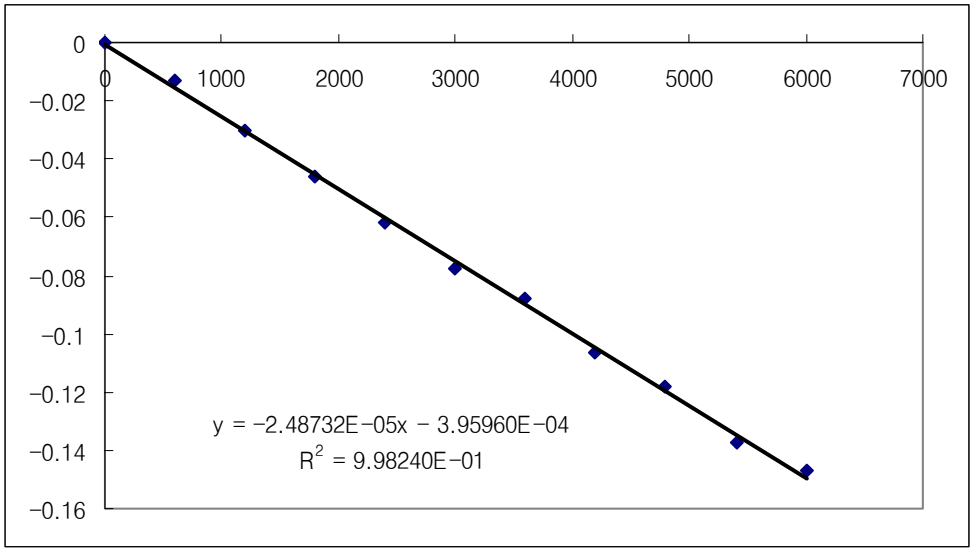

	20oC	3c + *CO		
time	0	300	600	900
ln([A]t/[A]0)	0	-0.02056283	-0.05690837	-0.10334
time	1200	1500		
ln([A]t/[A]0)	-0.14927806	-0.2009		

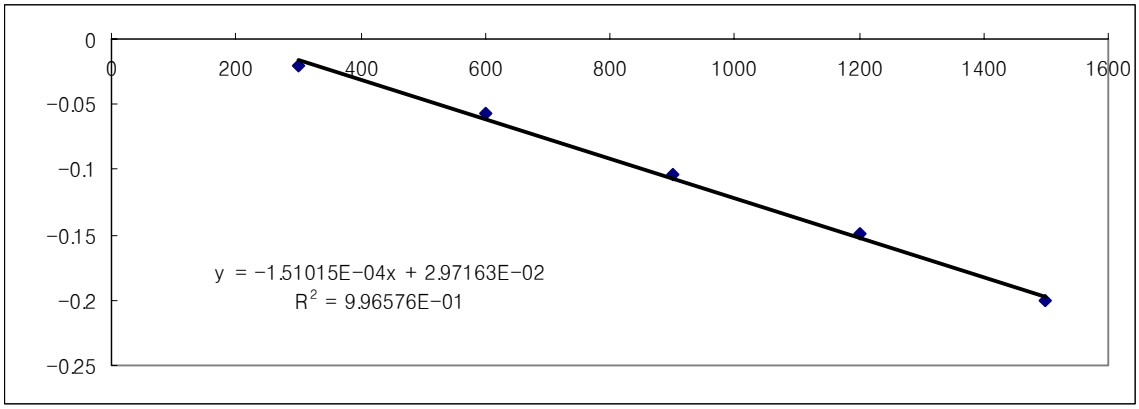

	0oC	3c + Imine +*CO		
time	900	1800	4500	8100
ln([A]t/[A]0)	-0.03204	-0.04018	-0.06273	-0.08966
time	11700			
ln([A]t/[A]0)	-0.11817			

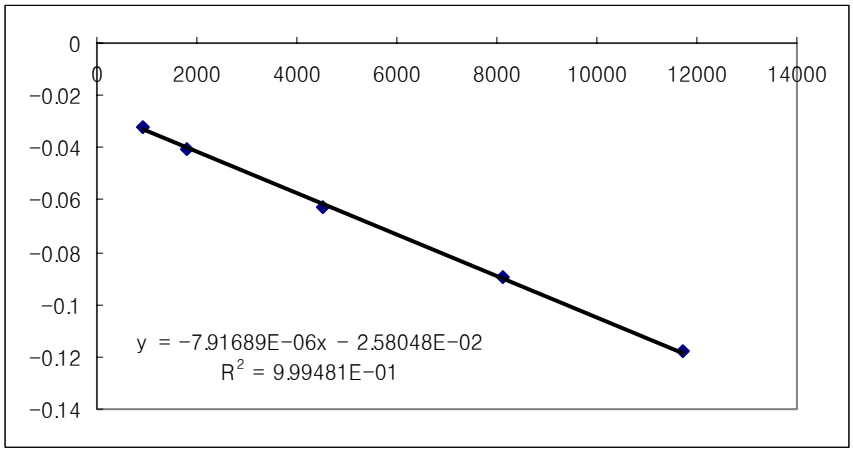

	10oC	3c + Imine +*CO		
time	900	1800	2700	3600
ln([A]t/[A]0)	-0.071465898	-0.102683789	-0.1067224	-0.13450993
time	4500	5400	6300	7200
ln([A]t/[A]0)	-0.15938	-0.16880611	-0.19135	-0.21295282
time	8100	9000	9900	
ln([A]t/[A]0)	-0.21279	-0.24288	-0.25921	

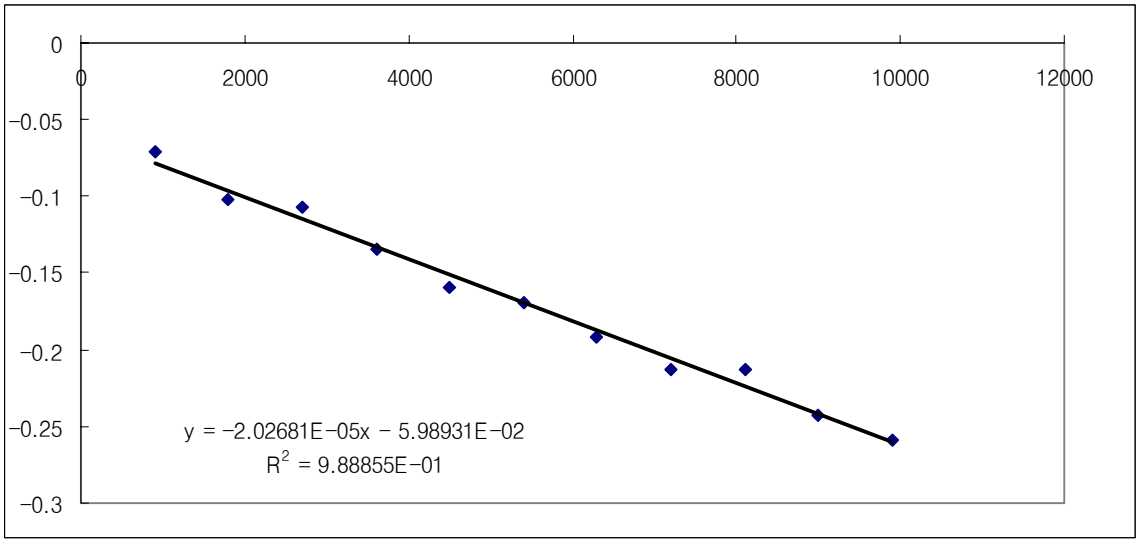

	20oC	3c + Imine +*CO		
time	300	600	900	1200
ln([A]t/[A]0)	-0.051832773	-0.07799489	-0.09829763	-0.12287
time	1500	1800	2100	
ln([A]t/[A]0)	-0.1487688	-0.17715	-0.19966078	

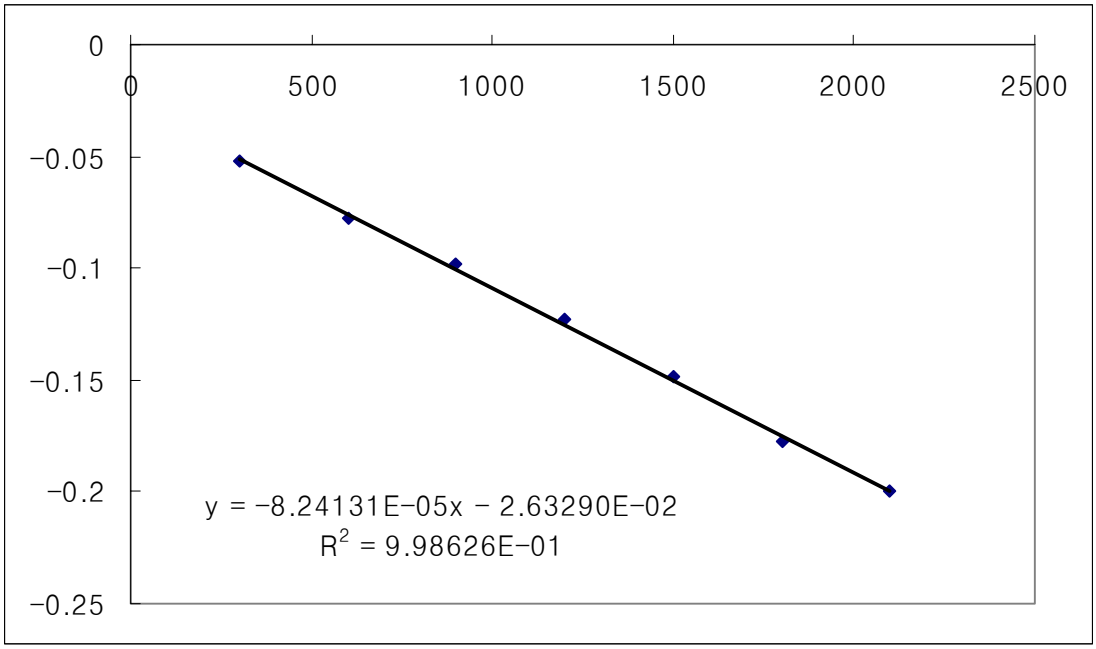

Temp. Calib. of NMR probe (DPX300)

y = 1.2431x - 65.562

R2 = 0.9997

		1.2431	65.562	
	273.15	339.552765	273.990765	0oC
	283.15	351.983765	286.421765	10oC
	293.12	364.377472	298.815472	20oC

3c +*CO

T	273.9908	286.4218	298.8155
k(/s)	7.48954E-06	2.48732E-05	1.51015E-04
kB(J/K)	1.38E-23	1.38E-23	1.38E-23
h(J s)	6.63E-34	6.63E-34	6.63E-34
R(J/K mol)	8.314	8.314	8.314
*D*G	9.38E+04	9.53E+04	9.50E+04
1/T	0.003649758	0.003491354	0.003346547
ln(k/T)	-17.41509771	-16.25918519	-14.49795771

*D*H(kJ/mol)	79686.3644	79.686
*D*S(J/K mol))	-52.47167092	-52.47167092

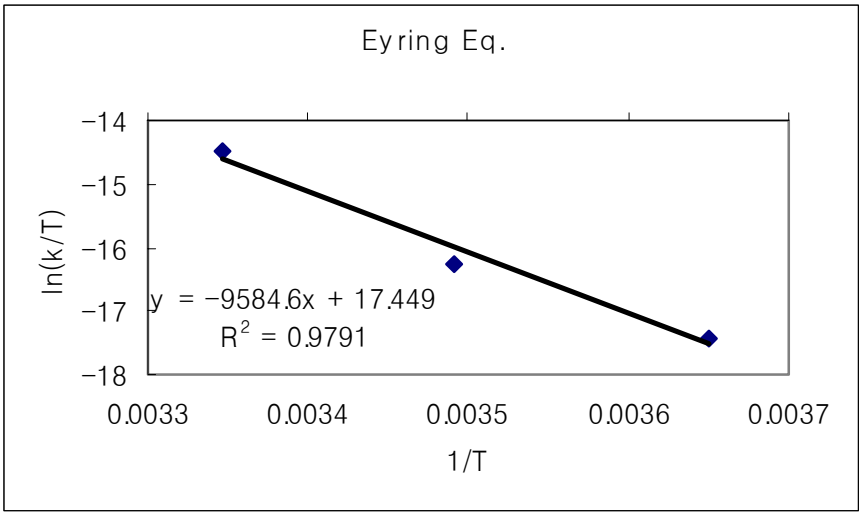

3c + Imine +*CO

T	273.9908	286.4218	298.8155
k(/s)	7.91689E-06	2.02681E-05	8.24131E-05
kB(J/K)	1.38E-23	1.38E-23	1.38E-23
h(J s)	6.63E-34	6.63E-34	6.63E-34
R(J/K mol)	8.314	8.314	8.314
*D*G	9.37E+04	9.58E+04	9.66E+04
1/T	0.003649758	0.003491354	0.003346547
ln(k/T)	-17.35960664	-16.46392789	-15.10359248

*D*H(kJ/mol)	61627.525	61.628
*D*S(J/K mol))	-117.6916753	-117.6916753

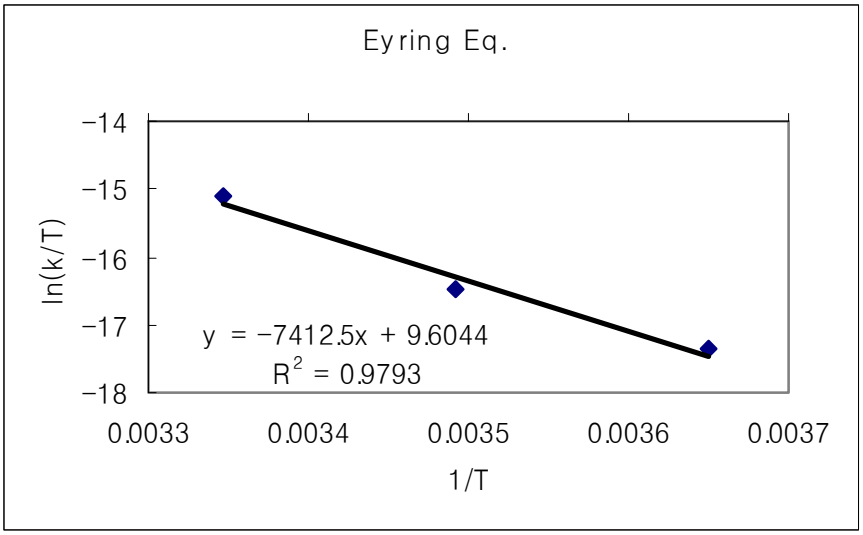

VITA

Myeongsoon Kang

Myeongsoon Kang graduated from Inha University, Inchon, S. Korea with a Bachelor's degree in Chemistry. He got Master's degree under the guidance of Prof. Dr. Ik-Mo Lee at Inha University. His thesis title was 'Synthesis of Sterically modified Zirconocenes [$(2\text{-R-Ind})_2ZrCl_2$ (R=methyl, i-propyl, phenyl and benzyl, Ind=Indenyl)] for polymerization of thermoplastic elastomer'. He joined Prof. Dr. Ayusman Sen's group in August 1999 to study late transition metal-based catalytic systems for polymerization of polar vinyl monomers. He received the Braucher Research Fellowship, 2003-2004 for his work on the mechanistic study of the reaction between a cationic palladium complex and vinyl halide. He will receive his doctoral degree in August 2004 and will continue working on metal-catalyzed polymerizations.